Universitat Autònoma de Barcelona

ADVANCES IN ENHANCED BIOLOGICAL PHOSPHORUS REMOVAL: AMINO ACIDS AS CARBON SOURCE AND ENVISAGING ITS INTEGRATION IN HIGH-RATE SYSTEMS

Natalia Rey Martínez

Universitat Autònoma de Barcelona

ADVANCES IN ENHANCED BIOLOGICAL PHOSPHORUS REMOVAL: AMINO ACIDS AS CARBON SOURCE AND ENVISAGING ITS INTEGRATION IN HIGH-RATE SYSTEMS

Doctoral thesis

Natalia Rey Martínez

Supervisors: Dr. Juan Antonio Baeza Labat

Dr. Albert Guisasola i Canudas

Academic tutor: Dr. Juan Antonio Baeza Labat

A thesis submitted in fulfilment of the requirements for the Doctoral degree in Environmental Science and Technology

GENOCOV research group

Department of Chemical, Environmental and Biological Engineering

Engineering School

Universitat Autònoma de Barcelona (UAB)

Bellaterra, September 2019

GENOCOV
Departament d'Enginyeria Química,
Biològica i Ambiental
Escola d'Enginyeria
Universitat Autònoma de Barcelona
Barcelona · Spain
info@genocov.com

Research Group on Biological Treatment and Valorisation of Liquid and Gaseous Effluents
GENOCOV

UAB
Universitat Autònoma de Barcelona

ALBERT GUISASOLA I CANUDAS, Professor Agregat i **JUAN ANTONIO BAEZA LABAT**, Catedràtic Laboral del Departament d'Enginyeria Química de la Universitat Autònoma de Barcelona,

CERTIFIQUEM:

Que l'enginyera NATALIA REY MARTÍNEZ ha realitzat sota la nostra direcció, el treball que amb títol "ADVANCES IN ENHANCED BIOLOGICAL PHOSPHORUS REMOVAL: AMINO ACIDS AS CARBON SOURCE AND ENVISAGING ITS INTEGRATION IN HIGH-RATE SYSTEMS" es presenta en aquesta memòria, i que constitueix la seva Tesi per optar al Grau de Doctor per la Universitat Autònoma de Barcelona.

I per a què se'n prengui coneixement i consti als efectes oportuns, presentem a l'Escola d'Enginyeria de la Universitat Autònoma de Barcelona l'esmentada Tesi, signant el present certificat.

Bellatera, 19 de setembre de 2019

Dr. Albert Guisasola i Canudas

Dr. Juan Antonio Baeza Labat

A Emilio, Gnomito y Chispi

SUMMARY

Nowadays, population and economic growth, changes in lifestyles and consumption patterns result in an increasing demand of water and energy. This leads to a huge wastewater production that needs to be treated before its discharge. Therefore, urban wastewater treatment plants (WWTPs) are widely implemented in industrialized countries and they must incorporate processes for nutrients removal (nitrogen (N) and phosphorus (P)). In this sense, biological processes are the most economical and sustainable processes for nutrients removal to prevent the eutrophication of water bodies.

Enhanced biological phosphorus removal (EBPR) has been highly studied at lab scale but, in the most cases, using simple substrates as carbon source, i.e. volatile fatty acids (acetic, propionic and butyric). As a result, a microbial population enriched in polyphosphate accumulating organisms (PAO) is developed, being *Candidatus* Accumulibacter phosphatis the species of PAO most frequently found. However, the new microbial identification technologies have demonstrated the presence of other PAO different than *Accumulibacter* in WWTPs. Since real wastewater is a complex matrix, mainly composed of lipids, proteins and carbohydrates, the need to study EBPR process using complex substrates has arisen. Furthermore, studies on a larger scale than lab-scale should be also performed.

In this thesis, the operation of a pilot plant (146 L) with A^2/O configuration for simultaneous removal of organic matter, N and P using glutamate as carbon and nitrogen source was proposed. As a result, a microbial community enriched in *Thiothrix* (37%), *Comamonadaceae* (15.6%) and *Accumulibacter* (7.7%) was developed. This microbial community performed anaerobic P-release with only 18-29% of the observed polyhydroxyalkanoate (PHA) storage in *Accumulibacter*-enriched sludge. Moreover, the denitrifying capabilities of this population were evaluated using nitrite and nitrate as electron acceptors. It was concluded that free nitrous acid was indeed the true inhibitor, instead of nitrite, and at concentrations of 2 $\mu g\ N\text{-}HNO_2^- \cdot L^{-1}$, the complete inhibition of P-uptake for this microbial community occured. Finally, a sequencing batch reactor (SBR) enriched in *Tetrasphaera* using casein hydrolysate as sole carbon source was operated. *Tetrasphaera* present important differences in comparison to *Accumulibacter*, since they are able to ferment complex organic compounds and they can take up some amino acids. However, they do not synthesize PHA. The degradation capacities of

different amino acids and the polymers stored was studied here, using *Tetrasphaera*-enriched biomass.

Conventional activated sludge process presents high energy consumption, mainly associated to aeration and sludge treatment. In addition, organic matter is mineralized or used for denitrification instead of being utilized for biogas production. For these reasons, WWTPs are energy consuming facilities. Nowadays, the transformation of conventional WWTPs into energy self-sufficient facilities is one of the main challenges to be faced by the wastewater treatment. A feasible approach to achieve this challenge is the A/B process, which consist of a first step, A-stage, which aims at maximizing the carbon capture into the sludge for being treated through an anaerobic digestion system for biogas production; and a second step, B-stage, where the nitrogen is removed through an autotrophic process. However, this process does not include biological P removal.

Therefore, this thesis aims to investigate the possible integration of the EBPR in the A-stage of the A/B process. To reach this objective, two systems (a high-rate activated sludge (HRAS) and an SBR) were compared to act as A-stage treating real wastewater from the primary settler and operating at SRT of 1 and 2 days. The HRAS system provided better organic matter removal efficiencies, however, higher mineralization of the organic matter was achieved (55.2%) compared to the SBR (13.2%). In addition, higher biogas production was obtained with the sludge of SBR (308 NL $CH_4 \cdot kg^{-1}VS$). Finally, the possible integration of EBPR in the first step of the A/B process was studied, by incorporating an anaerobic zone in order to allow PAO growth. But, PAO bacteria are washed from the system when the SRT is lower than 4 days, so it was needed to work at higher SRTs than those typically used in high-rate systems (SRT<2 days). In addition, real influent was also used in this study, but an external contribution of organic matter was required for the development of the PAO activity.

Hoy en día, el aumento de la población, el crecimiento de la economía, los cambios en los estilos de vida y los patrones de consumo llevan a una creciente demanda de agua y energía. Lo que se traduce en una enorme producción de agua residual que necesita ser tratada antes de su vertido. Por ello, las Estaciones Depuradoras de Aguas Residuales (EDARs) urbanas están ampliamente implantadas en los países industrializados y deben incorporar procesos que permitan la eliminación biológica de nutrientes (nitrógeno (N) y fósforo (P)) ya que es la manera más económica y sostenible de prevenir la eutrofización de las aguas.

A escala laboratorio, la eliminación biológica de P está altamente estudiada pero, en la mayoría de los casos, se ha utilizado como fuente de carbono sustratos sencillos tales como ácidos grasos volátiles (acético, propiónico y butírico). Esto da lugar al desarrollo de una población microbiana en la que predominan unas bacterias acumuladoras de P (Polyphosphate Accumulating Organisms, PAO) catalogadas como *Accumulibacter*. Sin embargo, el impulso de las nuevas técnicas de identificación microbiológicas ha demostrado la presencia de otras PAO diferentes a las *Accumulibater* en las EDARs. Debido a que el agua residual real es una matriz mucho más compleja, compuesta principalmente por lípidos, proteínas y carbohidratos, nace la necesidad de estudiar este proceso biológico utilizando sustratos más complejos y a una mayor escala.

En esta tesis se propuso operar una planta piloto (146 L) con configuración A^2/O para la eliminación biológica simultánea de materia orgánica, N y P utilizando glutamato como fuente de carbono y nitrógeno. Como resultado se obtuvo una población microbiana enriquecida en *Thiothrix* (37%) y *Comamonadaceae* (15.6%) además de la presencia de *Accumulibacter* (7.7%). La peculiaridad de esta población es la capacidad de liberar P almacenando solo un 18-29% del polihidroxialcanoato (PHA) que se acumularía en una biomasa enriquecida en *Accumulibacter*. Posteriormente se evaluaron las capacidades desnitrificantes de esta población utilizando como aceptores de electrones nitrito y nitrato. Se concluyó que el verdadero inhibidor es el ácido nitroso libre en lugar del nitrito y que a concentraciones de 2 $\mu g\ N\text{-}HNO_2^- \cdot L^{-1}$ se produce la completa inhibición de la captación de P para esta comunidad microbiana. Finalmente se ha operado un reactor discontinuo enriquecido en *Tetrasphaera* y utilizando caseína hidrolizada como única fuente de carbono. Las *Tetrasphaera* tienen rasgos diferenciadores de las *Accumulibacter*, ya que las primeras son capaces de fermentar compuestos orgánicos complejos y de captar

aminoácidos, sin embargo no son capaces de sintetizar PHA. Se han estudiado las capacidades de degradación de distintos aminoácidos utilizando esta biomasa enriquecida en *Tetrasphaera*, además de los polímeros de almacenamiento (PHA y glucógeno).

Por otra parte, los tratamientos convencionales de lodos activos presentan un gran consumo energético asociado principalmente a la aireación y al tratamiento de los lodos. Además, la materia orgánica es mineralizada o destinada a la desnitrificación en lugar de ser utilizada para la producción de biogás. Por todo esto, las EDARs son instalaciones consumidoras de energía. Sin embargo, el reto existente hoy en día es transformarlas en instalaciones autosuficientes energéticamente. Una manera de conseguirlo es mediante la implantación del proceso A/B, que consta de una primera etapa A en la cual trabajando a bajos tiempos de residencia celular (TRC) e hidráulico (TRH), se pretende minimizar la mineralización de la materia orgánica y que ésta se adsorba en el lodo para incrementar la producción de biogás. A continuación, en la segunda etapa B se eliminara autotróficamente el N. Sin embargo, este proceso tampoco contempla la eliminación biológica de P.

Por tanto, esta tesis pretende investigar la posible integración de la eliminación biológica de P en la etapa A del proceso A/B. Para ello se compararon dos sistemas (uno continuo y otro discontinuo) para actuar como etapa A tratando agua residual real procedente del sedimentador primario y operando a TRC de 1 y 2 días. El sistema continuo proporcionó mejores eficacias de eliminación de materia orgánica, sin embargo, se mineralizó un 55.2% de la materia orgánica inicial frente a un 13.2% mineralizado en discontinuo. Además, se observaron mayores producciones de biogás con el lodo del sistema discontinuo (308 NL $CH_4 \cdot kg^{-1}VS$). Finalmente se estudió la posibilidad de integrar la eliminación biológica de P en este primer paso del proceso A/B, mediante la incorporación de una zona anaerobia que permita el crecimiento de las PAO. Sin embargo, se ha estudiado que estas bacterias se lavan del sistema cuando el TRC baja de los 4 días, por tanto, se hace necesario trabajar a TRC mayores de los usados típicamente en los sistemas de alta carga (TRC<2 días). Además, el influente real utilizado en este estudio tenía un bajo contenido en materia orgánica, por lo que ha sido necesario aportarla externamente para desarrollar la actividad PAO.

Hoxe en día, o aumento da poboación, o crecemento da economía, os cambios nos estilos de vida e os patróns de consumo levan a unha crecente demanda de auga e enerxía. O que se traduce nunha enorme producción de auga residual que precisa de tratamento antes da súa descarga. Por iso, as estacións depuradoras de augas residuais (EDARs) urbanas están amplamente implantadas nos países industrializados e deben incorporar procesos que permitan a eliminación biolóxica de nutrintes (nitróxeno (N) e fósforo (P)) xa que é a maneira máis económica e sostible de evitar a autrofización das augas.

A escala laboratorio, a eliminación biolóxica de fósforo está altamente estudiada, pero na maioría dos casos, empregando substratos sinxelos (ácidos graxos volátiles) como fonte de carbono. Isto dá como resultado o desenvolvemento dunha poboación microbiana na que predominan unhas bacterias acumuladoras de fósforo (Polyphosphate Accumulating Organisms, PAO) clasificadas como *Accumulibacter*. Non obstante, o impulso das novas técnicas de identificación microbiolóxicas demostrou a presenza doutros PAO distintos dos Accumulibacter nas EDARs. Polo tanto, dado que a auga residual real é unha matriz complexa composta principalmente por lípidos, proteínas e carbohidratos, xorde a necesidade de estudiar este proceso biolóxico empregando substratos máis complexos e a unha maior escala.

Nesta tese propúxose operar unha planta piloto (146 L) cunha configuración A^2/O para a eliminación biolóxica simultánea de materia orgánica, N e P empregando glutamato como fonte de carbono e nitróxeno. Como resultado, obtívose unha poboación microbiana enriquecida en *Thiothrix* (37%) e *Comamonadaceae* (15.6%) ademáis da presenza de *Accumulibacter* (7.7%). A peculiaridade de esta poboación é a capacidade de liberar P almacenando soamente un 18-29% do polihidroxialcanoato (PHA) que se acumularía nunha biomasa enriquecida en *Accumulibacter*. Posteriormente avaliáronse as capacidades desnitrificantes desta poboación empregando como aceptores de electróns nitrito e nitrato. Concluíuse que o verdadeiro inhibidor é o ácido nitroso libre en lugar do nitrito, e que a concentracións de 2 $\mu g\ N\text{-}HNO_2^- \cdot L^{-1}$ prodúcese a completa inhibición da captación de P para esta comunidade microbiana. Finalmente, operouse un reactor discontinuo enriquecido en *Tetrasphaera* e empregando caseína hidrolizada como única fonte de carbono. As *Tetrasphaera* posúen trazos diferenciadores das *Accumulibacter*, xa que as primeiras son capaces de fermentar compostos orgánicos complexos e de captar aminoácidos, no entanto non son capaces de sintetizar PHA. Estudiáronse as capacidades

de degradación de distintos aminoácidos empregando esta biomasa enriquecida en *Tetrasphaera*, ademáis dos polímeros de almacenamento.

Por outra banda, os tratamentos convencionais de lodos activos presentan un alto consumo enerxético asociado principalmente á aireación e ao tratamento dos lodos. Ademais, a materia orgánica mineralízase ou destínase á desnitrificación en lugar de ser usada para a producción de biogás. Por isto, as EDARs son instalacións consumidoras de enerxía. Emporiso, o reto existente hoxe en día é transformalas en instalacións autosuficientes enerxéticamente. Un xeito de logralo é mediante a implantación do proceso A/B, que consta dunha primeira etapa A, na que se pretende minimizar a mineralización da materia orgánica e que ésta se adsorba no lodo para posteriormente destinar eses lodos á producción de biogás, traballando a baixos tempos de residencia celular (TRC) e hidráulico (TRH); e unha etapa B para a eliminación autotrófica de nitróxeno. No entanto, este proceso non contempla a eliminación biolóxica de fósforo.

Por iso, esta tese pretende investigar a posible integración da eliminación biolóxica de fósforo na etapa A do proceso A/B. Para isto, compáraronse dous sistemas (un continuo e outro discontinuo) para actuar como etapa A tratando auga residual real procedente do sedimentador primario e operando a TRC de 1 e 2 días. O sistema continuo proporcionou mellores eficacias de eliminación de materia orgánica, con todo, mineralizouse un 55.2% da materia orgánica inicial frente a un 13.2% mineralizada no reactor discontinuo. Ademais, observáronse maiores producción de biogás co lodo do sistema discontinuo (308 NL $CH_4 \cdot kg^{-1}VS$). Finalmente estudiouse a posibilidade de integrara eliminación biolóxica de P neste primeiro paso do proceso A/B, mediante a incorporación dunha zona anaerobia que permita o crecemento de PAO. Non obstante, as bacterias PAO lávanse do sistema cando o TRC é menor de 4 días, polo que se fai necesario traballar a TRC maiores dos empregados típicamente nos sistemas de alta carga (TRC<2 días). Ademais, o influente real empregado neste estudio tiña un baixo contido en materia orgánica, polo que se fixo necesario un aporte externo para desenrolar a actividade PAO.

Avui en dia, l'augment de la població, el creixement de l'economia, els canvis en els estils de vida i els patrons de consum porten a una creixent demanda d'aigua i energia. El que es tradueix en una enorme producció d'aigua residual que necessita ser tractada abans del seu abocament. Per això, les estacions depuradores d'aigües residuals (EDARs) urbanes estan àmpliament implantades en els països industrialitzats i han d'incorporar processos que permetin l'eliminació biològica de nutrients (nitrogen (N) i fòsfor (P)), ja que és la manera més econòmica i sostenible de prevenir l'eutrofització de les aigües.

A escala laboratori, l'eliminació biològica de fòsfor està altament estudiada però, en la majoria dels casos, utilitzant substrats senzills (àcids grassos volàtils) com a font de carboni. Això dona lloc al desenvolupament d'una població microbiana en la qual predominen uns bacteris acumuladors de fòsfor (Polyphosphate Accumulating Organisms, PAO) catalogats com *Accumulibacter*. No obstant això, l'impuls de les noves tècniques d'identificació microbiològiques ha demostrat la presència d'altres PAO, diferents als *Accumulibacter*, a les estacions depuradores d'aigües residuals (EDARs). Per tant, ja que l'aigua residual real és una matriu complexa composta principalment per lípids, proteïnes i carbohidrats, neix la necessitat d'estudiar aquest procés biològic utilitzant substrats més complexos i a una major escala.

En aquesta tesi es va proposar operar una planta pilot (146 L) amb configuració A^2/O per a l'eliminació biològica simultània de matèria orgànica, N i P usant glutamat com a font de carboni i nitrogen. Com a resultat es va obtenir una població microbiana enriquida en *Thiothrix* (37%) i *Comamonadaceae* (15.6%) a més de la presència d'*Accumulibacter* (7.7%). La peculiaritat d'aquesta població és la capacitat d'alliberar P emmagatzemant sols un 18-29% del polihidroxialcanoat (PHA) que s'acumularia en una biomassa enriquida en *Accumulibacter*. Posteriorment es van avaluar las capacitats desnitrificants d'aquesta població utilitzant com a acceptors d'electrons nitrit i nitrat. Es va concloure que el veritable inhibidor és l'acid nitrós lliure en comptes del nitrit, i que a concentracions de 2 $\mu g\ N\text{-}HNO_2^- \cdot L^{-1}$ es produeix la completa inhibició de la captació de fòsfor per aquesta comunitat microbiana. Finalment es va operar un reactor discontinu enriquit en *Tetrasphaera* i utilitzant caseïna hidrolitzada com a única font de carboni. Els *Tetrasphaera* tenen trets diferenciadors dels *Accumulibacter*, ja que els primers són capaços de fermentar compostos orgànics complexos i de captar aminoàcids, però no són capaços de sintetitzar PHA. S'han estudiat les capacitats de degradació de diferents

aminoàcids utilitzant aquesta biomassa enriquida en *Tetrasphaera* a més dels polimers d'enmagatzematge.

D'altra banda, els tractaments convencionals de fangs actius presenten un gran consum energètic associat principalment a l'aeració i al tractament dels llots. A més a més, la matèria orgànica es mineralitza o es destina a la desnitrificació, en comptes de ser utilitzada per la producció de biogàs. Per tot això, les EDARs són instal·lacions consumidores d'energia. Així doncs, el repte existent avui dia és transformar les EDARs en instal·lacions autosuficients energèticament. Una manera d'aconseguir-ho és mitjançant la implantació del procés A/B, que consta d'una primera etapa, etapa A, en la qual treballant a temps de residència cel·lular (TRC) i hidràulic (TRH) baixos, es pretén minimitzar la mineralització de la matèria orgànica i que aquesta s'adsorbeixi al fang per posteriorment destinar aquests llots a la producció de biogàs; i una etapa B per l'eliminació autotròfica del nitrogen. Malgrat això, aquest procés no contempla l'eliminació biològica de fòsfor.

Per tant, aquesta tesi pretén investigar la possible integració de l'eliminació biològica de fòsfor en l'etapa A del procés A/B. Per això es van comparar dos sistemes (un continu i un altre discontinu) per actuar com etapa A tractant aigua residual real procedent del sedimentador primari i operant a TRC de 1 i 2 dies. El sistema continu va proporcionar millors eficàcies d'eliminació de matèria orgànica, però es va mineralitzar el 55.2% de la matèria orgànica inicial enfront d'un 13.2% mineralitzada en el sistema discontinu. Tanmateix, es van observar majors produccions de biogàs amb el fang del sistema discontinu (308 NL $CH_4 \cdot kg^{-1}VS$). Finalment, es va estudiar la possibilitat d'integrar l'eliminació biològica de P en aquest primer pas del procés A/B, mitjançant la incorporació d'una zona anaeròbia que permeti el creixement de PAO. No obstant això, s'ha d'estudiat que aquest bacteris es renten del sistema quan el TRC baixa dels 4 dies, per tant es fa necessari treballar a TRC majors dels típicament utilitzats en els sistemes d'alta càrrega (TRC<2 dies). Per una altra banda, l'influent real utilitzat en aquest estudi tenia un baix contingut en matèria orgànica, pel que ha estat necessari aportar-la externament per desenvolupar l'activitat PAO.

LIST OF ACRONYMS AND ABBREVIATIONS

A/O	Anaerobic/Oxic
A^2/O	Anaerobic/Anoxic/Oxic
AOB	Ammonium Oxidizing Bacteria
A/O-HRAS	Anaerobic/Oxic High-Rate Activated Sludge
AS	Activated Sludge
BMP	Biochemical Methane Potential
BNR	Biological Nitrogen Removal
C	Carbon
CAS	Conventional Activated Sludge
Cas_aa	Sodium casein hydrolysate
CLSM	Confocal Laser Scanning Microscopy
COD	Chemical Oxygen Demand
COD_C	Colloidal COD
COD_F	Filtered COD
COD_P	Particulate COD
COD_S	Soluble COD
COD_T	Total COD
CRR	Carbon Recovery Ratio
DNA	Deoxyribonucleic Acid
DO	Dissolved Oxygen
DPAO	Denitrifying Polyphosphate Accumulating Organisms
EBPR	Enhanced Biological Phosphorus Removal
EPS	Extracellular Polymeric Substances
FISH	Fluorescence *in situ* hybridization
GAO	Glycogen Accumulating Organisms
GC	Gas Chromatography
Gly	Glycogen
HPLC	High-Performance Liquid Chromatography

HRAS	High-Rate Activated Sludge
HRT	Hydraulic Retention Time
HRSBR	High-Rate Sequencing Batch Reactor
Mix_aa	Mixture of arginine, lysine, cysteine, proline and tyrosine
N	Nitrogen
NOB	Nitrite Oxidizing Bacteria
OHO	Ordinary Heterotrophic Organisms
PAO	Polyphosphate Accumulating Organisms
PCR	Polymerase Chain Reaction
P	Phosphorus
PHA	Polyhydroxyalkanoates
Poly-P	Poly-Phosphate
PSE	Primary Settler Effluent
PSI	Primary Settler Influent
rRNA	Ribosomal Ribonucleic Acid
SBR	Sequencing Batch Reactor
SNA	Simultaneous Nitritation and Anammox
SRT	Sludge Retention Time
SVI	Sludge Volume Index
TOC	Total Organic Carbon
TCA	Tricarboxylic Acid Cycle
TSS	Total Suspended Solids
VFA	Volatile Fatty Acids
VSS	Volatile Suspended Solids
WWTP	Wastewater Treatment Plant
Y_{OBS}	Observed biomass growth yield

CONTENTS

Chapter 1

GENERAL INTRODUCTION

1.1. The importance of wastewater treatment

The increasing populations, growing economies, changing lifestyles and evolving consumption patterns led to a globally increasing demand for freshwater and energy (UNESCO, 2014). This can turn into a huge wastewater production, which is discharged into watercourses together with hazardous chemicals and materials. Therefore, an urgent need to control water quality in the wastewater-receiving bodies has emerged (UNEP, 2015), which brought up the necessity of a wastewater treatment before their discharge into the environment (UNESCO, 2014).

The main pollutants of wastewater are pathogens, organic matter, nutrients (mostly nitrogen (N) and phosphorus (P)), salts, acids, heavy metals, toxic organic compounds and inorganic suspended particles. N and P are key nutrients that must be removed from wastewater to avoid eutrophication in aquatic water systems, since they are usually limiting the growth of algae and other photosynthetic microorganisms such as cyanobacteria and hence their presence stimulate their growth. In turn, the proliferation of these microorganisms in the water may result in a shift in the composition of the flora and fauna and the depletion of oxygen, causing death of fish and other species (Ménesguen and Lacroix, 2018).

The conventional activated sludge (CAS) system continues being the most commonly used technology for urban wastewater treatment nowadays (Van Loosdrecht and Brdjanovic, 2014). This system allows the conversion of roughly half of the chemical oxygen demand (COD) to sludge and half to CO_2, however, it have developed significant improvements during the last decades, incorporating biological nutrient removal through nitrification/denitrification and enhanced biological phosphorus removal (EBPR) (Verstraete and Vlaeminck, 2011). The classical nitrification/denitrification process is the most common way to remove N from wastewater, nevertheless, there are more efficient and latest processes which are described below.

1.2. Biological nitrogen removal (BNR)

The removal of nitrogen by biological nitrification/denitrification is a two-step process. Nitrification is the first step, in which ammonium is converted aerobically to nitrite (Eq. 1.1) and then to nitrate (Eq. 1.2) by ammonium oxidizing bacteria (AOB) and nitrite oxidizing bacteria (NOB) respectively.

$$NH_4^+ + 1.5\ O_2 \rightarrow NO_2^- + 2\ H^+ + H_2O \quad (1.1)$$

$$NO_2^- + 0.5\ O_2 \rightarrow NO_3^- \quad (1.2)$$

Therefore, the nitrification process has the following stoichiometry (Eq. 1.3):

$$NH_4^+ + 2\ O_2 \rightarrow NO_3^- + 2\ H^+ + \ H_2O \quad (1.3)$$

The overall nitrification process with cell synthesis based on observed yield is described by means of the Eq. 1.4 (Asano et al., 2007).

$$NH_4^+ + 1.92\ O_2 + 0.08\ CO_2 \rightarrow$$
$$0.98\ NO_3^- + 0.016\ C_5H_7O_2N + \ 1.98\ H^+ + \ 0.95\ H_2O \quad (1.4)$$

In the second step (denitrification), nitrate is converted to nitrogen gas under anoxic conditions by facultative heterotrophic bacteria with organic carbon as electron donor (George Tchobanoglous et al., 2003). Similarly to nitrification, the denitrification involves several reduction steps:

$$NO_3^- \rightarrow NO_2^- \rightarrow NO \rightarrow N_2O \rightarrow \ N_2 \quad (1.5)$$

The stoichiometric equation for denitrification from nitrate considering methanol as carbon source and the synthesis of new bacteria is (Asano et al., 2007):

$$NO_3^- + 1.08\ CH_3OH \ + \ 0.073\ H_2CO_3 \rightarrow$$
$$0.47\ N_2 + 0.056\ C_5H_7O_2N + \ 0.83\ CO_2 + \ OH^- \quad (1.6)$$

Although this conventional treatment guarantees a good effluent quality, is not the most cost-effective solution for common wastewater treatment plants (WWTPs), mainly due to the high energy consumption. In fact, about 60-70% of the total energy consumption of an urban WWTP is allocated to aeration, which in turn is associated with nitrification and organic matter removal (Zessner et al., 2010); and up to 40% of the operational costs are associated to the sludge treatment and disposal (Verstraete and Vlaeminck, 2011). In recent years, more cost effective alternatives have been developed such as nitritation coupled with denitritation or anaerobic ammonium oxidation (Anammox), which lead to minimize carbon and oxygen requirements compared to conventional nitrification/denitrification.

1.3. Innovative nitrogen removal processes

1.3.1. Nitritation/denitritation

Nitritation/denitritation is the conversion of ammonium to nitrite followed by nitrite reduction. The main advantages of N-removal via the nitrite pathway when compared to conventional nitrification and denitrification processes are (Turk and Mavinic, 1989; Winkler and Straka, 2019):

- 25% lower oxygen consumption in the aerobic stage for N oxidation, thus reducing aeration costs.
- Up to 40% lower COD requirement in the anoxic stage, allowing N-removal from wastewater with low COD/N ratio and reducing costs incurred by the need of external carbon sources.
- Faster denitrification rate (1.5 to 2 times), thus requiring smaller anoxic basin.

1.3.2. Partial nitritation/Anammox

In more recent years, a cost-effective N-removal process dedicated to ammonia-rich effluents, called the simultaneous nitritation and Anammox (SNA) process has also been proposed (Sliekers et al., 2002). This process combines partial nitrification to nitrite with the Anammox reaction to achieve autotrophic N-removal, which represents an energy-saving improvement compared to nitritation/denitritation. Anammox bacteria oxidize ammonium directly to nitrogen gas using nitrite (produced by AOB during nitritation) as electron acceptor and without the addition of organic carbon (Winkler and Straka, 2019).

The Anammox process is given by the following reaction (Asano et al., 2007):

$$NH_4^+ + NO_2^- \rightarrow N_2 + 2\,H_2O \quad (1.7)$$

Strous et al. (1998) determined the elemental composition of the biomass and calculated the stoichiometry of the Anammox process showed in Eq. 1.8. In this process a small amount of nitrate is also produced in the anabolism of Anammox bacteria.

$$NH_4^+ + 1.32\,NO_2^- + 0.066\,HCO_3^- + 0.13\,H^+ \rightarrow 1.02\,N_2 + 0.26\,NO_3^- + 0.066\,CH_2O_{0.5}N_{0.15} + 2.03\,H_2O \quad (1.8)$$

The global stoichiometry of the total process combining partial nitrification and Anammox is represented in Eq. 1.9 (Vazquez, 2009).

$$NH_4^+ + 0.85\ O_2 + 1.11\ HCO_3^- \rightarrow 0.44\ N_2 + 0.11\ NO_3^- + 1.11\ CO_2 + 2.56\ H_2O \quad (1.9)$$

1.4. Biological phosphorus removal

1.4.1. Enhanced biological phosphorus removal (EBPR) process

As mentioned above, the demand for achieving low effluent P concentration without the addition of chemical precipitants is increasing across the world, so an alternative to chemical precipitation is needed to remove P. EBPR process is considered one of the most efficient, economical and sustainable ways to remove P from the wastewater (Oehmen et al., 2007). EBPR is based on the ability of polyphosphate accumulating organisms (PAO) to take up phosphorus and accumulate it intracellularly as polyphosphate (Poly-P) when exposed to alternating anaerobic and aerobic conditions (Figure 1.1).

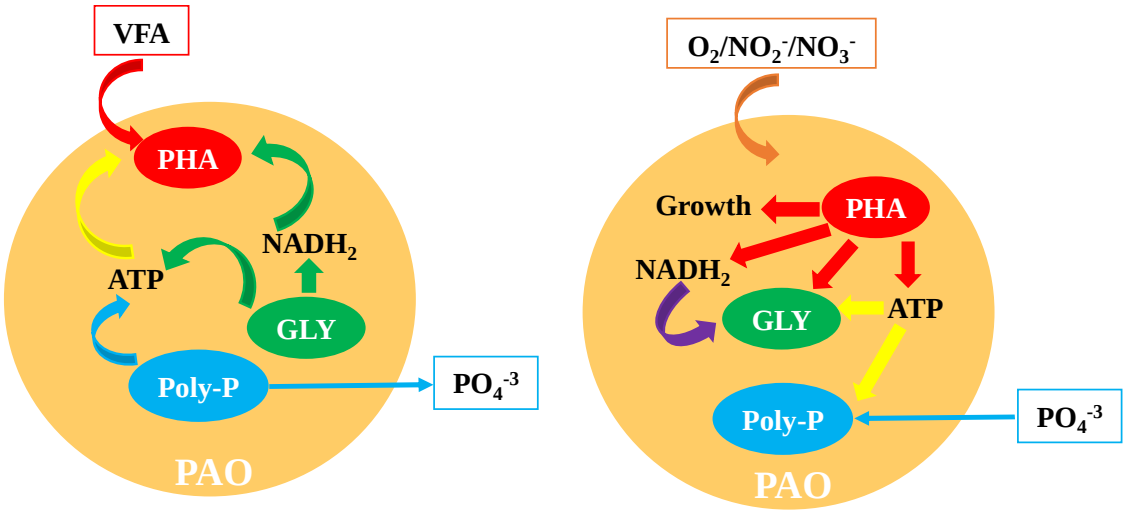

Figure 1.1. Schematic representation of PAO metabolism.

PAO take up volatile fatty acids (VFA) under anaerobic conditions and store them as polyhydroxyalkanoates (PHA), using the energy provided by the hydrolysis of the accumulated Poly-P and the reductive power and energy provided by glycogen consumption. In the aerobic stage, PHA is used as carbon and energy source for growth and for the replenishment of internal glycogen and poly-P pools. The wasting of sludge after the aerobic step ensures net P removal because biomass contains the highest level of poly-P (Mino et al., 1998).

When the electron acceptor is nitrate or nitrite instead of oxygen (i.e. anoxic conditions), a fraction of PAO called denitrifying PAO (DPAO) was demonstrated to uptake effectively P linked to denitrification (Carvalho et al., 2007). Ahn et al. (2001a) stated that the ability to use nitrite or nitrate in denitrification differs according to the type of PAO clade. However, the findings about the denitrification capabilities of PAO are contradictory (more details about this topic are discussed in Chapter 5). Most research on DPAO metabolism has been conducted using nitrate as an electron acceptor (Guisasola et al., 2009), but nitrite can also be used as an electron acceptor (Tayà et al., 2013a). Other studies have reported nitrite inhibition for anoxic P-uptake (Ahn et al., 2001b; Saito et al., 2004), but free nitrous acid (FNA), the protonated species of nitrite, has been identified as the true inhibitor (Zhou et al., 2010).

1.4.2. Putative PAO depending on the carbon source

Among the many parameters governing EBPR viability and stability, the type of carbon source is key. Moreover, it is also one of the main differences between lab-scale and full-scale systems (Qiu et al., 2019; Rubio-Rincón et al., 2019). To date, short-chain VFA are the most commonly used carbon substrates in lab-scale EBPR systems. However, municipal wastewater is not only composed of VFA, but also contains a complex combination of organic compounds (Marques et al., 2017). The main components in wastewater are typically proteins (25-35%), lipids (25-35%) and carbohydrates (15-25%) all of them measured as COD (Nielsen et al., 2010). In fact, processing industries such as abattoir, whey, cheese, casein, fish and certain vegetables processing also typically produce wastewater containing significant amounts of proteins (Ramsay and Pullammanappallil, 2001).

Hesselmann et al. (1999) found that bacteria phylogenetically related to the *Rhodocyclus* group were the dominant bacteria in an anaerobic-aerobic sequencing batch reactor (SBR) using acetate as carbon source. They proposed the name *Candidatus* Accumulibacter phosphatis (*Accumulibacter* hereafter) for this new genus and species. *Accumulibacter* has long been assumed to be the most important of the known PAO. This genus is commonly found in full-scale plants and is relatively easy to enrich in VFA fed lab-scale reactors (Nielsen et al., 2019). Nevertheless, in the recent years, other species have been also reported to be involved in EBPR in full-scale plants, such as *Tetrasphaera*, *Dechloromonas* and *Tessaracoccus* being *Tetrasphaera* the most abundant genus (Nielsen et al., 2019). In fact, Nguyen et al. (2011) reported that *Tetrasphaera* constituted

18-30% of the total biomass present in six well-working EBPR plants with nitrogen removal. (Lanham et al., 2013a) observed significant abundances of *Accumulibacter* (3.5-6%) and *Tetrasphaera* (17-28%) in full-scale EBPR systems in Portugal and Denmark. Finally, Stokholm-Bjerregaard et al. (2017) assessed the abundance and diversity of all proposed PAO and glycogen accumulating organisms (GAO) in 18 Danish EBPR plants over 9 years, obtaining that members of the genera *Tetrasphaera, Accumulibacter* and *Dechloromonas* were the most abundant known PAO. However, Zhang et al. (2017) observed a different microbial distribution in two municipal WWTPs in China. They found that *Nitrosomonas, Thauera* and *Dechloromonas* were the most abundant genera present. Therefore, it is evident that wastewater characteristics, operational parameters, and geographic locations affect the bacterial community (Cydzik-Kwiatkowska and Zielinska, 2016; Wang et al., 2012).

At lab-scale, the carbon source and the operational conditions influence the microbial community developed. Several studies investigated the EBPR performance with carbon sources more complex than VFA and the proliferation of other putative PAO besides *Accumulibacter* took place. However, it should be noted that the fermentation of complex substrates by other microorganisms cannot be avoided and *Accumulibacter* can live on those fermentation products, such as VFA. Hence, it is difficult to obtain a highly enriched sludge in other putative PAO without a minimum *Accumulibacter* presence. In fact, a recent study (Nielsen et al., 2019) highlighted the importance of fermentative organisms such as *Tetrasphaera*. The authors reported that *Tetraspahera* possess a different physiology from the conventional PAO models. *Tetrasphaera* can grow anaerobically by fermenting amino acids and sugars without cycling PHAs. Instead, they are able to store high concentrations of amino acids and possibly fermentation products intracellularly in the anaerobic phase for subsequent use under aerobic conditions. Marques et al. (2017) obtained a good EBPR performance with a *Tetrasphaera*-enriched culture working in an SBR using casein hydrolysate as carbon source. *Tetrasphahera* present some differences in comparison to *Accumulibacter*: i) they cannot uptake VFA under anaerobic conditions, ii) they do not store PHA and iii) the can take up some amino acids and glucose (Nguyen et al., 2011). In a recent work, *Thiothrix caldifontis* proliferated in a lab-scale EBPR system containing 100 mg $S \cdot L^{-1}$ of sulphide in the influent and the authors show that this species could behave like PAO with a mixotrophic metabolism. *Thiothrix caldifontis* was able to store carbon anaerobically as PHA and then, in subsequent aerobic conditions,

PHA was used for growth and for the replenishment of polyphosphate and glycogen (Rubio-Rincón et al., 2017b). Finally, members of the *Comamonadaceae* family proliferated in an EBPR system with short sludge retention time (SRT) when treating protein-rich wastewater (Ge et al., 2015).

1.5. Interactions during simultaneous N and P biological removal

The individual fundamentals of biological N removal or EBPR are nowadays well known. However, achieving simultaneous carbon, N and P removal implies an aerobic zone for nitrification, an anoxic zone for denitrification and an extra anaerobic zone before the anoxic reactor to favour PAO growth, which can be obtained in conventional continuous systems, such as A^2/O (Figure 1.2), UCT or in SBR configurations.

Many studies have reported that the transfer of nitrate or dissolved oxygen (DO) into the anaerobic zone (through the external recycle) results in utilization of some of the influent organic matter by ordinary heterotrophic organisms (OHOs), which reduces the substrates available to PAO and hence the biological P-removal (Comeau et al., 1987; Henze et al., 2008; Kuba et al., 1994). Patel and Nakhla, (2006) stated that concentrations of nitrate below 0.8 mg $N \cdot L^{-1}$ are essential for P-release, except if the substrate used is acetic acid, which supported simultaneous denitrification and P-release.

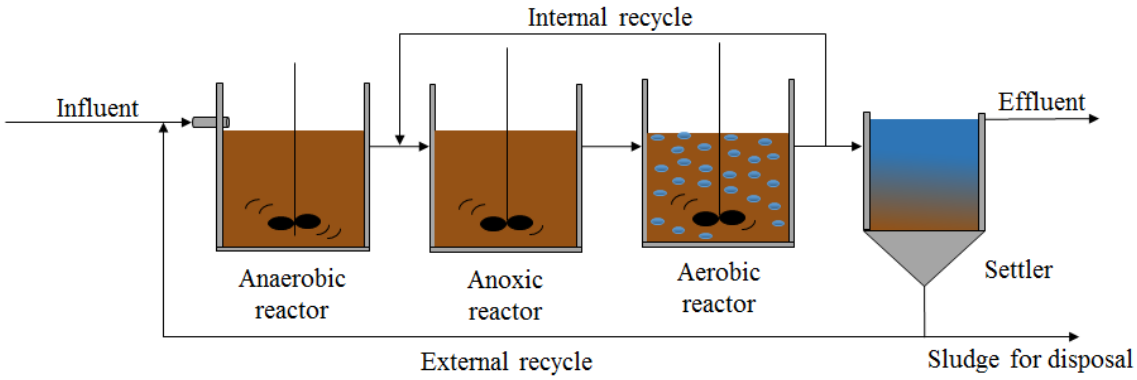

Figure 1.2. Scheme of the A^2/O process.

The problem of competition for the limited organic substrate can be addressed by DPAO, which can combine phosphorus removal and denitrification into one process using the same amount of organic substrate (Yuan and Oleszkiewicz, 2010). In fact, Tayà et al. (2013a) operated an SBR enriched in GAO, under anaerobic/anoxic configuration using nitrite as electron acceptor and fed with propionate. These operational conditions led to a PAO-enriched sludge where GAO were washed out of the system, demonstrating that nitrite is a key selection factor in the PAO/GAO competition. Moreover, this novel

strategy (the nitrite pathway) also allow lower aeration and COD requirements. Guerrero et al. (2011) also showed that the nature of the carbon source (fermentable versus non-fermentable substrate) is the key factor, which determines if PAO activity will be lost when nitrate is present.

1.6. New configuration for COD and nutrients removal: Energy self-sufficient WWTP

Nowadays, WWTPs are energy-demanding facilities, since all major procedures associated with them and sludge disposal technologies require energy, mostly electricity. The energy demand of a WWTP depends on the plant location, plant size, type of treatment process and aeration system, effluent requirements, age of plant and knowledge of the operators (Gu et al., 2017). Hence, as previously mentioned, most of the WWTPs are based on the CAS process, where aeration uses about 50-60% of the total electricity consumption while sludge treatment consumes 15-25% of the energy. Moreover, secondary sedimentation, including recirculation pumps, consumes 15% (Sancho et al., 2019). Conventional BNR processes result in the oxidation of a large fraction of organic carbon contained in wastewater, because long SRTs are needed for the growth of nitrifiers and organic matter is necessary for denitrification (Ge et al., 2017). The energy consumption associated to aeration increased from 0.305 $kWh \cdot m^{-3}$ to 0.405 $kWh \cdot m^{-3}$ in plants where the nitrification was implemented (Liu et al., 2018). However, the current goals of WWTPs are energy and nutrient recovery besides to accomplish the discharge limits. Namely, the transformation of conventional WWTPs into energy self-sufficient facilities is the main challenge to face by the wastewater treatment (Batstone et al., 2015). This cannot be achieved if the CAS process continues to be employed. Therefore, the research for alternative technologies towards the energy neutral or even positive operation is an urgent necessity.

The Adsorption/Bio-oxidation (A/B) process is a feasible approach for making an energy self-sufficient biological process. In fact, Liu et al. (2018) stated that the A/B process allows a larger energy recovery potential than the input energy consumption, since the process is based on maximize the energy recovery via capturing of COD from wastewater (A-stage), while minimizing energy consumption (B-stage to remove nitrogen). The general configuration of A/B process is shown in Figure 1.3.

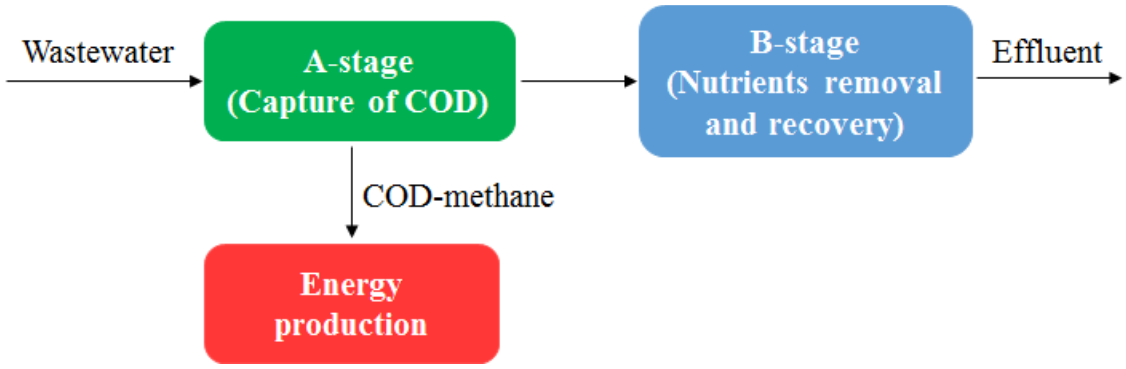

Figure 1.3. General scheme of an A/B process (Wan et al., 2016).

In the 1970s, a high-rate activated sludge (HRAS) process was reported by Böhnke (1977) that maximized energy recovery in the form of biogas, but, the interest in this process ceased because of the need for organic carbon (Van Loosdrecht and Brdjanovic, 2014). Originally, A/B process was not developed for nitrogen and phosphorus removal, since the biological removal of nitrogen and phosphorus require the alternate of anaerobic, anoxic and aerobic conditions and the supply of sufficient carbon source. Thus, to accomplish the stringent effluent limits, many novel technologies and processes have been developed, such as the creation of anaerobic and anoxic zones in the B-stage, which allow this stage to be operated in A/O, AAO and UCT mode. However, to solve the problem of the insufficient carbon reaching B-stage, several WWTP in Germany and China had to cut the COD removal in the A-stage (Wenyi et al., 2006).

Therefore, to becoming feasible the sustainable WWTPs, the use of anammox for nitrogen removal from sewage treatment has been proposed by Kartal et al. (2010). In this new WWTP configuration, the effluent from the A-stage would be treated using the partial nitritation-anammox process. Autotrophic BNR can be implemented as a one-stage system, where partial nitritation and anammox processes take place in the same reactor, or as a two-stage system, when these processes are separated in two different reactors. Two-stage systems present higher capital costs than one-stage systems but make possible a more stable performance and control. In addition, one-stage systems showed the failure of nitritation in the long-term operation at low temperature and low-strength wastewaters. Whereas, stable partial nitritation at 12.5 ºC and 10 ºC with a granular sludge reactor was reported by Isanta et al. (2015) and (Reino et al., 2016) respectively and a stable long-term operation of an anammox reactor at mainstream conditions was reported by (Reino et al., 2018). These studies demonstrate the feasibility of application of autotrophic BNR to mainstream conditions, so a B-stage with this two-stage configuration

seems to be a good option for the energy-neutral or even energy-positive WWTP (Figure 1.4).

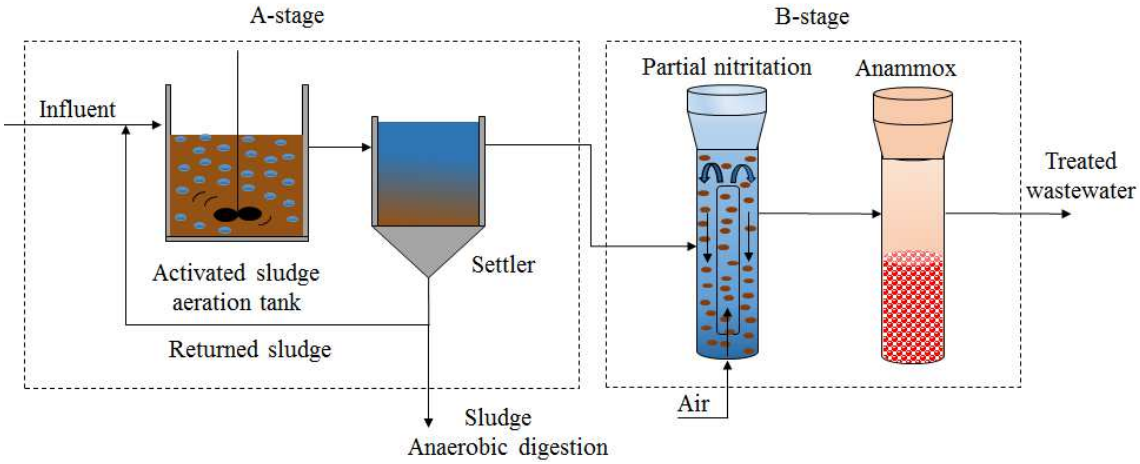

Figure 1.4. Scheme of the A/B process with partial nitritation-anammox process in two-stages.

Normally the biological phosphorus removal in the A/B process takes place in the B-stage (Xu et al., 2017). However, the B-stage configuration showed in Figure 1.4 does not allow phosphorus removal in the B-stage, causing that P-removal has to be included in the A-stage. Chan et al. (2017) studied the potential inclusion of EBPR in the A-stage phase working with three different A/O SBR enriched in *Accumulibacter* at low SRT. The authors reported that EBPR can be sustained with a minimal SRT of 3.6 d and lower values, SRT = 3 d, led to the PAO washout. Consequently, to achieve successful EBPR performance in the A-stage phase, it is necessary work at SRT of 4 d instead of the short SRTs used when only COD removal occurs. Wett et al. (2013) reported a successfully integration of HRAS and anammox process in the Strass WWTP, but it should be pointed out that this success is due to the return of anammox bacteria (harvested from the sidestream deammonification unit) to the B-stage. Nevertheless, biological phosphorus removal is not considered in this case, so further research is needed to achieve a sustainable WWTP including EBPR in the A-stage.

1.7. Research motivations and thesis overview

1.7.1. Research motivations

Phosphate is a key nutrient that has to be removed from wastewater because is one of the main sources of eutrophication in water bodies. Nowadays, EBPR is the most economical, efficient and sustainable process to remove P from wastewater. At lab-scale, VFA are the

most common carbon source used for the operation of EBPR systems. This has led to a very wide knowledge of the PAO that are favoured with this carbon source, i.e. *Accumulibacter*, since its metabolism has been thoroughly studied under different operational conditions. However, the recent developments on advanced microbiological techniques has shown the presence of other PAO than *Accumulibacter* since real wastewater is a complex matrix composed of proteins, carbohydrates, lipids and other complex substances. These novel PAO (such as *Tetrasphaera*, *Thiothrix* and *Comamonadaceae*) can coexist with *Accumulibacter* in real environments depending on the complexity of the influent carbon source. *Accumulibacter* can only consume a limited range of readily biodegradable carbon sources, but these novel PAO can use more complex carbon sources and can also release fermentation products than can be consumed by *Accumulibacter*.

Thus, the first research motivation of this thesis has been gaining understanding on this novel PAO and its coexistence with *Accumulibacter*. To this aim, a pilot plant has been operated to achieve stable carbon, nitrogen and phosphorus removal performance using a complex carbon source. Then, the microbial community developed has been studied in order to gain knowledge of the behaviour of these novel PAO and to unravel their potential role in full-scale systems.

On the other hand, the increasing demand for freshwater and energy to meet the needs of growing population and economy, changing lifestyles and evolving consumption patterns is forcing to transform the urban WWTPs from net power consumers into energy neutral or even energy positive facilities. The A/B process is a potential configuration to meet energy self-sufficient WWTPs: organic matter is removed in the first step (A-stage) and derived to biogas production whereas autrotrophic nitrogen removal is implemented in a second step (B-stage). However, phosphorus removal is not included in the initial design of the A/B process. Therefore, the second research motivation of this thesis has been to compare two high-rate systems that can be used to build an A-stage with EBPR integration.

1.7.2. Thesis overview

This document is divided into nine chapters. Chapter 1 presents a brief introduction of the topic, focused on the putative PAO other than *Accumulibacter* that can proliferate in an EBPR system when complex carbon sources are used. Moreover, the possible

integration of EBPR into the A-stage of the A/B process is investigated. Chapter 1 ends with the motivations and this thesis overview. Chapter 2 presents the main objectives of the thesis. Chapter 3 describes the chemical and microbial analyses performed as well as a general description of the different systems used in this work. Chapters 4 to 7 contain the results obtained during the development of the thesis. Chapters 4 and 5 comprise the results obtained during the long-term operation of the A^2/O pilot plant fed with glutamate as complex carbon source. Chapter 4 describes the development of the mixed microbial culture with high EBPR activity, mostly enriched in putative PAO bacteria other than *Accumulibacter*. Chapter 5 is focused on the denitrification capabilities of this microbial community, which is more similar to that observed in full-scale WWTPs. Chapter 6 deals with a *Tetrasphaera*-enriched sludge performing EBPR and its capability to use different amino acids. Chapter 7 compares the performance of two reactor configurations acting as an A-stage system fed with real urban wastewater. Moreover, this chapter, describes the possible integration of EBPR process in the A-stage phase working with a continuous high-rate system. Chapter 8 outlines main conclusions extracted from this thesis and, finally, Chapter 9 presents all references used.

Chapter 2

OBJECTIVES

The two main objectives of this thesis are to improve the knowledge about EBPR process by studying the microbial population developed when complex substrates are used as carbon sources and to investigate the possible integration of EBPR in the A-stage of an A/B process.

Following these objectives, the specific goals of this thesis are:

- To demonstrate the long-term stability of the EBPR process in an A^2/O pilot plant fed with glutamate as sole carbon and nitrogen sources.

- To study the development of the putative new PAOs under these conditions.

- To investigate the denitrification capabilities of the bio-P sludge developed using glutamate as carbon source with a microbial community similar to that obtained in conventional WWTPs.

- To investigate the degradation of different complex carbon sources (i.e. arginine, lysine, cysteine, proline and tyrosine) by a *Tetrasphaera*-enriched sludge and to study the possible additive, synergic or antagonistic effect of a mixture of these different complex substances.

- To correlate the abilities of a bio-P sludge for degrading different complex carbon sources with the bacterial community present.

- To compare the performance of a continuous and a batch configuration operating under high-rate conditions in order to a better understand of this process before to study the possible integration of EBPR in this first step.

Chapter 3

GENERAL MATERIALS AND METHODS

3.1. Description of the reactors and experimental set-up

3.1.1. A²/O Pilot plant

The anaerobic/anoxic/oxic (A^2/O) pilot plant consisted of three continuous stirred tank reactors with a total volume of 146 L and a 50 L settler (Figure 3.1). The first reactor (R1, 28L) was anaerobic, the second reactor (R2, 28L) was anoxic and the third reactor (R3, 90 L) worked under aerated conditions.

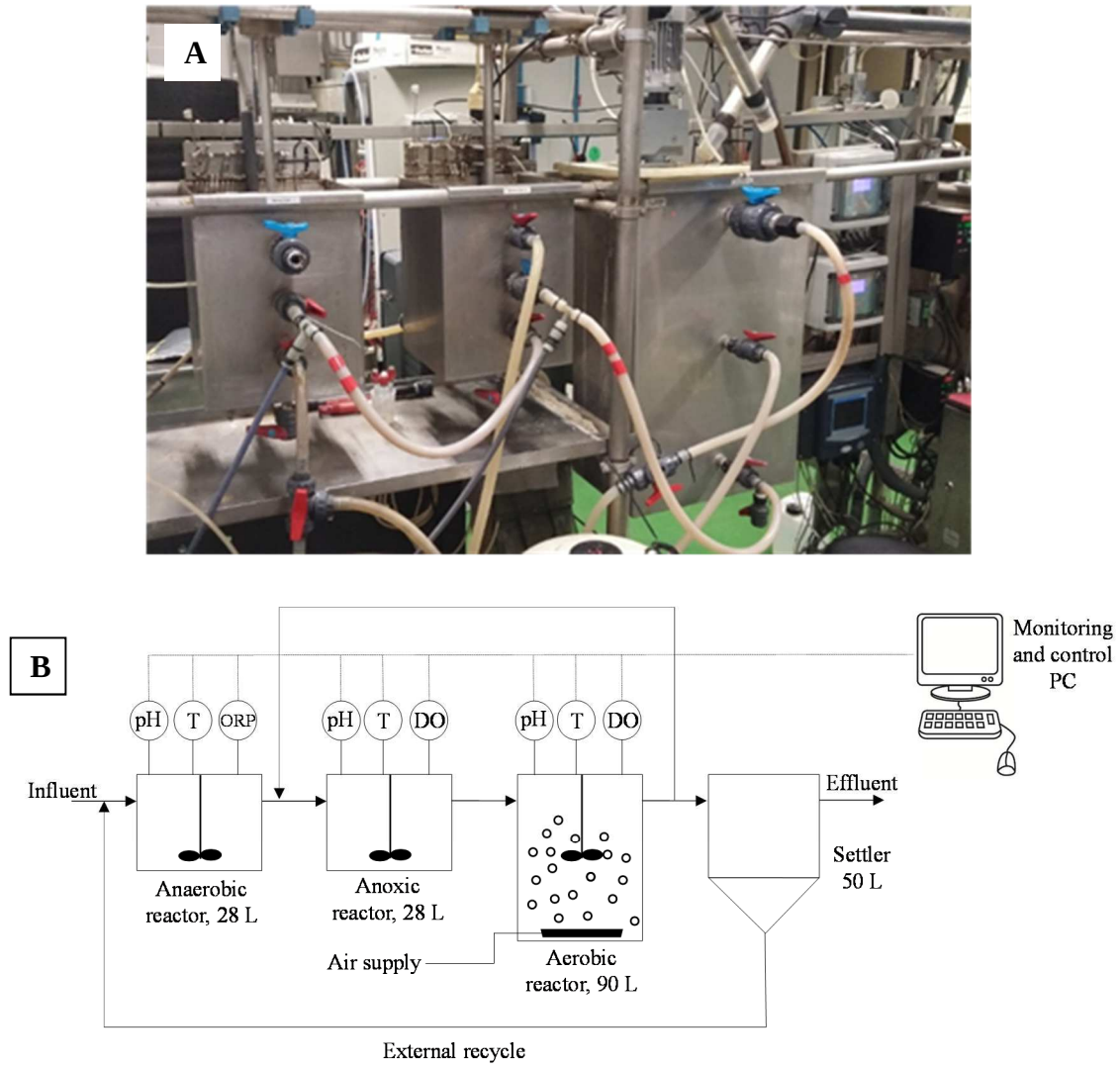

Figure 3.1. A^2/O pilot plant (A) and scheme and instrumentation used for monitoring (B).

The SRT was maintained between 10-15 days with daily sludge wastage from the aerobic reactor. The influent flow rate was 240 $L \cdot d^{-1}$ resulting in a HRT of 14.6 h. The pH was controlled at 7.5 using an on-off controller with sodium carbonate (1M) dosage in the aerobic reactor. Dissolved oxygen (DO) (HACH CRI6050) was also controlled in the aerobic chamber at 1 ± 0.1 $mg \cdot L^{-1}$ with a proportional-integral controller manipulating

the aeration flow-rate with a mass flowmeter F-201CV (Bronckhorst, The Netherlands). On-line data were acquired with a data acquisition card (Advantech PCI-1711) connected to a PC, with the Addcontrol software for process monitoring and control developed by the research group using NI LabWindows CVI 2017.

3.1.2. Lab-scale SBR

An anaerobic/oxic (A/O) SBR with a working volume of 10 L and a volume exchange ratio of 50% was used (Figure 3.2). The hydraulic residence time (HRT) was fixed at 12 h. It was inoculated with sludge from an EBPR-designed WWTP (Igualada, Barcelona). The reactor was monitored for oxygen, pH and temperature and controlled with a PLC (Siemens S7-226). The SBR was operated at a controlled temperature of 25 ± 1°C. HCl (1M) and NaOH (1M) were added automatically to control the pH at 7.50 ± 0.05. Nitrogen was sparged during the anaerobic phase to maintain strict anaerobic conditions. DO was controlled between 2.5 to 3.5 $mg \cdot L^{-1}$ in the aerobic phase by manipulating an on/off aeration valve. The reactor was stirred at 120 rpm during the reaction phases. Daily sludge wastage was performed to maintain a SRT between 10-15 days.

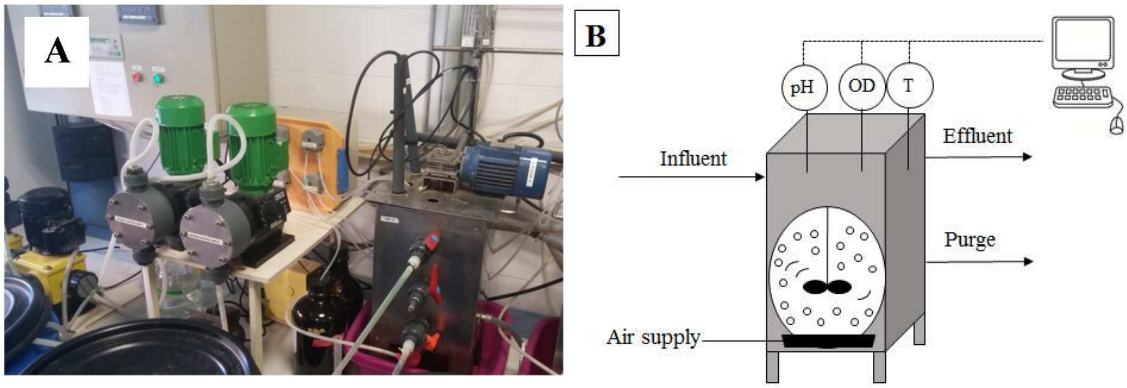

Figure 3.2. Lab-scale SBR (A) and schematic diagram of the set-up (B).

3.1.3 High-rate activated sludge (HRAS) reactor

The HRAS system consisted of a continuously stirred, aerobic reactor (19 L) and a settler (27 L) (Figure 3.3). It was operated at room temperature (18-22ºC) with an average influent flowrate of 165 $L \cdot d^{-1}$ (HRT = 2.8 h). Daily sludge wastage was performed to maintain a SRT between 1-2 days. The external recycle from the bottom of the settler to the reactor was 200 $L \cdot d^{-1}$, which results in an external recirculation ratio (R_{ext}) of 1.2. The HRAS system was inoculated with sludge collected from a municipal WWTP (Rubí, Barcelona). The HRAS reactor was managed with an on-line system based on an

Advantech PCI-1711 I/O card and an industrial PC running the Addcontrol software. DO was measured with a HACH-CRI6050 DO probe and controlled around 1 $mg \cdot L^{-1}$ by manipulating an on/off aeration valve. pH and temperature were monitored with a pH probe (HACH CRI5335) and a thermoresistance (Axiomatic Pt1000), respectively.

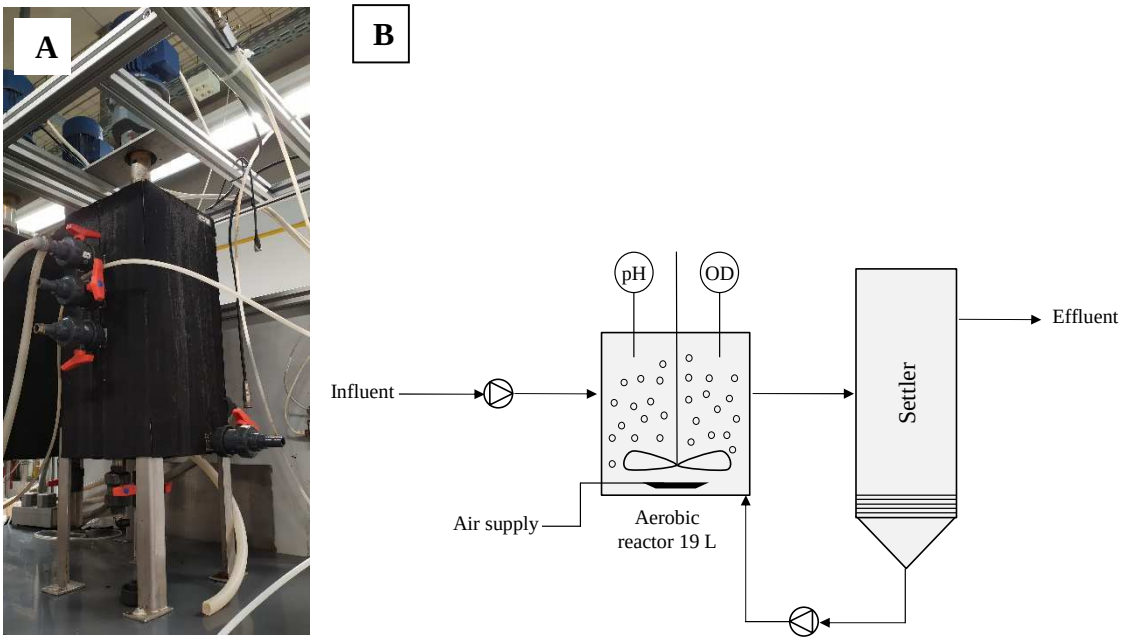

Figure 3.3. HRAS (A) and schematic diagram of the set-up (B).

3.1.4. Lab-scale High Rate Sequencing Batch Reactor (HRSBR)

The HRSBR used was a stirred and aerobic reactor with a working volume of 3.5 L and a volume exchange of 2.5 L (Fig. 3.4). It was inoculated with sludge collected from a WWTP (Rubí, Barcelona) and the HRT was fixed at 2.5 h. Daily sludge wastage was performed to maintain a SRT between 1 and 2 days. The reactor was monitored for DO, pH and temperature and controlled with a programmable logic controller. The temperature was controlled at 25 ± 1°C. The pH was not controlled, and its value was in the range 7.5-8.6 during the operation. DO was controlled during the aerobic phases by manipulating an on/off aeration valve. The DO set point was 5 $mg \cdot L^{-1}$ during the start-up period and 3 $mg \cdot L^{-1}$ afterwards.

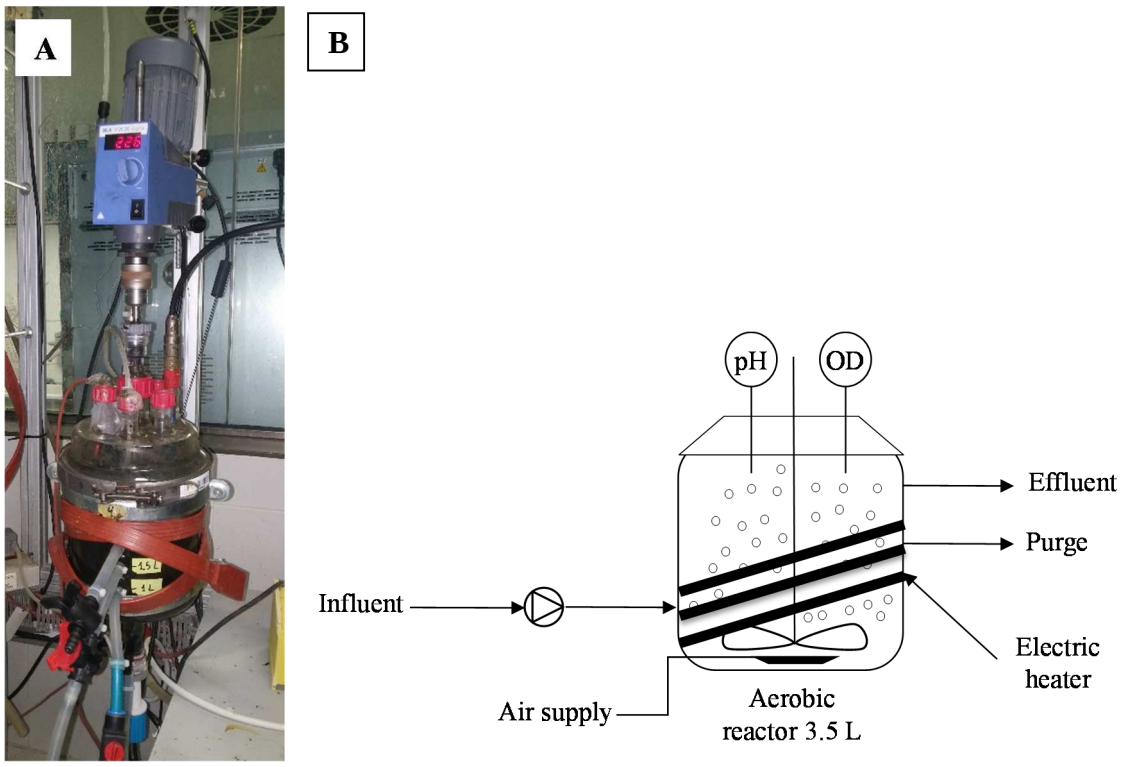

Figure 3.4. HRSBR (A) and schematic diagram of the set-up (B).

3.2. Chemical analysis

Samples were filtered with 0.22 µm Hydrophilic PES filters (Millipore).

Ortophosphate phosphorus (PO_4^{-3}-P) concentration was measured by a phosphate analyser (PHOSPHAXsc, Hach Lange) which is based on the vanadomolybdate yellow method.

Ammonia nitrogen concentration was analysed off-line by means of an ammonium analyser (AMTAXsc, Hach Lange, Germany), based on the potentiometric determination of ammonia. Analyses of nitrite and nitrate were performed with ionic chromatography using an ICS-2000 Integrated Reagent-Free IC system (DIONEX Corporation, USA).

Chemical oxygen demand (COD) was analysed by using colorimetric Hach Lange kits (LCK314 and LCK714) and the DR2800 Hach Lange spectrophotometer. Total COD was directly measured by using the kits, while soluble COD was analysed after filtering by 0.22 µm. Samples were analysed in triplicate.

Acetic, propionic and butyric acids were measured using an Agilent Technologies 7820 A gas chromatograph equipped with a DB-FFAP column (30 m x 0.25 mm x 0.25 µm) and a flame ionization detector (FID). A volume of 0.2 mL of hexanoic acid solution as

internal standard was added to 0.8 mL of filtered sample. 1 µL sample was injected at 275 ºC using helium as carrier gas with a split ratio of 10:1 at 2.9 $mL \cdot min^{-1}$. The temperature of the column was initially set at 85 ºC during one minute, followed by a temperature ramp of 3 $ºC \cdot min^{-1}$ to reach 130 ºC. Then, a second ramp of 35 $ºC \cdot min^{-1}$ was maintained until 220 ºC was reached. The run time was around 18 min per sample and the FID temperature was 275 ºC.

Total suspended solids (TSS) and volatile suspended solids (VSS) were analysed according to Standard Methods (APHA, 2005). Samples were analysed in triplicate. First, samples were filtered through previously weighted (W_1) standard glass microfiber filters of 0.7 µm (GF/F grade, Whatman, USA) and dried at 105 ºC until constant weight (W_2) (c.a. 2.5 hours). The relation between the difference between W_1 and W_2 and the sample volume was the concentration of TSS. Then, the sample was ignited at 550 ºC for about 45 min and weighted (W3). The difference between W1 and W3 per volume of the sample filtrated represented the concentration of VSS. Total solids (TS) and volatile solids (VS) concentrations were calculated following the same procedure without the filtering step. In this case, samples were weighted using metallic dishes.

SVI was analysed in duplicate according to Standard Methods (APHA, 2005). An Imhoff cone was filled with 1 L of sludge sample and the volume occupied by the suspension after 30 min was measured to determine V30. SVI was calculated as V30 divided by TSS.

3.3. Microbial analysis

Two molecular biology techniques were used to identify and quantify the microorganisms present in sludge samples: fluorescence *in situ* hybridization (FISH) and 16S-rRNA amplicon sequencing through Illumina platform.

3.3.1. Fluorescence in situ hybridization (FISH)

Sample fixation

For Gram-negative microorganisms, biomass was fixed by adding three volumes of 4% (v/v) paraformaldehyde solution to one volume of biomass suspension and held at 4 ºC for 1 to 3 hours. For Gram-positive microorganisms, biomass was fixed by adding equal volumes of sludge and 96% ethanol and held at 4 ºC for 5 hours.

Afterwards, biomass suspension was washed twice with 0.01M Phosphate Buffered Saline (PBS) solution (1:30 dilution of a solution 0.3M PBS which was prepared with

77.4 g of $Na_2HPO_4 \cdot 12H_2O$, 13.1 g of $NaH_2PO_4 \cdot 2H_2O$ and 226.2 g of NaCl) and it was re-suspended in one volume of 0.01M PBS per one volume of ice-cold ethanol 98%. Fixed biomass could be spotted onto glass slides to start the hybridization protocol or stored at -20 ºC for several months.

Hybridization

The hybridization protocol was adapted from Hugenholtz et al. (2002) and Manz et al. (1992). Suspended fixed biomass was spotted onto a glass slide and dehydrated in ethanol series of 50, 80 and 98% (v/v) (3 min each). After dehydration with ethanol and when glass slide was dry, 10 µL of hybridization buffer were added plus 1 µL of (each) probe working solution (probe concentration of 50 $ng \cdot \mu L^{-1}$). Solution was mixed without scratching the slide and cell layer. Hybridization buffer contained: 360 µL of 5M NaCL (autoclaved), 40 µL of 1M Tris/HCl (autoclaved), 2 µL of 10% SDS, 898 µL of Milli-Q-grade water and the corresponding amount of formamide for each molecular probe. The slide was placed in a 50 mL falcon tube containing a moistened tissue and the tube was closed and put in the hybridization oven at 46 ºC for 2 hours. After hybridization, the slides were quickly transferred to the washing buffer tube by immersing the whole slide in the pre-warmed washing buffer at 48 ºC for 15 min. Washing buffer contained 80 µL of NaCl 5M (autoclaved), 500 µL EDTA 0.5M, 1 mL Tris/HCl 1M (autoclaved), 43.8 mL Milli-Q-water (autoclaved) and 50 µL 10% SDS. After washing, the slide was rinsed with cold Milli-Q-grade water. Afterwards, all droplets of water were removed from the slide by directly applying compressed air to the slide. To finish, a mounting medium (specifically *Fluoprep*) was applied for the subsequent microscope observation.

Hybridizations were carried out using at the same time the general bacteria probe and the probes for the specific microorganisms to be identified. The general bacteria probe was an equal mixture of probes EUB338I, EUB338II and EUB338III for all Bacteria. All the probes used in this thesis are summarized in Table 3.1.

Table 3.1. FISH probes used in this thesis.

Probe	Target	Reference
Cy5-labelled EUBMIX	Most bacteria	(Daims et al., 1999)
Cy3-labelled PAOMIX, comprising PAO462, PAO651 and PAO846	*Candidatus* Accumulibacter phosphatis,	(Crocetti et al., 2000)
Cy3-labelled GAOMIX, comprising GAOQ431 and GAOQ989 probes	*Candidatus* Competibacter phosphatis	(Crocetti R. et al., 2002)
Cy3-labelled DFIMIX, comprising TFO_DF218 and TFO_DF618 probes	Cluster I of *Defluviicoccus vanus* GAO	(Wong et al., 2004)
Cy3-labelled DFIIMIX, comprising DF988 and DF1020 probes plus helper probes H966 and H1038	Cluster II of *Defluviicoccus vanus* GAO	(Nguyen et al., 2011)
Cy3-labelled Tet1-266	Clade I of *Tetrasphaera*	(Nguyen et al., 2011)
Cy3-labelled Tet2-892	Clade 2A of *Tetrasphaera*	(Nguyen et al., 2011)
Cy3-labelled Tet2-174	Clade 2B of *Tetrasphaera*	(Nguyen et al., 2011)
Cy3-labelled Tet3-654	Clade 3 of *Tetrasphaera*	(Nguyen et al., 2011)

Microscope observation and quantification

A Leica TCS-SP5 confocal laser scanning microscope (Leica Microsystem Heidelberg GmbH; Mannheim, Germany) using a Plan-Apochromatic 63x objective (NA 1.4 oil) was used for biomass quantification. The quantification was performed following an automated image analysis procedure described in Jubany et al. (2009), where at least 30 microscopic fields were analysed and a single-z position was selected on the highest intensity for each sample.

3.3.2. Next-generation sequencing analysis

16S-rRNA amplicon sequencing analysis was used for studying the diversity and relative abundance of different microorganisms in the sludge of the reactors.

First, DNA was extracted from biomass samples by applying the manufacturer protocol of MoBio PowerSoil™ DNA extraction kit (MoBio Laboratories, USA). Once the extraction was performed, NanoDrop 1000 Spectrophotometer (Thermo Fisher Scientific, USA) was used to measure the quantity and quality of the extracted DNA. A 260/280 nm ratio of 1.8 was used as quality cut-off and a minimum of 25 $ng \cdot \mu L^{-1}$ of extracted DNA was guaranteed to perform sequencing.

AllGenetics & Biology SL (A Coruña, Spain) (Chapter 5) and Servei Central de Suport a la Investigació Experimental – SCSIE (UV, Valencia, Spain) (Chapter 6), performed paired-end sequencing of the extracted DNA on an Illumina MiSeq platform using the bacterial primer pair 515F-806R. The data analysis pipeline (denoising and chimera), the microbial diversity analysis, the OUT selection clusters sequences and the taxonomic identification were performed by the external services.

Chapter 4

GLUTAMATE AS SOLE CARBON SOURCE FOR ENHANCED BIOLOGICAL PHOSPHORUS REMOVAL

A modified version of this chapter has been published as:

Natalia Rey-Martínez, Marina Badia-Fabregat, Albert Guisasola, Juan Antonio Baeza, 2019. Glutamate as sole carbon source for enhanced biological phosphorus removal. STOTEN 657, 1398-1408. doi: 10.1016/j.scitotenv.2018.12

ABSTRACT

Enhanced Biological Phosphorus Removal (EBPR) is based on the enrichment of sludge in polyphosphate accumulating organisms (PAO). *Candidatus* Accumulibacter is the bacterial community member most commonly identified as PAO in EBPR systems when volatile fatty acids (VFA) are the carbon source. However, it is necessary to understand the role of non-*Accumulibacter* PAO in the case of wastewater with low VFA content. This work shows the first successful long-term operation of an EBPR system with glutamate as sole carbon and nitrogen source, resulting in the enrichment of sludge in the genus *Thiothrix* (37%), the family *Comamonadaceae* (15.6%) and *Accumulibacter* (7.7%). The enrichment was performed in an anaerobic/anoxic/oxic (A^2/O) continuous pilot plant, obtaining stable biological N and P removal. This microbial community performed anaerobic P-release with only 18-29% of the observed polyhydroxyalkanoate (PHA) storage in *Accumulibacter*-enriched sludge and with slight glycogen storage instead of consumption, indicating the involvement of other carbon storage routes not related to PHA and glycogen. *Thiothrix* could be clearly involved in P-removal because it is able of accumulating Poly-P, probably without PHA synthesis, but with glutamate involvement. On the other hand, *Comamonadaceae* could participate in degradation of glutamate and denitrification, but its involvement in P-uptake cannot be reliably concluded.

4.1. Introduction

Candidatus Accumulibacter phosphatis (referred to as *Accumulibacter* hereafter) are the species of PAO most frequently found in many lab-scale studies (Crocetti et al., 2000) when using VFA-rich synthetic wastewaters or other easily fermentable carbon sources such as glucose (Fukushima et al., 2007), ethanol (Puig et al., 2008) or glycerol (Guerrero et al., 2012), among others. However, the concentration of these easily fermentable carbon sources in real wastewater is quite low. In fact, the organic substances found in wastewater are mostly proteins (50%), carbohydrates (40%) and fats and oils (10%) (Shon et al., 2007). Since the proportion of protein in real wastewater is very high, the amino acids could be potential carbon sources for EBPR (Zengin et al., 2011). Indeed, several studies have tested a wide range of amino acids as carbon source. Chua et al. (2006) and Zengin et al. (2011) worked with aspartate and glutamate, Nguyen et al. (2011) used casamino and glutamic acids and Marques et al. (2017) operated a SBR with casein hydrolysate and also performed batch tests with glutamate, aspartate and glycine.

Besides these reasons, the recent microbiological advances and the study of EBPR with different real wastewaters have shown that PAO other than *Accumulibacter* can proliferate as well. These other putative PAO belong to the genera *Tetrasphaera* (Fukushima et al., 2007; Nguyen et al., 2011), *Halomonas* (Nguyen et al., 2012), *Thiothrix* (Rubio-Rincón et al., 2017b) and to the family *Comamonadaceae* (Ge et al., 2015). For instance, Kong et al. (2005) found that Gram-positive *Tetrasphaera*-related organisms can be involved in P-removal and are abundant in many full-scale EBPR plants. Another study, considering 28 Danish municipal WWTPs, revealed that the genus *Tetrasphaera* was very abundant in all of them (Mielczarek et al., 2013). Despite their ability to accumulate phosphorus, *Tetrasphaera* present important differences in comparison to *Accumulibacter*: i) they cannot uptake VFA under anaerobic conditions, ii) they do not store PHA and iii) they can take up some amino acids and glucose (Nguyen et al., 2011).

Regarding *Comamonadaceae*, Khan et al. (2002) found that they are primary denitrifiers able to degrade 3-(hydroxybutyrate-co-3-hydroxyvalerate). Willems (2014) reported that many members of the *Comamonadaceae* family are capable of accumulating PHA in the cell based on phylogenetic analysis of the polyhydroxyalkanoate synthase gene. In addition, these bacteria have been identified in EBPR systems with short sludge retention time (SRT) when treating protein-rich (abattoir) wastewater (Ge et al., 2015).

Finally, regarding *Thiothrix*,Vaiopoulou et al. (2007) reported the growth of filamentous bacteria *Eikelboom* type 021N and *Thiothrix* for the first time in a multistage pilot-scale WWTP designed for EBPR occurrence, which caused activated sludge bulking. In a recent work, *Thiothrix caldifontis* proliferated in a lab-scale EBPR system containing 100 mg $S \cdot L^{-1}$ of sulphide in the influent and the authors showed that this species could behave like PAO with a mixotrophic metabolism. *Thiothrix caldifontis* was able to store carbon anaerobically as PHA and then, in subsequent aerobic conditions, PHA was used for growth and for the replenishment of polyphosphate and glycogen (Rubio-Rincón et al., 2017b). Bacteria belonging to the genus *Thiothrix* have been reported to: i) grow in media with low organic carbon concentration and reduced S-compounds (Rubio-Rincón et al., 2017b), ii) deteriorate settling properties of activated sludge and iii) store polyphosphate (Wanner et al., 1987).

Therefore, there is a range of genera, other than *Accumulibacter*, that can be related to full-scale EBPR WWTPs but their role and significance are still to be defined since most of the fundamental research conducted so far has led to bioreactors with *Accumulibacter*-enriched microbial communities. Hence, our work aims at obtaining a mixed microbial culture with high EBPR activity, mostly enriched in putative PAO bacteria other than *Accumulibacter*, by using a different carbon source. This is why we have used the amino acid glutamate to i) explore the possibility of using amino acids as EBPR carbon source and ii) obtain a consortium with high EBPR activity to gain more understanding of the behaviour of these “novel” PAO and to unravel their potential role in full-scale systems.

4.2. Materials and methods

4.2.1. Lab-scale Sequencing Batch Reactor (SBR)

The first experimental system used was an anaerobic/oxic (A/O) SBR with a working volume of 10 L and a volume exchange ratio of 50%. The detailed diagram of the reactor and set-up details are described in Section 3.1.2 of Chapter 3. The SBR was operated at a controlled temperature of 25 ± 1°C. The pH was controlled at 7.50 ± 0.05 by adding HCl (1M) and NaOH (1M). Nitrogen was sparged during the anaerobic phase to maintain strict anaerobic conditions. Dissolved oxygen (DO) was controlled between 2.5 to 3.5 $mg \cdot L^{-1}$ in the aerobic phase by manipulating an on/off aeration valve.

The reactor was fed with a mixture of aspartate and glutamate as carbon source for 68 days. The proportion of aspartate and glutamate varied throughout the operation, as well

as cycle and phase duration, but a concentration of 44-113 mg $COD \cdot L^{-1}$ was maintained in the influent. The phosphate concentration at the inlet was 10 mg $P \cdot L^{-1}$. The carbon source was added separately at minute 15 after achieving complete anaerobic conditions in the reactor. Allylthiourea was used to prevent nitrification activity. The SBR operation was divided into four operational periods according to the carbon source load (Table 4.1 and 4.2). Operating conditions were modified according to SBR performance and changes in the microbial community. Daily sludge wastage was performed to maintain a SRT between 10-15 days (Table 4.1).

4.2.2. Continuous pilot plant

The anaerobic/anoxic/oxic (A^2/O) pilot plant consisted of three continuous stirred tank reactors with a total volume of 146 L and a 50 L settler. The scheme of the reactor and the instrumentation used for monitoring it are detailed in section 3.1.1 of Chapter 3. The SRT was maintained around 10 days with daily sludge wastage from the aerobic reactor. The pH was controlled at 7.5 using an on-off controller with sodium carbonate (1M) dosage in the aerobic reactor. DO was also controlled in the aerobic chamber at 1.0 ± 0.1 $mg \cdot L^{-1}$.

This pilot plant operated at room temperature for 480 days treating a synthetic wastewater containing 10 mg PO_4^{-3}-$P \cdot L^{-1}$, 50 mg NH_4^{+}-$N \cdot L^{-1}$ and 400 mg $COD \cdot L^{-1}$ with glutamate as a sole carbon source. The glutamate used was food grade (AJINOMOTO) except in period II, when another supplier provided glutamate with different physical characteristics, which caused the system to fail. This new glutamate had a less compact texture, so some additive may have been used to keep it fresh and prevent moisture.

On day 250 of the operation, ammonium was removed from the synthetic wastewater to reduce the nitrogen concentration in the influent, and glutamate was used as both carbon and nitrogen source. The synthetic influent was prepared from a concentrated feed (Table 4.3) that was diluted with tap water resulting in a wastewater with the above concentrations.

Table 4.1. Operational conditions for the A/O SBR.

Period	Day (d)	SRT (d)	VSS ($g \cdot L^{-1}$)	Cycle length (h)	Anaerobic phase length (h)	Aerobic phase length (h)	Settling phase length (h)	Carbon source (G: glutamate and A: aspartate)
I	0-6	13 ± 3	0.99 ± 0.13	8	4	3	1	50% G + 50% A, 44 mg $COD \cdot L^{-1}$
	6-11	13 ± 3	0.99 ± 0.13	8	4	3	1	50% G + 50% A, 71 mg $COD \cdot L^{-1}$
II	11-15	15 ± 4	0.65 ± 0.11	6	2.5	2.5	1	50% G + 50% A, 71 mg $COD \cdot L^{-1}$
	15-32	15 ± 4	0.65 ± 0.11	6	2	3	1	50% G + 50% A, 71 mg $COD \cdot L^{-1}$
III	32-49	12 ± 1	1.08 ± 0.11	6	2	3	1	G, 113 mg $COD \cdot L^{-1}$
IV	49-68	13 ± 1	1.17 ± 0.06	6	2	3	1	50% G + 50% A, 71 mg $COD \cdot L^{-1}$

Table 4.2. Operation of the A/O SBR: EBPR ratios and rates observed for the different periods.

Period	Anaerobic phase		Aerobic phase	
	P/C (mol P·mol^{-1} C)	$P_{release}$ rate (mg P·g^{-1}VSS·h^{-1})	P_{uptake} rate (mg P·g^{-1}VSS·h^{-1})	$P_{uptake}/P_{release}$ (mol P·mol^{-1} P)
I	0.07 ± 0.03	1.0 ± 0.5	1.3 ± 0.8	1.2 ± 0.1
II	0.26 ± 0.06	9.6 ± 4.6	11.0 ± 5.2	1.2 ± 0.1
III	0.17 ± 0.11	6.4 ± 3.6	8.0 ± 4.	1.4 ± 0.3
IV	0.09 ± 0.06	1.2 ± 0.6	1.6 ± 0.6	1.4 ± 0.4

Table 4.3. Composition of the concentrated synthetic wastewater. It was diluted 18 times with tap water.

Composition	**g·L^{-1}**
Macronutrients	
Sodium glutamate ($C_5H_8NO_4Na$)	15.60
Ammonium chloride (NH_4Cl)	4.58
Dipotassium phosphate (K_2HPO_4)	0.44
Potassium phosphate (KH_2PO_4)	1.11
Micronutients*	
Ferric chloride ($FeCl_3 \cdot 6H_2O$)	1.50
Potassium iodide (KI)	0.18
Boric acid (H_3BO_3)	0.15
Cobalt chloride ($CoCl_2 \cdot 6H_2O$)	0.15
Manganese chloride ($MnCl_2 \cdot 4H_2O$)	0.12
Zinc sulphate ($ZnSO_4 \cdot 7H_2O$)	0.12
Sodium molybdate ($Na_2MoO_4 \cdot 2H_2O$)	0.06
Copper sulphate ($CuSO_4 \cdot 5H_2O$)	0.03
EDTA ($C_{10}H_{16}N_2O_8$)	10.00

*Trace solution: 1 mL per L of concentrated influent

4.2.3. Batch tests

Batch tests were conducted to investigate the involvement of PHA and glycogen in internal metabolites. Batch tests were conducted with 10L of mixed liquor from the aerobic reactor of the A^2/O pilot plant. These were transferred to a batch reactor where the sludge was subjected to anaerobic/aerobic conditions at controlled pH (7.5) and

temperature (20ºC). Samples were taken every 15 to 30 min and filtered with 0.22 μm Millipore filters for analysis of COD and phosphate concentration in the supernatant. Samples were also collected for the analysis of the PHA and glycogen content in the biomass.

4.2.4. Chemical analyses

The concentration of phosphorus, ammonium, nitrite, nitrate and COD were measured in 0.22 μm filtered samples according to Section 3.2 of Chapter 3. Total organic carbon (TOC) was quantified using an OI Analytical TOC Analyzer (Model 1020A, Shimadzu). Glycogen and PHA were measured in duplicate. PHA was measured with a GC (Agilent Technologies 7820A) according to the methodology described by Oehmen et al. (2005a). Lyophilised sludge samples were digested and methylated with 4 mL of acidulated methanol (10% H_2SO_4) and 4 mL of chloroform during 20 h at 100ºC. Benzoic acid was used as internal standard. Calibration of the method was performed using a copolymer of 3-hydroxybutyric acid and 3-hydroxyvaleric acid (7:3) as standard for PHB and PHV (Fluka, Buchs SG, Switzerland) and 2-hydroxycaproic acid as standard for PH2MV (Aldrich). Glycogen was determined as detailed in Chan et al. (2017) . Total suspended solids (TSS) and volatile suspended solids (VSS) were analysed according to APHA (1995).

4.2.5. Microbiological analyses

The biomass was characterized using the fluorescence in-situ hybridization (FISH) technique coupled with confocal laser scanning microscopy (CLSM) as described in Section 3.3.1 of Chapter 3. The nine probes used to quantify the amount of PAO, GAO and *Tetrasphaera* (EUBMIX, PAOMIX, GAOMIX, DFIMIX, DFIIMIX, Tet1-266, Tet2-892, Tet2-174 and Tet3-654) are detailed in Section 3.3.1 of Chapter 3.

The identification of the bacterial population was performed using next-generation sequencing. Deoxyribonucleic Acid (DNA) extraction, pyrosequencing settings and bioinformatics applied are described in Section 3.3.2 of Chapter 3.

4.3. Results and discussion

4.3.1. Enrichment with non-Accumulibacter PAO in a SBR

The A/O SBR for the sludge enrichment with non-*Accumulibacter* PAO was operated for 68 days under different conditions (Table 4.1). The concentration of phosphate in the

influent was maintained at 10 mg P· L^{-1}. However, the carbon concentration was increased in some periods to obtain a higher PAO activity. Figure 4.1 shows the evolution of phosphorus concentration at the start of the cycle and at the end of the anaerobic and aerobic phases, while Table 4.2 summarises the observed P/C ratio (i.e. phosphorus released over carbon taken up in molar basis) and the P-release and P-uptake rates for the different periods.

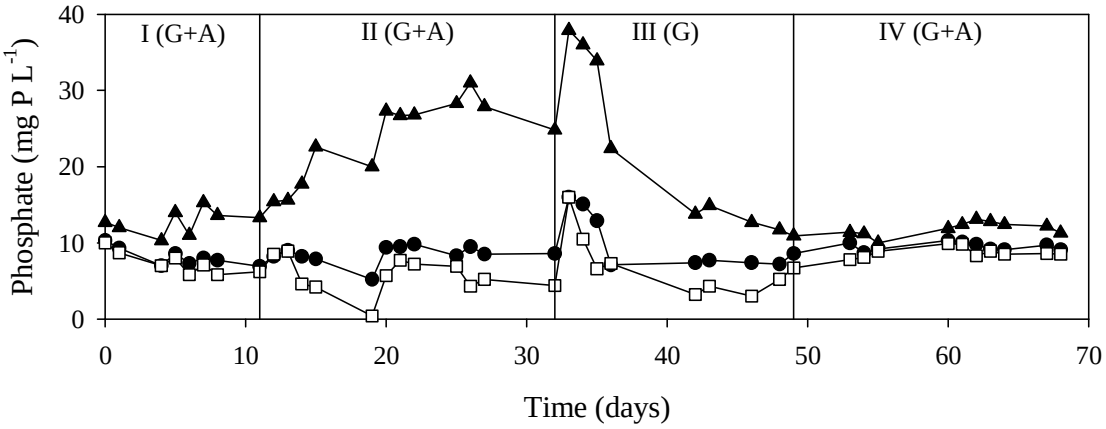

Figure 4.1. Operation of the A/O SBR with different carbon sources (G: glutamate and A: aspartate). Phosphorus concentration at the start of the cycle (●) and at the end of anaerobic (▲) and aerobic (□) phases.

The system was initially operated with a 1:1 mixture of glutamate and aspartate as carbon source. This choice was based on previous studies that reported a good EBPR performance using this mixture of amino acids (Chua et al., 2006; Kristiansen et al., 2013b; Satoh et al., 1998; Zengin et al., 2011). In fact, Zengin et al. (2011) stated that the highest EBPR activity was observed with aspartate and glutamate in the study developed by Satoh et al. (1998). The first period (11 days) showed a progressive increase in P-release activity but with a scarce net-P removal (i.e. around 1 mg· L^{-1}), probably limited by a low organic matter concentration. It is worth mentioning that this SBR operation showed that the system was much more sensitive to oxygen presence in the anaerobic phase than our previous research with conventional carbon sources (i.e. propionic, acetic, glycerol) and *Accumulibacter*-enriched sludge. Compared to our previous *Accumulibacter*-enriched operation, the nitrogen flow under anaerobic conditions had to be drastically increased to ensure complete anaerobic conditions.

The carbon influent concentration was raised from 44 to 71 mg COD· L^{-1} in period II and a gradual increase in P-release and P-uptake was observed. The P-release rate, the P-uptake rate and the P/C ratio reached the highest values of the entire operation (9.6 ± 4.6

mg P·g VSS^{-1}·h^{-1} 11.0 ± 5.2 mg P·g VSS^{-1}·h^{-1} and 0.26 ± 0.06 mol P·mol^{-1}C). The ratio P-uptake/P-release (i.e. phosphorus taken up under aerobic conditions over P released in anaerobic conditions) remained around 1.2-1.4 throughout the operation (Table 4.2). This EBPR activity resulted in a P-removal around 3.4 ± 1.2 mg P·L^{-1}.

Glutamate plays a central role in the metabolism of amino acids (Dionisi et al., 2004) and has three different potential metabolic routes: i) entering to the tricarboxylic acid cycle (TCA), ii) forming putrescine or iii) directly glutamine. We decided to focus on glutamate as sole carbon source from day 32 of the operation (period III). At the same time, the COD concentration was increased from 71 to 113 mg·L^{-1}. Unexpectedly, P-release progressively decreased despite the COD increase, leading to the system failure on day 48. The conditions used in period II were re-established in period IV with the objective of recovering the maximum observed activity, but the SBR became unstable and its recovery was not possible.

The deterioration in EBPR activity could be related to GAO growth as subsequently confirmed by FISH analyses (discussed below). Fast organic matter consumption was observed despite the poor P-release, a clear indicator of growth of microorganisms without EBPR phenotype but capable to consume organic matter under anaerobic conditions. Figure 4.2 shows two complete SBR cycles: one with successful P removal (day 46 in period III) and one with EBPR deterioration (day 68 in period IV). Similar stability problems for lab-scale EBPR systems fed with aspartate and glutamate were reported by Zengin et al. (2011) who, after 4 months of operation, had an unexpected EBPR deterioration and could not relate it to any operational condition.

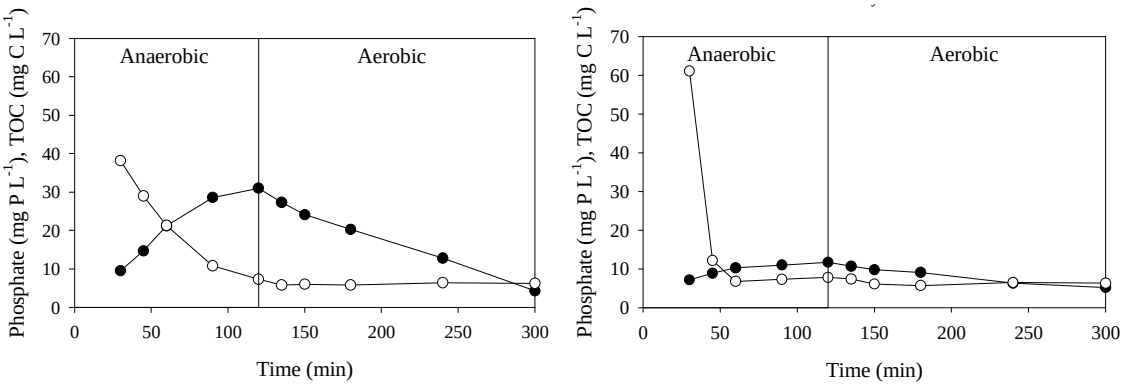

Figure 4.2. Monitoring of two A/O SBR cycles: day 46 during period III (left) and day 68 during period IV (right). Phosphorus concentration (●) and TOC concentration (○).

4.3.2. Long-term A^2/O continuous operation

The experimental period under batch conditions did not provide the desired results in terms of stability of P-removal and it was decided to switch to continuous mode. The A^2/O plant was chosen so that the EBPR would occur in a more realistic environment, i.e. coexisting with biological nitrogen removal. Glutamate was selected as sole carbon source to follow the SBR operation and to facilitate the interpretation of the results. The experimental profiles related to N- and P-removal during the 487 days of operation of the A^2/O pilot plant are shown in Figure 4.3.

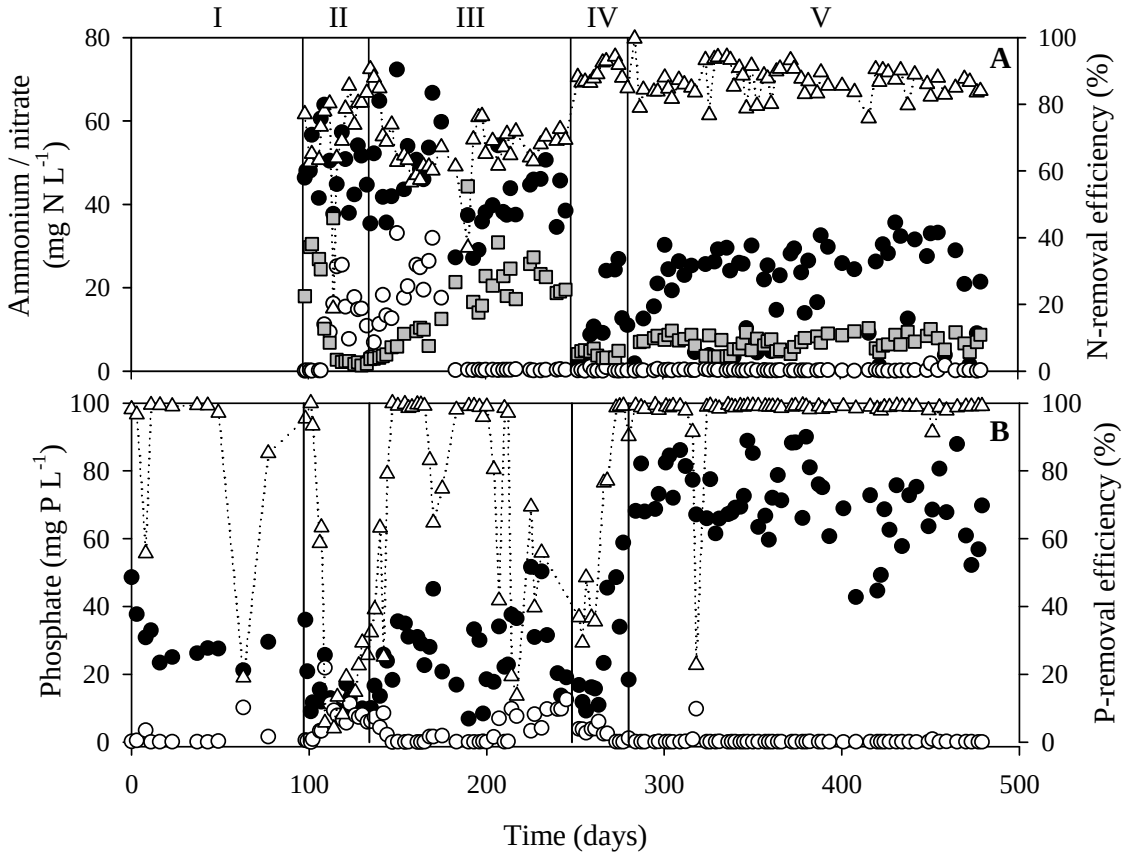

Figure 4.3. Continuous operation of the A^2/O plant. A) Ammonium concentration in the influent (●) and in the effluent (○), nitrate concentration in the effluent (■) and N-removal efficiency (Δ). B) Phosphorus concentration in the anaerobic chamber (●) and in the effluent (○) and P-removal efficiency (Δ).

The pilot plant operation was divided into five periods. The first period, the start-up, showed good P removal until EBPR activity and nitrification capacity were lost due to a batch of deteriorated glutamate that was used in period II (detailed in section 4.2.2 of this Chapter). The biomass concentration in the reactor decreased drastically in this period

(Figure 4.4) and, consequently, P-release and P-uptake decreased (Figure 4.3). The phosphate concentration (up to 22 mg PO_4^{-3}-P·L^{-1}) was even higher than that in the influent indicating depletion of intracellular polyphosphate or PAO decay.

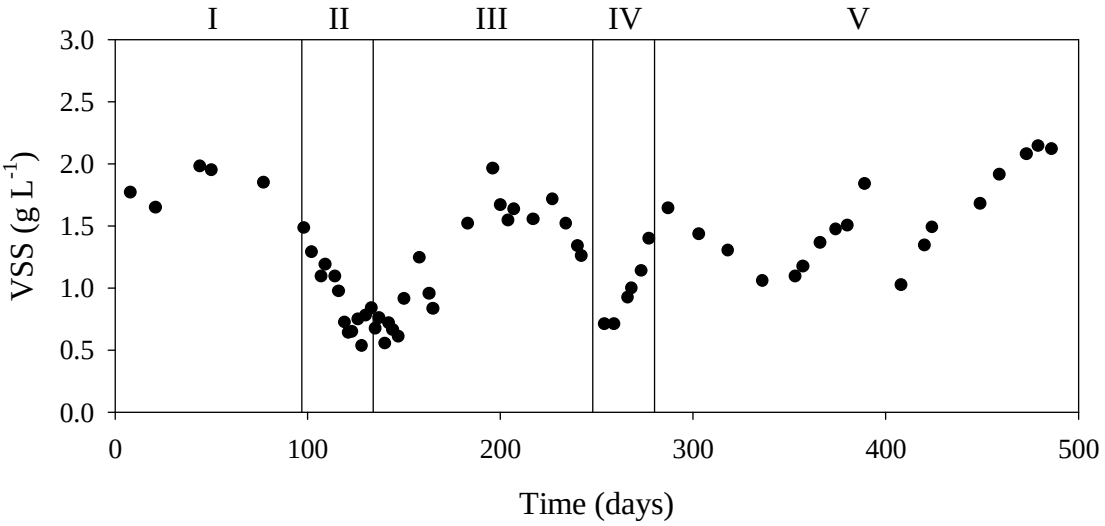

Figure 4.4. Volatile suspended solids concentration in the A^2/O pilot plant.

In period III, the batch of deteriorated feed was replaced and high N and P removal efficiencies were reached again after a few days of operation. Nitrification improved progressively during this period, resulting in complete ammonium oxidation to nitrate and, consequently, an increase in nitrate concentration in the effluent. The high nitrate input to the anaerobic reactor (0.24 ± 0.04 g N-NO_3^-·h^{-1}) finally caused a failure in EBPR activity between days 217 and 256. Nitrate entering through the external recycle is one of the most common causes of EBPR deterioration in real systems. Taking into account a reported average COD/N ratio for denitrification (8.6 g COD·g^{-1} N-NO_3^-) (Henze et al., 2008), an average of 2.05 ± 0.35 g COD·h^{-1} of the initial COD were consumed due to denitrification during this period, which is the 36 ± 15 % of the initial COD input. Again, we observed that the effect of nitrate was much more detrimental than in our previous works with the same pilot plant with *Accumulibacter*-enriched sludge (Guerrero et al., 2011). It was therefore decided to remove the ammonium chloride from the synthetic influent and use glutamate as both carbon and nitrogen source (period IV), since glutamate contains an important amount of organic nitrogen (0.083 mg N·mg^{-1} glutamate). The influent nitrogen was the reduced by 58.6 ± 0.3%. In fact, ammonium was still detected in the influent (an average of 20.5 ± 9.9 mg N·L^{-1}) due to some fermentation of glutamate in the storage tank, which also led to VFA production (mainly acetic acid, and less amounts of propionic and butyric acids, Table 4.4). The amount of

VFA measured in the storage tank after two days was equivalent to 8.9% of the initial COD and up to 63.4% after five days. Thus, fermentation of glutamate occurs but at a low rate and, hence, the contribution of glutamate fermentation was minor at least during the first days. It could be considered that most of the carbon source in our system was glutamate.

Table 4.4. VFAs concentration for the synthetic feed in the storage tank (initial COD concentration of 13.3 $gCOD \cdot L^{-1}$).

	Day 1	Day 2	Day 5
Acetic acid ($mg \cdot L^{-1}$)	n.d.	785.8	4521.1
Propionic acid ($mg \cdot L^{-1}$)	n.d.	5.6	70.4
Butyric acid ($mg \cdot L^{-1}$)	n.d.	187.1	1933.0

n.d: not detected

Finally, in period V, the internal recycle was increased to $R_{INT} = 4$ and the external recycle was decreased to $R_{EXT} = 0.5$ to further reduce the input of nitrate to the anaerobic reactor, which was still deleterious for the plant performance. The A^2/O plant operated for more than seven months (Period V) with a very stable performance for the simultaneous C, N and P removal with high efficiencies (97 ± 3%, 87 ± 5 and 97 ± 10% respectively) (Table 4.5), showing the first successful report of glutamate as sole carbon source for EBPR. The ratios P-uptake/P-release (1.1 ± 0.1) and P/C (0.32 ± 0.14 mol $P \cdot mol^{-1}$ C) were in the range of those obtained in the A/O SBR with successful performance at the end of its Period II. The P/C ratio was lower than that obtained with propionate or acetate (Carvalho et al., 2007; Oehmen et al., 2005b; Zeng et al., 2013) in *Accumulibacter*-enriched systems but correlated well with P/C ratios obtained with other less common carbon sources. In most of these cases, a prior step of degradation is required such as acetogenesis for methanol (Tayà et al., 2013b) or fermentation for glycerol (Guerrero et al., 2012) and glucose (Nielsen et al., 2012).

Despite the low P/C ratio observed, P removal was complete during the entire period V (207 days). Table 4.6 shows different ratios in the anaerobic, anoxic and aerobic phases during each experimental period.

Table 4.5. Operation of the A^2/O pilot plant: Nitrogen, phosphorus and organic matter removal efficiencies during each experimental period

Period	Day (d)		N removal (%)	P removal (%)	COD removal (%)
I	0-98	Start-up	no data	86 ± 26	no data
II	98-135	Deteriorated glutamate	71 ± 16	40 ± 35	91 ± 5
III	135-249	Nitrate input to the anaerobic reactor	67 ± 9	78 ± 28	91 ± 7
IV	249-280	Glutamate as C and N source	89 ± 3	64 ± 29	87 ± 9
V	280-487	Stable operation with high R_{int} and low R_{ext}	87 ± 5	97 ± 10	97 ± 3

Table 4.6. Operation of the A^2/O pilot plant: EBPR ratios and rates obtained during the different periods.

Period	Anaerobic phase		Anoxic phase	Aerobic phase	
	P/C (mol P·mol^{-1} C)	P-release rate (mg P·g^{-1}VSS·h^{-1})	P-uptake rate (mg P·g^{-1}VSS·h^{-1})	P-uptake rate (mg P·g^{-1}VSS·h^{-1})	P-uptake/P-release (mol P·mol^{-1} P)
I	no data	no data	no data	no data	no data
II	0.03 ± 0.05	3.3 ± 4.5	4.5 ± 5.2	1.3 ± 1.4	1.4 ± 0.7
III	0.14 ± 0.08	10.6 ± 5.8	3.9 ± 2.9	3.0 ± 2.0	1.2 ± 0.2
IV	0.28 ± 0.27	16.0 ± 10.5	11.2 ± 9.2	3.4 ± 1.9	1.1 ± 0.1
V	0.32 ± 0.14	23.9 ± 7.3	12.1 ± 6.8	4.1 ± 1.3	1.1 ± 0.1

The two periods with longer stability were period III and period V. In period III, 32% of the total phosphorus removed was taken up under anoxic conditions while the remaining 68% was removed in the aerobic reactor. However, in period V, when the external and internal recirculation were modified to minimise the entry of nitrate into the anaerobic reactor, up to 46% of the total phosphorus removed was taken up under anoxic conditions and 54% under aerobic conditions. These ratios reveal an important denitrifying PAO activity in the plant in spite of not being highly enriched in *Accumulibacter*, but in bacteria belonging to the genus *Thiothrix* and the family *Commamonadaceae* (see discussion below). In addition, anoxic phosphorus uptake rate was higher than under aerobic conditions for all the entire operation (Table 4.6), showing this high denitrifying PAO capability. This is especially significant in period V: 12.1 ± 6.8 and 4.1 ± 1.3 mg $P \cdot g\ VSS^{-1} \cdot h^{-1}$ were obtained for anoxic and aerobic uptake rates respectively.

4.3.3. Process stoichiometry. The role of intracellular polymers

The role of intracellular storage polymers (PHA and glycogen) is essential in the *Accumulibacter* metabolism. Batch experiments were conducted with glutamate as the sole carbon source to study the role of intracellular storage polymers in this case. Figure 4.5 shows two batch experiments under sequential anaerobic and aerobic conditions in which the internal storage polymers were measured: one with A/O SBR biomass (day 26) and one with A^2/O biomass (day 308).

The first key observation is the low relevance of PHA in the experimental profiles, especially with the sludge from the A^2/O pilot plant. The carbon source was completely taken up during the anaerobic phase linked to P-release but very low PHA increase was observed: only 0.2 mol $C \cdot mol^{-1}C$ (0.69 mmol $C \cdot g^{-1}$ VSS) and 0.07 mol $C \cdot mol^{-1}C$ (0.62 mmol $C \cdot g^{-1}$ VSS) for SBR and A^2/O pilot plant, respectively. In fact, the PHA concentration throughout the experiment was much lower than in conventional EBPR studies with VFA as the sole carbon source and *Accumulibacter*-enriched sludge. The average PHA concentration at the end of the anaerobic phase was 0.53 mol $C \cdot mol^{-1}$ C (1.83 ± 0.09 mmol $C \cdot g^{-1}$ VSS) (A/O SBR) and 0.17 mol $C \cdot mol^{-1}$ C (1.27 ± 0.04 mmol $C \cdot g^{-1}$ VSS) (A^2/O), while in the case of a conventional *Accumulibacter*-enriched SBR this concentration was 1.55 mol $C \cdot mol^{-1}C$ (4.59 mmol $C \cdot g^{-1}$ VSS) (Oehmen et al., 2005d). It should be noted that our sludge contained a high amount of *Thiotrix* and *Comamonadaceae* but also a certain amount of *Accumulibacter* (see discussion below) which uses PHA and, thus, it could be hypothesized that the non-*Accumulibacter* PAO

scarcely uses PHA. This observation of low PHA involvement is in agreement with several reports on EBPR with alternative PAO and may suggest a minor role of *Accumulibacter* in our system. For instance, a study with *Tetrasphaera* indicated the inability of these microorganisms to store PHA (Kristiansen et al., 2013a; Nguyen et al., 2011). On the other hand, Willems (2014) reported that many members of the *Comamonadaceae* group are able to accumulate PHA in the cell. Hui et al. (2016) obtained a PHA concentration of 1 mmol $C \cdot g^{-1}$ VSS at the end of the anaerobic phase in a SBR performing EBPR at a high temperature with a mixed microbial cultured with *Accumulibacter* and *Comamonadaceae.* Finally, Rubio-Rincón et al. (2017b) found that *Thiothrix caldifontis* could behave like a PAO with a mixotrophic metabolism for P-removal. In that case, the anaerobic PHA conversion was 0.75 mol $C \cdot mol^{-1}C$ (4.37 mmol $C \cdot g^{-1}$ VSS), but only 0.41 mol $C \cdot mol^{-1}C$ (1.61 mmol $C \cdot g^{-1}$ VSS) were attributed to *Thiothrix*. This value was higher than those obtained in our work: 0.2 mol $C \cdot mol^{-1}C$ and 0.07 mol $C \cdot mol\ C^{-1}$ for A/O SBR and A^2/O pilot plant respectively.

Regarding glycogen, most reports on EBPR (with *Accumulibacter*-enriched sludge) show that glycogen is degraded under anaerobic conditions to provide reducing power. However, in our experiments we observed that glycogen was slightly accumulated during the anaerobic phase (an increase of 0.14 mol $C \cdot mol\ C^{-1}$ (0.47 mmol $C \cdot g^{-1}$ VSS) for the A/O SBR). This observed low glycogen utilisation correlates with the low PHA involvement and casts doubts on the role of *Accumulibacter* in our system. Marques et al. (2017) also observed glycogen production under anaerobic conditions in the batch tests performed with glutamate, aspartate and glucose as carbon sources. On the other hand, glycogen accumulation with the sludge of the A^2/O plant was negligible (0.007 mol $C \cdot mol\ C^{-1}$, 0.06 mmol $C \cdot g^{-1}$ VSS). However, the glycogen concentration at the end of the anaerobic phase in the A/O SBR cycle was 1.34 mol $C \cdot mol^{-1}C$ (4.6 ± 0.2 mmol $C \cdot g^{-1}$ VSS), very similar to the concentration around 1.43 mol $C \cdot mol^{-1}C$ (4.25 mmol $C \cdot g^{-1}$ VSS) for the *Accumulibacter*-enriched sludge (Oehmen et al., 2005d). The glycogen concentration at the end of the anaerobic phase in the A^2/O test was only 0.2 mol $C \cdot mol^{-1}C$ (1.8 ± 0.3 mmol $C \cdot g^{-1}$ VSS), which is lower than the accumulation obtained in the A/O SBR. The difference in glycogen levels between the SBR and the $A^{2/}O$ operation could be related to the GAO proliferation: both the GAO presence and glycogen levels were drastically reduced in the $A^{2/}O$ operation compared to the A/O SBR operation.

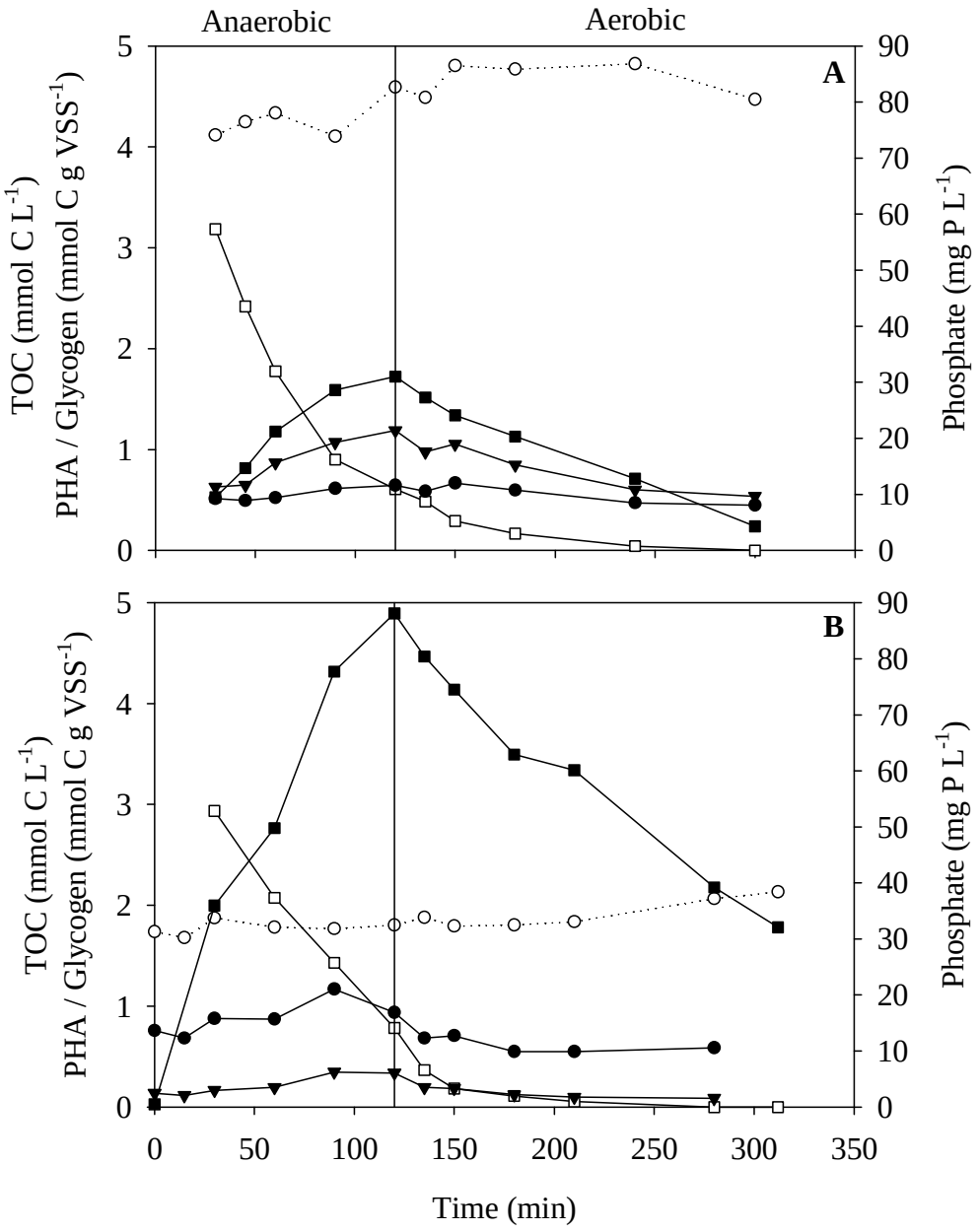

Figure 4.5. Monitoring of anaerobic/aerobic batch cycles. A) A/O SBR cycle at day 26 of operation and B) cycle performed with sludge from the A^2/O pilot plant obtained at day 308 of operation. Phosphorus concentration (■), TOC concentration (□), PHB concentration (●), PHV concentration (▼) and glycogen concentration (○).

Finally, the anaerobic yields and the carbon recovery ratio (CRR) for batch assays are summarized in Table 4.7 for both configurations and compared to related reports from the literature.

Table 4.7. Anaerobic yields for batch assays and comparison with other PAO-enriched systems in the literature.

Study		**Carbon source**	**P_{rel}/C_{upt} (mol P·mol^{-1} C)**	**PHA_{prod}/C_{upt} (mol C·mol^{-1} C)**	**$Glyc_{deg}/C_{upt}$ (mol C·mol^{-1} C)**	**CRR[1] (%)**
This study	SBR	Glutamate & aspartate	0.27	0.20	-0.14 (production)	34
	A^2/O	Glutamate (Batch)	0.21	0.07	-0.01 (production)	8
		Glutamate (Continuous mode)	0.32	0.41	$2.3 \cdot 10^{-4}$	28
Enriched Accumulibacter	Kapagiannidis et al. (2013)	Acetate	0.64	1.10	0.41	77
	Pijuan et al. (2009)	Propionic acid	0.27	0.64	0.45	44
	Lu et al. (2006)	Propionic acid	0.45	1.22	0.29	90
Accumulibacter + *Tetrasphaera*	Marques et al. (2017)	Casein hydrolysate	0.35	0.15	0.38	-
Rhodocyclus + *Actinobacteria*	Zengin et al. (2011)	Glutamate	0.39	0.24	0.45	10-37
Accumulibacter + *Thiothrix*	Rubio-Rincón et al. (2017)	Sodium acetate & Propionic acid	0.64-0.75	0.76-1.00	0.12-0.20	47-81
Accumulibacter + *Comamonadaceae*	Hui et al. (2016)	Acetate, yeast extract & Peptone	0.83	-	0.69	-

The carbon recovery ratio determines which part of the inlet carbon taken up and the glycogen consumed during the anaerobic phase is transformed to PHA. The low PHA and glycogen involvement in the cycle led to a low CRR compared to the results obtained for *Accumulibacter* enriched cultures. This suggests that another non-quantified carbon storage process is probably occurring. Since glycogen does not seem to be involved, our results indicate that other storage routes should be studied to identify the fate of the carbon stored under anaerobic conditions. Satoh et al. (1998) investigated the mechanisms of the anaerobic uptake of glutamate by EBPR activated sludge and stated that glutamate was accumulated as a polymer consisting of γ-aminobutyric acid and an unknown amino acid. This is in agreement with the fact that, in our work, PHA accumulation does not fully explain the fate of glutamate (i.e. CRR ratios of 0.34 for the A/O SBR and 0.08 and 0.28 for the A^2/O plant). Zengin et al. (2011) also found CRR values in the range of 10-37 % in their glutamate batch tests. In contrast, Rubio-Rincón et al. (2017b) obtained with VFA a higher COD balance of 47-81%. Regarding the aerobic ratios, the P_{UPT}/PHA_{DEG} ratios obtained in this work (1.3 and 2.2 mol $P \cdot mol^{-1}$ C for the A/O SBR and A^2/O plant respectively) were significantly higher than the aerobic PAO model prediction developed by Smolders et al. (1994a) (0.41 mol $P \cdot mol^{-1}$ C). These higher ratios suggest that there is a contribution of other putative PAO to EBPR activity.

4.3.4. Non-Accumulibacter PAO contribution to the EBPR process

The role of non-*Accumulibacter* PAO was investigated through the comparison of our experimental data with the values that can be predicted using the reported theoretical *Accumulibacter* stoichiometric ratios. Two different approaches were applied: i) based on the polyphosphate stored during the daily operation and ii) based on the anaerobic ratios obtained during batch tests.

On the one hand, the amount of VSS concentration required to achieve the overall P removal was estimated considering the *Accumulibacter* maximum Poly-P storage capacity (0.38 mg $P \cdot mg^{-1}$VSS, Wentzel et al. (1989)). The ratio between this required VSS concentration and the amount of solids removed from the system (through the purge and the effluent) was used to calculate the theoretical percentage of *Accumulibacter* needed to achieve the overall P removal. This theoretical value was compared to the biovolume quantification of *Accumulibacter* obtained through FISH analysis (Table 4.8).

Table 4.8. Estimation of the percentage of *Accumulibacter* required to perform the overall P-removal taking into account their maximum storage capacity (0.38 mg $P \cdot mg^{-1}VSS$) for the A/O SBR and for the A^2/O pilot plant.

System	Period	P-removal (mg $P \cdot d^{-1}$)	Required VSS (mg $VSS \cdot d^{-1}$)	Solids purged (mg $VSS \cdot d^{-1}$)	*Accumulibacter* required (%)	*Accumulibacter* obtained by FISH (%)
A/O SBR	I	24	62	1033	6	
	II	52	138	498	28	36
	III	79	209	1040	20	
	IV	22	57	1197	5	
A^2/O pilot plant	I	2336	6147	19757	31	
	II	860	2263	7666	30	26
	III	1434	3774	10005	38	
	IV	1332	3506	13213	27	
	V	2469	6496	13396	48	49

The overall P-removal can be explained with the percentage of *Accumulibacter* obtained through FISH analysis for both systems. Thus, with this approach, it cannot be evidenced the involvement of the non-*Accumulibacter* PAO. Nevertheless, this estimation considers that *Accumulibacter* are storing phosphate at their theoretical maximum capacity, which is only possible under well-controlled culture conditions with excess of phosphorus available. In addition, the calculations depend on the FISH percentages, which have also a degree of uncertainty (see discussion in section Bacterial community assessment).

On the other hand, the contribution of non-*Accumulibacter* PAO was assessed through the anaerobic conversions obtained in the batch tests (Tables 4.9 and 4.10) considering:

a) *Accumulibacter* PAO were capable to store up to 77% (A/O SBR) and 45% (A^2/O pilot plant) of the inlet COD. These calculations (detailed in Annex I.1) are based on the percentage of PAO according to FISH and the theoretical observed growth yield reported by Chan et al.(2017)
b) the experimental anaerobic yields (Table 4.7)
c) the stoichiometry for *Accumulibacter* reported by Welles et al. (2015) with acetic acid, Oehmen et al. (2005c) with propionic acid and Pijuan et al. (2004) with butyric acid
d) the theoretical ratios of acetate, propionate and butyrate produced per glutamate degraded: 0.57, 0.16 and 0.10 mol C·mol C^{-1}-glutamate, respectively (Annex I.2).
e) A theoretical anaerobic yield per mole of glutamate calculated based on data in c) and d) as detailed in Annex I.3.

Regarding phosphorus conversion for A/O SBR (Table 4.9), the measured P-release (0.73 mmol P·L^{-1}) was lower than the value theoretically estimated considering the amount of *Accumulibacter* obtained with FISH and the theoretical P/C ratio estimated for glutamate (0.93 mmol P·L^{-1}). As a result, all of the P-release could be attributed to *Accumulibacter*. On the contrary, the value of P-release measured for the A^2/O pilot plant (Table 4.10), was higher than the theoretically estimated for *Accumulibacter* (2.83 mmol P·L^{-1} vs 2.28 mmol P·L^{-1}). This observation suggests that some organisms other than *Accumulibacter* contributed to the biological P removal; these *non-Accumulibacter* PAO would be responsible of a P-release of 0.55 mmol P·L^{-1} (Table 4.10). Hence, using a theoretical P/C ratio for glutamate (Table A.1.3), only an 80.6% of the net phosphorus release can be attributed to *Accumulibacter*.

Table 4.9. Anaerobic conversions estimated for the non-*Accumulibacter* PAO organisms in the batch experiment conducted with sludge from the A/O SBR at day 26 of operation.

	Ratio	Unit	Measured	Estimated for *Accumulibacter*	Estimated for the non-*Accumulibacter* PAO
Anaerobic ratios	PHA/C_{upt}	mol C·mol^{-1}C	0.20	0.91	< 0
	PHB/C_{upt}	mol C·mol^{-1}C	0.04	0.79	< 0
	PHV/C_{upt}	mol C·mol^{-1}C	0.16	0.12	0.31
	P_{rel}/C_{upt}	mol P·mol^{-1}C	0.27	0.44	< 0
	Gly_{deg}/C_{upt}	mol C·mol^{-1}C	-0.14	0.28	-0.33
Anaerobic net conversion	PHA	mmol C·L^{-1}	0.55	1.91	< 0
	PHB	mmol C·L^{-1}	0.11	1.66	< 0
	PHV	mmol C·L^{-1}	0.44	0.25	0.19
	P	mmol P·L^{-1}	0.73	0.93	< 0
	C_{upt}	mmol C·L^{-1}	2.71	2.10	0.61
	Gly_{deg}	mmol C·L^{-1}	-0.38	0.58	-0.96

Table 4.10. Anaerobic conversions estimated for the non-*Accumulibacter* PAO organisms in the batch experiment conducted with sludge from the A^2/O pilot plant at day 308 of operation.

	Ratio	Unit	Measured	Estimated for *Accumulibacter*	Estimated for the non-*Accumulibacter* PAO
Anaerobic ratios	PHA/C_{upt}	mol $C \cdot mol^{-1}C$	0.07	0.91	< 0
	PHB/C_{upt}	mol $C \cdot mol^{-1}C$	0.05	0.79	< 0
	PHV/C_{upt}	mol $C \cdot mol^{-1}C$	0.02	0.12	< 0
	P_{rel}/C_{upt}	mol $P \cdot mol^{-1}C$	0.23	0.44	0.06
	Gly_{deg}/C_{upt}	mol $C \cdot mol^{-1}C$	-0.01	0.28	-0.21
Anaerobic net conversions	PHA	mmol $C \cdot L^{-1}$	0.85	4.71	< 0
	PHB	mmol $C \cdot L^{-1}$	0.56	4.09	< 0
	PHV	mmol $C \cdot L^{-1}$	0.29	0.62	< 0
	P	mmol $P \cdot L^{-1}$	2.83	2.28	0.55
	C_{upt}	mmol $C \cdot L^{-1}$	11.49	5.17	6.32
	Gly_{deg}	mmol $C \cdot L^{-1}$	-0.09	1.45	-1.54

Regarding the carbonaceous compounds, the amount of PHA produced under anaerobic conditions (0.55 and 0.85 mmol $C \cdot L^{-1}$ for A/O SBR and A^2/O pilot plant, respectively) was only 29% and 18% of the theoretical amount expected for *Accumulibacter* considering C-uptake (1.91 and 4.71 mmol $C \cdot L^{-1}$). Thus, there seems to be a population able to release P under anaerobic conditions with a minor storage of PHA.

Finally, glycogen production was observed in both systems (Gly_{deg} = -0.38 and -0.09 mmol $C \cdot L^{-1}$) compared to the predicted degradation of 0.58 and 1.45 mmol $C \cdot L^{-1}$. This result shows the low involvement of glycogen in this microbial community as already observed in the section "Process stoichiometry. The role of intracellular polymers".

4.3.5. Bacterial community assessment

Illumina and FISH-CSLM techniques were used to evaluate the enrichment of the biomass in other putative PAO different from *Accumulibacter*, such as *Tetrasphaera* and *Thiothrix* genus and *Comamonadaceae* family, as well as the presence of "conventional" PAO and GAO in the sludge of both systems.

In the A/O SBR sludge (day 47), FISH quantification detected 36 ± 1% of bacteria that hybridize with PAOMIX and 21 ± 1% with GAOMIX probe (Figure 4.6). This was in agreement with the phosphorus activity failure observed later in the reactor. Neither any of the four probes used for the detection of *Tetrasphaera* nor DFIMix or DFIIMix hybridizations were detected in the sludge.

Illumina was used, then, to examine the microbial community of the A/O SBR on the same sample of day 47 (Figure 4.7-up). With this analysis, *Accumulibacter* accounted for only 1.45% of total bacteria, although some unclassified bacteria belonging to the *Rhodocyclaceae* family, which is closely related to *Accumulibacter* (Zhou et al., 2015), were also detected (5.22%). The existing discrepancy between FISH analyses and the values obtained by Illumina, could be partly explained by a lack of probe specificity for the commonly applied PAOMIX probe. In fact, Albertsen et al. (2016) found that the FISH probe sets for the '*Candidatus* Accumulibacter' (PAOMIX) also target the *Propionivibrio* GAO.

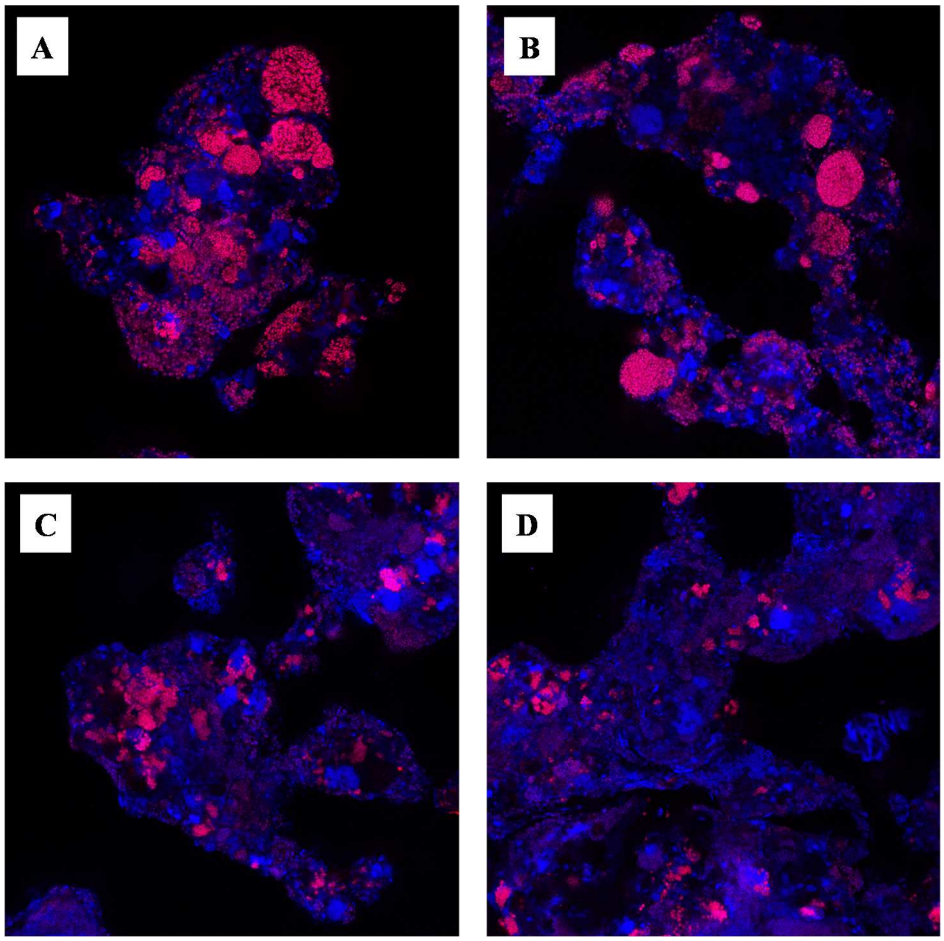

Figure 4.6. CLSM micrographs of FISH for the biomass of the A/O SBR after 47 days of operation. A and B: blue, all bacteria; magenta, *Accumulibacter*. C and D: blue, all bacteria; magenta, *Competibacter*.

This overestimation by FISH analyses was also reported by Stokholm-Bjerregaard et al. (2017). Nonetheless, DNA extraction, primer choice, various PCR settings and the DNA from dead cells have also a large effect on the observed community structure (Albertsen et al., 2015). Furthermore, the 16S rRNA copy numbers vary largely (1 to 15 copies per genome), whereas *Accumulibacter* genome has only two copies (He et al., 2007), which can lead to its underrepresentation when using Illumina in comparison to FISH. As a conclusion, if possible both techniques should be used to complement each other (Albertsen et al., 2012).

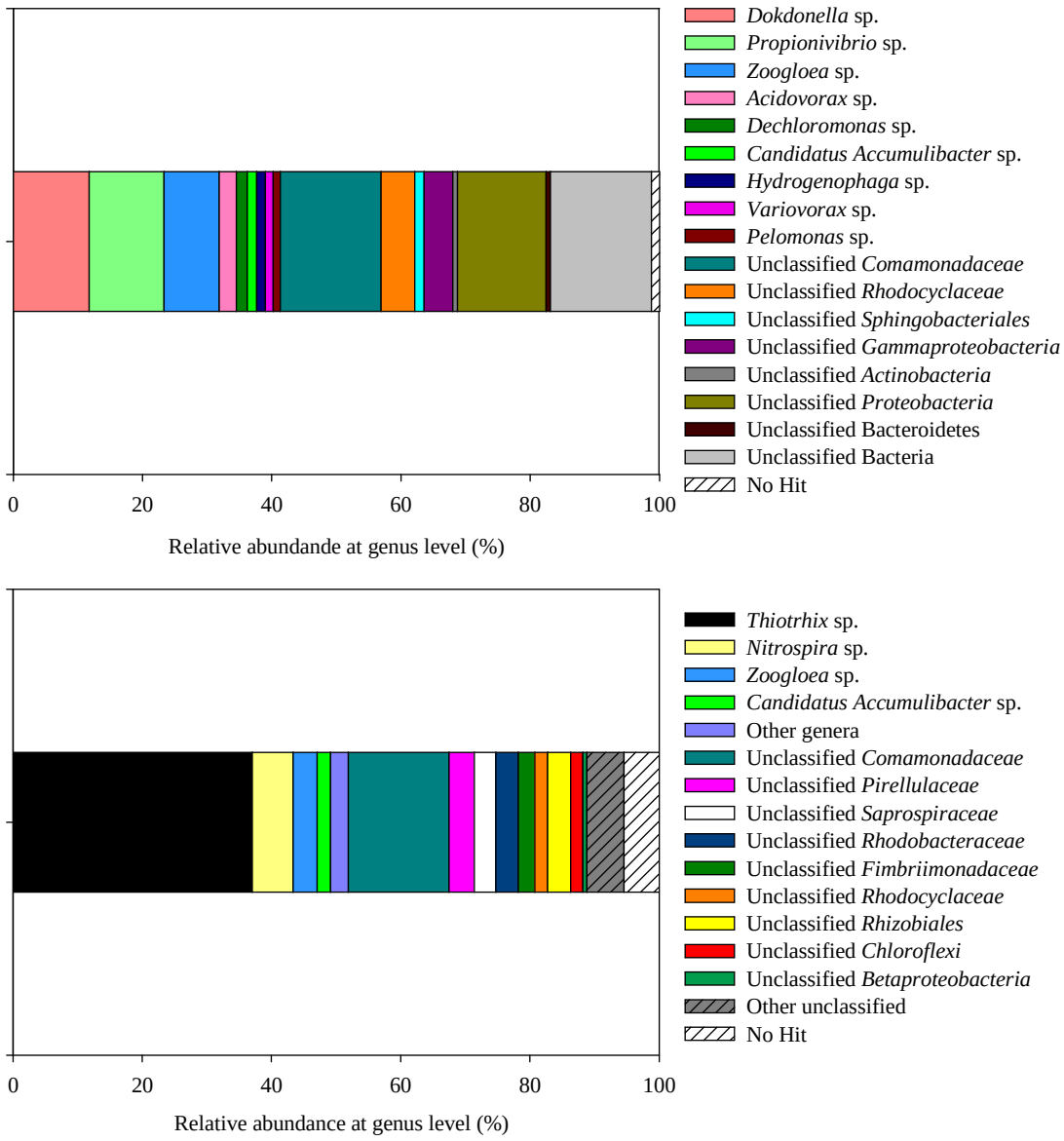

Figure 4.7. Microbial diversity in the A/O SBR (UP) and in the A^2/O pilot plant (DOWN) at genus level. Relative abundance was calculated only considering those microorganisms in which the number of 16S copies was higher than 0.5% of the total copies.

In fact, *Propionivibrio* and *Dokdonella* were the most abundant genera, representing 11.57% and 11.74% of the total bacteria, respectively. *Propionivibrio* are fermentative bacteria of the *Rhodocyclaceae* family. Hence, certain species of *Propionivibrio* could be postulated as putative PAO (Coats et al., 2017). Nevertheless, it is worth mentioning that Albertsen et al. (2016) recently reported the discovery of GAO belonging as well to the genus *Propionivibrio*. *Dechloromonas* and *Zoogloea* were also significant in this sludge, being 1.7% and 8.58% of the total bacteria, respectively. They are assigned to the order *Rhodocyclus*, which is also related to *Accumulibacter* genus. Bacteria from the *Comamonadaceae* family represented up to 21.8% from the A/O SBR sludge.

Variovorax, Acidovorax, *Pelomonas* and *Hydrogenophaga* genera, which belong to the *Comamonadaceae* family, have been identified in short SRT-EBPR systems treating protein-rich (abattoir) wastewater (Ge et al., 2015). A 1.4% of *Sphingobacteriales* order was also observed. This order belongs to the phylum Bacteroidetes and is capable of hydrolysis and utilization of complex carbon sources (McIlroy and Nielsen, 2014). Summarizing, taking into account *Dechloromonas*, *Zoogloea*, *Candidatus* Accumulibacter, *Propionivibrio* and unclassified bacteria from the *Rhodocyclaceae* family, a 25% of the total population in the A/O SBR system could be microorganisms capable of accumulating phosphate.

Regarding the A^2/O biomass, hybridization in FISH analysis of PAOMIX probe (26 ± 4%) was still observed on day 106, while hybridization of GAOMIX was very weak (less than 1 ± 1% of total bacteria) (Figure 4.8 A and B). On day 351, a 49 ± 10% of PAOMIX and a 14 ± 6% of GAOMIX were observed (Figure 4.8 C and D). Neither DFIMix nor DFIIMix hybridizations were detected in the sludge. No hybridization was observed with probes targeting *Tetrasphaera* in the A^2/O biomass. The relatively high presence of bacteria belonging to the *Accumulibacter* genus in both reactors highlights the difficulties in obtaining a highly-enriched sludge in other putative PAO with minimum *Accumulibacter* presence. It is not a straightforward issue since the fermentation of amino acids (in this case, glutamate) by other microorganisms cannot be avoided and *Accumulibacter* can live on those fermentation products, such as VFA.

The data obtained by Illumina from the samples of the A^2/O pilot plant at day 277 showed only 7.7% of *Accumulibacter* and other close related bacteria (*Zoogloea* genus (3.7%) and *Rhodocyclaceae* family (2%)). In fact, bacterial community developed in the A^2/O continuous reactor differed considerably from that observed in the A/O SBR reactor. Indeed, *Thiothrix* (37%) was the most abundant genus in the continuous reactor, suggesting that they could be involved in the EBPR cycle as also stated by Valverde-Pérez et al. (2016) and Rubio-Rincón et al. (2017b). This observation is very significant since we achieved high EBPR activity with low abundance of *Accumulibacter*. Enriching the system in *Thiothrix* without the presence of any sulphur species is also very relevant and an interesting outcome of this work, since previous reports on *Thiothrix* enrichment (Rubio-Rincón et al., 2017b) reported sulphide as the driving factor for this enrichment. In this work, low VFA/COD ratio of our wastewater and the high glutamate content clearly favoured the presence of *Thiothrix*. To our knowledge, this observation has not

been reported before in the literature. Additionally, the sludge volume index (SVI) along the operation was 374 ± 61 mL· g VSS^{-1}, indicating the presence of filamentous bacteria.

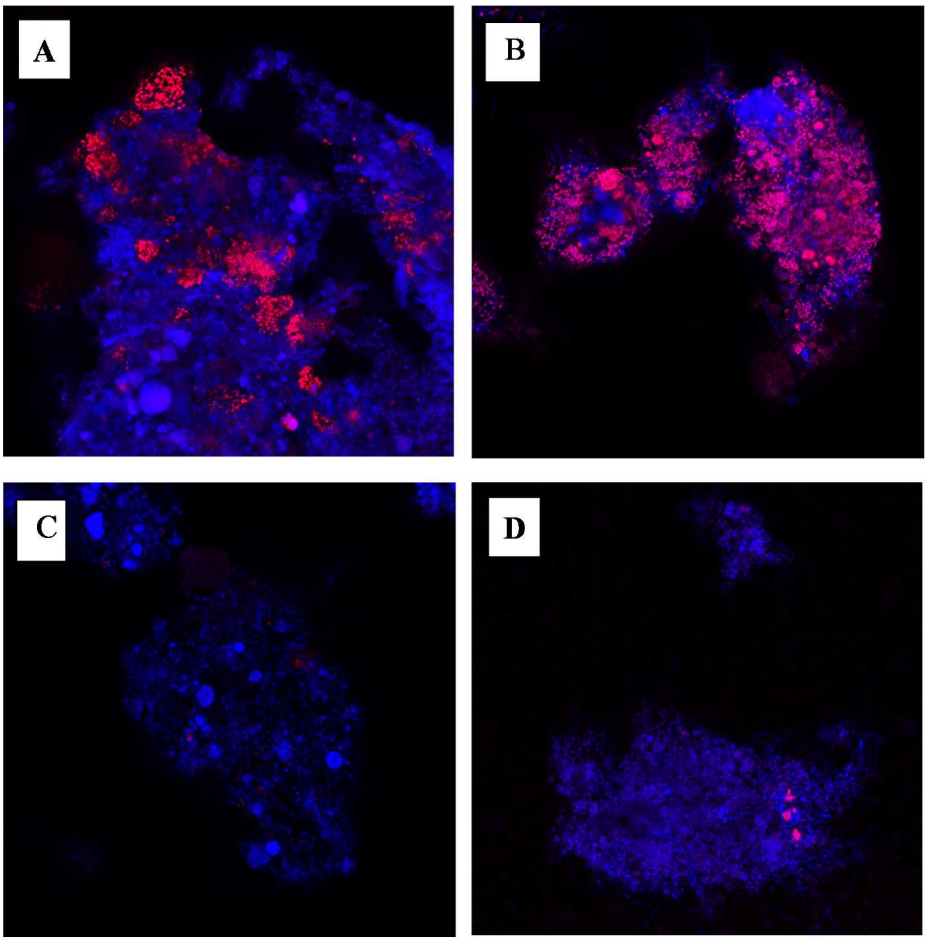

Figure 4.8. CLSM micrographs of FISH for the biomass of the A^2/O pilot plant after 8 days (A and C) and after 351 days of operation (B and D). A and B: blue, all bacteria; magenta, *Accumulibacter*; C and D: blue, all bacteria; magenta *Competibacter*.

The Comamonadaceae family, with members recognised as important denitrifiers in activated sludge Systems (Khan et al., 2002), represented around 15.6% of the microbial community of the A^2/O sludge. Bacteria belonging to the genus *Nitrospira* were present in the biomass at 6.3%. They are nitrite-oxidizing bacteria (NOB) and can exploit low amounts of nitrite because they are k-strategists (Kim and Kim, 2006). Bacteria from the *Rhodobacteraceae* family were detected in the pilot plant with an abundance of 3.4%. These bacteria have been reported to accumulate phosphorus during denitrification (Zheng et al., 2016). Moreover, bacteria from the families *Rhodobacteraceae* and *Rhodocyclaceae*, which has also been detected at 2%, usually play an important role in organic matter degradation(Zheng et al., 2016). Many genera belonging to the *Rhizobiales*

order (accounting. for 3.5% of total bacteria in the reactor), are considered anaerobic fermentative bacteria, which have the ability of fermenting complex organics through producing extracellular polymeric substances (EPS). Moreover, most of them are related to nitrate reduction (Feng et al., 2017). Bacteria from the *Pirellulaceae* family (3.9%) and *Chloroflexi* order (1.9%), have been also identified in marine and freshwater nitrification filters (Rud et al., 2017). In addition, *Pirellulaceae* family, have the ability of utilizing ammonia (Zhao et al., 2017). *Fimbriimonadaceae* family (2.5%) was previously detected in an anammox consortia (Qin et al., 2017). A 3.4% of *Saprospiraceae* family, which has the ability for the hydrolysis and utilization of complex carbon sources (McIlroy and Nielsen, 2014) was also observed in the A^2/O sludge.

To sum up, a higher variety of genus and families was obtained in the A^2/O pilot plant, which can be attributed to the many biological processes that took place in this system. Thus, the EBPR occurred in the A^2/O pilot plant in a more realistic environment than the sample in the A/O SBR. A stable EBPR system with a mixed microbial culture enriched in genera other than *Accumulibacter* was obtained with glutamate as sole carbon and nitrogen source in an A^2/O with high N and P removal efficiencies.

4.3.6. Enzymes reported for the main genus detected

The enzymes reported for *Accumulibacter*, *Thiothrix* and *Comamonadaceae* (Kristiansen et al., 2013a; Schomburg, 2015) were studied to elucidate the potential role of these genus in carbon storage and P-removal processes. The genes of special interest are shown in Table A.I.4. All three possess enzymes related to glycolysis, which is a required process to supply the reducing power for the anaerobic conversion of VFA to PHA according to Zhou et al. (2009). However, the enzymes required for glycogen synthesis have not been reported for *Thiothrix*. This fact, coupled with the high *Thiothrix* fraction observed in the A^2/O sludge, could explain the low involvement of glycogen in this system.

As for the use of Poly-P, *Accumulibacter* and *Thiothrix* possess polyphosphate kinase, which is an enzyme that catalyses the intracellular synthesis of Poly-P (Zeng et al., 2018), and it would indicate a role of these species in the uptake of phosphate. On the other hand, the presence of polyphosphate kinase has not been reported for *Comamonadaceae*, but the absence of this enzyme in current databases does not guarantee the absence of this enzyme in all genus of *Comamonadaceae*.

With respect to PHA synthesis, the presence of poly(3-hydroxybutyrate) depolymerase has been reported for *Accumulibacter* and *Comamonadaceae*. Regarding PHA synthesis for *Thiothrix*, this enzyme is not reported in the Brenda database (Schomburg, 2015), although (Rubio-Rincón et al., 2017b) reported PHA storage by *Thiothrix caldifontis*. Finally, *Comamonadaceae* and *Thiothrix* have some enzymes related to amino acid metabolism. In particular, the presence of glutamate dehydrogenase would indicate their involvement in glutamate degradation. In summary, *Thiothrix* could be clearly involved in P-removal in the A^2/O pilot plant because it is able to accumulate Poly-P, probably without PHA synthesis, but with glutamate involvement. On the other hand, *Comamonadaceae* family has some PAO characteristics, such as synthesis of PHA and glycogen, but to date no Poly-P storage has been reported. Therefore, it could participate in glutamate degradation and denitrification, which are important processes in the A^2/O system, but its involvement in P-uptake cannot be reliably concluded, and hence it should be studied further.

The contribution of non-*Accumulibacter* genus such as *Thiothrix* to the EBPR performance can be additionally supported by the anaerobic net conversions achieved in this study (showed in Tables 4.9 and 4.10, and explained in the section "Non-*Accumulibacter* PAO contribution to the EBPR process"). This observation widens the spectra of EBPR-related genera but a complete understanding of the individual role of *Thiothrix* and bacteria belonging to the *Commamonadaceae* family in this consortium and in the EBPR process needs further research.

4.4. Conclusions

This work shows for the first time the successful operation of an EBPR system using glutamate as both C and N source in a continuous pilot plant with successful results of simultaneous biological N and P removal, and high denitrifying PAO activity. Two systems were operated: i) an A/O SBR with glutamate and aspartate as C sources resulted in a microbial community enriched in *Comamonadaceae* (21.8%) and *Accumulibacter* (1.45%), and ii) an A^2/O pilot plant with glutamate as sole C and N source, resulted in enrichment of *Comamonadaceae* (15.6%), *Thiothrix* (37%) and a smaller fraction of *Accumulibacter* (7.7%) living on glutamate fermentation products. The increase in PHA during the anaerobic phase was only 18-29% of that observed in *Accumulibacter*-enriched sludge, indicating that other storage routes not related to PHA and glycogen should be

studied to identify the fate of the carbon source stored under anaerobic conditions. The contribution to P-removal from microorganisms other than *Accumulibacter* was needed to explain the low production of PHA and the lack of glycogen degradation during the anaerobic phase. *Thiothrix* is the main candidate to be involved in P-removal, as it can accumulate Poly-P, consume glutamate and probably without involving PHA metabolism.

Chapter 5

NITRITE AND NITRATE INHIBITION THRESHOLDS FOR A GLUTAMATE-FED BIO-P SLUDGE

A modified version of this chapter is being prepared for publishing as:

Natalia Rey-Martínez, Gökçe Merdan, Albert Guisasola, Juan Antonio Baeza, 2019. Nitrite and nitrate inhibition thresholds for a glutamate-fed bio-P sludge. *In preparation*.

ABSTRACT

Enhanced biological phosphorus removal (EBPR) is an efficient and sustainable technology to remove phosphorus from wastewater. However, the accumulation of nitrite or the excessive amount of oxygen recycled into the anaerobic reactor has been reported as factors that may deteriorate the efficiency of EBPR in wastewater treatment plants (WWTPs). Nevertheless, most of the existing studies on the investigation of denitrification capabilities, free nitrous acid (FNA) inhibition and P-release under permanent aerobic conditions are focused on *Accumulibacter* and *Tetrasphaera*-enriched biomass. Therefore, it is necessary to examine these conditions on a more diverse microbial community similar to the one observed in a full-scale WWTP. This work shows for the first time, the study of the denitrification capabilities of a biomass developed using glutamate as sole carbon and nitrogen source in an anaerobic/anoxic/oxic (A^2/O) configuration. The microbial community was more diverse, mimicking that of a WWTP, and was able to use nitrite and nitrate as electron acceptors for P-uptake. Moreover, net P-removal was observed under permanent aerobic conditions. However, this microbial culture resulted more sensitive to FNA and to permanent aerobic conditions when compared to *Accumulibacter*-enriched sludge.

5.1. Introduction

Anoxic conditions (nitrite or nitrate as electron acceptors) also allow P-uptake, which is advantageous because i) both nitrogen and phosphorus are removed in the same process, ii) organic matter is used for both nitrogen and phosphorus removal and aeration costs can be reduced and iii) less biomass is produced (Kerrn-Jespersen and Henze, 1993; Kuba et al., 1993). The organisms with the anaerobic-anoxic P-removal phenotype i.e., the microorganisms able to conduct simultaneous nitrogen and P-removal are known as denitrifying PAO or DPAO (Patel and Nakhla, 2006; Zeng et al., 2003). Ahn et al. (2001a) stated that the ability to use nitrite or nitrate in denitrification differs according to the type of PAO clade. However, some reported findings about the denitrification capabilities of PAO are contradictory. On one hand, many authors considered that clade PAO I is able to use nitrite and nitrate as electron acceptors and PAO II is only capable of use nitrite (Carvalho et al., 2007; Flowers et al., 2009; Guisasola et al., 2009; Tayà et al., 2013a). On the other hand, Kim et al. (2013), Saad et al. (2016) and Rubio-Rincón et al. (2017a) stated that PAO I was not capable of using nitrate.

However, despite nitrite-based P-uptake is feasible, the presence of nitrite under aerobic conditions is one of the most reported causes of EBPR failure. Several works reported that high concentration of nitrite in the mixed liquor resulted inhibitory for anoxic P-uptake (Kuba et al., 1996; Meinhold et al., 1999; Saito et al., 2004). Zhou et al. (2007) reported that the protonated species of nitrite, free nitrous acid (FNA i.e. HNO_2) is the true inhibitor of P-uptake and FNA concentrations in the range of 0.002-0.2 mg HNO_2-N$\cdot L^{-1}$ resulted in a decrease in the anoxic P-uptake. Moreover, nitrite can inhibit both anoxic and aerobic P-uptake by PAO (Zhou et al., 2012).

Nitrite is an intermediate of both nitrification and denitrification processes and, thus, it can be accumulated under aerobic or anoxic conditions (Philips et al., 2002). For example, in the aerobic phase, conditions of low sludge residence time (SRT), high temperature (above 30ºC) and low dissolved oxygen (DO) can cause the wash-out nitrite oxidizing bacteria (NOB) (Jia et al., 2018; Rongsayamanont et al., 2014) and, thus, nitrite accumulation. Under anoxic conditions, nitrite accumulation can also occur under low pH, high temperature and low carbon to nitrogen ratios, which can lead to an imbalance between nitrate and nitrite reduction rates (Zhou et al., 2011).

Another potential cause of EBPR deterioration in full-scale WWTPs is an increment of the oxygen amount entering to the anaerobic reactor through the external recycle (for example, due to excessive aeration or heavy rainfalls periods). These situations can be simulated at lab-scale when the electron donor (substrate) and the electron acceptor (nitrite, nitrate or oxygen) are present simultaneously (Pijuan et al., 2006; Vargas et al., 2009).

The abovementioned causes of EBPR failure (i.e. nitrite/nitrate inhibition and oxygen presence under anaerobic conditions) have been widely studied in the literature at lab-scale with bio-P sludge maintained under conditions different from those found in a real environment (particularly the carbon source). Consequently, the microbial community developed in these lab-scale systems was mostly *Accumulibacter* or *Tetrasphaera*-enriched sludge, which may be different from the real bacterial communities abundant in WWTPs. It has been demonstrated that the microbial communities involved in EBPR systems can be very diverse depending on the carbon source supplied. When simple carbon sources are used such as propionate, butyrate or acetate, the microbial community is enriched in *Accumulibacter* PAO (Oehmen et al., 2005; Maite Pijuan et al., 2004; Welles et al., 2015). Nevertheless, with more complex carbon sources not only of *Accumulibacter* but also other microorganisms proliferate such as *Tetrasphaera* (casamino acid, Marques et al., 2017), *Comamonadaceae* (abattoir wastewater, Ge et al., 2015), *Thiothrix* (glutamate, Chapter 4) and fermentative bacteria capable of hydrolyzing complex substrates. Therefore, there is a niche on investigating the extent of FNA inhibition on the bio-P microbial communities abundant in WWTPs.

We have analyzed the toxic effects of FNA, nitrate and oxygen in a glutamate-fed EBPR community with a diverse microbial community structure, similar to the bacterial population observed in a full-scale WWTP. Anaerobic-anoxic/aerobic batch tests with different carbon sources, with nitrite and nitrate and under permanent aerobic conditions were conducted to evaluate the denitrifying capabilities and contribution towards anoxic P-uptake.

5.2. Materials and methods

5.2.1. Continuous pilot plant description

The A^2/O pilot plant consisted of three continuous stirred tank reactors with a total volume of 146 L and a 50 L settler. The detailed diagram of the reactor and set-up details are described in Section 3.1.1 of Chapter 3. The first reactor (R1, 28L) was anaerobic so that PAO were selected against other ordinary heterotrophic organisms (OHO). Nitrate entering to the second reactor (R2, 28L) with the internal recycling was denitrified by either OHO or DPAO. The third reactor (R3, 90L) worked under aerated conditions: organic matter was completely removed, phosphorus was taken up and nitrification took place. The SRT was maintained around 15 days with daily sludge wastage from the aerobic reactor. The pH was controlled at 7.5 using an on-off controller with sodium carbonate (1M) dosage in the aerobic reactor. DO was also controlled in the aerobic chamber at 1.0 ± 0.1 mg L^{-1}. The pilot plant operated at room temperature.

The starting point of this work is an A^2/O system fed with glutamate as sole carbon and nitrogen source aiming at simultaneous phosphorus and nitrogen removal. This plant was previously run for more than 480 days under different operational conditions as described in Chapter 4. Hence, the biomass was adapted to this new carbon source. The glutamate was fed from an individual storage tank and a partial fermentation to VFA was detected, which resulted in a gradual increase of the VFA content in the storage tank: from 0% just after preparation to 8.9% of the initial COD after two days and up to 63.4% after five days.

The results reported in this work show 261 days of operation after a change in the feeding strategy to limit the amount of VFA entering the system. To avoid this fermentation to VFA, fresh feed was prepared three times per week. As a result of this new strategy, VFAs were not detected in the storage tank and glutamate was the only carbon source entering the anaerobic reactor.

The synthetic influent was prepared from a concentrated feed that was diluted with tap water as described in Chapter 4, with a final content of 10 mg PO_4^{-3}-P·L^{-1} and 400 mg COD·L^{-1} and using glutamate as sole carbon and nitrogen source.

5.2.2. Batch experiments

Several batch tests were conducted in a magnetically stirred vessel (2 L) inoculated with biomass withdrawn from the aerobic reactor of the A^2/O pilot plant. Three sets of batch

experiments were performed to investigate the behaviour of the biomass in terms of: i) carbon consumption under different electron donors (acetate, propionate and glutamate), ii) simultaneous denitrification and P-removal with different electron acceptors (nitrite, nitrate and oxygen) and iii) P-release under permanent aerobic conditions by means of different DO. All batch tests mimicked the pilot plant configuration and consisted of an anaerobic phase by sparging nitrogen until the carbon source had been fully consumed (2 h) followed by an aerobic or anoxic phase depending on the set. The aerobic phase was obtained with air sparging. An initial pulse of concentrated feed resulted in the initial desired conditions inside the reactor. pH (WTW Sentix 81) and DO (WTW CellOx 352) probes were connected to a multiparametric terminal (WTW INOLAB 3), which was in turn connected to a PC with a specific software allowing for data monitoring and manipulation of a high precision microdispenser (Crison Multiburette 2 S) for pH control with acid/base addition (HCl and NaOH at 1 M, respectively).

Three sets of batch tests were conducted:

i) The first set of experiments consisted on the monitoring of anaerobic-aerobic carbon and phosphorus profiles using different electron acceptors. Acetic acid, propionic acid and glutamate were the substrates used with an initial concentration in the reactor of 195 mg acetic acid·L^{-1} (208 mg COD·L^{-1}), 125 mg propionic acid·L^{-1} (189 mg COD·L^{-1}) and 270 mg COD·L^{-1} as glutamate.

ii) The second set of experiments consisted of anaerobic-anoxic assays by dosing a concentrated solution of nitrite (14.75 - 92.11 mg N·L^{-1} in the reactor) or nitrate (15 - 82.93 mg N·L^{-1} in the reactor). The batch experiments using nitrite as electron acceptor were performed at different pH values (7.5, 8 and 8.5) in order to evaluate the effect of different FNA concentrations in the biomass. Some of the nitrite and nitrate batch tests were followed by an aerobic phase.

iii) Aerobic P-release was studied under different aeration flowrates. Compressed air was sparged during the entire experiment.

The batch tests were sampled every 15 or 30 minutes for chemical analysis of the supernatant. Samples were filtered by 0.22 µm (Millipore) for the analysis of phosphate, nitrite, nitrate, ammonia, acetate, propionate and COD. The specific process rates were calculated as the slope of a linear regression including the first points of consumption or production, standardized against the biomass concentration.

The FNA concentration was calculated using the equation 1 and with K_a value determined using the equation 2 for a given temperature (ºC) (Zhou et al., 2007).

$$[FNA] = \frac{S_{N-NO_2}}{K_a \cdot 10^{pH}} \quad (1)$$

$$K_a = e^{-\frac{2300}{(273+T)}} \quad (2)$$

5.2.3 Chemical and microbiological analyses

The concentration of phosphorus, ammonium, nitrite, nitrate and COD were measured in 0.22 μm filtered samples according to Section 3.2 of Chapter 3. Total suspended solids (TSS) and volatile suspended solids (VSS) were analysed according to Section 3.2 of Chapter 3.

Biomass was characterized using fluorescence in-situ hybridization (FISH) technique coupled with confocal laser scanning microscopy (CLSM) as described in Section 3.3.1 of Chapter 3. The nine probes used to quantify the amount of PAO and GAO (EUBMIX, PAOMIX, GAOMIX) are detailed in Section 3.3.1 of Chapter 3.

Identification of bacterial population was performed using next-generation sequencing. DNA extraction, pyrosequencing settings and bioinformatics applied are described in Section 3.3.2 of Chapter 3. Paired-end sequencing of the extracted DNA was performed on an Illumina MiSeq platform by an external service (Scsie UV, Valencia, Spain) using the bacterial primer pair 515F-806R.

5.3. Results and discussion

5.3.1. Pilot plant performance and microbial community composition

The experimental profiles related to N- and P-removal during the 261 days of operation of the A^2/O pilot plant under the new feeding strategy without VFA are shown in Figure 5.1. High N- and P-removal efficiencies (85% and 99% respectively) were obtained during the entire operation. The solids concentration was maintained around 1.85 ± 0.29 g VSS·L^{-1} (Figure 5.2).

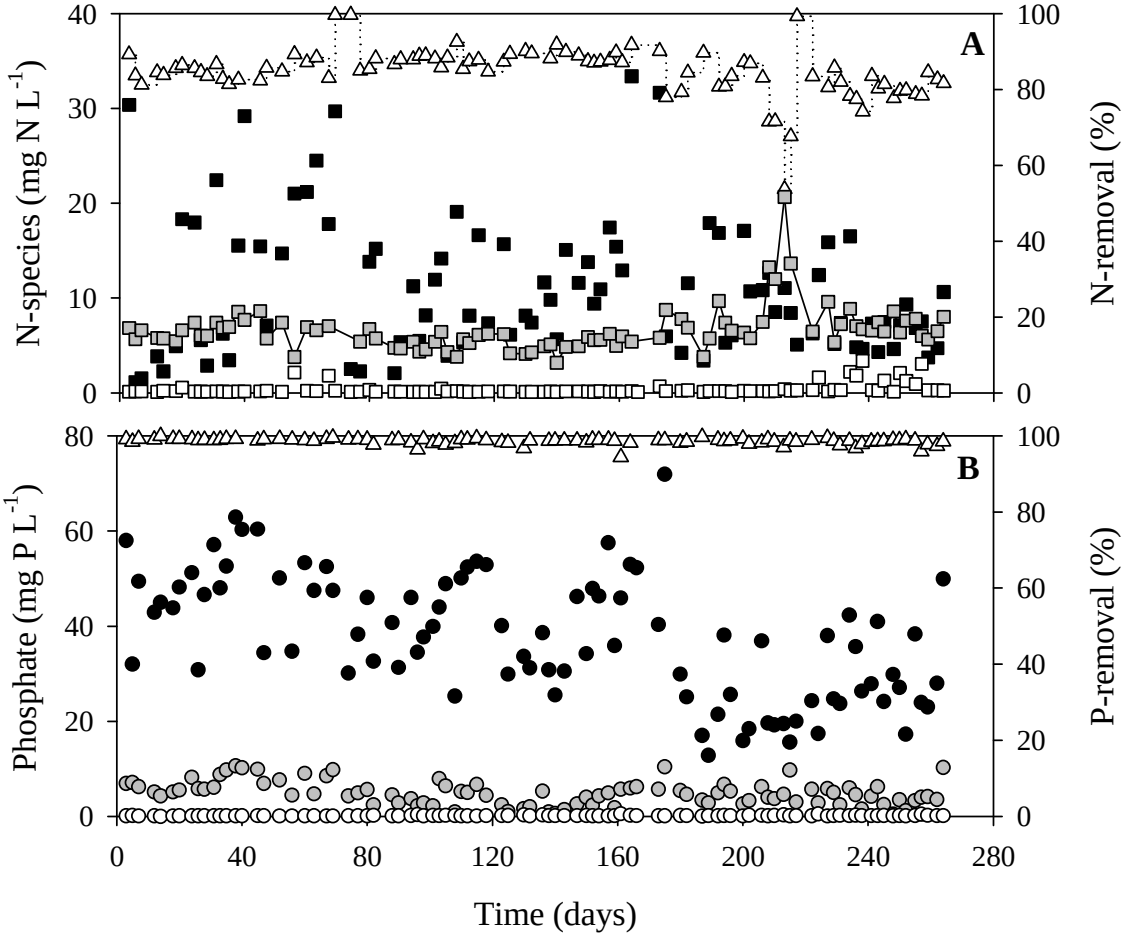

Figure 5.1. Experimental profiles during the 261 d of operation of the A^2/O plant. A) Ammonium concentration in the influent (■) and effluent (□), nitrate concentration in the effluent (■) and N-removal efficiency (Δ). B) Phosphorus concentration in the anaerobic reactor (●), anoxic reactor (●) and effluent (○) and P-removal efficiency (Δ).

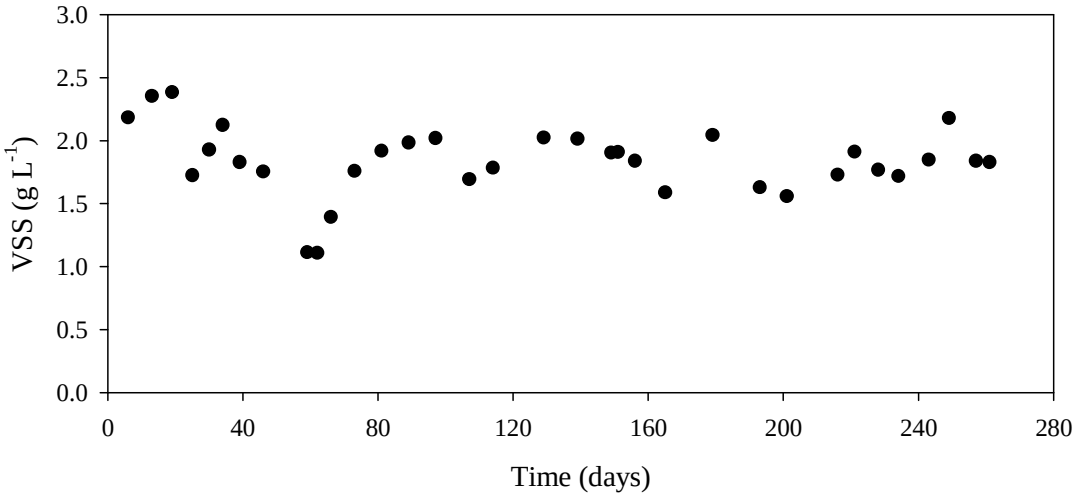

Figure 5.2. Volatile suspended solids concentration in the A^2/O pilot plant.

Between days 208 and 215, technical problems with the external recirculation pump led to an increase in its flowrate, which in turn, caused a high nitrate input to the anaerobic reactor by means of external recirculation. That led to a decrease of the anaerobic PAO activity (i.e. lower P-release) but it did not affect the P-removal efficiency, being the concentration of phosphorus in the effluent 0.16 ± 0.08 mg $P \cdot L^{-1}$ (Figure 5.1). Moreover, the nitrate present in the anaerobic reactor resulted in low COD available for denitrification in the anoxic reactor, which in turn caused an increase of nitrate concentration in the effluent (15 ± 4 mg NO_3^--$N \cdot L^{-1}$).

No nitrite was ever observed, so complete nitrification was achieved during the pilot plant operation. The P/C ratio was very low (0.15 ± 0.07 mol $P \cdot$mol C^{-1}) particularly when compared to P/C ratio for conventional PAO electron donors such as acetate (0.5 mol $P \cdot$mol C^{-1}, Smolders et al., 1994b) or propionate (0.42 mol $P \cdot$mol C^{-1}, Oehmen et al., 2005d).

The P/C ratio (0.15 ± 0.07 mol $P \cdot$mol C^{-1}) was also much lower than in the previous operational period (0.32 ± 0.14 mol $P \cdot$mol C^{-1}, Table 5.1). Lower P/C ratios are obtained when *Accumulibacter* PAO are the dominating PAO and fermentable substrates are used instead of VFA, such as the case of glycerol (0.2 mol $P \cdot$mol C^{-1}) as obtained by Lv et al. (2014) and Guerrero et al. (2012). Some COD is used during the fermentation process, resulting in less COD available for PAO. Glutamate is also a complex substrate that has to be firstly hydrolysed by fermentative bacteria during the anaerobic phase to produce VFA. In fact, the new feeding strategy led to a severe increase of fermentative bacteria in the reactor as will be shown below. Then, the P/C ratio and the P-release rate were lower to the values obtained in the previous work (Table 5.1). This decrease was due to the lower amount of *Accumulibacter* in the system, being the FISH percentages 21% in the current operation and 49% during the last period of the previous operation. This fact would indicate that other non *Accumulibacter* PAO were also part of the microbial community. In any case, P-removal was complete during the entire operation.

Table 5.1. EBPR ratio and rates obtained and comparison with the previous work.

Study	Anaerobic		Anoxic phase	Aerobic phase
	P/C (mol P·mol^{-1} C)	P-release rate (mg P·g^{-1}VSS·h^{-1})	P-uptake rate (mg P·g^{-1}VSS·h^{-1})	P-uptake rate (mg P·g^{-1}VSS·h^{-1})
Chapter 4	0.32 ± 0.14	23.9 ± 7.3	12.1 ± 6.8	4.1 ± 1.3
This study	0.15 ± 0.07	9.84 ± 4.63	6.49 ± 3.14	2.91 ± 1.98

Regarding the P-uptake activity, Figure 5.1 shows that the most of the phosphorus was taken up under anoxic conditions. 56% of the total phosphorus removed was taken up under anoxic conditions while the 44% remaining was removed aerobically, in spite of the volume of the aerobic reactor being three times higher (90L) than the anoxic reactor (28L). The average amount of phosphorus that entered to the aerobic reactor was 5±2 mg P·L^{-1} in contrast with the higher amounts entering to the anoxic reactor (38±13 mg P·L^{-1}). The specific anoxic and aerobic P-uptake rates were also lower than those found in the previous operational period. However, the anoxic P-uptake rate was again higher than that under aerobic conditions (Table 5.1), confirming the high denitrifying activity of this culture.

The Illumina technique was used to examine the microbial community developed in the A^2/O pilot plant on day 158. As shown in Figure 5.3-up, *Proteobacteria* and *Bacteroidetes* were clearly the most abundant phyla, accounting for 47.2% and 37.9% respectively. The next major phyla were *Armatimonadetes* (3.3%), *Nitrospirae* (2.8%) and *Verrucomicrobia* (2.1%). Finally, *Planctomycetes*, *Firmicutes*, *Chloroflexi* and *Acidobacteria* were in abundance below 2%. This microbial distribution is similar, in terms of the predominant phyla, to the community structure observed in WWTPs (Cydzik-Kwiatkowska and Zielinska, 2016; Hu et al., 2012; Wang et al., 2012). Nevertheless, this is a comparison at phylum or class level, because the microbial composition at family or genus level varies with influent organic matter fractionation and dissolved oxygen concentration in the reactor (Zhang et al., 2017).

At family level (Figure 5.3-down), within *Proteobacteria* phylum, *Rhodocyclaceae* (23.4%) was the most dominant family, which is closely related to *Accumulibacter* (Zhou et al., 2015). Three genera were identified within *Rhodocyclaceae* family, 13.6% correspond to *Candidatus* Accumulibacter phosphatis, 2.4% to *Propionivibrio* and 1.5%

to *Dechloromonas*. *Accumulibacter* is broadly recognized as the model PAO (Oehmen et al., 2007) and, although it has not been formally categorized, their reference sequences are classified as belonging to *Rhodocyclaceae* family (Coats et al., 2017). *Propionivibrio* are fermentative bacteria and certain species could be postulated as putative PAO (Coats et al., 2017), but also Albertsen et al. (2016) reported the discovery of GAO belonging to this genus. Finally, *Dechloromonas* are a genus frequently reported as PAO in EBPR reactors (Liu et al., 2005).

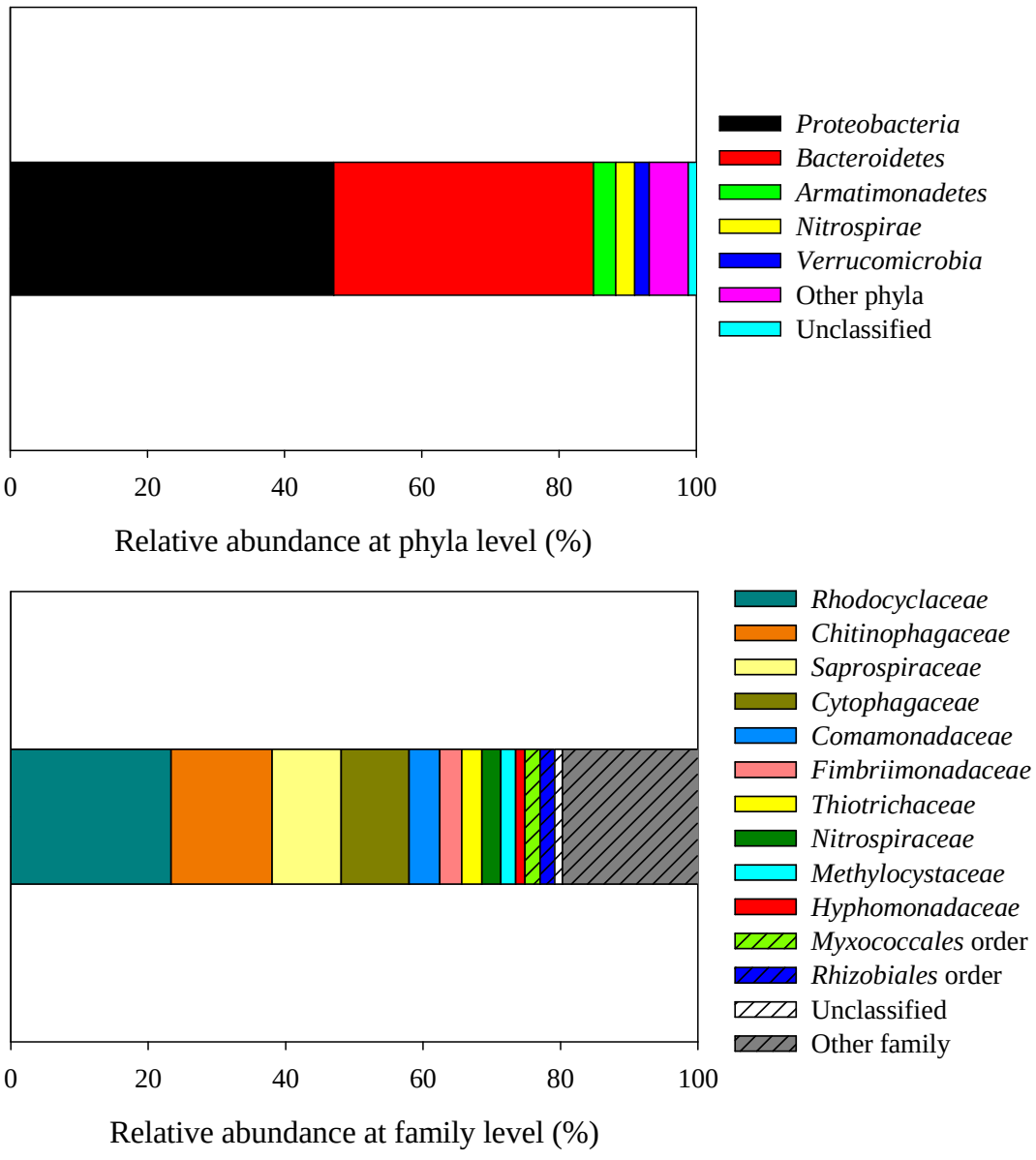

Figure 5.3. Microbial community distribution in the biomass from the A^2/O pilot plant at phyla level (UP) and family level (DOWN).

Within *Bacteroidetes* phylum, *Chitinophagaceae*, *Saprospiraceae* and *Cytophagaceae* families accounted for 14.7%, 10.1% and 9.8% of the total bacteria. These families

exhibit the ability to hydrolyse complex carbon sources, like proteins and polysaccharides (Rosenberg et al., 2014), and hence, they could be involved in the glutamate degradation. The *Comamonadaceae* family, 4.5% of the microbial community, has been identified in short SRT-EBPR systems treating protein-rich wastewater (Ge et al., 2015). Moreover, some members have been recognised as important denitrifiers in activated sludge Systems (Khan et al., 2002). *Thiothrichaceae* family had an abundance of 2.9% and the genus associated to this family was *Thiothrix*. In the previous operation of the pilot plant, *Thiothrix* represented 38% of the total bacteria; hence, they experienced a sharp decline in the new operation. In fact, this decrease was corroborated by the lower sludge volume index (SVI): 158 ± 55 mL$\cdot$ g^{-1} VSS, which was almost half of that obtained in the previous operation (around 300 mL$\cdot$ g^{-1} VSS). *Nitrospiraceae* family accounted for 2.7% corresponding totally to *Nitrospira* genus which are nitrite-oxidizing bacteria (NOB), generally adapted to low substrate concentrations and can exploit a low amount of nitrite (Kim and Kim, 2006).

This complex microbial distribution of the bio-P sludge obtained in this study is closer to that found in a conventional WWTP. To the best of our knowledge, most of the reported studies on PAO inhibition and the DPAO denitrification capabilities were performed with *Accumulibacter* or *Tetrasphaera*-enriched cultures. Therefore, the importance of our work lays on the comparison of our experiments with those already reported for less complex microbial communities.

5.3.2 Denitrification capabilities of the culture

Batch tests with different electron acceptors were performed to study the denitrifying capacities of the mixed microbial culture. The electron acceptors, i.e. nitrite and nitrate, were dosed at different concentrations of both compounds.

5.3.2.1 Nitrite as electron acceptor

The objective of these batch tests was to understand the denitrifying capabilities of our bio-P sludge and to compare the inhibition threshold for FNA and nitrite with the reported values for *Acccumulibacter*-enriched sludge. FNA has been reported as the real inhibiting agent (Zhou et al., 2007). For that reason, several batch tests with different nitrite concentrations and at different pH values (7.5, 8 and 8.5) were performed. It has been reported that FNA-adapted and non FNA-adapted PAO have different response to FNA inhibition, being the non FNA-adapted PAO more sensible to the FNA presence

(Meinhold et al., 1999; Saito et al., 2004; Zhou et al., 2012). It is worth mentioning that the sludge used in the current study was obtained from an A^2/O plant where simultaneous P and N removal was achieved. Hence, this sludge was adapted to nitrate but not necessarily to high concentrations of nitrite, since nitrification was complete and no nitrite accumulation was observed in the reactor during the entire operation. On the other hand, Zhou et al. (2007) suggests that adaptation to nitrite/FNA does not necessarily increases the tolerance of *Accumulibacter* PAO to FNA, so there is not a consensus in this need of acclimatization to FNA.

Figure 5.4 displays the experimental profiles of two typical batch tests. In Figure 5.4A, 90% of initial glutamate was consumed in the first 30 min of the anaerobic phase linked to P-release. In the anoxic phase, nitrite (initial concentration of 23 mg NO_2^--N L^{-1}) was supplied and simultaneous P-uptake and nitrite consumption was observed. When nitrite was depleted, a slight P-release occurred. Finally, under aerobic conditions, P-uptake took place again leading to complete P-removal. The batch test presented in Figure 5.4A was performed at pH of 7.5 resulting in an initial concentration of FNA of 1.63 µg HNO_2-N L^{-1}. Zhou et al. (2007) found that FNA inhibition on anoxic P-uptake starts at these low levels (1-2 µg HNO_2-N L^{-1}). Total inhibition occurred at 20 µg HNO_2-N L^{-1}. In contrast, Figure 5.4B shows a batch test where the initial nitrite concentration (34.5 mg NO_2^--N L^{-1}) resulted in FNA concentration of 2.45 µg HNO_2-N L^{-1} that completely inhibited the uptake process. A low nitrite consumption rate 1.9 mg NO_2-N $g^{-1}VSS \cdot h^{-1}$ compared to the 10.9 mg NO_2-N $g^{-1}VSS \cdot h^{-1}$ obtained for the batch test of Figure 5.4A was observed. Moreover, P-release instead of P-uptake was detected. At the beginning of the aerobic phase, nitrite concentration was 20 mg NO_2^--N L^{-1} (1.34 µg HNO_2-N L^{-1}).

This FNA concentration was even lower than that of Figure 5.4A (1.63 µg HNO_2-N L^{-1}), where no inhibition was observed for the anoxic P-uptake. Surprisingly, no P-uptake was observed despite nitrite and oxygen were present, even though it has been reported that some DPAO can use both electron acceptors simultaneously leading to a higher metabolic rate (Zhou et al., 2012). In any case, Lanham et al. (2011) also never observed aerobic P-uptake after a nitrite spike for concentrations ranging 25-65 mg $NO_2^- \cdot$-N L^{-1}, which were equivalent to 1.1-5.4 µg HNO_2-N L^{-1}. Our results show that when the biomass was subjected to an inhibitory FNA concentration, P-uptake was affected even after recovering aerobic conditions. On the other hand, other possible explanation for this phenomenon could be that the aerobic P-uptake was more sensitive to FNA inhibition

than the anoxic P-uptake. This is in agreement with the report of Saito et al. (2004), who working at a pH of 7.47±0.10 observed that less than 0.4 mg NO_2^--N g^{-1}VSS and around 2 mg NO_2^--N g^{-1}VSS were observed as threshold for aerobic and anoxic P-uptake, respectively. In our case, the anoxic phase tolerated up to 13 mg NO_2^--N g^{-1}VSS at a pH of 7.5. In the case of the aerobic phase, we never observed P-uptake if nitrite concentration resulted inhibitory in the previous anoxic phase. This observation is somehow controversial since other studies stated that the anoxic P-uptake was more sensitive to nitrite/FNA inhibition (Meinhold et al., 1999; Zhou et al., 2012).

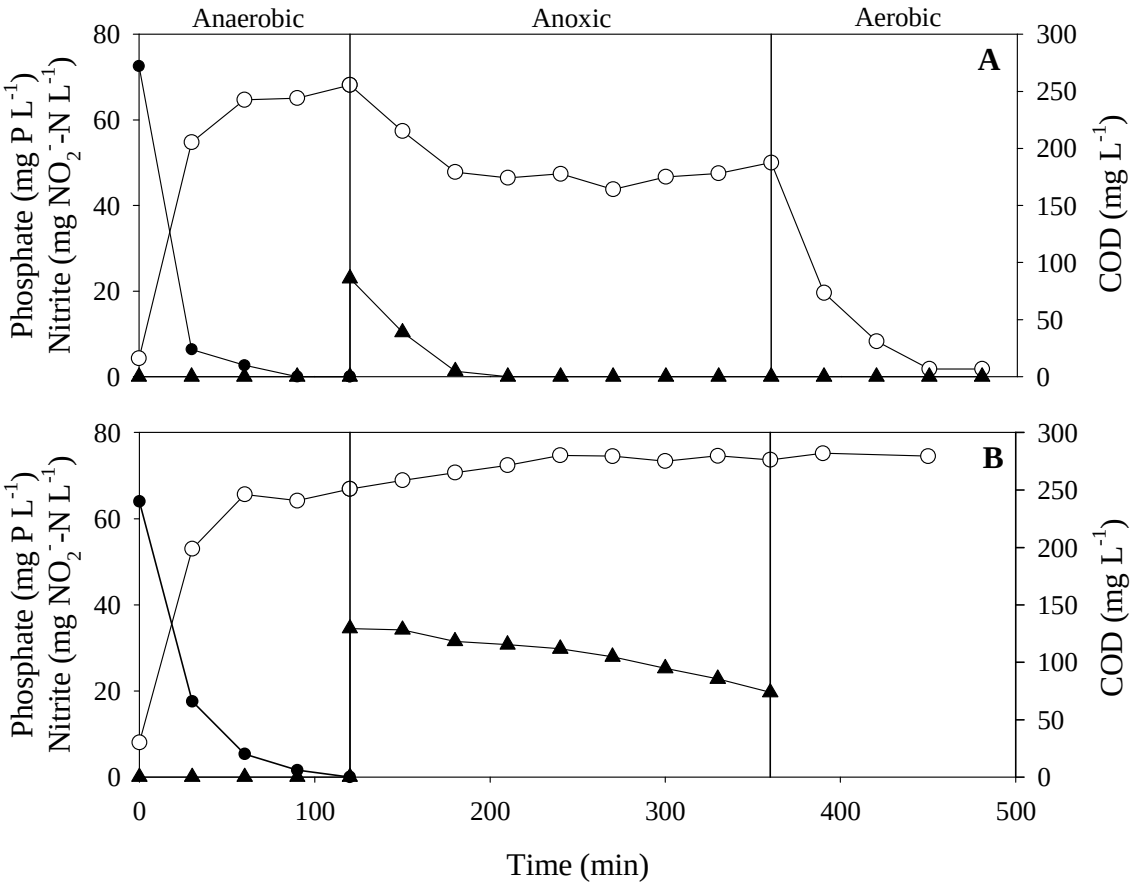

Figure 5.4. Monitoring of anaerobic/anoxic/aerobic batch experiments with nitrite as sole electron acceptor at pH 7.5 A) With a spike of nitrite of 23 mg NO_2^--N L^{-1} and FNA concentration of 1.63 µg HNO_2-N L^{-1} B) With a spike of nitrite of 34.5 mg NO_2^--N L^{-1} and FNA concentration of 2.45 µg HNO_2-N L^{-1}. Phosphorus concentration (○), COD concentration (●) and nitrite concentration (▲).

The threshold of FNA inhibition depends on the microbial population, its FNA adaptation and on the type of microbial culture (suspended or attached biomass) (Jabari et al., 2016; Zhou et al., 2011). Zhou et al. (2012) observed that anoxic P-uptake was 100% inhibited

at FNA concentration of 5 µg HNO_2-N L^{-1} with a FNA-adapted sludge with 45% of *Accumulibacter*. In another study, Zhou et al. (2007) stated that anoxic P-uptake was totally inhibited when the FNA concentration was greater than 20 µg HNO_2-N L^{-1} with an *Accumulibacter*-enriched sludge (85%).

Several batch tests were performed at different FNA concentrations to determine the maximum FNA at which anoxic P-uptake could occur. Different nitrite concentrations at different pHs were used to reach different FNA amounts. Figure 5.5 shows the phosphorus (A) and nitrite (B) uptake rates for each FNA concentration tested.

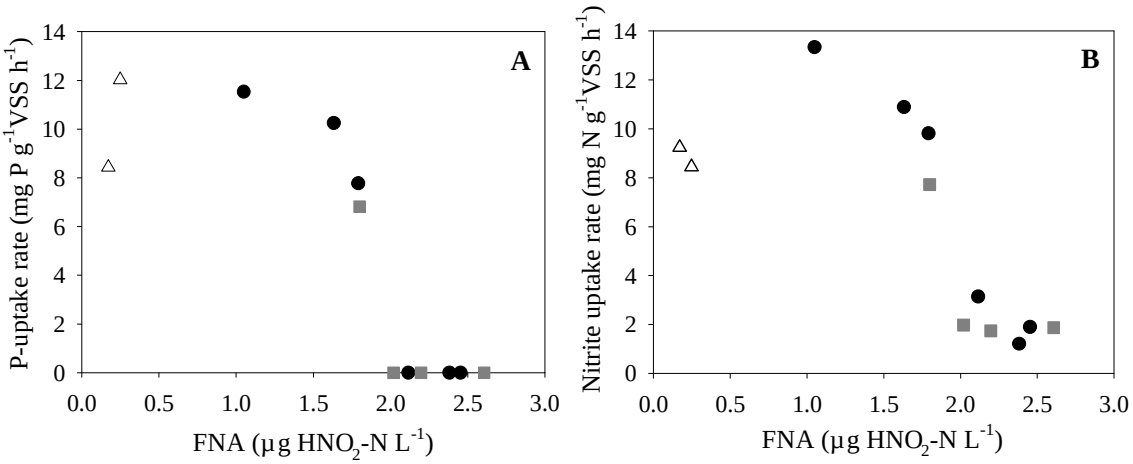

Figure 5.5. Correlation between P-uptake (A) and N-uptake (B) rates with FNA concentration at different pH values: 7.5 (●), 8 (■) and 8.5 (Δ).

A decrease in both rates was observed with the increase in FNA concentration, resulting in 2 µg HNO_2-N L^{-1} the concentration that completely stopped P-uptake. When our bio-P sludge was subjected to an inhibitory FNA concentration, P-release instead of P-uptake was observed during anoxic phase, indicating that FNA concentration directly affects P-uptake mechanisms rather than P-release. Three batch tests performed with different inhibitory FNA concentrations are shown in Figure 5.6. A P-release of 15.7, 13.1 and 16.6 mgP·L^{-1} was observed during the anoxic phase in figures 5.6A, 5.6B and 5.6C respectively. Moreover, nitrite denitrification by DPAO was also inhibited by FNA. However, the inhibitory effect was weaker than that on P-uptake, since nitrite uptake rates around 2 mg N·g^{1} VSS·h^{-1} were obtained for FNA concentrations between 2-2.5 µg HNO_2-N L^{-1}. This represents 76.5% of inhibition in the nitrite uptake rate when the FNA concentration increased from 1.05 to 2.11 µg HNO_2-N L^{-1}. This FNA values led to a complete P-uptake inhibition.

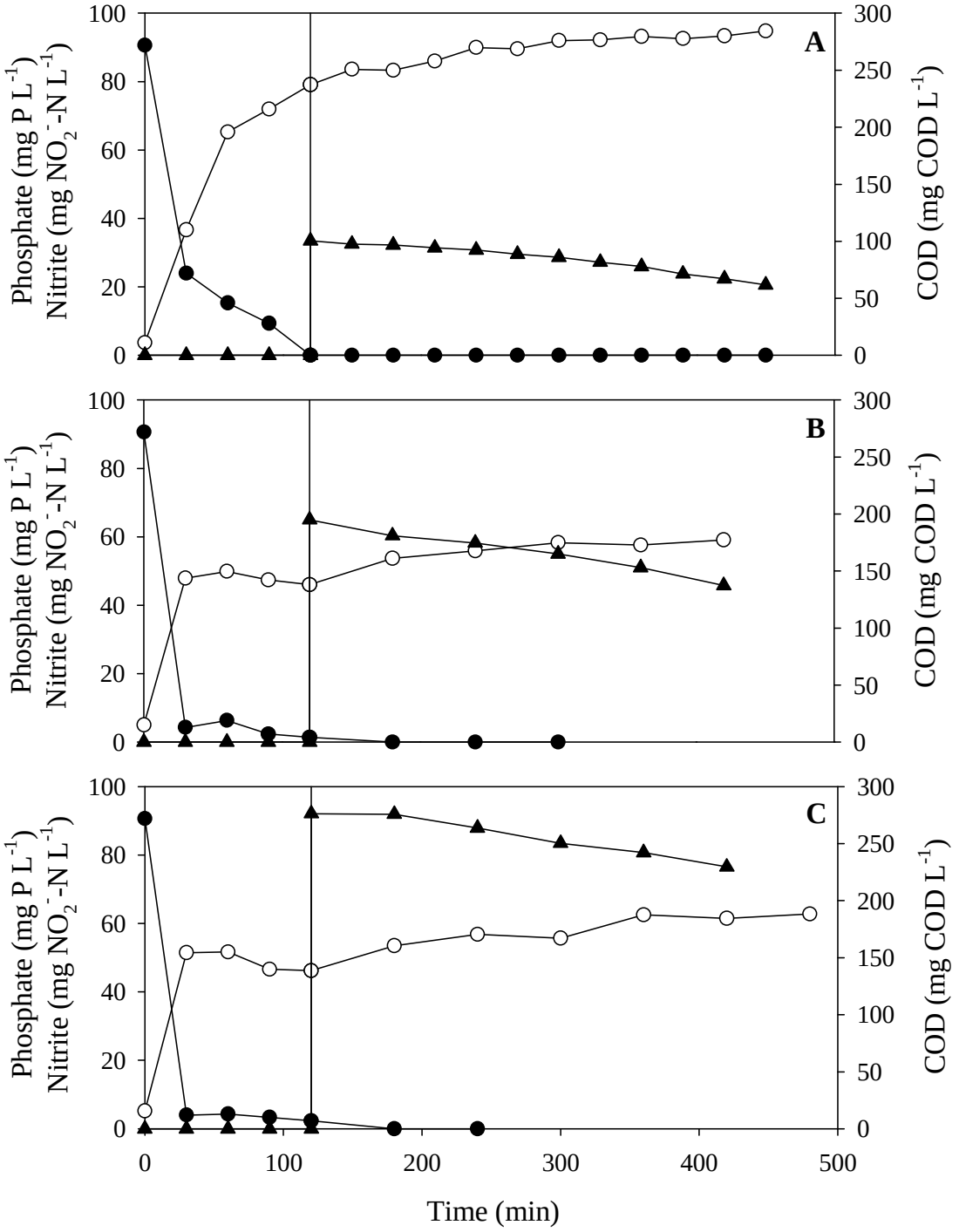

Figure 5.6. Different batch tests with inhibitory FNA concentrations showing P-release during the anoxic phase. A) With a spike of nitrite of 33.5 mg NO_2^--N L^{-1} (FNA= 2.38 µg HNO_2-N L^{-1}) at a pH of 7.5. B) With a spike of nitrite of 65.0 mg NO_2^--N L^{-1} (FNA= 2.02 µg N-$HNO_2 \cdot L^{-1}$) at a pH of 8.0. C) With a spike of nitrite of 92.1 mg NO_2^--N L^{-1} (FNA= 2.61 µg HNO_2-N L^{-1}). Phosphorus concentration (○), COD concentration (●) and nitrate concentration (▲).

A summary of the FNA and nitrite concentrations used and the nitrite, nitrate and P-uptake rates and P/N ratios obtained for each batch test is presented in Table 5.2. The anoxic P-uptake rates were in the range 6.8-12.0 mg $P \cdot g^{-1}VSS \cdot h^{-1}$ under FNA concentrations around 1.80-0.25 µg HNO_2-N L^{-1} respectively. The maximum FNA concentration that the biomass could tolerate while maintaining P-uptake was 1.80 µg HNO_2-N L^{-1}, as P-release instead of P-uptake was observed for higher FNA values. This threshold is lower than in other works with bio-P sludge, where P-uptake was observed with higher FNA concentrations (2.45 and 2.88 µg HNO_2-N L^{-1}) (Guisasola et al., 2009; Saito et al., 2004). However, the P-uptake rates obtained in our work in the range of no FNA inhibition were higher than some values reported in the literature (Table 5.3). Zhou et al. (2007) obtained anoxic P-uptake rates around 1 mg $P \cdot g^{-1}$ $VSS \cdot h^{-1}$ for an *Accumulibacter*-enriched sludge and for FNA concentrations ranging 0.85-38.8 µg HNO_2-N L^{-1}. Moreover, Jabari et al. (2016) obtained anoxic P-uptake rates of 7.6-8.7 mg $P \cdot g^{-1}$ $VSS \cdot h^{-1}$ with 0.2-1.8 µg HNO_2-N L^{-1} respectively in an integrated fixed-film activated sludge system. Guisasola et al. (2009) obtained an anoxic P-uptake rate of 3.42 mg $P \cdot g^{-1}$ $VSS \cdot h^{-1}$ when the FNA concentration was 2.45 µg HNO_2-N L^{-1} with sludge adapted to nitrite and enriched in PAOMIX (42%). Finally, Saito et al. (2004) obtained anoxic P-uptake rates between 11.5-7 mg $P \cdot g^{-1}VSS \cdot h^{-1}$ for FNA concentrations ranging 0.72-2.88 µg HNO_2-N L^{-1}. From these results, our bio-P sludge possesses a lower FNA inhibition threshold; nevertheless, the P-uptake rates obtained were together with the presented by Saito et al. (2004), the higher anoxic P-uptake rates reported in the literature., only comparable with those obtained by Saito et al. (2004).

Table 5.2. Summary of batch tests results with nitrite and nitrate as electron acceptors

Electron acceptor	pH	NO_X dosed (mg NO_X-N L^{-1})	FNA concentration (µg HNO_2-N L^{-1})	NO_X uptake rate (mg NO_X-N g^{-1} VSS·h^{-1})	Anoxic P-uptake rate (mg P·g^{-1} VSS·h^{-1})	P/N ratio (mol P·mol^{-1} N)
NO_2^-	7.5	14.8	1.05	13.3	11.5	0.39
		23.0	1.63	10.9	10.3	0.43
		25.2	1.79	9.8	7.8	0.36
		29.8	2.12	3.1	-1.7	-0.55
		33.5	2.38	1.2	-2.4	-2.00
		34.5	2.45	1.9	-1.9	-1.00
	8	50.5	1.80	7.7	6.8	0.40
		65.0	2.02	2.0	-2.7	-1.35
		77.6	2.20	1.7	-2.2	-1.29
		92.1	2.61	1.9	-1.9	-1.00
	8.5	24.1	0.17	9.2	8.4	0.41
		34.8	0.25	8.5	12.0	0.64
NO_3^-	7.5	15.0		5.0	9.8	0.89
		23.6		3.4	5.3	0.71
		27.7		4.0	6.7	0.75
		41.6		3.2	5.6	0.79
		61.9		2.6	4.7	0.83
		70.4		2.7	3.0	0.49
		82.9		2.5	2.7	0.49

Table 5.3. Comparison of the P-uptake rates with nitrite found in this work with some values reported in the literature

Study	pH	FNA concentration ($\mu g\ HNO_2\text{-}N\ L^{-1}$)	P-uptake rate ($mg\ P \cdot g^{-1}\ VSS \cdot h^{-1}$)	FNA-adaptation biomass
Saito et al. (2004)	7	0.24	0.5	
		0.48	3.0	
		0.72	11.5	
		1.68	10.5	
		2.88	7.0	
Zhou et al. (2007)	8	0.86	1.06	
Guisasola et al. (2009)	7.5	2.45	3.42	Adapted
Jabari et al. (2016)	7.8	0.2	7.6	Adapted
		0.4	7.7	
		1.2	8.3	
		1.8	8.7	
		0.55	6.0	Non-adapted
		1.35	3.89	
This work	8.5	0.25	12.0	Non-adapted
	8	1.80	6.8	
	7.5	1.79	7.8	
		1.63	10.3	
		1.05	11.5	

The ratio of phosphorus removed to nitrogen denitrified during anoxic conditions (P/N ratio) describes the whether the energy obtained from nitrite denitrification is used for P-uptake. The average P/N ratio was 0.4 mol $P \cdot mol^{-1}$ N for all the batch tests except for the inhibited batch tests (Table 5.2). However, a decrease in the P/N ratios and even negative values were obtained for inhibitory FNA concentrations, therefore, it seems that FNA had a negative impact on P/N ratio, in accordance with the results obtained in other studies (Jabari et al., 2016).

5.3.2.2 Nitrate as electron acceptor

Different nitrate concentrations were used to study its effect on the biomass (Table 5.2, Figure 5.7). Simultaneous P-removal and nitrate denitrification were observed in all batch tests. The experimental profiles of carbon, phosphorus and nitrate monitored in a conventional cycle are presented in Figure 5.7A.

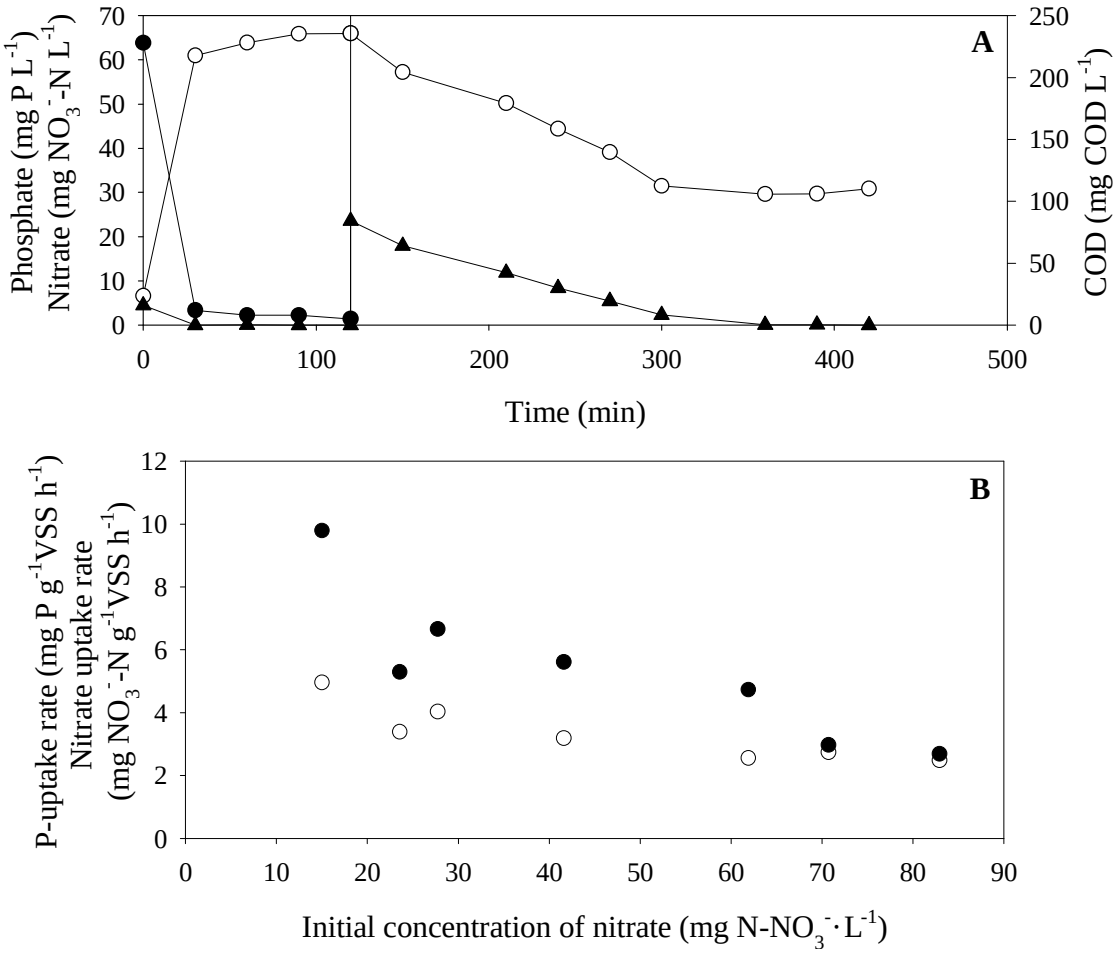

Figure 5.7. Batch experiments with nitrate as sole electron acceptor. A) Monitoring of an anaerobic/anoxic batch test: concentrations of phosphorus (○), COD (●) and nitrite (▲). B) Effect of the initial concentration of nitrate in the different batch experiments on nitrate uptake rate (○) and P-uptake rate (●).

Glutamate was completely taken up during the anaerobic phase linked to P-release. Then, in the subsequent anoxic phase, an initial amount of nitrate (23.6 mg NO_3^--N L^{-1}) was supplied and simultaneous phosphorus and nitrate uptake were observed. P-uptake ceased when nitrate was fully reduced and no nitrite accumulation was observed during the experiment. Nitrite was never accumulated when nitrate was dosed in any of the batch tests performed in this work. This lack of nitrite build-up could suggest that complete

nitrate reduction was conducted by a single population (Carvalho et al., 2007) or it could be hypothesized the coexistence of bacteria capable only to reduce nitrate to nitrite, while DPAO could denitrify from nitrite onwards (Guisasola et al., 2009). The absence of nitrite was also observed by Lanham et al. (2011) and Carvalho et al. (2007) in propionate-fed systems. However, Carvalho et al. (2007), observed nitrite accumulation when the carbon source was acetate. In the same way, Zhou et al. (2010) observed a low nitrite accumulation in all experiments with high initial concentrations of nitrate (30, 60 and 120 $mg \cdot L^{-1}$). On the other hand, Flowers et al. (2009) did not observe nitrite accumulation during the batch tests with a sludge that had not been exposed to nitrate.

Figure 5.7B shows the phosphorus and nitrate uptake rates for each of the initial nitrate concentrations tested. The higher the initial concentration of nitrate, the lower both rates were. Nevertheless, contrarily to the case of nitrite, nitrate caused a decrease in the consumption rates but not complete inhibition. In fact, P-uptake occurred even at the highest concentration tested (82.9 mg NO_3^--N L^{-1}), which was also observed by Zhou et al. (2010). P-uptake rate experimented a reduction of 72% when the initial nitrate concentration increase from 15 to 82.9 mg NO_3^--N L^{-1} whereas the nitrate uptake rate decreased a 50% (Figure 5.7B). The lowest nitrate concentration tested was 15 mg NO_3^--N L^{-1}, which led to the highest P-uptake and nitrate uptake rates. In the case of Zhou et al. (2010), both uptake rates were higher with nitrate concentration in a range of 5-30 mg $N\text{-}NO_3^- \cdot L^{-1}$. Then, higher concentrations such as 60 and 120 mg NO_3^--N L^{-1} caused a decrease in the uptake rates. It is worth to be mentioned that the P-uptake rate was an average of 30% faster when nitrite was used as electron acceptor than with nitrate. The same trend was observed by Lee et al. (2001) when nitrite concentrations up to 10 mg NO_2^--N L^{-1} (2.57 µg HNO_2-N L^{-1}) were supplied. A comparison of the P-uptake rates using nitrate obtained in this work with some values reported in literature are shown in Table 5.4. The values obtained by Flowers et al. (2009) were lower than the values observed in this study even for higher nitrate concentrations. Nevertheless, other authors reported higher values (Zeng et al., 2003; Zhou et al., 2010). The low P-uptake rates could be explained by the microbial community developed using complex substrates, since in both, our work and the study developed by Flowers et al. (2009), the carbon source were glutamate and a mixture of acetate and casaminoacids respectively. In the other studies, simple carbon sources such as acetate or propionate were used. Nevertheless, the concentrations of nitrate used in this work were very high in comparison with the typical

values observed in real WWTPs. For example in the Manresa WWTP, the average influent for nitrate was 3.5 and 2 mg NO_3^--N L^{-1} in winter and summer respectively (Machado et al., 2014). In the work developed by Vieira et al. (2019), the maximum nitrate concentration (13 mg NO_3^--N L^{-1}) was obtained in the aeration tank of a conventional activated sludge in the WWTP of Lisbon.

Table 5.4. Comparison of the P-uptake rates with nitrate found in this work with other values reported in the literature.

Study	Initial nitrate concentration (mg NO_3^--N L^{-1})	P-uptake rate (mg P·g^{-1} VSS·h^{-1})	NO_3^- Acclimatization (carbon source)
Zeng et al. (2003)	53.2	16.90	Yes (Acetate)
Carvalho et al. (2007)	10	8.36	Yes (Acetate)
	50	19.51	Yes (Propionate)
Flowers et al. (2009)	25	1.42	No (Acetate +
	25	2.94	Yes casaminoacids)
Zhou et al. (2010)	20	14.61	No (Acetate)
	30	18.29	
	60	8.44	
	120	2.67	
This work	15	9.79	Yes (Glutamate)
	23.6	5.29	
	61.9	4.73	
	82.9	2.69	

Concerning the P/N ratio (Table 5.2), it was in the range 0.71-0.89 mol P·mol N^{-1} for initial nitrate concentrations ranging 15.0-61.9 mg NO_3^--N L^{-1}. For the higher nitrate concentrations tested (70.7 and 82.9 mg NO_3^--N L^{-1}) the P/N ratio decreased down to 0.49 mol P·mol N^{-1}. Lv et al. (2014) conducted a study consisting on three SBRs using acetate, propionate and glycerol as sole carbon sources. P/N ratios of 0.75, 0.76 and 0.57 mol P·mol^{-1} N were obtained for acetate, propionate and glycerol, respectively, with an initial nitrate concentration of 20 mg N·L^{-1}. The P/N ratio obtained for acetate and propionate are in the range of the average P/N ratio (0.78 ± 0.09 mol P·mol^{-1}N) observed in this study for initial nitrate concentrations between 15-27.7 mg NO_3^--N L^{-1}. Finally, Carvalho et al. (2007) obtained a P/N value of 0.82 mol P·mol^{-1}N in a PAOI-enriched sludge, which is in agreement with the values obtained in this study for nitrate concentrations ranging 15-

61.9 mg NO_3^--N L^{-1}. Different P/N ratios for nitrite and nitrate were obtained in the present study when the inhibition was not present. This difference can be explained by the different oxygen equivalence in both species, being 1.67 times higher for the nitrate than for the nitrite therefore, lower nitrogen is required per unit of phosphorus uptake. The average P/N ratio for nitrate was 0.79 ± 0.07 mol P·mol^{-1}N which was 1.67 times higher than the average P/N ratio for nitrite (0.44 ± 0.10 mol P·mol^{-1}N).

The maximum P-uptake rate in our work (9.8 mg P·g^{1} VSS·h^{-1}) was obtained with an initial nitrate concentration of 15 mg NO_3^--N L^{-1}. However, lower concentrations were not tested. On the other hand, Zhou et al. (2010), observed an increase in the P-uptake rate with the increase in the initial nitrate concentration until 30 mg NO_3^--N L^{-1}, which was considered as the optimal concentration in their study.

5.3.3. Different electron donors

Textbook knowledge states that a high VFA/COD ratio is a key factor to achieve efficient phosphorus removal (Guerrero et al., 2012; Lv et al., 2014; Merzouki et al., 2005). However, in a glutamate-fed system, the effect of VFA is not clear a priori, as some microorganisms may be able to use glutamate without a fermentation step, while others as *Accumulibacter* PAO need the previous fermentation of glutamate to VFA for a good EBPR performance. Considering that acetic and propionic acids are the two most common VFA present in domestic wastewaters (Pijuan et al., 2004b), batch experiments with acetic acid, propionic acid and glutamate as sole carbon sources were conducted to study the behavior of our glutamate-fed bio-P sludge. Figure 5.8 shows the experimental profiles for three batch experiments under sequential anaerobic and aerobic conditions. Similar trends were observed in all batch tests: the carbon source was anaerobically consumed linked to P-release and phosphorus was taken up in the subsequent aerobic phase.

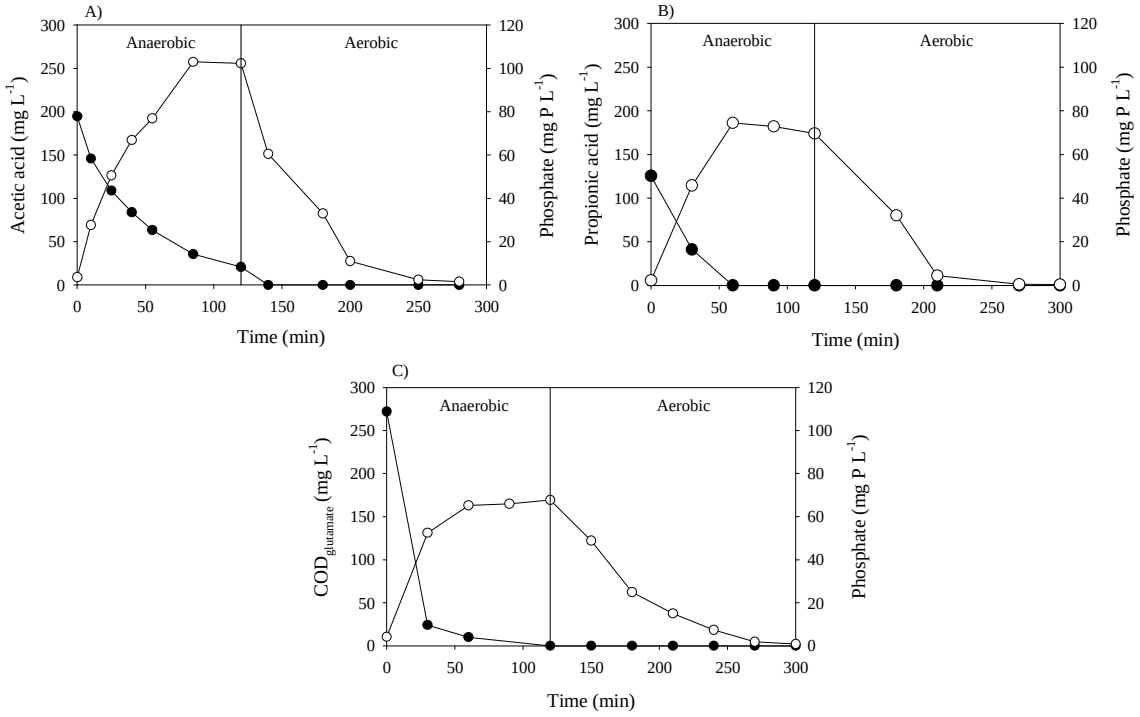

Figure 5.8. Batch tests performed with different carbon sources. A) Acetic acid. B) Propionic acid. C) Glutamate. Carbon source (●), phosphorus (○).

The carbon uptake rate for glutamate (57.8 mg C·g^{-1} VSS·h^{-1}) was higher in comparison to that found with acetic and propionic (27.4 and 41.0 mg C·g^{-1} VSS·h^{-1} respectively) (Table 5.5), since the biomass was acclimatized to this carbon source. The P/C ratio observed for acetic acid (0.55 mol P·mol^{-1} C) was in accordance with the literature values for *Accumulibacter* PAO: 0.32 to 0.66, being 0.5 the most accepted value (Oehmen et al. (2004), Zeng et al., 2003 and Mcmahon et al., 2002). The P/C ratio obtained for propionic acid was 0.45, which was similar to the value obtained by Pijuan et al. (2004b). Finally, the P/C ratio observed for glutamate in the batch tests (0.21 mol P·mol^{-1} C) was slightly higher than that obtained in the continuous operation (0.15 ± 0.07 mol P·mol C^{-1}). It is a low value in the range of similar ratios obtained using complex carbon sources such as glycerol (0.2 mol P·mol C^{-1}, Guerrero et al. (2012)) or casein hydrolysate (0.35 mol P·mol^{-1} C, Marques et al. (2017)). Regarding P, the highest P-release rate was obtained for propionic acid; however, the P-uptake rate was the highest for acetic acid. This is in contrast with the results obtained by Patel and Nakhla (2006) , where the P-release and P-uptake rates were higher in the case of acetic acid than for propionic acid and other carbon sources such as butyric acid and primary effluent. For propionic acid and glutamate, the P-uptake rates were similar. In the case of the batch test with glutamate,

no VFA were detected during the anaerobic phase, which indicated that the VFA consumption rate was probably limited by the VFA formation rate. The fast glutamate consumption could indicate that some microorganisms are able to use glutamate directly without a fermentation step. However, unavoidably, some glutamate is fermented to VFA, which explain the high P-release with acetate and propionate (Figures 5.8A and 5.8B).

Table 5.5. Observed uptake and release rates for different carbon sources

Carbon source	Specific P release rate (mg P·g^{-1} VSS·h^{-1})	Carbon uptake rate (mg C·g^{-1} VSS·h^{-1})	Specific P-uptake rate (mg P·g^{-1} VSS·h^{-1})	P/C ratio (mol P·mol C^{-1})
Acetic acid	24.3	27.4	31.5	0.55
Propionic acid	36.1	41.0	21.3	0.45
Glutamate	30.6	57.8	21.4	0.21

5.3.4 Phosphorus removal under permanent aerobic conditions

Four batch experiments were performed using different aeration flowrates to assess the behavior of the mixed culture when the electron donor (glutamate) and the electron acceptor (nitrate and oxygen) were present simultaneously. Glutamate contains nitrogen, which is degraded to ammonia, and this ammonia is oxidized to nitrate when oxygen is present. P-release under aerobic conditions is observed in Figure 5.9 and the presence of nitrate is due to the carbon source used. As observed in previous studies (Guisasola et al., 2004; Pijuan et al., 2005), two different phases (feast and famine) could be distinguished, despite the aeration conditions were not changed along the experiment. In the feast phase, glutamate was consumed linked to P-release and oxygen consumption. Moreover, nitrate concentration at the end of the feast phase was 15.7 mg NO_3^--N L^{-1}. When glutamate was depleted, oxygen concentration started to increase and P-uptake took place.

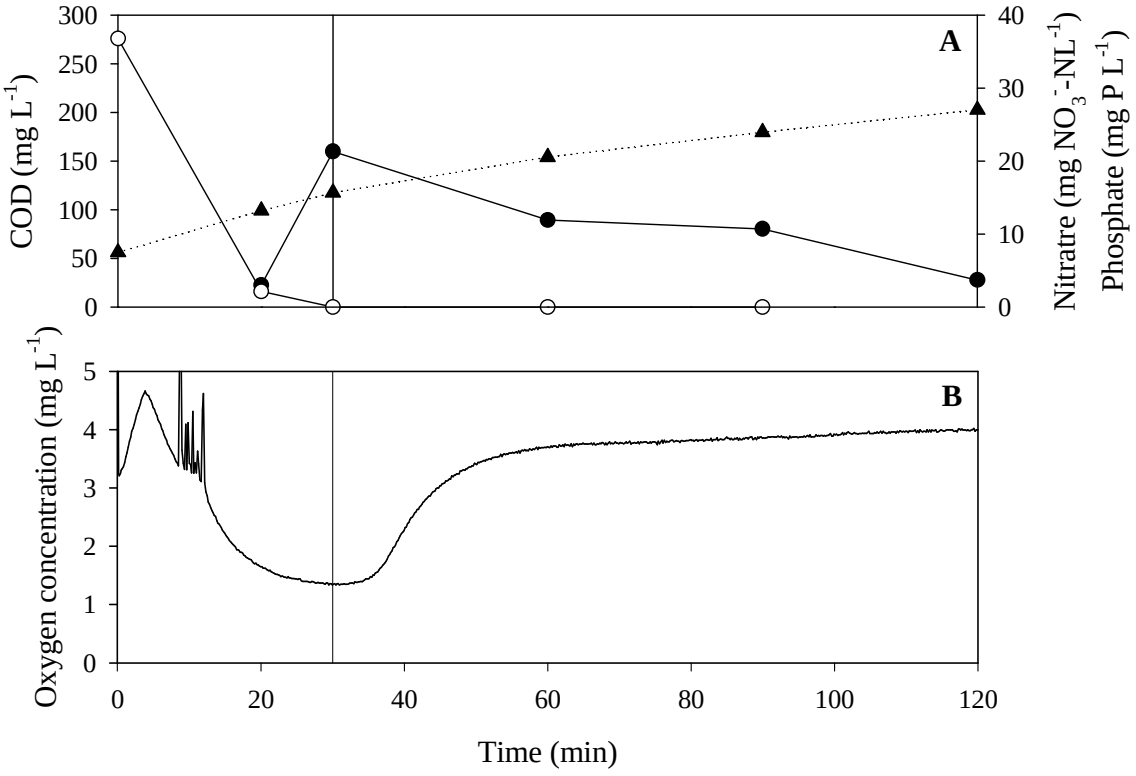

Figure 5.9. Batch experiment performed with sludge withdrawn from the aerobic chamber under permanent aerobic conditions. (A) Experimental profiles of different compounds: Phosphorus (●), COD (○) and nitrate (▲). (B) DO profile obtained for an oxygen flowrate of 500 mL min^{-1}.

The different phosphate profiles obtained in the batch tests using different aeration flowrates are shown in Figure 5.10. The maximum value achieved for P-release (44.5 mg P L^{-1}) was obtained under strong oxygen limited conditions (DO concentration in the bulk liquid was near zero during the experiment), when aeration flowrate was 50 mL min^{-1}. However, when the aeration flowrate was increased to 500 mL min^{-1} (with a DO concentration between 4 and 1.5 mg L^{-1}), the P-release resulted in 21.3 mg P L^{-1} (Figure 5.9). In this sense, Pijuan et al. (2005) obtained higher values (ca. 49 mg P L^{-1}) in the feast phase, at 2 mg L^{-1} of oxygen concentration. Therefore, the mixed culture used in this study was able to release phosphorus when the carbon source and oxygen were present simultaneously, moreover, net P-removal was observed in the whole range of DO applied. The lower the aeration flowrate, the higher phosphorus release was (Figure 5.10). Nevertheless, some oxygen limitation when the aeration flowrate were 50, 150 and 250 mL min^{-1} could allow such P-release. In fact, DO concentration reached zero values during the feast phase when the metioned aeration flowrates were used and this could

difficult oxygen penetration in the biomass, creating anaerobic conditions inside the floccules. Contrarily, the minimum DO concentration achieved during the feast phase was 1.35 mg L^{-1} when the aeration flowrate was 500 mL min^{-1}. Another explanation to the behavior observed in Figure 5.10 can be the glutamate fermentation degree, i.e. the higher the oxygen presence during the feast phase, the lower glutamate fermentation was. Therefore, *Accumulibacter* which live on fermentation products, can not contribute to the P-release.

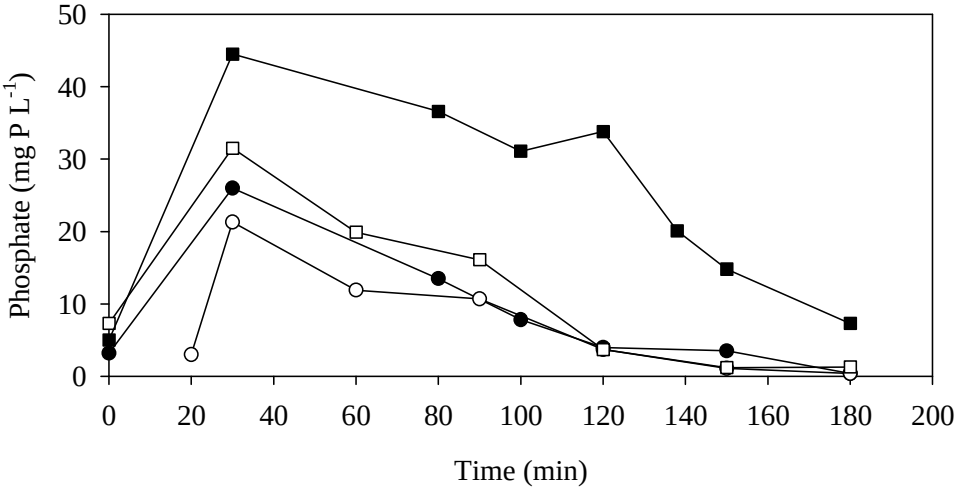

Figure 5.10. Phosphate concentration profiles of different batch tests under permanent aerobic conditions using different aeration flows: 50 mL·min^{-1} (■), 150 mL·min^{-1} (□), 250 mL·min^{-1} (●) and 500 mL·min^{-1} (○).

Vargas et al. (2009) indicated that it is possible to maintain EBPR activity under permanent aerobic conditions in a long term with propionate as sole carbon source. Nittami et al. (2011) operated an SBR under strictly aerobic conditions for one cycle every three or four days alternating with anaerobic-aerobic operation with acetate as carbon source. Another studies reporting that the simultaneous presence of electron donor and acceptor does not affect the long-term operation of the EBPR were Ahn et al. (2007) and Yadav et al. (2016). Nevertheless Pijuan et al. (2006), observed that net phosphorus removal was achieved under permanent aerobic conditions only during the first 4 days of operation when acetate was used as carbon source. In the same line, Zafiriadis et al. (2017) reported that the simultaneous presence of electron donor and acceptor in the mixed liquor inhibited phosphorus uptake. These discrepancies may be attributed to differences in the biomass community structure and functionality, which was affected by the carbon source used, indicating the necessity for further experimentation (Nittami et al., 2017).

5.4. Conclusions

This is the first report that studies the denitrifying capabilities of a bio-P sludge with a microbial community as diverse as bio-sludge from real WWTPs. The biomass was enriched in *Rhodocyclaceae* (23.36%), *Chitinophagaceae* (14.7%), *Saprospiraceae* (10.05%) and *Cytophagaceae* (9.84%). *Comamonadacae* (4.49%) and *Thiothrichaceae* (2.93%) were also detected. This microbial community was capable to use both nitrite and nitrate as electron acceptors for P-uptake. P-uptake was affected by the FNA concentration and the process completely stopped at FNA values of 2 µg HNO_2-N L^{-1}. This value is lower than the inhibitory concentrations reported for *Accumulibacter*-enriched cultures. In the case of nitrate, a decrease in the consumption rates instead of complete inhibition was observed. A reduction of 72% on the P-uptake rate was observed when the initial nitrate concentration increased from 15 to 82.9 mg N-NO_3^- L^{-1}.

The amount of phosphorus uptake using nitrate was a 38% higher than when the electron acceptor is nitrite for the same initial concentration of both electron donors. However, the P-uptake rates were an average of 30% higher using nitrite.

The microbial culture developed in this work was able to perform EBPR under permanent aerobic conditions however, the concentrations of P released obtained were lower than the observed by Pijuan et al. (2006). Further research is needed because there is no agreement in the effect of the simultaneous presence of electron donor and acceptor on EBPR activity.

Finally, it seems that our biomass is more sensitive to nitrite and to oxygen presence than other cultures highly enriched in different types of *Accumulibacter*.

Chapter 6

AMINO ACIDS AS COMPLEX CARBON SOURCE FOR EBPR

This work has been done at the Facultade de Ciências e Tecnologia, Universidade Nova de Lisboa (Caparica, Portugal) under the supervision of Dr. Ricardo Marques (*in memóriam*).

ABSTRACT

Tetrasphaera and *Candidatus* Accumulibacter are two abundant polyphosphate accumulating organisms (PAOs) in full-scale enhanced biological phosphorus removal (EBPR) systems. Although real wastewater is composed by a combination of lipids, carbohydrates and proteins, only volatile fatty acids (VFAs) are typically used as carbon source in lab-scale EBPR studies. Thus, it is important to study EBPR performance with other complex carbon sources that can be found in full scale wastewater treatment plants (WWTPs). Specifically, this work shows the performance of a mixed culture composed by mostly *Tetrasphaera* and with *Accumulibacter* presence that was developed in an SBR using casein hydrolysate as sole carbon source. Batch tests were conducted to study the utilization capabilities of different amino acids (arginine, lysine, cysteine, proline and tyrosine) by this mixed culture. The *Tetrasphaera*-enriched culture was able to use all the amino acids as carbon source for EBPR except for cysteine. Moreover, the fermentation products of the different amino acids were involved on polyhydroxyalkanoates (PHA) and glycogen as storage polymers. Moreover, four additional batch tests were conducted with other types of sludge (two withdrawn from lab-scale SBRs and two from WWTPs) to investigate the relation between the microbial community and the capability to use different complex carbon sources.

6.1. Introduction

The type of carbon source is a key parameter for EBPR viability and stability (Shen and Zhou, 2016). In fact, it is one of the main differences between lab-scale and full-scale systems. Simple carbon sources such as volatile fatty acids (VFAs) are normally supplied at lab scale, resulting in the proliferation of *Candidatus* Accumulibacter phosphatis (Crocetti et al., 2000). Nevertheless, it is known that *Tetrasphaera*-related organisms are present in a higher abundance (up to 30% of the total bacteria) than *Accumulibacter* in full-scale EBPR systems in Denmark and Portugal (Lanham et al., 2013a; Stokholm-Bjerregaard et al., 2017). In contrast to *Accumulibacter*, *Tetrasphaera* are more versatile in substrate uptake capabilities, as they can take up amino acids and glucose (Nguyen et al., 2015, 2011), and are capable of fermenting complex organics (Marques et al., 2017). Other distinguishing trait between *Accumulibacter* and *Tetrasphaera* is the capability to store PHA. Kong et al. (Kong et al., 2005) reported that *Tetrasphaera* is not able to store PHA, while Mckenzie et al. (Mckenzie et al., 2006) concluded that only three filamentous species (*T. veronensis, T. jenkinsii* and *T. vanveenii*) are able to synthesize PHA. Hence, the utilization of other storage polymer in *Tetrasphaera* is rather plausible, although they can synthesize glycogen. In fact, Nguyen et al. (2015), using amino acids as carbon sources, showed that during the anaerobic phase labelled glycine was consumed and the majority was store intracellularly as free glycine and fermentation products. In the subsequent aerobic phase, the stored glycine was consumed. In addition, Marques et al. (2017) identified amino acids, amines, sugars and acids as intracellular metabolites during a cycle study performed in an SBR with a *Tetrasphaera*-enriched culture using sodium casein hydrolysate (hereafter refer as Cas_aa) as carbon source.

All current metabolic models for EBPR were developed based on acetate (García Martín et al., 2006) or glucose (Kristiansen et al., 2013a), and hence do not cover the use of amino acids. This fact, together with wastewater being a complex matrix composed by proteins (25-35%), lipids (25-35%) and carbohydrates (15-25%) (Nielsen et al., 2010) highlights the importance of understanding the role of *Tetrasphaera* in EBPR systems when amino acids are used as carbon source. To the best of our knowledge, only Marques et al. (2017) and Nguyen et al. (2015) studied the storage products and metabolic pathways in a *Tetrasphaera*-enriched sludge with amino acids as carbon source. Likewise, investigations at full-scale level are still few, and the existing studies are performed with acetate (Lanham et al., 2013a) or are focused in describing the microbial

diversity in WWTPs (Cydzik-Kwiatkowska and Zielinska, 2016; Wang et al., 2012). Therefore, is also essential to study the metabolic performance of the microbial communities in WWTPs with amino acids as carbon source.

In this study, anaerobic/aerobic bath tests with different amino acids were conducted to investigate the preferred carbon source by a *Tetrasphaera*-enriched culture, besides to study the EBPR performance. Another set of anaerobic/aerobic batch tests with different types of sludge were performed using two complex carbon sources: casein hydrolysate (Cas_aa) and a mixture of five amino acids (arginine, lysine, cysteine, proline and tyrosine) (Mix_aa). Four sludge samples were used, two withdrawn from lab-scale reactors (*Tetrasphaera*-enriched and *Accumulibacter*-enriched sludge) and two withdrawn from WWTPs (one of them with EBPR and the other only with biological nitrogen removal (BNR)). The aim of this set of batch tests was to explore the associations between the utilisation of the two complex carbon sources and the PAO-GAO bacterial community of each sludge, characterised using fluorescence *in situ* hybridization (FISH). We hypothesised that differential utilisation of carbon sources is related to a distinct PAO community. Furthermore, the involvement of storage polymers (PHA and glycogen) may also be associated to the microbial community and their capabilities to uptake different complex substrates.

6.2. Materials and methods

6.2.1. SBR operation

A sequencing batch reactor (SBR) of 2 L was enriched in *Tetrasphaera* and operated for several months. The inoculum was obtained from the same set-up as in the work of Marques et al. (2017). The SBR was operated with cycles of 8 h, including an anaerobic phase (4 h), a settling/extraction/idle phase (1 h) and an aerobic phase (3 h). A settling/extraction/idle phase was introduced between the anaerobic and aerobic phases to minimise the organic carbon entering to the aerobic phase. 1 L of supernatant was extracted before the start of the aerobic phase. The reactor was continuously fed during the first 3 h of the anaerobic phase with a flow rate of 133.3 $mL \cdot h^{-1}$ with Cas_aa (Fluka, USA) as sole carbon source and mineral media (400 mL). Phosphate medium (600 mL) was fed at the start of the aerobic phase during 2 min which implied a concentration of 1.8 mmol $P \cdot L^{-1}$ inside the reactor besides the P concentration coming from the release in the anaerobic phase. The SBR was operated with a hydraulic retention time (HRT) and sludge retention time (SRT) of 16 h and 20 days respectively. Anaerobic/aerobic

conditions were obtained by bubbling either argon or air, respectively. pH was controlled at 7.1 ± 0.1 by automatic addition of 0.1 M HCl and temperature was also controlled at 20 ± 1 ºC. The stirring rate was kept constant at 300 rpm during the anaerobic and aerobic phases. The reactor performance was assessed weekly through routine biological and chemical analyses.

6.2.2. Culture media

The composition of the SBR culture media was similar to that used in Marques et al. (2017), briefly: the mineral medium with carbon source contained per litre 0.77 g Cas_aa, 0.37 g NH_4Cl, 0.59 g $MgSO_4 \cdot 7H_2O$, 0.28 g $CaCl_2 \cdot 2H_2O$, 0.01 g N-Allythiourea (ATU), 0.02 g ethylene-diaminetetraacetic (EDTA) and 1.98 mL of micronutrient solution. The micronutrient solution was prepared based on Smolders et al. (1994a) and contained (g/L): 1.5 $FeCl_3 \cdot 6H_2O$, 0.15 H_3BO_3, 0.03 $CuSO_4 \cdot 5H_2O$, 0.18 KI, 0.12 $MnCl_2 \cdot 4H_2O$, 0.06 $Na_2MoO_4 \cdot 2H_2O$, 0.12 $ZnSO_4 \cdot 7H_2O$ and 0.15 $CoCl_2 \cdot 6H_2O$. The phosphate medium contained (g/L) 0.47 K_2HPO_4 and 0.29 KH_2PO_4. The mineral medium and the micronutrient solution were autoclaved, but prior to this, pH was set to 7.4 ± 0.1 in the Cas_aa and the mineral medium. In the batch tests, the mineral and phosphate media had the same composition as that described for the SBR. For the batch tests with only one carbon source, it was selected an initial concentration of 5 C-mM for each of the carbon sources (Cas_aa, Arginine, Lysine, Cysteine, Proline and Tyrosine). For the test with combination of carbon sources, it was selected an initial concentration in the reactor of 1 C-mM for each carbon source (Arginine, Lysine, Cysteine, Proline and Tyrosine, 5aa). In all carbon source media, the pH was set to 7.0 ± 0.1 by the addition of 2 M NaOH.

6.2.3. Batch tests

Anaerobic/aerobic batch tests were performed with different amino acids in order to investigate the preferred carbon source by the different cultures. Moreover, the experimental phosphorus, TOC, PHA and glycogen profiles were measured for each of the cultures. Four sets of batch tests were carried out:

A) Tests performed with the enriched *Tetrasphaera* sludge obtained in this study with A1) Five individual amino acids (Arginine, Lysine, Cysteine, Proline and Tyrosine), A2) Cas_aa, A3) a balanced mixture of the aforementioned amino acids and A4) a blank test without any carbon source.

B) Tests performed with sludge withdrawn from Beirolas WWTP (SIMTEJO, Lisbon, Portugal) which includes EBPR process with B1) Cas_aa, B2) the balanced mixture of amino acids and B3) a blank test without any carbon source.

C) Tests performed with sludge withdrawn from Chelas WWTP (Lisbon, Portugal) which has BNR process and chemical phosphorus removal with C1) Cas_aa, C2) the balanced mixture of amino acids and C3) a blank test without any carbon source.

D) Tests performed with an enriched *Accumulibacter* culture with D1) Cas_aa, D2) the balanced mixture of amino acids and D3) a blank test without any carbon source.

The whole protocol for the batch tests was:

Pre-tests: 400 mL of sludge was left to settle, the supernatant was removed and the sludge was washed twice with mineral media M1 (Table 6.1). The sludge was suspended in 250 mL of solution M2 (Table 6.1). If the settling phase was not efficient enough, the sludge was centrifuged at 6000 rpm for 10 min and resuspended in 250 mL of M2.

Anaerobic phase: The SBR for the batch tests (500 mL) was inoculated with 250 mL of the sludge resuspended in mineral medium M2 and 150 mL of phosphorus medium (Table 6.2). Argon was bubbled to ensure that no oxygen was present before adding the carbon source (100 mL) (or water in the case of blank assays). Argon was also bubbled in the carbon sources (or water) before their addition to the inoculated sludge.

Settle/extraction phase: This phase was introduced between the anaerobic and aerobic phases to avoid the organic carbon entering to the aerobic phase. Therefore, the sludge was left to settle, the supernatant was removed and the sludge was washed twice with mineral media M1. The sludge was suspended in 250 mL of solution M2. If the settling phase was not efficient enough, the sludge was centrifuged at 6000 rpm for 10 min and resuspended in 250 mL of M2.

Aerobic phase: 250 mL of the sludge resuspended in mineral medium M2, 150 mL of phosphorus medium and 100 mL of water were added to the SBR. The sludge was the last to be added. The aerobic phase started with biomass addition and the sparging of compressed air.

Samples were withdrawn for total organic carbon (TOC), PHA, glycogen, phosphate, ammonia, poly-P concentration, as well as for FISH. Samples were also taken at the

beginning and end of each phase for the determination of the total suspended solids (TSS) and the volatile suspended solids (VSS).

Finally, the carbon recovery ratio (CRR) was calculate for all batch tests. The carbon recovery ratio determines which part of the inlet carbon taken up and the glycogen consumed during the anaerobic phase is transformed to PHA.

6.2.4. Chemical analyses

Inorganic phosphate and ammonia were analysed by segmented flow analysis (Skalar 5100, Skalar Analytical, The Netherlands). Total P concentration was determined as described by Carvalheira et al. (2014). The VFA concentration in the supernatant was determined by high-performance liquid chromatography (HPLC) using a Metacarb 87 H (Varian) column and a refractive index detector (RI-71, Merk) as described in Carvalheira et al. (2014). Glycogen was determined as described by Lanham et al. (2013a) (conditions: 2 mg biomass, HCl 0.9 M and 3 h of digestion time). PHA was determined by gas chromatography (GC) using the method described by Lanham et al. (2013b), using a Bruker 430-GC gas chromatograph equipped with a FID detector and a BR-SWax column (60m, 0.53 mm internal diameter, 1 mm film thickness, Bruker, USA). The carbon source uptake was assessed through the analysis of total organic carbon (TOC) by a Shimadzu TOC-VCSH (Shimadzu, Japan). Total suspended solids (TSS) and volatile suspended solids (VSS) were analysed according to APHA, (1995).

Table 6.1. Composition of the mineral media M1 and M2 used in the batch tests for washing the sludge (pH adjusted to 7.0 and autoclaved).

Compound	M1 ($g \cdot L^{-1}$)	M2 ($g \cdot L^{-1}$)
NH_4Cl	0.074	0.148
$MgSO_4 \cdot 7H_2O$	0.098	0.196
$CaCl_2 \cdot 2H_2O$	0.055	0.110
ATU	0.001	0.003
EDTA	0.004	0.008
Micronutients*	0.396	0.792

*(Smolders et al., 1994b)

Table 6.2. Phosphorus media used in batch tests (pH adjusted to 7.0).

Compound	$g \cdot L^{-1}$
K_2HPO_4	0.316
KH_2PO_4	0.193

6.2.5. Microbial characterisation

FISH was performed at the end of the anaerobic phase using the following oligonucleotide probes: EUBMIX (equimolar concentrations of EUB338, EUB338II and EUB338III) (Amann et al., 1990; Daims et al., 1999), which target all bacteria; PAOMIX (PAO651, PAO462 and PAO846 (Crocetti et al., 2000)), which targets most members of the Accumulibacter cluster; and Tet1-266, Tet2-892, Tet2-174 and Tet3-654, which target most *Tetrasphaera*-related PAOs (Nguyen et al., 2011). GAOMIX (GAOQ431, GAOQ989 and GB_G2) targeting *Competibacter* GAOs (Crocetti et al., 2000; Kong et al., 2002). FISH samples were observed using an Olympus BX51 epifluorescence microscope.

6.3. Results and discussion

6.3.1. SBR performance and microbial composition

The SBR was operated during more than 14 weeks with Cas_aa as sole carbon source. During this period, periodic monitoring and several cycle studies were conducted to evaluate the reactor performance and to ensure that a pseudo steady state operation was achieved. Figure 6.1 shows the monitoring of a conventional SBR cycle obtained after 4 weeks of operation.

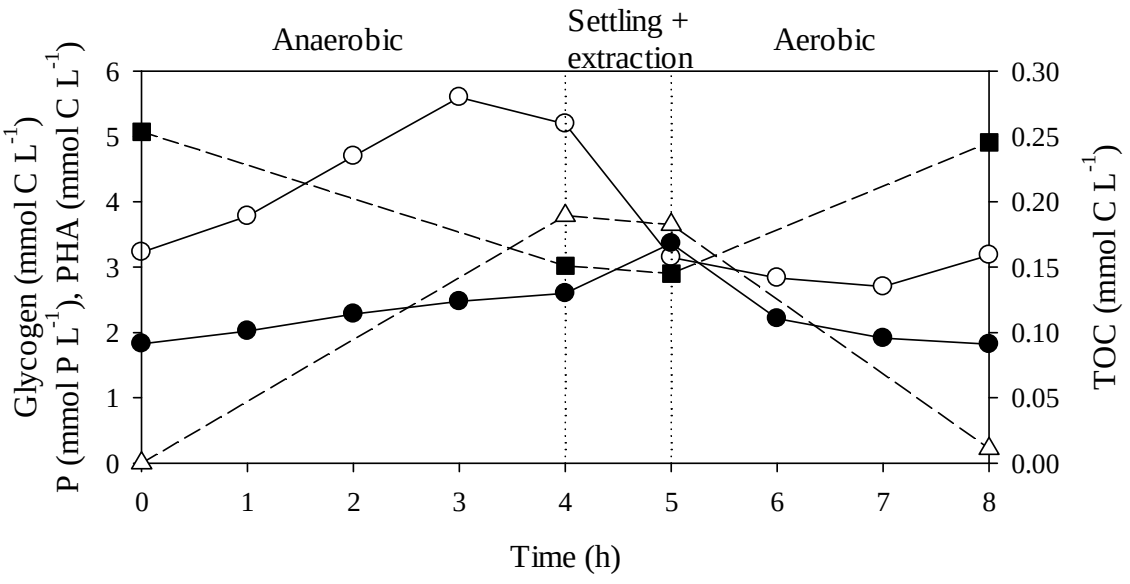

Figure 6.1. Conventional batch experiment conducted during the SBR operation with continuous feed during the first three hours. Phosphorus (●), TOC (○), PHA (Δ) and glycogen (■).

Cas_aa was taken up during the anaerobic phase, linked to P-release, glycogen hydrolysis and PHA production. TOC (i.e. the sole organic source, Cas_aa) increased during the anaerobic phase because Cas_aa was continuously dosed during the first three hours of anaerobic phase up to a total addition of 17 mmol C. This strategy was adopted to elude substrate inhibition problems under anaerobic conditions. The deleterious effect of the carbon source being present in the aerobic phase was avoided by settling the sludge between the anaerobic and aerobic phases and replacing the reactor supernatant by a fresh P-rich medium without TOC. In the subsequent aerobic phase, PAO were able to replenish their poly-P and glycogen pools.

High PAO activity was clearly detected and the P-uptake was 1.54 mmol $P \cdot L^{-1}$, similar to the valued obtained by Marques et al. (2017) with a 0.5 L SBR enriched in *Tetrasphaera* (1.5 mmol $P \cdot L^{-1}$). However in the later study, a complete P-removal was observed and no P was detected in the effluent, in contrast to concentrations about 1.82 mmol $P \cdot L^{-1}$ observed in the effluent of the current research. Since PHA are scarcely involved in the *Tetrasphaera* metabolism (i.e. most *Tetrasphaera*-related organisms are not able to produce or oxidize PHA (Kristiansen et al., 2013a)), the lower the PHA involvement in an EBPR system, the higher the *Tetrasphaera* enrichment. We detected a higher PHA involvement (PHA_{prod}/C_{upt} = 0.23 mol $C \cdot mol^{-1}C$ and aerobic PHA consumption of 3.56 mmol $C \cdot L^{-1}$) compared to the work of Marques et al. (2017) (0.15 mol $C \cdot mol^{-1}C$ and 0.75 mmol $C \cdot L^{-1}$, respectively). Nevertheless, the PHA contribution in this study was significantly lower than the typical values observed for *Accumulibacter* enriched systems (1.33 mol $C \cdot mol^{-1}C$ (Smolders et al., 1994b) and 7.60 mmol $C \cdot L^{-1}$ (Oehmen et al., 2005c), respectively). Regarding the other storage polymer implied in the PAOs metabolism, glycogen, the Gly_{deg}/C_{upt} ratio was 0.12 mol $C \cdot mol^{-1}C$, lower than the 0.38 mol $C \cdot mol^{-1}C$ obtained by Marques et al. (2017) and also lower than typical values observed for *Accumulibacter* enriched systems with values between 0.3-0.5 (Oehmen et al., 2005c; Smolders et al., 1994b). However, under aerobic conditions, glycogen consumption was higher (2.01 mmol $C \cdot L^{-1}$) when compared to the work of Marques et al. (2017) (1.38 mmol $C \cdot L^{-1}$). These anaerobic and aerobic ratios are summarized in Table 6.3, together with the P/C ratio (0.14 mol $P \cdot mol^{-1}C$), which was lower than the values obtained in the previous work (0.35 mol $P \cdot mol^{-1}C$).

Table 6.3. Anaerobic/aerobic ratios from typical cycle studies during SBR operation and comparison with previous results

	Accumulibacter + *Tetrasphaera* (Cas_aa)		*Accumulibacter*
	This study	(Marques et al., 2017)	Acetate
Anaerobic results			
P/C ratio (mol P·mol^{-1}C)	0.14	0.35	0.48[a]
PHA_{prod}/C_{upt} (mol C·mol^{-1}C)	0.23	0.15	1.33[a]
Gly_{deg}/C_{upt} (mol C·mol^{-1}C)	0.12	0.38	0.50[a]
Aerobic results			
P_{uptake} (mmol P·L^{-1})	1.54	1.76	2.50[b]
PHA consumption (mmol C·L^{-1})	3.56	0.75	7.60[b]
Gly production (mmol C·L^{-1})	2.01	1.38	3.62[c]

[a] (Smolders et al., 1994b)
[b] (Oehmen et al., 2005c)
[c] (Smolders et al., 1994a)

FISH analyses were conducted to evaluate the presence of *Accumulibacter* in our system. The amount of *Accumulibacter* observed in this work (Figures 6.2A and 6.2B) was clearly higher than the abundance of 20% reported by Marques et al. (2017). This fact, could explain the higher role of PHA in the system. In addition, the lower P/C ratio obtained in this work could be attributed to a higher presence of *Competibacter* (Figures 6.2C and 6.2D) when compared with the previous work where an abundance for GAOMIX below 1% was reported. A higher presence of *Competibacter* should be an indicator of a higher involvement of glycogen, in fact, glycogen production under aerobic conditions was higher (2.01 mmol C·L^{-1}) than the obtained for Marques et al. (2017) with a value of 1.38 mmol C·L^{-1}. However, unexpectedly, the Gly_{deg}/C_{upt} ratio was lower (0.12 mol C·mol^{-1}C) than the obtained for Marques et al. (2017) with a value of 0.38 mol C·mol^{-1}C.

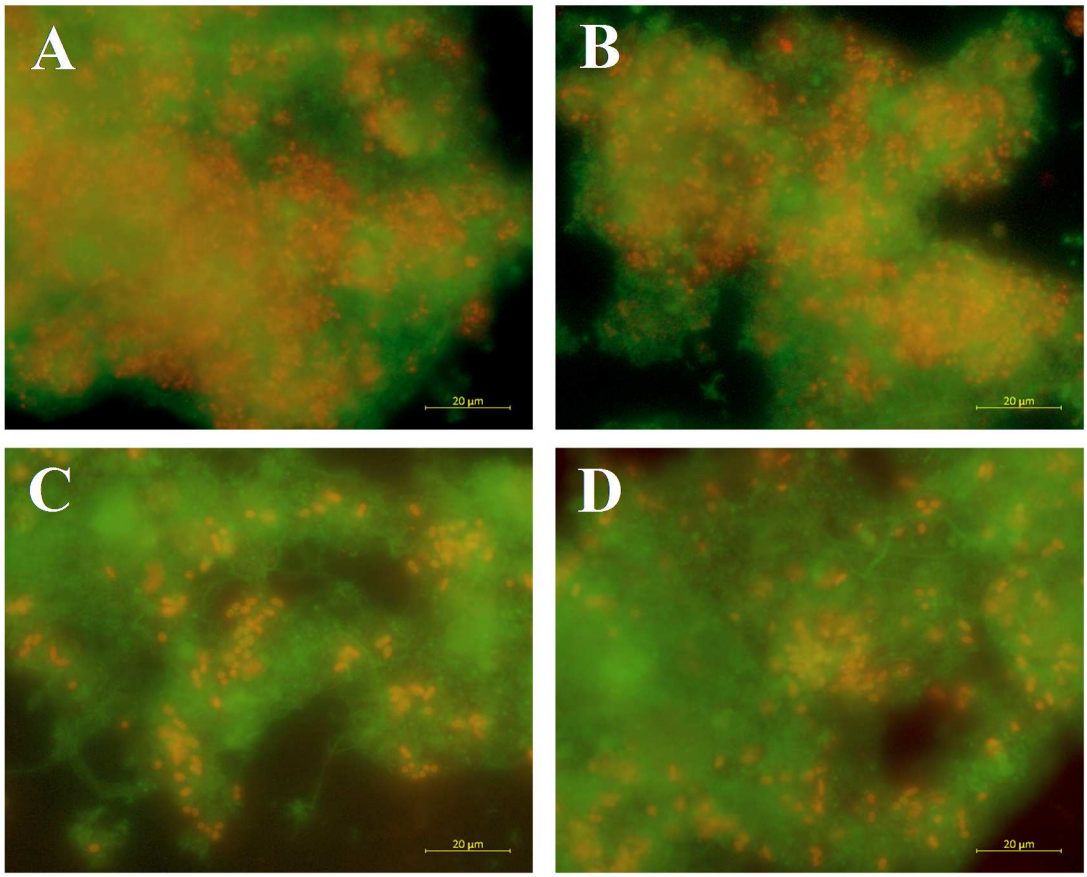

Figure 6.2. CLSM micrographs of FISH for the biomass of SBR. A and B: green, all bacteria; orange, *Accumulibacter*. C and D: green, all bacteria; orange, *Competibacter*.

6.3.2. Tetrasphaera-enriched sludge batch tests with amino acids as carbon source

Tetrasphaera have been found to take up different carbon sources, such as glucose, casamino acids, glutamic acid (Nguyen et al., 2011) and also acetate, propionate, glutamate and aspartate (Kristiansen et al., 2013a). Previously, Marques et al. (2017) identified intracellular metabolites such as amino acids, amines, sugars an acids during a cycle study using Cas_aa in a *Tetrasphaera*-enriched sludge. These compounds could be used as potential electron donors. Therefore, amino acids were tested as sole carbon source to examine the preferred amino acid in terms of consumption rate and to evaluate the influence of the carbon source in the phosphorus release and uptake.

6.3.2.1. Individual amino acids as sole carbon source

The following carbon sources were tested: Arginine, cysteine, lysine, proline, tyrosine and Cas_aa. Figure 6.3 displays the experimental profiles of TOC (Figure 6.3A) and P (Figure 6.3B) for the batch experiments for each amino acid tested. The carbon source

was consumed during the anaerobic phase linked to P-release, while P-uptake was observed under aerobic conditions.

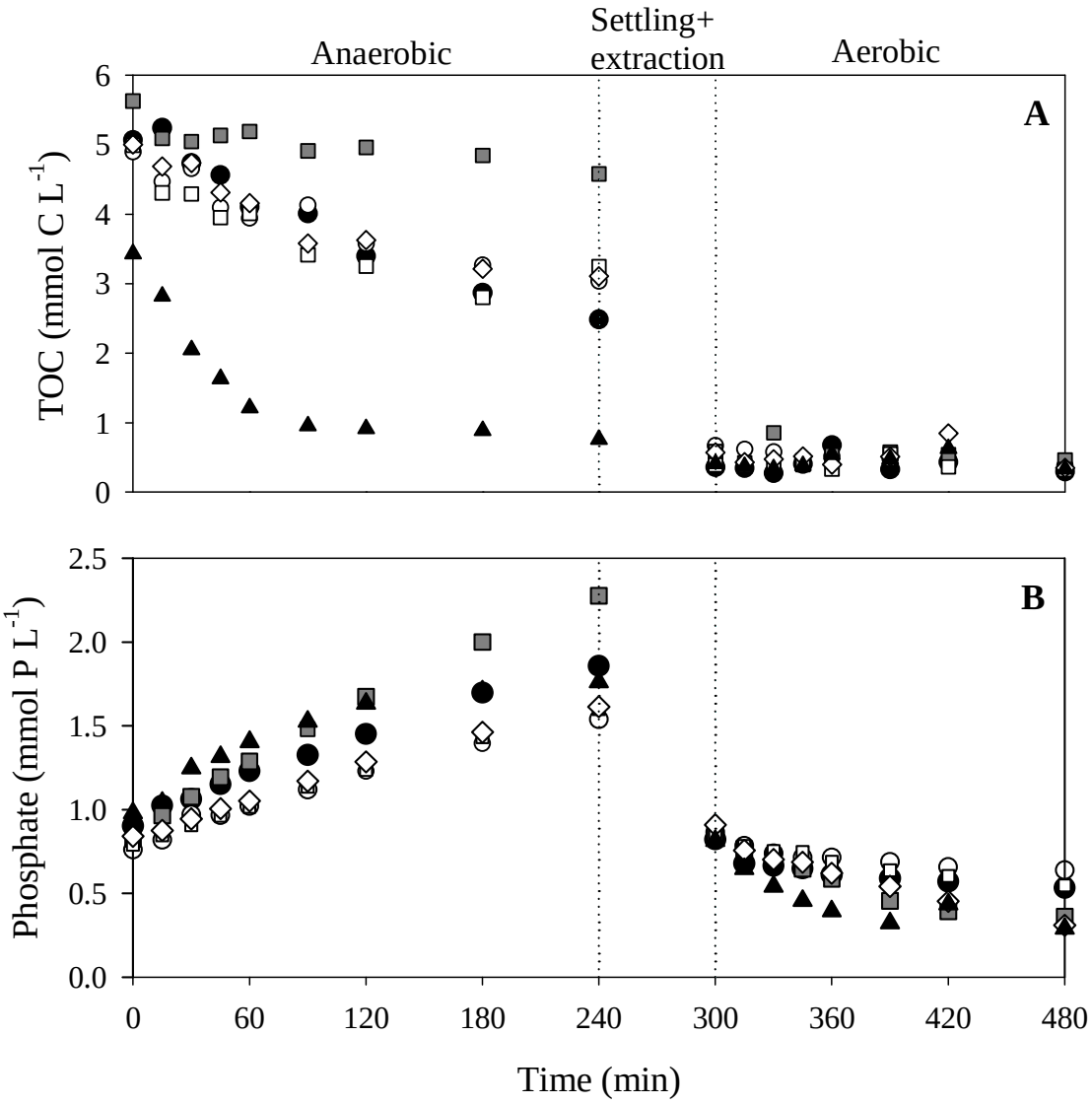

Figure 6.3. Anaerobic/aerobic batch experiments with a single amino acid as carbon source. A) TOC and B) phosphorus. Arginine (●), lysine (○), cysteine (■), proline (□), tyrosine (◊) and Cas_aa (▲).

All the amino acids exhibited a similar behaviour in terms of carbon consumption rate except of cysteine (grey squares), which was slower, and Cas_aa (black triangles), which was the highest by far. The EBPR ratios, rates and the anaerobic and aerobic yields for the six batch tests are shown in Table 6.4.

Different carbon uptake values were obtained for each amino acid despite the initial carbon concentration was the same for all batch tests. Around 41 ± 7% of the initial carbon was consumed except for Cas_aa (78%) and cysteine (19%). Regarding the P/C ratio, an

average of 0.42 ± 0.04 mol P·mol^{-1}C can be calculated if the two extreme ratios (Cysteine and Cas_aa) are excluded. This P/C is higher than the obtained for Cas_aa (0.29) but similar to the P/C ratios observed for other carbon sources such as propionate (Lu et al., 2006; Oehmen et al., 2005b; Pijuan et al., 2004b) or glutamate (Zengin et al., 2011). To the best of our knowledge, only Marques et al. (2017) tested different amino acids (glutamate, aspartate and glycine) as carbon source with an enriched-*Tetrasphaera* sludge. However, they observed lower P-release, obtaining a P/C ratio of 0.04 mol P·mol^{-1}C for glutamate. There are some other studies using amino acids (Nguyen et al., 2015; Qiu et al., 2019) and VFAs (Lanham et al., 2013a) as carbon sources, but with sludge withdrawn from full-scale WWTPs, as will be discussed in the next section.

Cysteine was not significantly consumed during the anaerobic phase, detecting only a total consumption of 1.05 mmol C·L^{-1} (Table 6.4). However, cysteine was surprisingly the carbon source with the highest P-release (1.45 mg P·L^{-1}). The P/C value obtained for cysteine (1.38 mol P·mol^{-1}C) was highly influenced by the low consumption of this carbon source during the batch test. Moreover, the ratio glycogen consumed per carbon uptake was higher (0.59 mmol C·mmol^{-1}C) than the ratios obtained for the other amino acids (0.21-0.37 mmol C·mmol^{-1}C) (Table 6.4 and Figure 6.3B). This fact would indicate that cysteine uptake and storage requires additional energy, leading to higher P-release and glycogen degradation as observed. Nevertheless, PHA involvement in this batch test was negligible and the CRR was very low (1.6%), suggesting that cysteine may have been converted into other intracellular storage compounds, probably amino acids. Unfortunately, internal amino acids could not be measured during the batch tests.

Regarding the Cas_aa, 78% of this substrate was consumed during the anaerobic phase and the carbon and P-uptake rates obtained were the highest (13.37 mg C·gVSS^{-1}·h^{-1} and 6.87 mg P· gVSS^{-1}·h^{-1}) compared with the individual amino acids tested (Table 6.5). These high rates could be attributed to the fact that Cas_aa is the usual carbon source in the SBR and hence, the *Tetrasphaera*-enriched sludge is acclimatized to this substrate. Regarding the P-release rate, this value was only slightly lower than that of cysteine (7.73 mg P·gVSS^{-1}·h^{-1} vs 6.87 mg P·gVSS^{-1}·h^{-1} obtained with Cas_aa).

The results obtained for the different amino acids are probably dependent on their fermentation pathways. However, predicting the nature of the fermentation products of each single amino acid is not straightforward. The range of the different fermentation products depends on the microbial community present and on the operational conditions.

Besides that, the nature of fermentation products is essential to understand the performance of the posterior EBPR process. In this sense, to the best of our knowledge, there is no previous report detailing the metabolism of *Tetrasphaera* using amino acids and, thus, the different fermentation products obtained in this case with a *Tetrasphaera*-enriched sludge. Therefore, we have to draw upon other existing works with different bacteria (e.g. *Clostridia*) to understand the possible metabolic pathways occurring in our system.

Tyrosine is an aromatic amino acid and, therefore, its structure is more complex than the rest of amino acids tested. Barker (1981) reported that the fermentation products derived from the anaerobic degradation of tyrosine by various *Clostridia* were aromatic compounds: hydroxyphenylacetic acid, hydroxyphenyl-lactic acid, hydroxyphenylpropionic acid, phenol and p-cresol, because the aromatic rings are apparently not modified by *Clostridia*. Only some groups of *Clostridia* are able to use the aromatic amino acids and ferment them to VFAs (Barker, 1981). Moreover, Cai et al. (2017) reported that the phyla Firmicutes, Actinobacteria and Proteobacteria can degrade the tyrosine present in extracellular polymeric substances. Cai et al. (2017) showed that tyrosine was directly metabolized into tyramine and phenol and, in addition, through indirect reactions, tyrosine could be converted into salidroside, succinate, fumarate and acetoacetate. Thus, given that *Tetrasphaera* is a genus belonging to Actinobacteria, the tyrosine fermentation products could be aromatic or complex compounds that *Accumulibacter* cannot use. This fact could explain that both PHA and glycogen were not involved during the anaerobic fermentation of tyrosine and in consequence would result in the low CRR value observed (1%). Despite the low involvement of PHA and glycogen during the anaerobic phase, some PHA consumption (0.12 mmol $C \cdot L^{-1}$) and glycogen production (0.24 mmol $C \cdot L^{-1}$) were observed under aerobic conditions. However, these values are obtained from a single cycle with this new carbon source, and are probably due to the residual activity of the polymers stored in previous cycles and could not be maintained under long-term feeding with this carbon source.

Likewise, proline is reduced to γ-aminovaleric acid by amino acid-degrading *Clostridia* (Barker, 1981). Although the fermentation product is an amino acid, there was no PHA involvement in the proline batch test. On the other hand, lysine and arginine produced PHA in the anaerobic phase and glycogen under aerobic conditions, with similar values to those obtained with Cas_aa. The fermentation products of these amino acids reported

in the literature are: i) lysine is converted to acetate, butyrate and ammonia by *Fusobacterium nucleatum* and lysine-fermenting *Clostridia* (Barker et al., 1982) and ii) arginine can be fermented to ornithine, acetate and formate or to methane and propionate depending on the culture used (Baena et al., 1999). Given that some fermentation products of these two amino acids are VFAs, *Accumulibacter* can use them as carbon source and store PHA and utilize glycogen. Moreover, the CRR for these two amino acids arginine and lysine, were higher (19 and 24%) than the obtained for the rest of individual amino acids. As a conclusion, amino acid fermentation products are very diverse and difficult to predict, but they are essential to understand the involvement of PHA and glycogen in the batch tests.

Finally, it is worth to mention that the P_{upt}/PHA_{oxid} ratios obtained in this study are higher than the model predictions for *Accumulibacter*-enriched cultures (0.41 mol $P \cdot mol^{-1}C$), and in some cases values of up to 8.76 mol $P \cdot mol^{-1}C$ clearly indicate that PAOs other than *Accumulibacter* are also key actors in P-removal. Moreover, this mixed culture also showed a high intracellular P content, accounting between 6 and 8% of the TSS concentration (Table 6.4). Nevertheless, the intracellular P values obtained in this study are lower than those observed by Marques et al. (2017), with a range between 8-19% and also lower than the range reported for *Accumulibacter*-enriched cultures which values are around 7-17% (Oehmen et al., 2007).

Table 6.4. EBPR ratios, rates and anaerobic and aerobic yields observed for the different batch tests

Anaerobic	Arginine	Lysine	Cysteine	Proline	Tyrosine	Cas_aa	Mix_aa
P_{rel}/C_{upt} (mol $P \cdot mol^{-1}C$)	0.37	0.42	1.38	0.46	0.41	0.29	0.37
P_{rel} (mmol $P \cdot L^{-1}$)	0.95	0.78	1.45	0.81	0.77	0.78	1.14
C_{upt} (mmol $C \cdot L^{-1}$)	2.58	1.86	1.05	1.75	1.90	2.67	3.08
Gly_{deg}/C_{upt} (mol $C \cdot mol^{-1}C$)	0.11	0.35	0.59	0.21	0.06	0.43	0.34
PHA_{prod}/C_{upt} (mol $C \cdot mol^{-1}C$)	0.21	0.32	0.03	-	0.01	0.31	0.37
CRR (%)	19	24	1.6	-	1	21	28
Aerobic							
P_{upt} (mmol $P \cdot L^{-1}$)	0.29	0.23	0.50	0.30	0.60	0.52	0.60
% P in TSS	8.1	6.5	6.4	8.0	7.6	6.1	6.9
Gly production (mmol $C \cdot L^{-1}$)	0.46	0.21	0.49	0.24	0.24	0.49	1.05
PHA consumption (mmol $C \cdot L^{-1}$)	0.80	0.48	0.06	-	0.12	0.84	1.16
Gly/PHA (mol $C \cdot mol^{-1}C$)	0.58	0.44	8.59	-	2.00	0.58	0.91
P_{upt}/PHA_{oxid} (mol $P \cdot mol^{-1}C$)	0.36	0.47	8.76	-	5.01	0.62	0.52

Table 6.5. Anaerobic/aerobic carbon and phosphorus rates

	Anaerobic phase		Aerobic phase
Amino acid	P-release rate (mg $P \cdot gVSS^{-1} \cdot h^{-1}$)	C-uptake rate (mg $C \cdot gVSS^{-1} \cdot h^{-1}$)	P-uptake rate (mg $P \cdot gVSS^{-1} \cdot h^{-1}$)
Arginine	4.93	8.78	5.55
Lysine	4.38	5.79	3.96
Cysteine	7.73	3.98	4.83
Proline	3.72	5.81	2.36
Tyrosine	3.48	5.67	4.55
Cas_aa	6.87	13.37	7.51
Mix_aa	6.54	14.57	8.03

6.3.2.2. Mixture of amino acids as carbon source

Besides the individual tests, a batch test was conducted with a proportionate mix of all the amino acids (1 mM C each). The objective was determining the effect of the mixture on the P-removal performance: additive (i.e. the performance of the mixture is similar to that calculated from the addition of the individual effects), synergic (i.e. the performance of the mixture is higher than the addition of the individual effects) or antagonistic (i.e. the

performance of the mixture is lower than the addition of the individual effects). The typical EBPR rates and ratios and anaerobic and aerobic yields for this mixture of amino acids are also detailed in Tables 6.4 and 6.5. The mixture provided the highest anaerobic P-release (1.14 mmol $P \cdot L^{-1}$), carbon uptake (3.08 mmol $C \cdot L^{-1}$), PHA_{prod}/C_{upt} ratio (0.37 mol $C \cdot mol^{-1}C$) and CRR (28%), thanks to the synergic effect of the five amino acids. This mixture also obtained the highest values for some aerobic parameters: P-uptake (0.60 mmol $P \cdot L^{-1}$), glycogen production (1.05 mmol $C \cdot L^{-1}$) and PHA consumption (1.16 mmol $C \cdot L^{-1}$). On the other hand, the theoretical P-release and P-uptake (mmol $P \cdot gVSS^{-1}$) of the mixture was calculated by considering the concentration of each amino acid and their individual values. The experimental P-release for the mix of amino acids was 0.56 mmol $P \cdot gVSS^{-1}$, which was 12% higher than the theoretical (0.50 mmol $P \cdot gVSS^{-1}$). In the case of P-uptake, it was 30 % higher for the experimental vs. the theoretical (0.30 vs. 0.21 mmol $P \cdot gVSS^{-1}$). Overall, the contribution of the mix allows the activation of several types of microorganisms with different metabolisms, which appears to have a synergic effect in the case of P removal.

6.3.3. Comparison of the use of amino acids with different sludge

This section compares the performance of several sludge samples with different PAO populations. For this aim, four different sludge samples were chosen:

1) Sludge from the Beirolas WWTP (Lisbon, Portugal), which includes EBPR process and, therefore, the sludge was expected to be enriched in PAOs (*Accumulibacter*, *Tetrasphaera* or whatever PAO is more favoured in this full scale environment).

2) Sludge from the Chelas WWTP (Lisbon, Portugal) which has only BNR process and, thus, a low presence of PAO is expected.

3) *Tetrasphaera*-enriched sludge (tests performed in section 6.3.2).

4) *Accumulibacter*-enriched sludge obtained from a SBR operating under pseudo steady state conditions and treating a mixture of acetic acid (75%) and propionic acid (25%).

All the batch tests were conducted with Cas_aa and with the mixture of the five amino acids (in the same proportion) as carbon sources. Moreover, a batch test without carbon source (blank) was conducted for each case to obtain the cell maintenance. The TOC, phosphorus, PHA and glycogen profiles for the all batch tests are shown in Figure 6.4. The anaerobic and aerobic stoichiometric data obtained for these tests are compared in

Table 6.6 with the values obtained with the sludge from the Beirolas WWTP using acetate (Lanham et al., 2013a) and the sludge from WWTP3 in Singapore, where glutamate and aspartate were used as carbon source (Qiu et al., 2019).

The complete profiles for the batch tests with the *Tetrasphaera*-enriched culture using Cas_aa and Mix_aa are shown in Figure 6.4. This sludge was able to use Cas_aa and Mix_aa as carbon sources with good P-removal. The values of P-release and P-uptake were higher for Mix_aa than for Cas_aa, probably related to the higher carbon uptake with Mix_aa (3.08 vs 2.67 mmol $C \cdot L^{-1}$, Table 6.6). Nevertheless, the carbon uptake rate was higher in the case of Cas_aa (14.65 vs 8.94 mg $C \cdot g^{-1}VSS \cdot h^{-1}$, Table 6.7). The ratio Gly_{deg}/C_{upt} was also higher for Cas_aa, however the ratio PHA_{prod}/C_{upt} was slightly higher for Mix_aa. CRR values of 21 and 28% were obtained when Cas_aa and Mix_aa were used as carbon source respectively, indicating the importance of non-identified fermentation products and other intracellular storage polymers different from PHA that were not quantified.

The *Accumulibacter*-enriched culture was able to use Cas_aa as carbon source and perform complete P-removal, but no TOC degradation was measured when Mix_aa was supplied. *Accumulibacter* rarely use complex carbon sources and, thus, the small consumption of 1.13 mmol $C \cdot L^{-1}$ of Cas_aa (compared to 2.67 and 3.08 mmol $C \cdot L^{-1}$ obtained for the *Tetrasphaera* culture, and 2.12 mmol $C \cdot L^{-1}$ obtained with the Beirolas WWTP sludge, Table 6.6) could be attributed to some fermentation of Cas_aa but also to the presence of 10% of *Tetrasphaera* as measured by FISH. The reason for the different behaviour of the sludge is clearly related to the microbial community in each case, as for example the presence of different *Tetrasphaera* clades in each sample. In fact, we observed much more abundance of clade 3 (targeted by probe Tet3-654) in the *Tetrasphaera*-enriched sludge, whereas Beirolas WWTP sludge had a higher abundance of clade 2 (targeted by probe Tet2-892). The different clades of *Tetrasphaera* can possess different affinities for different substrates (Nguyen et al., 2011). Nevertheless, this was only an approximation because the use of techniques other than FISH (e.g. quantitative polymerase chain reaction, qPCR) is necessary to quantify the abundance of each clade.

Despite there was no consumption of Mix_aa by the *Accumulibacter*-enriched sludge, a P-release of 1.07 mmol $P \cdot L^{-1}$ was obtained, which was similar to the obtained in the batch test with Cas_aa (1.16 mmol $P \cdot L^{-1}$, Table 6.6). This P-release cannot be attributed to the cell maintenance, since values around 0.4 mmol $P \cdot L^{-1}$ were achieved in the batch tests

without carbon addition. Furthermore, there was no involvement of both PHA and glycogen under anaerobic conditions due to the absence of carbon uptake. In the case of Cas_aa, the ratio PHA_{prod}/C_{upt} was similar to the obtained for the same carbon source in the *Tetrasphaera*-enriched sludge. However, the ratio Gly_{deg}/C_{upt} achieved negative values, indicating a production instead of degradation. Higher CRR was obtained for this culture (48%) when compared with the *Tetrasphaera*-enriched sludge. Total P-uptake was observed during the aerobic phase (0.83 mmol $P \cdot L^{-1}$, Table 6.6 and Figure 6.4), while lower P-uptake (0.26 mmol $P \cdot L^{-1}$, Table 6.6) was obtained for the Mix_aa.

Similar P-release values were obtained for both WWTP sludge (Beirolas and Chelas), which was surprising since a higher P-release was expected at the Beirolas WWTP with implemented EBPR process. Carbon uptake can be considered negligible for the Chelas batch test performed with Cas_aa, and slight carbon consumption was observed for the batch tests performed with Mix_aa and the Chelas and Beirolas WWTP sludge. The highest carbon consumption was achieved with the Beirolas WWTP sludge when using Cas_aa as carbon source. This fact could be due to a higher abundance of *Tetrasphaera* in the Beirolas sludge comparing to Chelas sludge (Figures 6.5D and 6.5G respectively) and also due to the more abundance of clade 3 (above mentioned). There was no PHA involvement in any of the batch tests performed with the Chelas WWTP sludge, which agrees with the sludge composition, which presents lower abundance of *Tetrasphaera* and *Accumulibacter* compared to the sludge from Beirolas WWTP and to the *Tetrasphaera*-enriched culture (Figure 6.5). Despite the higher carbon uptake in Beirolas WWTP when Cas_aa was used as substrate, the anaerobic PHA and glycogen involvement were negligible. In fact, a CRR of 7% was obtained, increasing up to 27% when Mix_aa was added as carbon source.

Intracellular P content for the different sludge are shown in Table 6.6 and *Accumulibacter* biomass had the higher P content with values between 9.6-12.2%, which are in the range of the values obtained by Oehmen et al. (2007). Lower intracellular P was achieved with the *Tetrasphaera* sludge which values were below 7% with the carbon sources used. Finally, a higher P content was observed for the sludge from Beirolas WWTP compared to the sludge from Chelas WWTP, with values between 3.6-4.4% and 3.1-3.7% respectively. In fact, higher P content was expected for the sludge from Beirolas WWTP since this plant includes EBPR process.

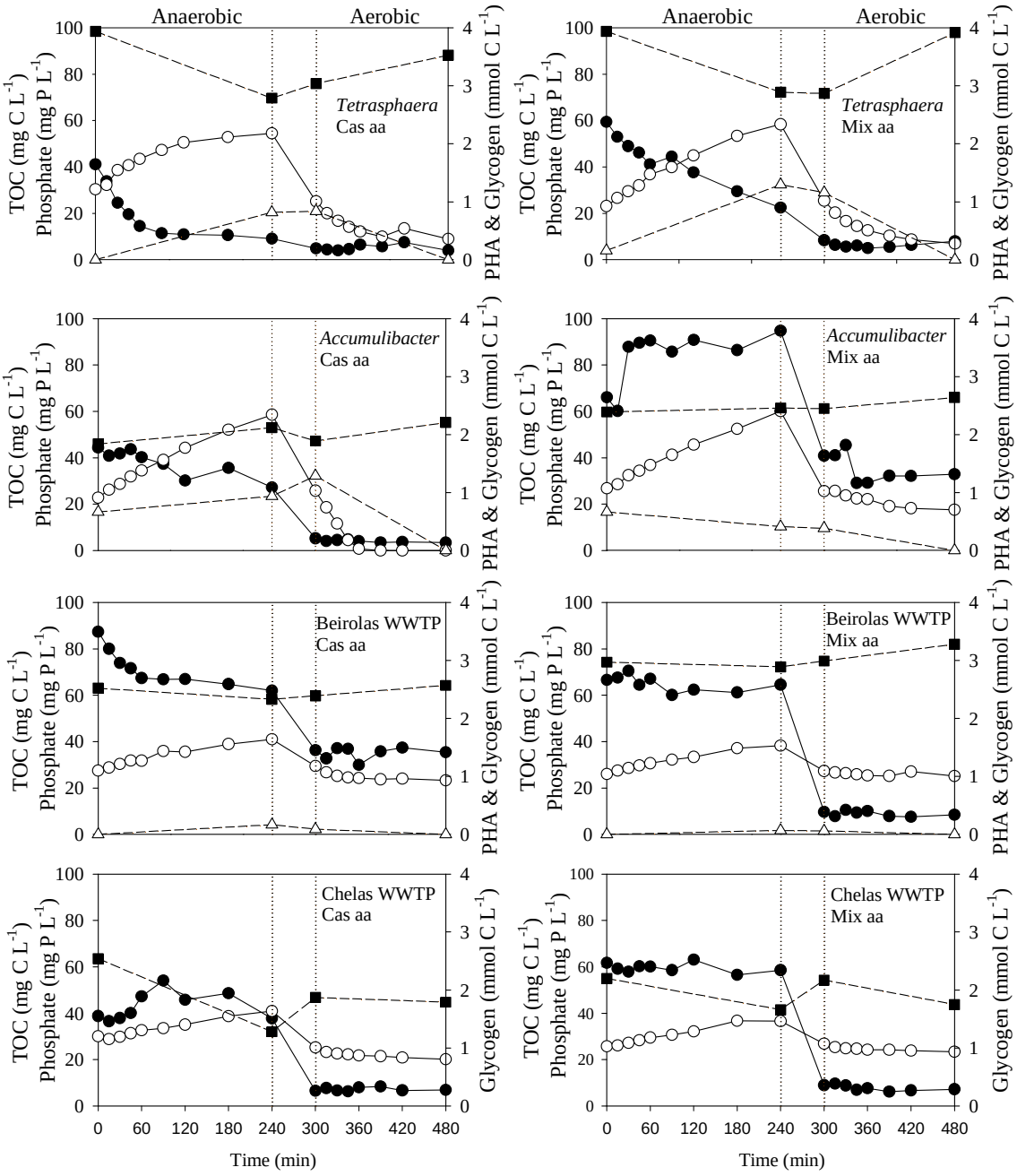

Figure 6.4. Anaerobic/aerobic batch tests performed with the different sludge using Cas_aa or the mixture of amino acids. Concentration of TOC (●), phosphorus (○), PHA (Δ) and glycogen (■).The dotted lines indicate the period with settling and extraction.

Table 6.6. Typical EBPR ratios and rates and anaerobic and aerobic yield s obtained for the different batch tests

	Experimental results								Literature values		
	Tetrasphaera		*Accumulibacter*		Beirolas WWTP		Chelas WWTP		Beirolas WWTP[a]	WWTP3[b]	WWTP3[b]
Anaerobic results	Cas aa	Mix aa	Cas aa	Mix aa	Cas aa	Mix aa	Cas aa	Mix aa	Acetate	Aspartate	Glutamate
P_{rel}/C_{upt} (mol $P \cdot mol^{-1}C$)	0.29	0.37	1.02	-	0.21	2.32	3.95	1.34	0.60	0.16	0.20
P_{rel} (mmol $P \cdot L^{-1}$)	0.78	1.14	1.16	1.07	0.44	0.40	0.35	0.35	2.26	0.32	0.32
C_{upt} (mmol $C \cdot L^{-1}$)	2.67	3.08	1.13	-	2.12	0.17	0.09	0.26	1.25	2.05	1.58
Gly_{deg}/C_{upt} (mol $C \cdot mol^{-1}C$)	0.43	0.34	-0.25	-	0.09	0.47	14.20	2.06	0.20	n.a.	n.a.
PHA_{prod}/C_{upt} (mol $C \cdot mol^{-1}C$)	0.31	0.37	0.24	-	0.08	0.40	-	-	0.80	0.35	0.04
CRR (%)	21	28	48	-	7	27	-	-	67	n.a.	n.a.
Aerobic results											
P_{upt} (mmol $P \cdot L^{-1}$)	0.52	0.60	0.83	0.26	0.20	0.07	0.16	0.11	0.97	0.18	0.14
% P in TSS	6.1	6.9	12.2	9.6	4.4	3.6	3.1	3.7			
Gly production (mmol $C \cdot L^{-1}$)	0.49	1.05	0.32	0.19	0.18	0.29	-0.08	-0.42	0.42	n.a.	n.a.
PHA consumption (mmol $C \cdot L^{-1}$)	0.84	1.16	1.29	0.39	0.09	0.06	-	-	1.33	0.63	0.07
Gly/PHA (mol $C \cdot mol^{-1}C$)	0.58	0.91	0.25	0.49	2.02	5.02	-	-	0.70	n.a.	n.a.
P_{upt}/PHA_{oxid} (mol $P \cdot mol^{-1}C$)	0.63	0.52	0.65	0.67	2.22	1.22	-	-	1.30	0.29	2

[a] (Lanham et al., 2013a)
[b] (Qiu et al., 2019)
n.a.: not avalilable

Table 6.7. Anaerobic/aerobic carbon and phosphorus rates

		Anaerobic phase		Aerobic phase
Sludge	Carbon source	P-release rate (mg $P \cdot gVSS^{-1} \cdot h^{-1}$)	C-uptake rate (mg $C \cdot gVSS^{-1} \cdot h^{-1}$)	P-uptake rate (mg $P \cdot gVSS^{-1} \cdot h^{-1}$)
Tetrasphaera	Cas_aa	6.87	14.65	7.51
	Mix_aa	6.54	8.94	7.26
Accumulibacter	Cas_aa	6.44	2.96	16.97
	Mix_aa	5.42	-	2.65
Beirolas WWTP	Cas_aa	1.97	7.43	3.02
	Mix_aa	1.48	1.34	0.62
Chelas WWTP	Cas_aa	1.89	-	2.10
	Mix_aa	1.37		1.41

Lanham et al. (2013a) also performed some experiments with sludge from the Beirolas WWTP, but using acetate as carbon source. Since they were adding a preferred VFA, anaerobic ratios were higher than in our experiment with Cas_aa and Beirolas WWTP sludge: the P/C ratio was 0.6 vs 0.21 mol $P \cdot mol^{-1}C$ and the CRR (67% vs. 7%), indicating a typical *Accumulibacter* metabolism with high PHA production and glycogen degradation. The aerobic phase also showed higher glycogen production and PHA consumption in the experiments with acetate, as in the typical *Accumulibacter* phenotype. Another work performed by Qiu et al. (2019) reported some experiments with the sludge withdrawn from a WWTP in Singapore with high in-situ EBPR activity, high temperatures 28.7-31.6 ºC and with amino acids (glutamate and aspartate) among other carbon sources. The P/C ratios obtained for both substrates aspartate and glutamate (0.16 and 0.20 mol $P \cdot mol^{-1}C$, Table 6.6) were in the range of those observed for Beirolas WWTP and *Tetrasphaera*-enriched sludge when the Cas_aa was the carbon source. The negligible PHA detection with glutamate suggests that this carbon source may have been converted into other intracellular storage compounds. Low PHA involvement was also observed in the A^2O pilot plant using glutamate (Chapter 4). The PHA_{prod}/C_{upt} in the case of aspartate was similar to those obtained for *Tetrasphaera*-enriched sludge. Under aerobic conditions, similar P-uptake values were obtained for both amino acids. However, in the case of glutamate, the P-uptake was allowed without the necessity for anaerobic conversion of this carbon source to PHA. Glycogen analysis were not conducted in these batch tests.

Finally, the P_{upt}/PHA_{oxid} ratios ob tained for all batch tests were higher than the reported in the metabolic models for acetate (0.41 mol $P \cdot mol^{-1}C$ (Smolders et al., 1995)), indicating that *Tetrasphaera* were contributors to the P-uptake besides *Accumulibacter*. The small differences in P-release values for the different sludge and carbon sources, underscores the potential role of other compounds than VFA which could serve as complementary carbon sources in full-scale WWTP.

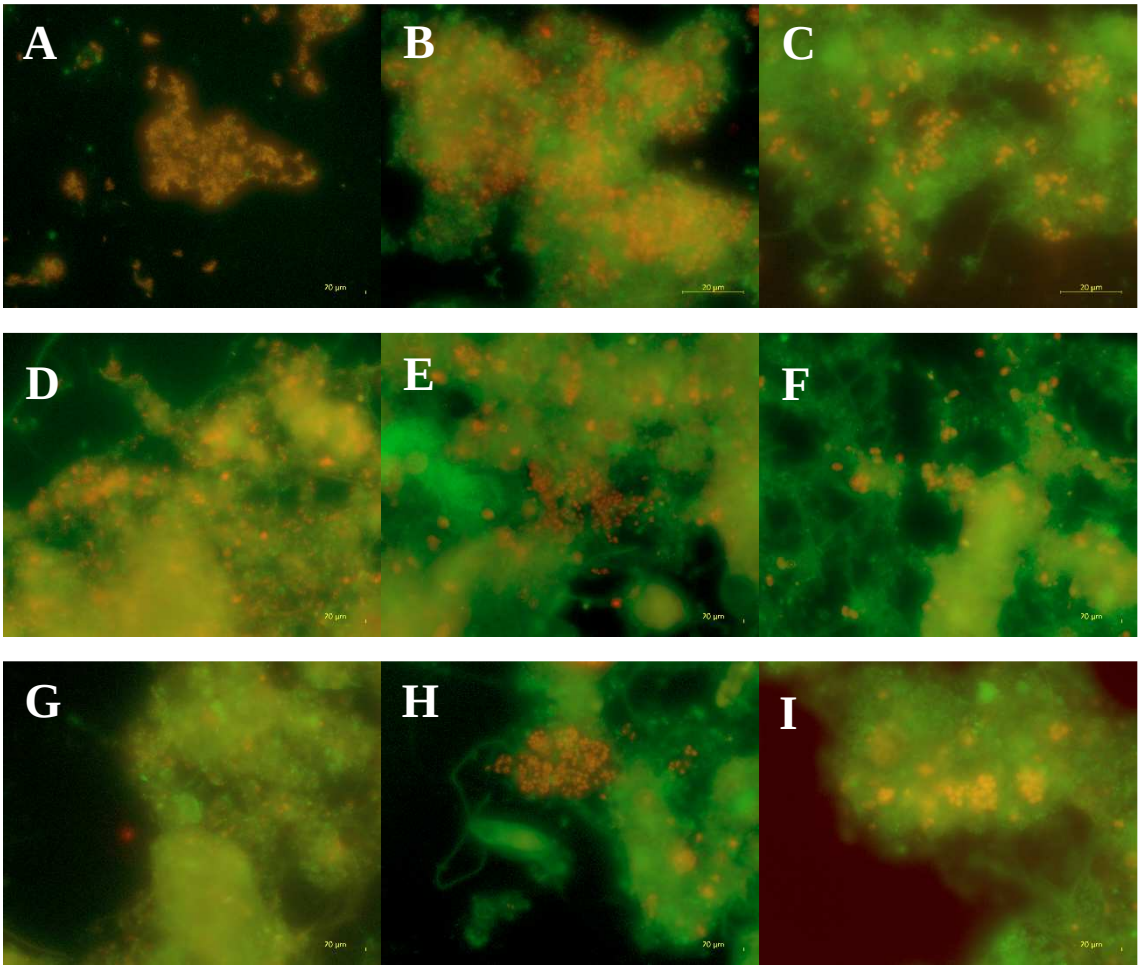

Figure 6.5. CLSM micrographs of FISH for the different sludge tested. A, B and C: *Tetrasphaera*-enriched sludge. D, E and F: Beirolas WWTP sludge. G, H and I: Chelas WWTP sludge. Green, all bacteria. A, D and G: orange, *Tetrasphaera*. B, E and H: orange, *Accumulibacter*. C, F and I: orange, *Competibacter*.

6.4. Conclusions

This work shows the importance of amino acids in full-scale EBPR systems, where they can play a significant role in the performance of a WWTP. The presence of amino acids content in the influent of a WWTP will develop a microbial community with EBPR

activity not related to *Accumulibacter* and hence with a wider range of carbon sources able to contribute to biological P-removal.

To show the importance of amino acids in EBPR systems, the operation of an SBR using Cas_aa as carbon source was tested. The system was enriched in *Tetrasphaera* and *Accumulibacter* and this culture was able to perform the uptake of different amino acids (arginine, lysine, cysteine, proline and tyrosine) under anaerobic conditions. The preferred carbon source was Cas_aa, since it was the substrate used for the reactor operation. On the other hand, the *Tetrasphaera* culture was not capable to use cysteine, with a consumption of 19% of the initial carbon source. For the rest of amino acids, around 41±7% of the initial carbon was consumed. The batch test conducted with the mixture of the five amino acids improved the individual addition of amino acids, showing a synergic effect on the bio-P removal performance. The different involvement of PHA and glycogen in the batch tests could be connected to the fermentation products generated, which is an essential feature to understand the performance of the posterior EBPR process.

The preliminary results for the batch tests performed with different sludge, allowed us to infer that the capability to consume Cas_aa and Mix_aa by the different cultures is related to the abundance of a particular clade within the genus *Tetrasphaera*. In fact, the sludge withdrawn from the Beirolas WWTP, with a higher abundance of clade 2 (targeted by TET 2-892 probe), was able to uptake Cas_aa but not Mix_aa, while the sludge from the Chelas WWTP, with a higher fraction of clade 1 (targeted by TET 1-266 probe) was not able to uptake either Cas_aa or Mix_aa.

Chapter 7

COMPARING CONTINUOUS AND SBR OPERATION FOR HIGH-RATE TREATMENT OF URBAN WASTEWATER IN VIEW OF EBPR INTEGRATION

Part of this chapter is being prepared for publishing as:

Natalia Rey-Martínez, Aloia Barreiro-López, Albert Guisasola, Juan A. Baeza, 2019 Comparing continuous and SBR configurations for high-rate treatment of urban wastewater. *In preparation.*

ABSTRACT

Water-energy nexus has changed the perception of wastewater treatment plants (WWTPs), which should move from power consumers into energy neutral or even energy positive facilities. The A/B process is a potential configuration to meet energy self-sufficient WWTPs: organic matter is removed in the first step (A-stage) and derived to biogas production whereas autotrophic nitrogen removal is implemented in a second step (B-stage). This work compares two high-rate systems that can be used as A-stage for organic matter removal: a continuous high rate activated sludge (HRAS) reactor and for the first time, a high-rate sequencing batch reactor (HRSBR). Both systems were operated with real urban wastewater at a short hydraulic retention time (2.5 h) and at short sludge retention time (SRT) of 1-2 d to minimize COD mineralization and to maximise organic matter diversion to methane production. The HRAS showed higher COD removal efficiencies and lower effluent solids. On the other hand, the HRSBR was better to avoid undesired nitrification and provided lower COD mineralization for all the SRTs tested (13.2% of mineralised COD in HRSBR vs 55.2% in HRAS at SRT of 1 day).The biochemical methane potential (BMP) of the sludge was measured at different SRT values (range of 187-308 NL $CH_4 \cdot kg^{-1}VS$), obtaining higher BMP for HRSBR sludge. Finally, this study also explores the potential integration of enhanced biological phosphorus removal (EBPR) into the A-stage for simultaneous COD and P removal, as this is not included in the design of conventional A/B processes, where chemical precipitation is normally implemented if required.

7.1. Introduction

The activated sludge (AS) process is still the most commonly used technology for urban wastewater treatment since its first description in 1914 (Van Loosdrecht et al., 2014). Although this technology is robust and provides a good effluent quality, it presents high operational costs and does not use the potential energy of the organic compounds present in sewage (Akanyeti et al., 2010). Moreover, nitrogen and phosphorus must be also removed to avoid eutrophication and oxygen depletion in water bodies. Conventional AS systems for nitrogen removal through nitrification/denitrification require high sludge retention times (SRTs), around 10-20 days, to ensure nitrification (Kartal et al., 2010). The major costs in these WWTPs are related to the energy consumption and sludge treatment: aeration uses about 60% of the total energy consumption (Gu et al., 2017), while sludge treatment and disposal account for up to 40% (Verstraete et al., 2011).

Urban WWTPs are currently energy-demanding facilities and, thus, novel approaches are needed for achieving a self-sustainable or even energy-positive WWTPs (Gu et al., 2017). The two-stage A/B process is a configuration targeting this goal (Versprille et al., 1985) that has recently received more attention (Liu et al., 2018; Xu et al., 2017). In the first step (A-stage) the objective is to maximize the capture of carbon into the sludge through mostly physicochemical (adsorption, flocculation and coagulation) processes and to divert this sludge towards an anaerobic digestion system for biogas production. An A-stage system operates at very short sludge retention times (SRTs) and short hydraulic retention times (HRTs) to minimise biological oxidation of COD. The effluent of the first step is treated in the second step (stage B) through the autotrophic biological nitrogen removal (BNR): partial nitritation and anaerobic ammonium oxidation (anammox) processes. Autotrophic BNR results in significant economic and energetic cost savings when compared to the conventional nitrification/denitrification process. The performance of the B-stage depends on the COD and solids removal of the A-stage. Moreover, the A-stage acts as a shock absorber of unexpected toxic loads that could be very detrimental for the B-stage (Smitshuijzen et al., 2016).

The increasing concern towards the achievement of an energy-neutral wastewater treatment makes necessary to maximize the capture of organic matter in A-stage rather than oxidation processes. The sludge produced in the A-stage has a high potential for energy recovery via anaerobic digestion (Meerburg et al., 2015).

The A-stage is usually designed as a continuous HRAS under short SRT and HRT. For example, Jimenez et al. (2015) studied the effect of SRT, HRT and dissolved oxygen (DO) on a HRAS pilot plant performance. Ge et al. (2017) evaluated the impact of sludge age on nutrient removal using a HRAS pilot plant. Finally, a review of new alternatives for carbon redirection to improve the energy balance of WWTPs (Sancho et al., 2019), demonstrated that HRAS is an acceptable technology to redirect carbon in WWTPs. However, a batch process in a sequencing batch reactor (SBR) operated at the same HRT and SRT could also be a good option because SBRs present some advantages when compared with continuous systems: i) higher tolerance facing toxic or inhibitory compounds (Jiang et al., 2016), ii) higher operation flexibility (Tomei et al., 2016), iii) they retain sludge more effectively than continuous reactors, because the supernatant is discharged only after the sludge has been settled (Sekine et al., 2018) and iv) they can have lower installation cost and less space requirement, because the process occurs in only one tank and in this way the settler is avoided (Jaramillo et al., 2018).

On the other hand, the fate of phosphorus (P) in this new A/B configuration has not been deeply studied yet and, currently, a chemical precipitation in the tertiary step is the most common option. Thus, there is a need to rethink this configuration in order to include biological P removal. The possible integration of EBPR into this configuration requires the modification of the A-stage to include EBPR as well as carbon removal. The inclusion of an anaerobic phase and to expose the biomass to alternating anaerobic and aerobic stages is required to obtain a sludge enriched in polyphosphate accumulating organisms (PAOs). Then, the content of P in the biomass generated would increase as the purge would be more enriched in poly-phosphate (poly-P). This could allow a posterior P recovery as struvite after the anaerobic digestion. However, the lower growth rate of PAO compared to ordinary heterotrophic organisms hinders the possibility of working at very low SRTs.

The main objective of this work was to compare the performance of a continuous HRAS and a high-rate SBR (HRSBR) acting as an A-stage under the same SRT and HRT conditions and fed with real urban wastewater. Based on the experimental results obtained, the possible integration of an EBPR system and a posterior B-stage was tested and discussed. Finally, the methanogenic potential of the sludge generated in both systems was assessed.

7.2. Materials and methods

7.2.1. Characteristics of the real wastewater

Two different real wastewaters were used in this work: primary settler influent (PSI) and primary settler effluent (PSE), both from a municipal WWTP (Rubí, Barcelona). Fresh wastewater was collected once a week and stored in a refrigerated tank at 5 ºC. Table 7.1 summarizes the most important parameters of these wastewaters during the entire operation.

Table 7.1. Summary of wastewater characteristics for primary settler influent (PSI) and primary settler effluent (PSE).

	Influent average	
Parameter	PSI	PSE
TSS (g/L)	0.18 ± 0.17	0.08 ± 0.06
VSS (g/L)	0.16 ± 0.15	0.07 ± 0.05
Total COD (mg/L)	496 ± 214	359 ± 128
Particulate COD (mg/L)	239 ± 203	124 ± 93
Soluble COD (mg/L)	185 ± 54	157 ± 53
Colloidal COD (mg/L)	72 ± 26	76 ± 27
NH_4^+-N (mg/L)	76 ± 13	65 ± 21
PO_4^{-3}-P (mg/L)	9 ± 4	9 ± 3
pH	7.6 ± 0.2	7.6 ± 0.3

7.2.2. High-rate activated sludge (HRAS) system

The HRAS system consisted of a continuously stirred, aerobic reactor (19 L) and a settler (27 L). The detailed diagram of the reactor and the operation conditions are described in Section 3.1.3 of Chapter 3. The HRAS system was inoculated with sludge collected from the same municipal WWTP (Rubí, Barcelona) and was operated for 175 days treating PSE wastewater. The operation characteristics of each period are shown in Table 7.2.

Table 7.2. Operational conditions for each period of HRAS.

Period	Days (d)	Carbon source	Purge flow ($L \cdot d^{-1}$)	SRT (d)
I	0-24	PSE	5	2.5 ± 0.2
II	26-87	PSE	3.5	2.1 ± 0.6
III	89-175	PSE	2.5	1.2 ± 0.6

7.2.3. High Rate Sequencing Batch Reactor (HRSBR)

The HRSRB was a stirred aerobic system with a working volume of 3.5 L and an exchange volume of 2.5 L. The operation (253 days) was divided into different periods according to the operational conditions and the cycle configuration for each period is reported in Table 7.3. It was inoculated with sludge collected from the same WWTP. The HRSBR was fed with PSI during periods I and II and with PSE for the rest of periods. DO was controlled during the aerobic phases by manipulating an on/off aeration valve. The DO set point was 5 $mg \cdot L^{-1}$ during the start-up period and 3 $mg \cdot L^{-1}$ afterwards. The detailed diagram of the reactor and the operation conditions are described in Section 3.1.4 of Chapter 3.

Table 7.3. Operational conditions for each period for HRSBR.

Period	Days (d)	Carbon source	Purge flow ($L \cdot d^{-1}$)	SRT (d)	Cycle length (min)	Reaction phase (min)	Settling phase (min)	Discharge phase (min)
I	0-30	PSI	Variable to obtain constant SRT	1.8 ± 0.9	106	75	30	1
II	58-105	PSI	0.576	1.2 ± 0.5	116	85	30	1
IIIA	107-191	PSE	0.576	2.2 ± 1.0	116	85	30	1
IIIB	194-231	PSE	0.576	1.3 ± 0.8	116	85	30	1
IV	236-253	PSE	0.993	1.0 ± 0.3	116	85	30	1

7.2.4. Anaerobic/aerobic (A/O) high-rate activated sludge system (A/O-HRAS)

The anaerobic/aerobic (A/O-HRAS) pilot plant consisted of two continuous stirred tank reactors with a total volume of 42 L and a 25 L settler. It was operated at room temperature (18-22ºC) with an average influent flow rate of 102 $L \cdot d^{-1}$ (HRT = 10.8 h). The SRT was maintained around 3-4 days with daily sludge wastage from the aerobic reactor. The external recycle from the bottom of the settler to the anaerobic reactor was 56.6 $L \cdot d^{-1}$, which resulted in an external recirculation ratio (R_{ext}) of 0.51. The plant was fed with PSE, but propionic acid was also supplied to increase the ratio of readily degradable

organic matter available (an average concentration of 2373 ± 154 mg $COD \cdot L^{-1}$ was maintained in the influent). The A/O-HRAS system was inoculated with sludge collected from the same WWTP and was operated for 35 days. The reactor was managed with an on-line system based on an Advantech PCI-1711 I/O card and an industrial PC running the Addcontrol software developed in our research group. Dissolved oxygen (DO) was measured with a HACH-CRI6050 DO probe and controlled around 1 $mg \cdot L^{-1}$ by manipulating an on/off aeration valve. pH and temperature were monitored with a pH probe (HACH CRI5335) and a thermoresistance (Axiomatic Pt1000), respectively.

7.2.5 Anaerobic digestion batch tests

The biochemical methane potential (BMP) of the sludge purged in both systems was studied through anaerobic batch digestion tests. BMP assays were performed in 160 mL glass bottles (125 mL of working volume) with rubber stoppers and screw caps according to Angelidaki et al. (2009). The inoculum used in the tests was obtained from the anaerobic digester of the Rubí WWTP and was pre-incubated at 37ºC in order to deplete the residual biodegradable organic matter. All tests were performed in triplicate in an incubator at T = 37ºC and manually mixing of the bottles once a day. A substrate to inoculum (S/I) ratio of 1 (on VS basis) with 2 $gVS \cdot L^{-1}$ of inoculum was used. Negative control assays with only inoculum and MilliQ water were conducted in parallel to measure the background BMP from the inoculum and this value was subtracted from the test prior to parameter estimation. Additionally, a positive control with cellulose as substrate was performed to confirm the activity of the inoculum. The liquid phase and the headspace of the bottles were flushed with nitrogen to provide anaerobic conditions. A pressure transducer was used to measure the pressure increase. The biogas was sampled regularly and its composition was determined by gas chromatography. The moles of methane were calculated by the ideal gas law (Equation 1):

$$CH_4 \text{ moles} = \frac{P_T \cdot X_{CH_4} \cdot V_{headspace}}{R \cdot (T+273)} \quad (1)$$

where P_T is the total pressure measured by the transducer (mmHg), X_{CH4} is the methane molar fraction, $V_{headspace}$ is the headspace volume (mL), R is the ideal gas constant (62320 $mmHg \cdot mL \cdot mol^{-1} \cdot K^{-1}$) and T is the temperature (ºC). Then, the corresponding volume of methane was calculated and converted to standard temperature and pressure conditions (0ºC and 1 atm).

7.2.6. Specific analytical methods and calculations

Phosphorus, ammonium, nitrate and nitrite concentrations were measured off-line according to Sections 3.2.1 and 3.2.2 of Chapter 3. SVI and TSS and VSS were analysed according to sections 3.2.5 and 3.2.6 respectively of Chapter 3.

Influent and effluent COD fractions were measured according to Jimenez et al. (2015). Particulate COD (COD_P) was the difference between total COD (COD_T) and the COD filtered through a 1.5 µm filter (COD_F). The soluble COD (COD_S) was the flocculated and filtrated COD (COD_{ff}) as defined by Mamais et al. (1993). Colloidal COD fraction (COD_C) was defined as the difference between COD_P and COD_S. These COD fractions were measured using COD kits (Lovibond Vario LR and Vario MR) and a spectrophotomer (Photometer system MD100 Lovibond).

Biogas composition (CH_4 and CO_2) was analysed with a Hewlett Packard gas chromatograph (HP 5890) equipped with a thermal conductivity detector (TCD) and a Supelco Porapack Q (250ºC) 3 m x 1/8" column. Helium was the carrier gas at 338 kPa, and the oven, injector and detector temperatures were 70, 150 and 180ºC respectively. A total sample volume of 100 µL was used for chromatography.

The observed yield (Y_{obs}) under different SRT conditions was calculated using the experimental biomass production (P_X, equation 2).

$$P_X = Q_P \cdot X_P + Q_e \cdot X_e - Q_{in} \cdot X_{in} \quad (2)$$

Where Q_P, Q_e and Q_{in} are the flowrates of purge, effluent and influent ($L \cdot d^{-1}$) and X_P, X_e and X_{in} are the VSS concentrations in the purge, in the effluent and in the influent ($gVSS \cdot L^{-1}$).

The experimental observed yield (Y_{obs}, $gCOD \cdot g^{-1}COD$) was calculated with equation 3.

$$Y_{obs} = \frac{P_X \cdot 1.416}{Q_{in} \cdot (COD_{in} - COD_{out})} \quad (3)$$

where 1.416 is a stoichiometric factor converting VSS into COD ($gCOD \cdot g^{-1}VSS$), Q_{in} is the influent flowrate ($L \cdot d^{-1}$) and COD_{in} and COD_{out} are the COD concentrations in the influent and effluent respectively ($mgCOD \cdot L^{-1}$).

7.3. Results and discussion

7.3.1. Continuous HRAS system performance

The HRAS system was operated for 175 days under two different SRTs and real PSE as feed. During the start-up (period I), the average COD_S removal efficiency was 66 ± 6 %. Figure 7.1 shows the average values of influent/effluent COD_T and the sludge volume index (SVI) for periods II and III.

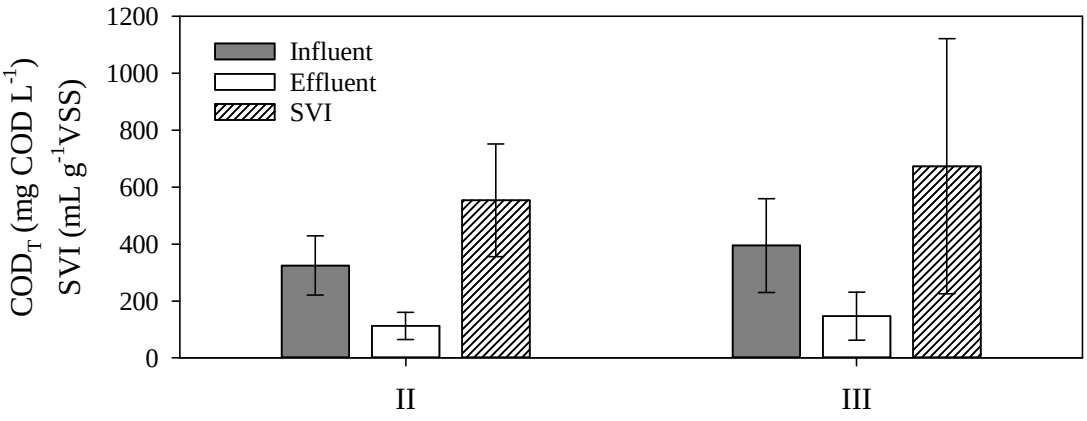

Figure 7.1. HRAS operation. Average influent and effluent COD_T and SVI in periods II and III.

The COD_T in the effluent was not affected by the reduction of the SRT from 2 d (period II) to 1 d (period III). In fact, the COD_T removal efficiencies were 70 ± 16% and 65 ± 15% respectively for periods II and III. The slight increase in the effluent COD_T concentration from period II to period III could also be due to the 18% increase in the influent COD_T (Figure 7.1).

The settleability of the sludge in the HRAS reactor was never good as can be deduced from the high SVI values (Figure 7.1), being 568 ± 329 $mL \cdot g^{-1}$ VSS the average value during the entire operation. These settleability problems led to an extremely low solids concentration (Figure 7.2): the VSS reached values around 0.13 $g \cdot L^{-1}$ during period III. In fact, from day 140 to 168 of operation, the purge had to be turned off because of this low VSS concentration. Settleability issues are very relevant when implementing novel technologies and, in this case, a settler with higher surface would be needed after the continuous HRAS reactor. In this sense, Rahman et al. (2019) performed a parallel comparison of the A-stage and high-rate contact-stabilization technology for carbon and nutrient redirection. In this case, the settler was three times bigger than the reactor. In

contrast, Jimenez et al. (2015) did not reported settleability problems working with a biological reactor consisted of 260 L and a sedimentation tank of 280 L.

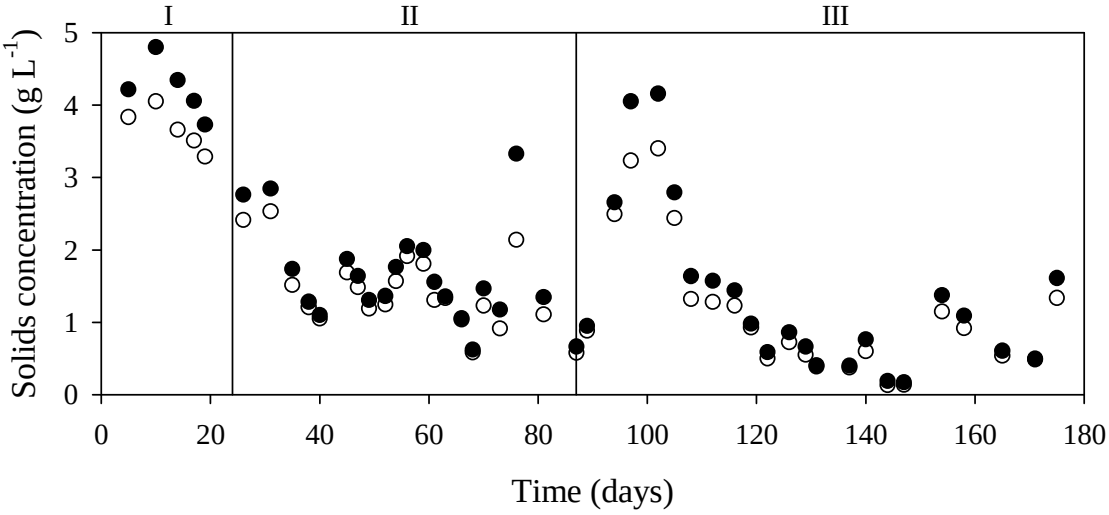

Figure 7.2. HRAS operation. Suspended solids concentration in the reactor. (●) TSS and (○) VSS.

7.3.2. HRSBR performance

The HRSBR was operated for 253 days under different conditions (Table 7.3). Period I corresponds to the start-up of the reactor. The objective of this period was operating with a constant SRT of 2 days, but this required a daily modification of the purge flow, which could lead to an unstable operation. Thus, it was decided to maintain a constant purge flow in the subsequent periods II and III (0.576 $L \cdot d^{-1}$ and 0.993 $L \cdot d^{-1}$ respectively) and, thus, the SRT fluctuated in a range of 1.2-2.2 days. Period III was divided into periods IIIA and IIIB because there was an incident and the reactor had to be inoculated again with biomass from the purges of previous days, which had been stored at 4ºC. Finally, the purge flow was increased to 0.993 $L \cdot d^{-1}$ in period IV and the system operated at a SRT of 1.0 ± 0.3 day. The evolution of the solids in the HRSBR is presented in Figure 7.3.

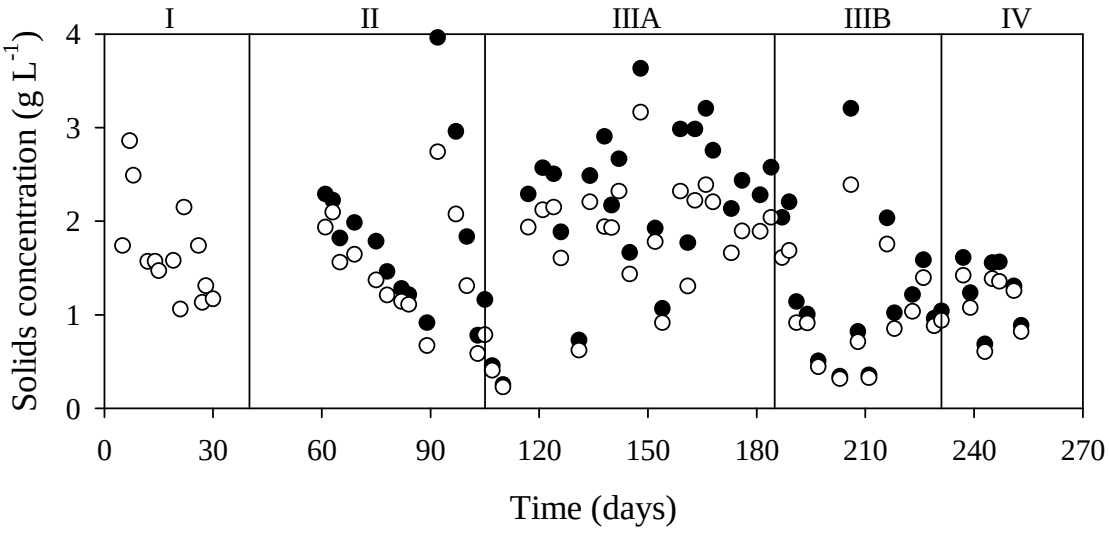

Figure 7.3. HRSBR operation. Suspended solids concentration in the reactor. (●) TSS and (○) VSS.

It is worth mentioning that biomass attachment to the walls of the reactor was observed in periods I and II. Therefore, the decrease in the solids concentration during period II might be unreliable. The walls of the reactor were scratched once a week from period IIIA onwards in order to detach this biomass. Attached biomass can distort the total solids concentration in the reactor and consequently the real SRT would be higher than desired. The solids concentration increased during period IIIA because of the detachment of the biomass grown on the walls of the reactor, however TSS and VSS diminished again during periods IIIB and IV when the SRT was decreased from 2.2 ± 1.0 d (period IIIA) to 1.3 ± 0.8 and 1.0 ± 0.3 d respectively.

Figure 7.4 shows the evolution of the COD_T and the average SVI. The effluent COD_T was below 200 mgCOD·L^{-1} during periods I, II and IIIA, and it increased around 300 mgCOD·L^{-1} for periods IIIB and IV. High effluent COD_T is linked to the poor settleability of the sludge (SVI reached values of 300-500 mL·g^{-1}VSS). The fractionation of the effluent COD (Figure 7.5) shows that during periods IIIB and IV the effluent COD_P increased (the fraction related to the sludge settling characteristics) (Rössle and Pretorius, 2001).

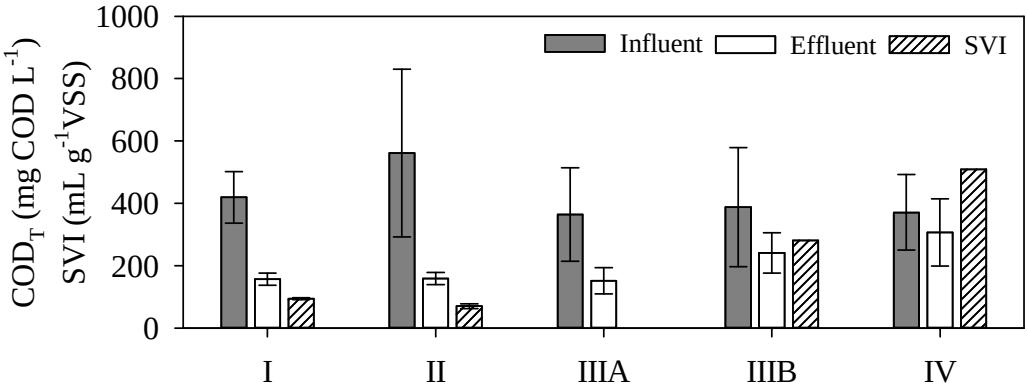

Figure 7.4. HRSBR operation. COD_T in the influent and in the effluent and SVI.

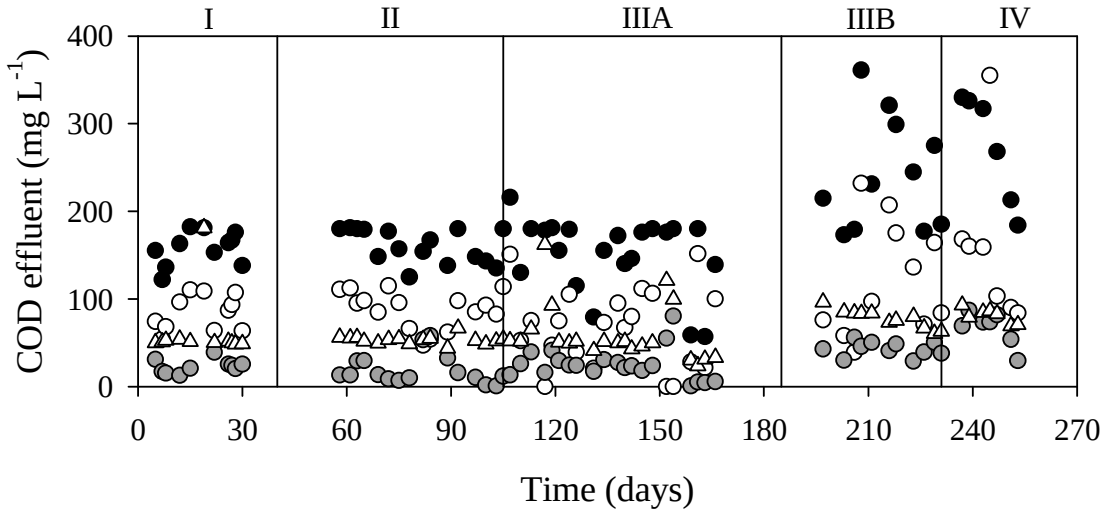

Figure 7.5. HRSBR operation. Fractionation of COD in the effluent: Total (●), particulate (○), colloidal (●) and soluble (Δ).

7.3.3. Comparison of effluent quality and carbon removal in both systems

The effluent quality of both systems was evaluated in terms of solids concentration and the different effluent COD fractions (Table 8.4 and Figure 8.6 respectively). The average TSS values in the effluent of each reactor were similar, but the average SVI for the HRAS sludge (568 ± 329 mL· g VSS^{-1}) was much higher than the observed for the HRSBR sludge (206 ± 192 mL· g VSS^{-1}), indicating that the former had worsen settleability properties (Table 7.4).

Table 7.4. Total suspended solids concentration in reactor and in effluent for both high rate systems.

System	TSS reactor ($g \cdot L^{-1}$)	TSS effluent ($g \cdot L^{-1}$)	SVI ($mL \cdot gVSS^{-1}$)
HRAS			
I (startup)	2.5 ± 0.2	0.059 ± 0.039	171
II	2.1 ± 0.6	0.060 ± 0.068	553 ± 198
III	1.2 ± 0.6	0.075 ± 0.069	673 ± 448
HRSBR			
I	1.8 ± 0.9	0.097 ± 0.048	95 ± 3
II	1.2 ± 0.5	0.134 ± 0.058	71 ± 8
IIIA	2.2 ± 1.0	0.070 ± 0.040	-
IIIB	1.3 ± 0.8	0.081 ± 0.038	282
IV	1.0 ± 0.3	0.097 ± 0.040	510

Figure 7.6 shows the average values of the different COD fractions as function of the SRT in both experimental systems. In the case of the HRAS reactor, the effluent COD_T, COD_F and COD_P concentrations increased (23.5, 11.7 and 31.2% respectively) when the SRT decreased from 2.1 d to 1.5 d. COD_C had similar concentrations between 8 and 15 $mgCOD \cdot L^{-1}$ in all cases and COD_S was below 50 $mgCOD \cdot L^{-1}$ for both SRT. Similar results of the effect of SRT on the effluent COD fractions was also observed by Rahman et al. (2016) when comparing continuous systems treating raw wastewater.

Regarding the HRSBR operation, effluent COD_T, COD_F and COD_P increased when SRT decreased, except for SRT = 1.2 d (period II). This fact could be explained by the attached biomass on the walls of the reactor, which resulted in an effective SRT higher than that calculated considering only planktonic biomass. The rest of the COD fractions were less affected by the SRT: COD_S was in the range 59.4 - 80.8 $mgCOD \cdot L^{-1}$ in all cases whereas COD_C had a minor role due to the low influent concentrations (14.5-21.2% of influent COD_T) (Table 7.1).

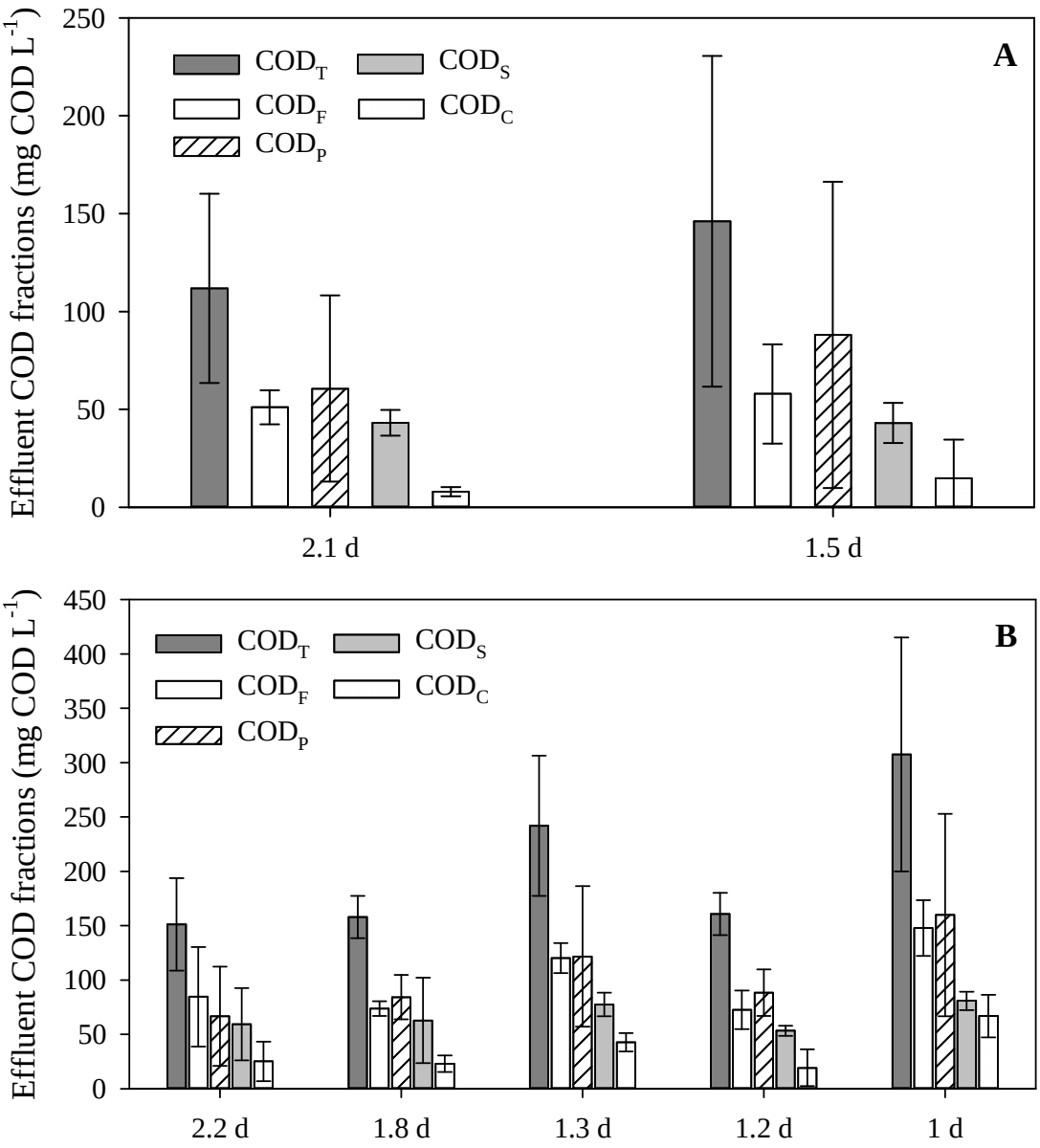

Figure 7.6. Average COD fractionation in the effluent of A) HRAS and B) HRSBR.

COD removal efficiencies for both systems are shown in Table 7.5. The HRAS system showed slightly lower COD removal efficiency (from 70 to 65 % COD_T removal) when decreasing the SRT from 2.1 to 1.2 d. Higher variations were observed for the HRSBR. If the results of periods I and II are discarded due to the problems of biomass attached to the reactor walls, a clear decreasing trend of COD removal is observed when SRT decreases. For example, the removal efficiency of COD_T decreases from 54 to 15% when the SRT decreases from 2.2 to 1 d. Thus, the lower the SRT, the higher the total COD in the effluent. Understanding the behaviour of the removal efficiencies of each individual COD fraction is not straightforward since many non-controlled interactions happen (from hydrolysis to aggregation). Moreover, the values of these fractions in the reactor are

dynamic and, thus, some positive or negative accumulation of these fractions may occur. Removal efficiencies lower than 50% were achieved for COD_P during the entire operation. In fact, negative COD_P removal efficiencies were obtained when SVI increased and the solids content in the reactor was reduced (periods IIIB and IV corresponding to the lower SRT tested of 1 d). That led to a high effluent COD_P value, which was transitorily higher than the influent COD_P. A decrease in the COD_C removal efficiency during the same periods (Table 7.5) was also observed. Therefore, the efficiency removal of COD_P and COD_C decreased in parallel to the decrease in the SRT but with limited impact on the COD_S. Faust et al. (2014) reported that extracellular polymeric substances were lower at lower SRTs, which negatively affects bioflocculation, which is the mechanism responsible for removing particulate and colloidal COD from wastewater (Rahman et al., 2014). Jimenez et al. (2015) obtained a similar trend, the efficiencies for COD_P and COD_C removal decreased from 70% to around 40% and 60% respectively when the SRT decreased from 2 to 1 day.

Table 7.5. COD removal efficiencies (%) for both high rate systems

	SRT (d)	Period	COD_T	COD_F	COD_P	COD_S	COD_C	COD (0.22 µm)
HRAS	Start up	I	-	-	-	-	-	66 ± 6
	2.1 ± 0.6	II	70 ± 16	64 ± 5	70 ± 32	60 ± 7	77 ± 7	
	1.2 ± 0.6	III	65 ± 15	63 ± 18	66 ± 23	55 ± 17	71 ± 22	
HRSBR	1.8 ± 0.9	I	60 ± 10	68 ± 5	38 ± 36	58 ± 27	72 ± 17	
	1.2 ± 0.5	II	66 ± 13	72 ± 8	44 ± 39	73 ± 7	67 ± 27	
	2.2 ± 1.0	IIIA	54 ± 17	62 ± 9	25 ± 99	57 ± 12	57 ± 20	
	1.3 ± 0.8	IIIB	27 ± 19	50 ± 4	-	51 ± 10	42 ± 15	
	1.0 ± 0.3	IV	15 ± 27	43 ± 5	-	47 ± 10	33 ± 18	

-: negative removal efficiencies

The presence of either solids or organic matter in the influent of a B-stage can decrease its performance (Smitshuijzen et al., 2016). Thus, the effluent of the high-rate system should not represent a significant organic load to the B-stage process. Otherwise, this organic matter would result in the increase of the heterotrophic bacterial population, which would compete with the autotrophic bacteria for the electron acceptor (i.e. mostly nitrite) resulting in a limitation of the autotrophic nitrogen removal (Miller et al., 2016; Mozumder et al., 2014) and an increase of the aeration requirements. Considering this COD removal criterion, the effluent of the HRAS reactor was more adequate than that

from the HRSBR, as the COD_T removal efficiencies were systematically higher. Moreover, a higher impact of SRT on COD removal efficiencies was observed for the HRSBR (Table 7.5). The periods with the same SRT for both systems, as for example when SRT was around 2 days (period II of the HRAS and period IIIA of the HRSBR), have similar COD_S removal efficiency (60 vs. 57%). However, higher COD_P removal efficiency was obtained for the HRAS (70 vs. 25%), showing the higher capacity of separation of particulate compounds in the continuous HRAS.

7.3.4. COD_T mass balances

COD_T mass balances were performed at different SRTs for both systems using the steady-state operation data, obtaining the average COD fractions illustrated in Figures 7.7A and 7.7B. In addition, Figures 7.7C and 7.7D show the COD mass balance distribution in a perfect settling scenario (no solids lost in the effluent) and considering that all of the effluent biomass could be redirected to the anaerobic digestion. Mineralization was estimated as in Akanyeti et al. (2010), i.e. the COD fraction required to close the COD mass-balance.

Figure 7.7A and B show the COD distribution for the continuous HRAS and for the HRSBR. The data of the mineralization of the COD and the COD distribution was very dependent on the effluent solids. These variable concentrations of effluent solids can be attributed to a settling issue rather than a problem with the reactor configuration and, hence, the discussion of figures 7.7 C and D becomes much more meaningful.

The COD distribution obtained in the perfect settling scenario is shown in Figures 7.7C and 7.7D. These values were estimated assuming that: i) effluent COD_S was the only effluent COD fraction and ii) the experimental solids in the effluent were considered as part of the purge and the COD content in these solids was estimated using the same procedure as in the purge and with the stoichiometric factor (1.416 $gCOD \cdot g^{-1}VSS$).

The extent of mineralization in the HRAS system was important (Figure 7.7C) where values around 41-57% were observed. These values are in the range obtained by Jimenez et al. (2015) and Akanyeti et al. (2010) at SRT of 1 d. Moreover, the fraction of the inlet COD directed to the purge decreased from 34% to 30% when the SRT decrease from 2 to 1 d. This distribution was not expected because previous works (Akanyeti et al., 2010; Jimenez et al., 2015) reported carbon redirection improvement at lower SRT. This observation (i.e. similar COD distribution independently of the SRT) could be attributed

to the SRT range tested in this work, always higher than 1 day. In fact, Jimenez et al. (2015) and Rahman et al. (2016) did not observe differences between the COD distribution for 1-2 d SRT, and a clear difference was only observed at SRT below 0.5 d. Akanyeti et al. (2010) also worked with SRT below 1 d (0.25, 0.5 and 1 d), obtaining a mineralization of 27%, 41% and 54%, respectively.

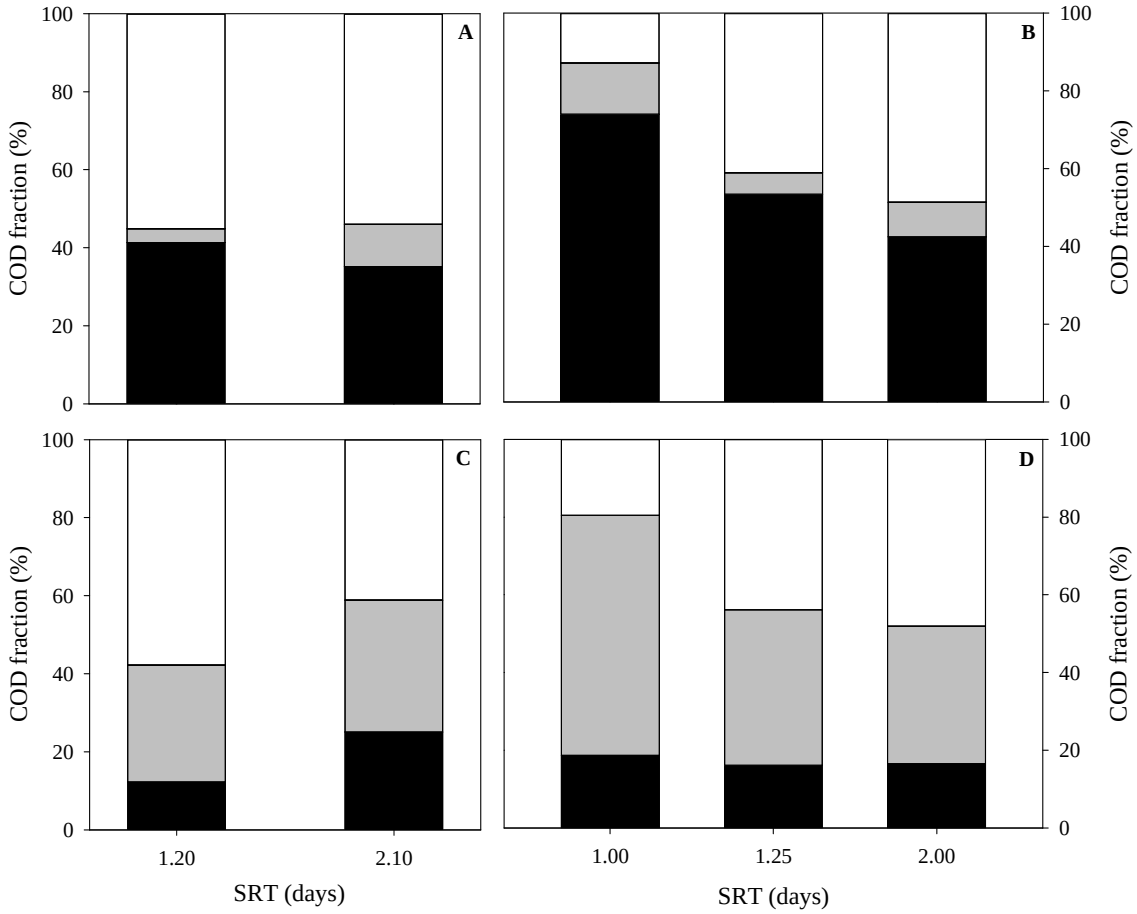

Figure 7.7. COD distribution as a fraction of influent COD at different SRT conditions for A) HRAS and B) HRSBR. C) and D) correspond to HRAS and HRSBR in the perfect settling scenario. Effluent (■), purge (▭) and mineralization (□).

Regarding HRSBR, a decrease in the SRT implied an increase of the COD redirected to the purge, up to 62% when the SRT was 1 d. Consequently, the COD fraction in the effluent decreased considerably: the values obtained in this hypothetical scenario were in the range of 16-19% whereas the values reached in the real mass balance were between 42-74%. This is the first report where a HRSBR was used as an A-stage and, therefore, there is no available literature to compare the results. However, the COD redirected to purge obtained in this work at a SRT of 1 d (62%) was higher than the values observed in other studies with continuous systems operating at even lower SRTs. In fact, Rahman

et al. (2019) observed percentages of COD in purge around 43% only at SRT of 0.3 d. The extent of mineralization was lower in the HRSBR (19.5%) than in the continuous HRAS system (58%) when the SRT was 1 d. This mineralization was also lower than the obtained by Jimenez et al. (2015) for the same SRT (60%). However, when the authors worked at shorter SRTs (0.3-0.1 d) the mineralization decreased until 20%, which is the value obtained for the HRSBR. As a conclusion, the HRSBR allowed a better control of the extent of mineralization process, which means that there was more COD in the purge and available for redirection to anaerobic digestion.

7.3.5. Observed biomass growth yield (Y_{OBS})

The values of Y_{OBS} calculated for each SRT are presented in Table 7.6. Y_{OBS} seems to be higher at high SRT conditions for HRAS. The start-up (period I) was the period with the highest SRT value (2.5 d), and with highest Y_{OBS} (1.05 ± 0.38 gVSS·g^{-1}COD). Values higher than one are not possible when accounting only for biological processes. However, higher Y_{OBS} values have sense if other non-biological processes such as adsorption occur. There may be a fraction of COD, which is not degraded, that is adsorbed in the solids of the effluent. Therefore, the solids of the effluent are highly overestimated and, thus, the solids production is overestimated too. Ge et al. (2017) also observed the same behaviour operating a lab-scale HRAS system with Y_{OBS} values between 10-13 gVSS·g^{-1}COD for SRT of 2-3 d and 3-6 gVSS·g^{-1}COD for SRT of 0.5-1 d (Table 7.6). In contrast, in the HRSBR, at longer SRTs (2.2 d) the Y_{OBS} (0.58 ± 0.34 gVSS·g^{-1}COD) was lower compared to short SRT conditions (1 d) with Y_{OBS} values of 1.35 ± 0.54 gVSS·g^{-1}COD. This effect of SRT on the Y_{OBS} was similar to the observed by Jimenez et al. (2015) and Rahman et al. (2016) (Table 7.6).

Table 7.6. Observed yield as a function of SRT

System	Period	SRT (d)	Y_{obs} ($gCOD \cdot g^{-1}COD$)	Y_{obs} ($gVSS \cdot g^{-1}COD$)	$\frac{N_{growth}}{N_{influent}}$ (%)	N-removal (%)
HRAS	III	1.2 ± 0.6	0.53 ± 0.35	0.37 ± 0.25	22 ± 19	11 ± 4
(This study)	II	2.1 ± 0.6	0.92 ± 0.80	0.65 ± 0.56	23 ± 16	19 ± 7
	I	2.5 ± 0.2	1.48 ± 0.54	1.05 ± 0.38	31 ± 4	32 ± 9
HRSBR	IV	1.0 ± 0.3	1.91 ± 0.77	1.35 ± 0.54	24 ± 2	6 ± 2
(This study)	II	1.2 ± 0.5	0.69 ± 0.37	0.49 ± 0.26	20 ± 6	20 ± 10
	IIIB	1.3 ± 0.8	0.83 ± 0.43	0.59 ± 0.31	13 ± 7	4 ± 2
	I	1.8 ± 0.9	0.76 ± 0.54	0.54 ± 0.38	21 ± 9	22 ± 6
	IIIA	2.2 ± 1.0	0.81 ± 0.49	0.58 ± 0.34	18 ± 10	6 ± 3
HRAS		0.5		0.47 ± 0.11		
Jimenez et al. (2015)		1.0		0.38 ± 0.08		
		2.0		0.33 ± 0.10		
CSTR		0.2	0.54 ± 0.06			
Rahman et al. (2016)		0.8	0.47 ± 0.08			
		2.2	0.45 ± 0.13			
HRAS		0.5-1		3-6		
Ge et al. (2017)		2-3		10-13		

7.3.6. Nutrient removal

Figure 7.8 shows the nitrogen and phosphorus concentrations in the influent and effluent of the continuous HRAS and the HRSBR for the entire operation. Some nitrification was observed in the case of HRAS (Figure 7.8A): ammonia removal efficiencies of 53 ± 11% and 47 ± 17% were obtained during periods I and II respectively. However, from day 115 until day 145, ammonia removal efficiency decreased down to 10 ± 5%. This ammonia removal could be attributed to assimilation for microbial growth rather than to nitrification. The amount of nitrogen incorporated into the biomass during the cellular synthesis (Table 7.6) was estimated with mass balances, considering the COD removal, the Y_{OBS} and the typical stoichiometric factor of 0.086 g $N \cdot g^{-1}COD$ reported by Henze et al. (1987) for modelling studies. Results on Table 8.6 demonstrate that during periods I and II, 31% and 23% of the influent nitrogen was removed by heterotrophs growth. The assimilative nitrogen uptake was higher in period I due to the higher Y_{OBS}. Ammonia assimilation in this case is also overestimated since it is considered that all the solids in the effluent are biomass and, as discussed above, a fraction of adsorbed COD might be

present. The occurrence of nitrification in periods I and II at SRT values of 2.5 days and T=20 ºC was unexpected. However, the proliferation of some nitrifiers as a biofilm grown on the reactor walls could explain the detection of some nitrification activity. On the other hand, nitrification was not detected during period III (SRT = 1 d). The percentage of nitrogen attributed to growth was higher than the nitrogen removal efficiency (Table 7.6).

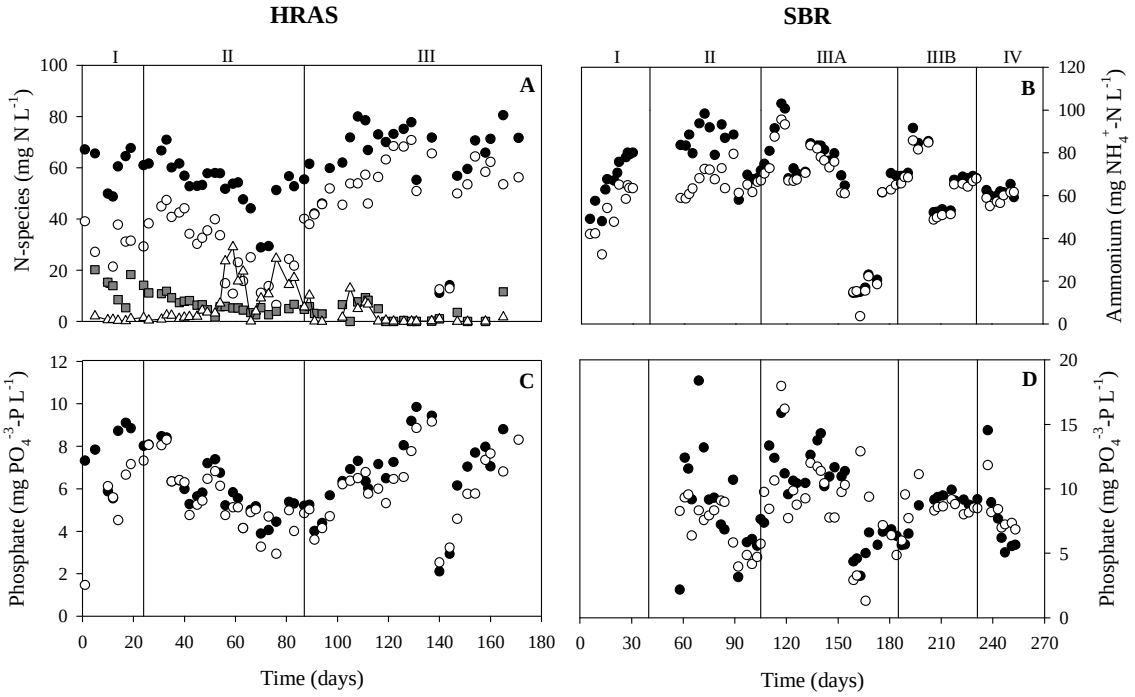

Figure 7.8. Ammonium concentration in the influent (●) and in the effluent (○) A) for HRAS and B) for HRSBR. Nitrite (■) and nitrate (Δ) concentrations in the effluent for HRAS. Phosphate concentration in the influent (●) and in the effluent (○) C) for HRAS and D) for HRSBR.

In the case of the HRSBR, the average ammonia removal was 21 ± 8% for periods I and II, however in the subsequent periods this value decreased down to 7 ± 1% (Figure 7.8B). In this case, 19% of the nitrogen influent was removed via biomass assimilation or adsorption for the higher SRT tested (2 d) and corresponding with the lower Y_{OBS}. A 24% of the nitrogen influent was removed by heterotrophs growth when SRT was 1 d and a higher Y_{OBS} was obtained (Table 7.6).

Nitrification is neither expected nor desired in a high rate system, as only COD should be removed during this step. It was only observed in the HRAS when the growth of a biofilm in the reactor walls was not avoided. The significance of the reactor walls is an inherent

problem only for lab-scale reactors and it is not expected to be important at full-scale systems.

Regarding phosphorus, the slight phosphorus removal observed could be attributed to assimilation during microbial growth for both systems. P-removal efficiencies of 9.5-12% were obtained in HRAS whereas higher values between 7-28% were obtained in HRSBR (Figure 7.8C and 7.8D respectively). The oscillations in the influent phosphorus concentration were due to variations of the real.

7.3.7. Biochemical methane potential (BMP)

Anaerobic digestion assays of the sludge generated in both systems and in periods under different SRTs were performed (Figure 7.9 and table 7.7). The highest BMP (307.8 ±6.7 L $CH_4 \cdot kg^{-1}$VS-added) was obtained for the lowest SRT (0.8 d) and the lowest BMP (187.2 ± 4.2 L $CH_4 \cdot kg^{-1}$VS-added) was obtained for the sludge generated at SRT of 2 days (both from the HRSBR). This is in accordance with Ge et al. (2013) who observed an increase in the anaerobic degradability of the sludge with decreasing the SRT. Finally, the sludge generated in the HRAS had a BMP of 275.6 ± 7.4 L $CH_4 \cdot kg^{-1}$VS-added (Table 7.7) when the SRT of the system was 1.2 d. The BMP values obtained in this study were lower than those obtained by Ge et al. (2017) (335.5 ± 8.7 and 357 ± 12.8 L $CH_4 \cdot kg^{-1}$VS-added) for the same SRT interval (2-1 d).

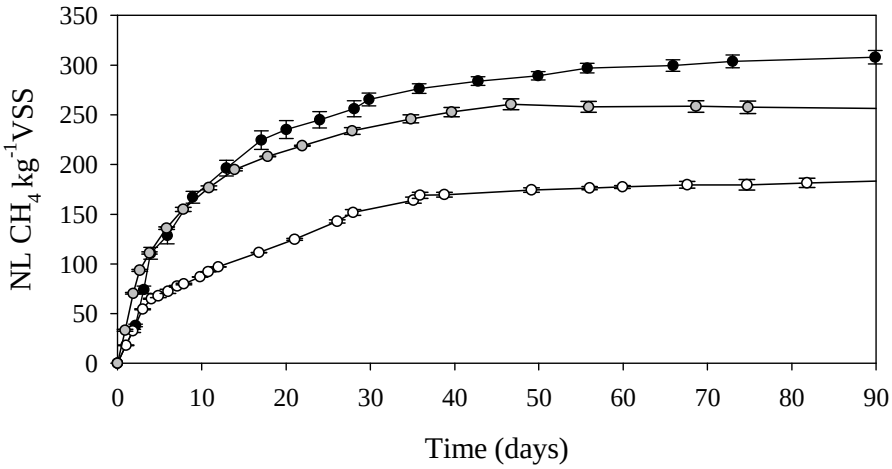

Figure 7.9. Cumulative methane production from mesophilic anaerobic digestion batch tests for different SRTs sludge. HRAS: 1.2 d (●).HRSBR: 2 d (○), 0.8 d (●).

Table 7.7. Ultimate methane production for the different sludge studied in this work.

System	SRT (d)	Ultimate methane production (NL $CH_4 \cdot kg^{-1}$VS-added)
HRAS	1.2	275.6 ± 7.4
HRSBR	0.8	307.8 ± 6.7
	2.0	187.2 ± 4.2

7.3.8 EBPR integration in high-rate systems

According to the results presented above, the integration of EBPR in A-stage systems could be a favourable option. Operating at SRTs somehow higher than 1 or 2 days does not seem to decrease the performance severely of these systems and, besides that, PAOs could enhance COD removal. The extra anaerobic phase would not increase the chances of nitrification appearance provided the aerobic SRT is not increased.

The results obtained in this chapter have opened the possibility of integrating EBPR in a high rate system (either a HRSBR or in a HRAS). Both objectives are very ambitious and, thus, out of the scope of the present thesis. Therefore, this possibility was finally studied in a single PhD thesis by another member of the research group. The case of integrating EBPR in a HRSBR system was studied in Chan (2018), who proved that EBPR could be integrated in an HRSBR system with a short SRT. The exact minimum value is highly dependent on the temperature but a value around 3.5 and 4 days may be suitable at room temperature.

The integration of EBPR in a HRAS system was preliminary studied in this thesis and the results were promising. This research is currently continued in the frame of a new PhD thesis in the group. The preliminary results were obtained in the anaerobic/aerobic pilot WWTP described in section 7.2.4 of materials and methods (A/O-HRAS) of the present chapter. Figure 7.10 shows an example of this EBPR integration in the period of SRT around 2-3 days and a DO value of 1 mg/L.

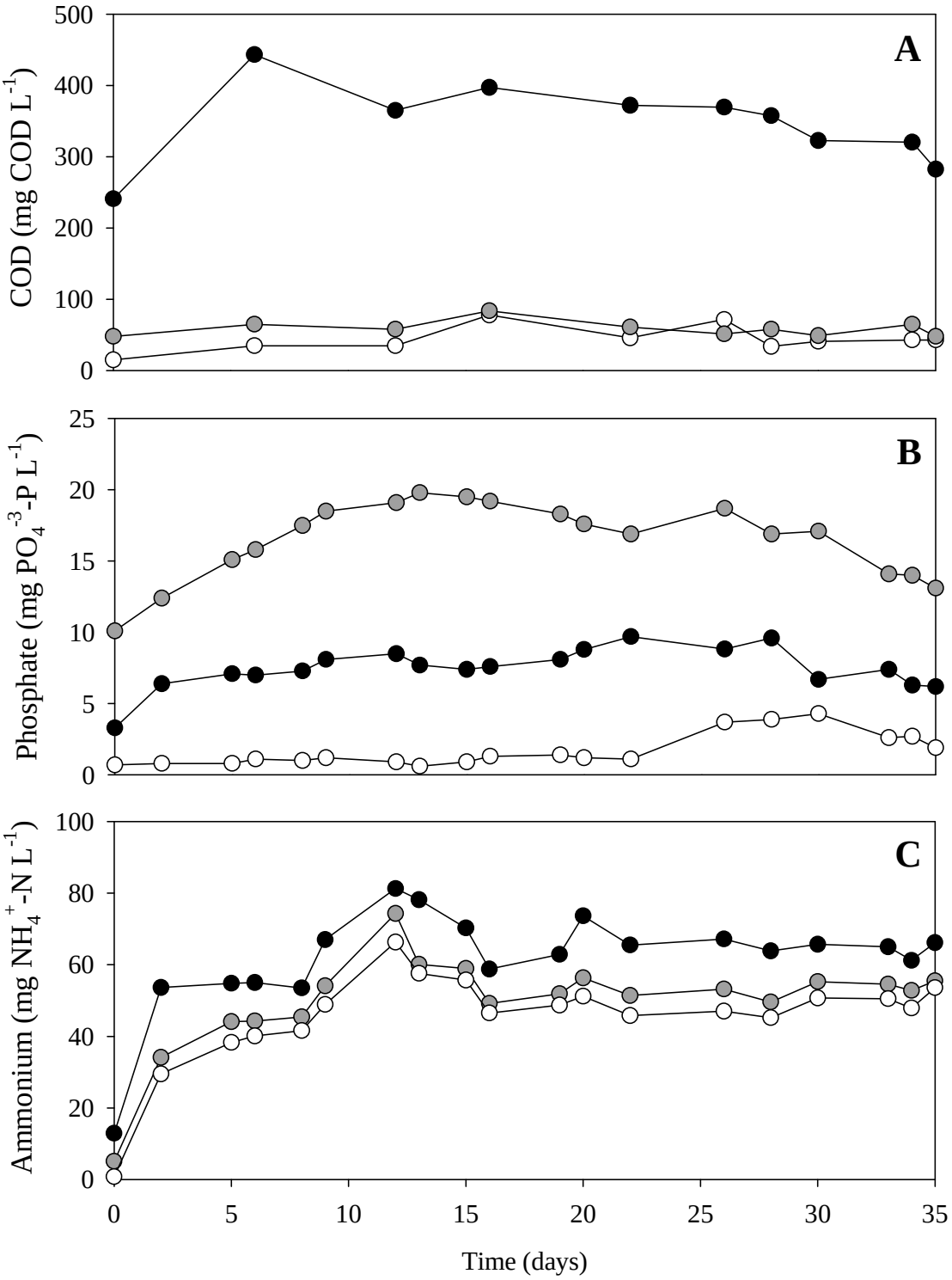

Figure 7.10. Concentrations C,N and P during the integration of EPBR in the HRAS system: COD (A), Phosphate (B) and Ammonium (C) in the influent (●), in the anaerobic chamber (●) and in the effluent (○).

In general, the results showed that DO had to be as low as possible in order to prevent the growth of nitrifiers but high enough to not affect aerobic PAO kinetics or sludge

settleability. Since DO limitation on kinetics is highly relevant, the effect of temperature is non-negligible and, thus, this parameter has to be considered and monitored. Throughout the experimental period, high COD removal was reached (87.4 ± 4.5%) with most of the organic carbon depleted in the anaerobic phase (more than 80% of total COD removed) ensuring an oxygen saving (Figure 7.10A). P-removal efficiencies of 84.9 ± 3.8% were obtained until day 26, when P-release decreased from values around 19 mg $P \cdot L^{-1}$ to 13 mg $P \cdot L^{-1}$ and as a consequence, P concentrations in the effluent increased from 1 mg $P \cdot L^{-1}$ to 4 mg $P \cdot L^{-1}$ and P-removal efficiency dropped to values of 53.5 ± 12.6% (Figure 7.10B).

Nitrification appearance is the main barrier towards maintaining EBPR at low SRT conditions. In this case, nitrification could be effectively repressed (Figure 7.6C) during this period without production of nitrite neither nitrate. Therefore, the decrease in P-removal efficiency since day 26 cannot be attributed to nitrate presence in the anaerobic phase but to a loss of solids in the reactor (Figure 7.7). The solids in both anaerobic and aerobic chambers decreased to values below 1 $gVSS \cdot L^{-1}$ after day 16.

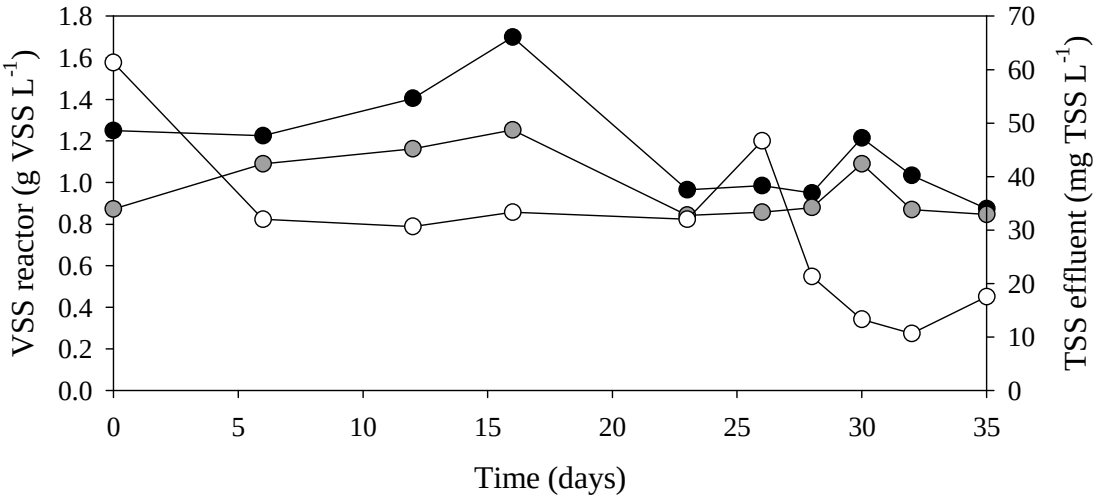

Figure 7.7. Solids concentration in: anaerobic phase (●), aerobic phase (●) and effluent (○).

Therefore, further research is currently being conducted to find the optimal conditions to reach a satisfactory EBPR performance at very low SRT with very low nitrifying activity and with a sludge with proper settleability characteristics.

7.4. Conclusions

The continuous HRAS system yielded higher COD removal efficiencies for all fractions (>60%) when compared to the HRSBR. In this latter system, the particulate COD fraction never reached the 50% of removal. Similar solids content in the effluent was observed for both systems. Obtaining low COD content and solids presence in the effluent of the A-stage is an essential feature of an A-stage system, since they affect the performance of the B-stage.

Mineralization was calculated for the perfect settling scenario, obtaining values around 20% for the HRSBR, and 41-57% for the HRAS. Hence, the COD mineralization in the HRSBR was lower, which enhances the potential energy recovery of the system, since more COD could be diverted to anaerobic digestion.

Nitrification was more easily repressed in the HRSBR. This is an important factor to guarantee a suitable ammonia influent concentration for the subsequent B-stage.

Values of Y_{OBS} higher than 1 were obtained for both systems, indicating that other non-biological processes (such as adsorption) occurred. As a consequence, a fraction of COD was adsorbed in the solids of the effluent and their production was overestimated.

A dilemma between the two high-rate systems arises. On the one hand, better results were obtained with the HRAS in terms of COD removal and solids presence. On the other hand, the extent of mineralization and the degree of nitrification were lower in the case of HRSBR. Therefore, the HRSBR seems to be the best option, because the solids content in the effluent was similar for both systems and the COD removal efficiencies could be improved by increasing the oxygen transfer with a better agitation conditions or by lengthening the aerobic phase. Nevertheless, an optimization of the SBR cycle configuration is recommended to demonstrate the feasibility and reliability of the HRSBR as an A-stage in an A/B configuration.

Finally, this work explored the possibility of integrating EPBR into A-stage systems. Promising results were obtained using an A/O-HRAS (continuous anaerobic-aerobic) system at SRT of 2.5 ± 0.2 d, in line with the good EBPR performance obtained by Chan (2018) in an SBR working at a SRT of 3.5-4 d. The A/O-HRAS system is currently being studied by other PhD students in the research group.

Chapter 8

GENERAL CONCLUSIONS

The overall results obtained in this thesis contributed to a deeper understanding of the behaviour of the microbial populations developed in an EBPR system using complex substrates as carbon source and to evaluate the possibility of integrating the EBPR process in the A-stage of the A/B configuration.

Hence, two blocks of conclusions can be withdrawn considering both objectives separately:

EBPR performance using complex carbon sources

- A continuous A^2/O pilot plant was successfully operated using glutamate as carbon and nitrogen source with simultaneous biological N and P removal and high denitrifying PAO activity.
- A microbial community enriched in *Comamonadaceae*, *Thiothrix* and a smaller fraction of *Accumulibacter* living off glutamate fermentation products were obtained. The contribution to P-removal from microorganisms other than *Accumulibacter* was needed to explain the low production of PHA and the lack of glycogen degradation during the anaerobic phase.
- The microbial community was capable to use both nitrite and nitrate as electron acceptors for P-uptake. A dependence of P-uptake with FNA concentration was observed: the higher the FNA concentration the lower the P-uptake. The process completely stops when the FNA reach values of 2 $\mu g\ N\text{-}HNO_2^- \cdot L^{-1}$. The mixed microbial culture seems to be more sensitive to nitrite inhibition than other cultures highly enriched in *Accumulibacter*.
- Higher P-uptake values were achieved when nitrate is the electron acceptor, however higher P-uptake rates were obtained using nitrite.
- An SBR performing carbon and P removal and using casein hydrolysate as carbon source was operated resulting in a mixed culture enriched in *Tetrasphaera* with presence of *Accumulibacter*. This culture was able to uptake different amino acids (arginine, lysine, cysteine, proline and tyrosine) under anaerobic conditions.
- A mixture with the previous five amino acids has a synergic effect on the bio-P removal performance.

- The fermentation products of the amino acids were an essential feature to understand the EBPR performance and they could be connected to the different involvement of PHA and glycogen in the batch tests.
- The capability to consume casein hydrolisate and a mixture of five amino acids (arginine, lysine, cysteine, proline and tyrosine) by the different cultures is related to the abundance of a particular clade within the genus *Tetrasphaera*.

Integration of EBPR process in the A-stage step

- A continuous system and an SBR were compared, obtaining better results with the continuous reactor in terms of COD removal and solids presence. However, the extent of mineralization and nitrification were lower in the case of HRSBR. Moreover, the sludge from HRSBR achieved higher BMP.
- Promising results were obtained using an A/O-HRAS system at SRT of 2.5 ± 0.2 d.

Chapter 9

REFERENCES

Ahn, J., Daidou, T., Tsuneda, S., Hirata, A., 2001a. Selection and dominance mechanisms of denitrifying phosphate-accumulating organisms in biological phosphate removal process. Biotechnol. Lett. 23, 2005–2008. doi:https://doi.org/10.1023/A:1013726812529

Ahn, J., Daidou, T., Tsuneda, S., Hirata, A., 2001b. Metabolic behavior of denitrifying phosphate-accumulating organisms under nitrate and nitrite electron acceptor conditions. J. Biosci. Bioeng. 92, 442–446. doi:10.1016/S1389-1723(01)80293-0

Ahn, J., Schroeder, S., Beer, M., McIlroy, S., Bayly, R.C., May, J.W., Vasiliadis, G., Seviour, R.J., 2007. Ecology of the microbial community removing phosphate from wastewater under continuously aerobic conditions in a sequencing batch reactor. Appl. Environ. Microbiol. 73, 2257–2270. doi:10.1128/AEM.02080-06

Akanyeti, I., Temmink, H., Remy, M., Zwijnenburg, A., 2010. Feasibility of bioflocculation in a high-loaded membrane bioreactor for improved energy recovery from sewage. Water Sci. Technol. 61, 1433–1439. doi:10.2166/wst.2010.032

Albertsen, M., Hansen, L.B.S., Saunders, A.M., Nielsen, P.H., Nielsen, K.L., 2012. A metagenome of a full-scale microbial community carrying out enhanced biological phosphorus removal. ISME J. 6, 1094–106. doi:10.1038/ismej.2011.176

Albertsen, M., Karst, S.M., Ziegler, A.S., Kirkegaard, R.H., Nielsen, P.H., 2015. Back to basics - The influence of DNA extraction and primer choice on phylogenetic analysis of activated sludge communities. PLoS One 10, 1–15. doi:10.1371/journal.pone.0132783

Albertsen, M., Mcilroy, S.J., Stokholm-bjerregaard, M., Karst, S.M., Tyson, G.W., 2016. "Candidatus Propionivibrio aalborgensis": A Novel Glycogen Accumulating Organism Abundant in Full-Scale Enhanced Biological Phosphorus Removal Plants. Front. Microbiol. 7, 1–17. doi:10.3389/fmicb.2016.01033

Amann, R.I., Binder, B.J., Olson, R.J., Chisholm, Sallie, W., Devereux, R., Stahl, D.A., 1990. Combination of 16S rRNA-targeted oligonucleotide probes with flow cytometry for analyzing mixed microbial populations . Combination of 16S rRNA-Targeted Oligonucleotide Probes with Flow Cytometry for Analyzing Mixed Microbial Populations. Appl. Environ. Microbiol. 56, 1919–1925. doi:10.1111/j.1469-8137.2004.01066.x

Angelidaki, I., Alves, M., Bolzonella, D., Borzacconi, L., Campos, J.L., Guwy, A.J., Kalyuzhnyi, S., Jenicek, P., Van Lier, J.B., 2009. Defining the biomethane potential (BMP) of solid organic wastes and energy crops: A proposed protocol for batch assays. Water Sci. Technol. 59, 927–934. doi:10.2166/wst.2009.040

APHA, 2005. Standard Methods for the Examination of Water and Wastewater., 21st ed. American Public Health Association, Washington D.C.

APHA, 1995. Standard methods for the examination of water and wastewater. American Public Health Association, Washington, DC. USA.

Asano, T., Burton, F.L., Leverenz, H.L., Tsuchihashi, R., Tchobanoglous, G., 2007. Water Reuse: Issues, Technologies and applications, McGraw-Hill Professional, New York.

Baena, S., Fardeau, M.L., Ollivier, B., Labat, M., Thomas, P., Garcia, J.L., Patel, B.K.C., 1999. *Aminomonas paucivorans* gen. nov., sp. nov., a mesophilic, anaerobic, amino-acid-utilizing bacterium. Int. J. Syst. Bacteriol. 49, 975–982.

Barker, H.A., 1981. Amino acid degradation by anaerobic bacteria. Annu. Rev. Biochem. 50, 23–40. doi:10.1038/npg.els.0001388

Barker, H.A., Kahn, J.M., Hedrick, L., 1982. Pathway of lysine degradation in Fusobacterium nucleatum. J. Bacteriol. 152, 201–207.

Batstone, D.J., Hülsen, T., Mehta, C.M., Keller, J., 2015. Platforms for energy and nutrient recovery from domestic wastewater: A review. Chemosphere 140, 2–11. doi:10.1016/j.chemosphere.2014.10.021

Böhnke, B., 1977. Das adsorptions-Belebungsverfahren. Korresp. Abwasser, 24, 121-127

Buckel, W., 2001. Unusual enzymes involved in five pathways of glutamate fermentation. Appl. Microbiol. Biotechnol. 57, 263–273. doi:10.1007/s002530100773

Buckel, W., Barker, H.A., 1974. Two pathways of glutamate fermentation by anaerobic bacteria. J. Bacteriol. 117, 1248–1260.

Cai, L., Krafft, T., Chen, T. Bin, Lv, W.Z., Gao, D., Zhang, H.Y., 2017. New insights into biodrying mechanism associated with tryptophan and tyrosine degradations during sewage sludge biodrying. Bioresour. Technol. 244, 132–141. doi:10.1016/j.biortech.2017.07.118

Carvalheira, M., Oehmen, A., Carvalho, G., Reis, M.A.M., 2014. The effect of substrate competition on the metabolism of polyphosphate accumulating organisms (PAOs). Water Res. 64, 149–159. doi:10.1016/j.watres.2014.07.004

Carvalho, G., Lemos, P.C., Oehmen, A., Reis, M.A.M., 2007. Denitrifying phosphorus removal: Linking the process performance with the microbial community structure. Water Res. 41, 4383–4396. doi:10.1016/j.watres.2007.06.065

Chan, C., Guisasola, A., Baeza, J.A., 2017. Enhanced Biological Phosphorus Removal at low Sludge Retention Time in view of its integration in A-stage systems. Water Res. 118. doi:10.1016/j.watres.2017.04.010

Chua, A.S.M., Onuki, M., Satoh, H., Mino, T., 2006. Examining substrate uptake patterns of Rhodocyclus-related PAO in full-scale EBPR plants by using the MAR-FISH technique. Water Sci. Technol. 54, 63–70. doi:10.2166/wst.2006.372

Coats, E.R., Brinkman, C.K., Lee, S., 2017. Characterizing and contrasting the microbial ecology of laboratory and full-scale EBPR systems cultured on synthetic and real wastewaters. Water Res. 108, 124–136. doi:10.1016/j.watres.2016.10.069

Comeau, Y., Oldham, W.K., Hall, K.J., 1987. Dynamics of Carbon Reserves in Biological Dephosphatation of Wastewater, Biological Phosphate Removal from Wastewaters. International Association on Water Pollution Research and Control. doi:10.1016/b978-0-08-035592-4.50010-9

Crocetti, G.R., Hugenholtz, P., Bond, P.L., Schuler, A., Keller, J., Jenkins, D., Blackall, L.L., 2000. Identification of polyphosphate-accumulating organisms and design of 16S rRNA-directed probes for their detection and quantitation. Appl. Environ. Microbiol. 66, 1175–1182. doi:10.1128/AEM.66.3.1175-1182.2000

Crocetti R., G., Banfield F., J.F., Keller, J., Bond, P.L., Blackall, L.L., 2002. Glycogen-accumulating organisms in laboratory-scale and full-scale wastewater treatment processes. Microbiology 148, 3353–3364. doi:10.1099/00221287-148-11-3353

Cydzik-Kwiatkowska, A., Zielinska, M., 2016. Bacterial communities in full-scale wastewater treatment systems. World J Microbiol Biotechnol 32. doi:10.1007/s11274-016-2012-9

Daims, H., Brühl, a, Amann, R., Schleifer, K.H., Wagner, M., 1999. The domain-specific probe EUB338 is insufficient for the detection of all Bacteria: development and evaluation of a more comprehensive probe set. Syst. Appl. Microbiol. 22, 434–44. doi:10.1016/S0723-2020(99)80053-8

Dionisi, D., Majone, M., Miccheli, A., Puccetti, C., Sinisi, C., 2004. Glutamic acid removal and

PHB storage in the activated sludge process under dynamic conditions. Biotechnol. Bioeng. 86, 842–851. doi:10.1002/bit.20091

Faust, L., Temmink, H., Zwijnenburg, A., Kemperman, A.J.B., Rijnaarts, H.H.M., 2014. High loaded MBRs for organic matter recovery fromsewage: Effect of solids retention time on bioflocculation and on the role of extracellular polymers. Water Res. 56, 258–266. doi:10.1016/j.watres.2014.03.006

Feng, L., Chen, K., Han, D., Zhao, J., Lu, Y., Yang, G., Mu, J., Zhao, X., 2017. Comparison of nitrogen removal and microbial properties in solid-phase denitrification systems for water purification with various pretreated lignocellulosic carriers. Bioresour. Technol. 224, 236–245. doi:10.1016/j.biortech.2016.11.002

Flowers, J.J., He, S., Yilmaz, S., Noguera, D.R., Mcmahon, K.D., 2009. Denitrification capabilities of two biological phosphorus removal sludges dominated by different 'Candidatus Accumulibacter' clades. Environ. Microbiol. Rep. 1, 583–588. doi:10.1111/j.1758-2229.2009.00090.x

Fukushima, T., Uda, N., Okamoto, M., Onuki, M., Satoh, H., Mino, T., 2007. Abundance of Candidatus 'Accumulibacter phosphatis' in Enhanced Biological Phosphorus Removal Activated Sludge Acclimatized with Different Carbon Sources. Microbes Environ. 22, 346–354. doi:10.1264/jsme2.22.346

García Martín, H., Ivanova, N., Kunin, V., Warnecke, F., Barry, K.W., Mchardy, A.C., Yeates, C., He, S., Salamov, A.A., Szeto, E., Dalin, E., Putnam, N.H., Shapiro, H.J., Pangilinan, J.L., Rigoutsos, I., Kyrpides, N.C., Blackall, L.L., McMahon, K.D., Hugenholtz, P., 2006. Metagenomic analysis of two enhanced biological phosphorus removal (EBPR) sludge communities. Nat. Biotechnol. 24, 1263–1269. doi:10.1038/nbt1247

Ge, H., Batstone, D.J., Keller, J., 2015. Biological phosphorus removal from abattoir wastewater at very short sludge ages mediated bynovel PAO clade Comamonadaceae. Water Res. 69, 173–182. doi:10.1016/j.watres.2014.11.026

Ge, H., Batstone, D.J., Keller, J., 2013. Operating aerobic wastewater treatment at very short sludge ages enables treatment and energy recovery through anaerobic sludge digestion. Water Res. 47, 6546–6557. doi:10.1016/j.watres.2013.08.017

Ge, H., Batstone, D.J., Mouiche, M., Hu, S., Keller, J., 2017. Nutrient removal and energy recovery from high-rate activated sludge processes – Impact of sludge age. Bioresour. Technol. 245, 1155–1161. doi:10.1016/j.biortech.2017.08.115

Gu, Y., Li, Y., Li, X., Luo, P., Wang, H., Robinson, Z.P., Wang, X., Wu, J., 2017. The feasibility and challenges of energy self-sufficient wastewater treatment plants. Appl. Energy 204, 1463–1475. doi:10.1016/J.APENERGY.2017.02.069

Guerrero, J., Guisasola, A., Baeza, J.A., 2011. The nature of the carbon source rules the competition between PAO and denitrifiers in systems for simultaneous biological nitrogen and phosphorus removal. Water Res. 45, 4793–4802. doi:10.1016/j.watres.2011.06.019

Guerrero, J., Tayà, C., Guisasola, A., Baeza, J.A., 2012. Glycerol as a sole carbon source for enhanced biological phosphorus removal. Water Res. 46, 2983–2991. doi:10.1016/j.watres.2012.02.043

Guisasola, A., Pijuan, M., Baeza, J.A., Carrera, J., Casas, C., Lafuente, J., 2004. Aerobic Phosphorus Release Linked to Acetate Uptake in Bio-P Sludge: Process Modeling Using Oxygen Uptake Rate. Biotechnol. Bioeng. 85, 722–733. doi:10.1002/bit.10868

Guisasola, A., Qurie, M., Vargas, M. del M., Casas, C., Baeza, J.A., 2009. Failure of an enriched nitrite-DPAO population to use nitrate as an electron acceptor. Process Biochem. 44, 689–

695. doi:10.1016/j.procbio.2009.02.017

He, S., Gall, D.L., McMahon, K.D., 2007. "Candidatus Accumulibacter" population structure in enhanced biological phosphorus removal sludges as revealed by polyphosphate kinase genes. Appl. Environ. Microbiol. 73, 5865–5874. doi:10.1128/AEM.01207-07

Henze, M., Grady, C.P.L., Gujer, W., Marais, G. v. R., Matsuo, T., 1987. Activated Sludge Model No . 1. IAWPRC Sci. c Tech. Reports 1223, 19–21. doi:10.1016/S0273-1223(98)00785-9

Henze, M., van Loosdrecht, M.C.., Ekama, G., Brdjanovic, D., 2008. Biological wastewater treatment : principles, modelling and design. IWA Pub.

Hesselmann, R.P.X., Werlen, C., Hahn, D., Van Der Meer, J.R., Zehnder, A.J.B., 1999. Enrichment, phylogenetic analysis and detection of a bacterium that performs enhanced biological phosphate removal in activated sludge. Syst. Appl. Microbiol. 22, 454–465. doi:10.1016/S0723-2020(99)80055-1

Hu, M., Wang, X., Wen, X., Xia, Y., 2012. Microbial community structures in different wastewater treatment plants as revealed by 454-pyrosequencing analysis. Bioresour. Technol. 117, 72–79. doi:10.1016/j.biortech.2012.04.061

Hugenholtz, P., Tyson, G.W., Blackall, L.L., 2002. Design and Evaluation of 16S rRNA-Targeted Oligonucleotide Probes for Fluorescence In Situ Hybridization. Gene Probes (pp. 029–042). New Jersey Humana Press 179, 29–42. doi:10.1385/1-59259-238-4:029

Hui, Y., Seak, A., Chua, M., Tzu, Y., Cheng, G., 2016. The microbial community in a high-temperature enhanced biological phosphorus removal (EBPR) process. Sustain. Environ. Res. 26, 14–19. doi:10.1016/j.serj.2016.04.001

Isanta, E., Reino, C., Carrera, J., Pérez, J., 2015. Stable partial nitritation for low-strength wastewater at low temperature in an aerobic granular reactor. Water Res. 80, 149–158. doi:10.1016/j.watres.2015.04.028

Jabari, P., Munz, G., Yuan, Q., Oleszkiewicz, J.A., 2016. Free nitrous acid inhibition of biological phosphorus removal in integrated fixed-film activated sludge (IFAS) system. Chem. Eng. J. 287, 38–46. doi:10.1016/j.cej.2015.10.117

Jaramillo, F., Orchard, M., Muñoz, C., Zamorano, M., Antileo, C., 2018. Advanced strategies to improve nitrification process in sequencing batch reactors - A review. J. Environ. Manage. 218, 154–164. doi:10.1016/j.jenvman.2018.04.019

Jia, W., Zhang, J., Lu, Y., Li, G., Yang, W., Wang, Q., 2018. Response of nitrite accumulation and microbial characteristics to low-intensity static magnetic field during partial nitrification. Bioresour. Technol. 259, 214–220. doi:10.1016/j.biortech.2018.03.060

Jiang, Y., Wei, L., Zhang, H., Yang, K., Wang, H., 2016. Removal performance and microbial communities in a sequencing batch reactor treating hypersaline phenol-laden wastewater. Bioresour. Technol. 218, 146–152. doi:10.1016/j.biortech.2016.06.055

Jimenez, J., Miller, M., Bott, C., Murthy, S., De Clippeleir, H., Wett, B., 2015. High-rate activated sludge system for carbon management - Evaluation of crucial process mechanisms and design parameters. Water Res. 87, 476–482. doi:10.1016/j.watres.2015.07.032

Jubany, I., Lafuente, J., Carrera, J., Baeza, J.A., 2009. Automated thresholding method (ATM) for biomass fraction determination using FISH and confocal microscopy. J. Chem. Technol. Biotechnol. 84, 1140–1145. doi:10.1002/jctb.2146

Kapagiannidis, A.G., Zafiriadis, I., Aivasidis, A., 2013. Comparison between aerobic and anoxic metabolism of denitrifying-EBPR sludge: Effect of biomass poly-hydroxyalkanoates

content. N. Biotechnol. 30, 227–237. doi:10.1016/j.nbt.2012.05.022

Kartal, B., Kuenen, J.G., Van Loosdrecht, M.C.M., 2010. Sewage treatment with anammox. Science (80-.). 328, 702–703. doi:10.1126/science.1185941

Kerrn-Jespersen, J.P., Henze, M., 1993. Biological phosphorus uptake under anoxic and aerobic conditions. Water Res. 27, 617–624. doi:10.1016/0043-1354(93)90171-D

Khan, S.T., Horiba, Y., Yamamoto, M., Hiraishi, A., 2002. Members of the Family Comamonadaceae as Primary Denitrifiers in Activated Sludge as Revealed by a Polyphasic Approach. Appl. Environ. Microbiol. 68, 3206–3214. doi:10.1128/AEM.68.7.3206

Kim, D.-J., Kim, S.-H., 2006. Effect of nitrite concentration on the distribution and competition of nitrite-oxidizing bacteria in nitratation reactor systems and their kinetic characteristics. Water Res. 40, 887–894. doi:10.1016/j.watres.2005.12.023

Kim, J.M., Lee, H.J., Lee, D.S., Jeon, C.O., 2013. Characterization of the Denitrification-Associated Phosphorus Uptake Properties of "*Candidatus* accumulibacter phosphatis" Clades in Sludge Subjected to Enhanced Biological Phosphorus Removal. Appl. Environ. Microbiol. 79, 1969–1979. doi:10.1128/AEM.03464-12

Kong, Y., Nielsen, J.L., Nielsen, P.H., 2005. Identity and ecophysiology of uncultured actinobacterial polyphosphate-accumulating organisms in full-scale enhanced biological phosphorus removal plants. Appl. Environ. Microbiol. 71, 4076–4085. doi:10.1128/AEM.71.7.4076-4085.2005

Kong, Y., Ong, S.L., Ng, W.J., Liu, W., 2002. Diversity and distribution of a deeply branched novel proteobacterial group found in anaerobic – aerobic activated sludge processes. Environ. Microbiol. 4, 753–757.

Kristiansen, R., Nguyen, H.T.T., Saunders, A.M., Nielsen, J.L., Wimmer, R., Le, V.Q., McIlroy, S.J., Petrovski, S., Seviour, R.J., Calteau, A., Nielsen, K.L., Nielsen, P.H., 2013a. A metabolic model for members of the genus Tetrasphaera involved in enhanced biological phosphorus removal. ISME J. 7, 543–54. doi:10.1038/ismej.2012.136

Kristiansen, R., Thi, H., Nguyen, T., Saunders, A.M., Lund Nielsen, J., Wimmer, R., Le, V.Q., Mcilroy, S.J., Petrovski, S., Seviour, R.J., Calteau, A., Lehmann Nielsen, K., Nielsen, P.H.H., Nguyen, H.T.T., Saunders, A.M., Nielsen, J.L., Wimmer, R., Le, V.Q., Mcilroy, S.J., Petrovski, S., Seviour, R.J., Calteau, A., Nielsen, K.L., Nielsen, P.H.H., 2013b. A metabolic model for members of the genus Tetrasphaera involved in enhanced biological phosphorus removal. ISME J. 7, 543–554. doi:10.1038/ismej.2012.136

Kuba, T., Murnleitner, E., Van Loosdrecht, M.C.M., Heijnen, J.J., 1996. A metabolic model for biological phosphorus removal by denitrifying organisms. Biotechnol. Bioeng. 52, 685–695. doi:10.1002/(SICI)1097-0290(19961220)52:6<685::AID-BIT6>3.0.CO;2-K

Kuba, T., Smolders, G., van Loosdrecht, M.C.M., Heijnen, J.J., 1993. Biological phosphorus removal from wastewater by anaero-bic-anoxic sequencing batch reactor. Water Sci. Technol. 27, 241–252.

Kuba, T., Wachtmeister, A., van Loosdrecht, M.C.M., Heijnen, J.J., 1994. Effect of Nitrate on Phosphorus Release in Biological Phosphorus Removal Systems. Water Sci. Technol. 30, 263–269. doi:https://doi.org/10.2166/wst.1994.0277

Lanham, A.B., Moita, R., Lemos, P.C., Reis, M.A.M., 2011. Long-term operation of a reactor enriched in Accumulibacter clade I DPAOs: Performance with nitrate, nitrite and oxygen. Water Sci. Technol. 63, 352–359. doi:10.2166/wst.2011.063

Lanham, A.B., Oehmen, A., Saunders, A.M., Carvalho, G., Nielsen, P.H., Reis, M.A.M., 2013a. Metabolic versatility in full-scale wastewater treatment plants performing enhanced

biological phosphorus removal. Water Res. 47, 7032–7041. doi:10.1016/j.watres.2013.08.042

Lanham, A.B., Ricardo, A.R., Albuquerque, M.G.E., Pardelha, F., Carvalheira, M., Coma, M., Fradinho, J., Carvalho, G., Oehmen, A., Reis, M.A.M., 2013b. Determination of the extraction kinetics for the quantification of polyhydroxyalkanoate monomers in mixed microbial systems. Process Biochem. 48, 1626–1634. doi:10.1016/j.procbio.2013.07.023

Lee, D.S., Jeon, C.O., Park, J.M., 2001. Biological nitrogen removal with enhanced phosphate uptake in a sequencing batch reactor using single sludge system. Water Res. 35, 3968–3976. doi:10.1016/S0043-1354(01)00132-4

Liu, Y., Zhang, T., Fang, H.H.P., 2005. Microbial community analysis and performance of a phosphate-removing activated sludge. Bioresour. Technol. 96, 1205–1214. doi:10.1016/j.biortech.2004.11.003

Liu, Y.J., Gu, J., Liu, Y., 2018. Energy self-sufficient biological municipal wastewater reclamation: Present status, challenges and solutions forward. Bioresour. Technol. 269, 513–519. doi:10.1016/j.biortech.2018.08.104

Lu, H., Oehmen, A., Virdis, B., Keller, J., Yuan, Z., 2006. Obtaining highly enriched cultures of Candidatus Accumulibacter phosphates through alternating carbon sources. Water Res. 40, 3838–3848. doi:10.1016/j.watres.2006.09.004

Lv, X. mei, Shao, M. fei, Li, C. lin, Li, J., Xia, X., Liu, D. yang, 2014. Bacterial diversity and community structure of denitrifying phosphorus removal sludge in strict anaerobic/anoxic systems operated with different carbon sources. J. Chem. Technol. Biotechnol. 89, 1842–1849. doi:10.1002/jctb.4265

Machado, V.C., Lafuente, J., Baeza, J.A., 2014. Activated sludge model 2d calibration with full-scale WWTP data: Comparing model parameter identifiability with influent and operational uncertainty. Bioprocess Biosyst. Eng. 37, 1271–1287. doi:10.1007/s00449-013-1099-8

Mamais, D., Jenkins, D., Prrr, P., 1993. A rapid physical-chemical method for the determination of readily biodegradable soluble COD in municipal wastewater. Water Res. 27, 195–197. doi:10.1016/0043-1354(93)90211-Y

Manz, W., Amann, R., Ludwig, W., Wagner, M., Schleifer, K.H., 1992. Phylogenetic Oligodeoxynucleotide Probes for the Major Subclasses of Proteobacteria: Problems and Solutions. Syst. Appl. Microbiol. 15, 593–600. doi:10.1016/S0723-2020(11)80121-9

Marques, R., Santos, J., Nguyen, H., Carvalho, G., Noronha, J.P., Nielsen, P.H., Reis, M.A.M., Oehmen, A., 2017. Metabolism and ecological niche of Tetrasphaera and Ca. Accumulibacter in enhanced biological phosphorus removal. Water Res. 122, 159–171. doi:10.1016/j.watres.2017.04.072

McIlroy, S.J., Nielsen, P.H., 2014. The Family Saprospiraceae. The Prokaryotes Springer, 863–889. doi:https://doi.org/10.1007/978-3-642-38954-2_138

Mckenzie, C.M., Seviour, E.M., Schumann, P., Maszenan, A.M., Liu, J., Webb, R.I., Monis, P., Saint, C.P., Steiner, U., Seviour, R.J., 2006. Isolates of ‘ Candidatus Nostocoida limicola ’ Blackall et al . 2000 should be described as three novel species of the genus Tetrasphaera , as Tetrasphaera jenkinsii sp . nov ., Tetrasphaera vanveenii sp . nov . and Tetrasphaera veronensis sp . Int. J. Syst. Evol. Microbiol. 56, 2279–2290. doi:10.1099/ijs.0.63978-0

Mcmahon, K.D., Dojka, M. a, Pace, N.R., Jenkins, D., Keasling, J.D., 2002. Polyphosphate Kinase from Activated Sludge Performing Enhanced Biological Phosphorus Removal Polyphosphate Kinase from Activated Sludge Performing Enhanced Biological Phosphorus Removal †. Appl. Environ. Microbiol. 68, 4971–4978. doi:10.1128/AEM.68.10.49710

Meerburg, F.A., Boon, N., Van Winckel, T., Vercamer, J.A.R., Nopens, I., Vlaeminck, S.E., 2015. Toward energy-neutral wastewater treatment: A high-rate contact stabilization process to maximally recover sewage organics. Bioresour. Technol. 179, 373–381. doi:10.1016/j.biortech.2014.12.018

Meinhold, J., Arnold, E., Isaacs, S., 1999. Effect of nitrite on anoxic phosphate uptake in biological phosphorus removal activated sludge. Water Res. 33, 1871–1883. doi:10.1016/S0043-1354(98)00411-4

Ménesguen, A., Lacroix, G., 2018. Modelling the marine eutrophication: A review. Sci. Total Environ. 636, 339–354. doi:10.1016/j.scitotenv.2018.04.183

Merzouki, M., Bernet, N., Delgenès, J.P., Benlemlih, M., 2005. Effect of prefermentation on denitrifying phosphorus removal in slaughterhouse wastewater. Bioresour. Technol. 96, 1317–1322. doi:10.1016/j.biortech.2004.11.017

Mielczarek, A.T., Nguyen, H.T.T., Nielsen, J.L., Nielsen, P.H., 2013. Population dynamics of bacteria involved in enhanced biological phosphorus removal in Danish wastewater treatment plants. Water Res. 47, 1529–1544. doi:10.1016/j.watres.2012.12.003

Miller, M.W., De Armond, J., Elliot, M., Kinyua, M., Kinnear, D., Wett, B., Murthy, S., Bott, C.B., 2016. Settling and Dewatering Characteristics of an A-stage Activated Sludge Process Proceeded by Shortcut Biological Nitrogen Removal. Int. J. Water Wastewater Treat. 2. doi:10.16966/2381-5299.133

Mino, T., Loosdrecht, M.C.M.V. a N., Heijnen, J.J., 1998. Microbiology and biochemistry of the enhanced biological phosphate removal process. Water Res. 32, 3193–3207.

Mozumder, M.S.I., Picioreanu, C., Van Loosdrecht, M.C.M., Volcke, E.I.P., 2014. Effect of heterotrophic growth on autotrophic nitrogen removal in a granular sludge reactor. Environ. Technol. 35, 1027–1037. doi:10.1080/09593330.2013.859711

Nguyen, H.T.T., Kristiansen, R., Vestergaard, M., Wimmer, R., Nielsen, P.H., 2015. Intracellular Accumulation of Glycine in Polyphosphate-Accumulating Organisms in Activated Sludge, a Novel Storage Mechanism under Dynamic Anaerobic-Aerobic Conditions. Appl. Environ. Microbiol. 81, 4809–4818. doi:10.1128/aem.01012-15

Nguyen, H.T.T., Le, V.Q., Hansen, A.A., Nielsen, J.L., Nielsen, P.H., 2011. High diversity and abundance of putative polyphosphate-accumulating Tetrasphaera-related bacteria in activated sludge systems. FEMS Microbiol. Ecol. 76, 256–267. doi:10.1111/j.1574-6941.2011.01049.x

Nguyen, H.T.T., Nielsen, J.L., Nielsen, P.H., 2012. “Candidatus Halomonas phosphatis”, a novel polyphosphate-accumulating organism in full-scale enhanced biological phosphorus removal plants. Environ. Microbiol. 14, 2826–2837. doi:10.1111/j.1462-2920.2012.02826.x

Nielsen, J.L., Nguyen, H., Meyer, R.L., Nielsen, P.H., 2012. Identification of glucose-fermenting bacteria in a full-scale enhanced biological phosphorus removal plant by stable isotope probing. Microbiology 158, 1818–1825. doi:10.1099/mic.0.058818-0

Nielsen, P.H., McIlroy, S.J., Albertsen, M., Nierychlo, M., 2019. Re-evaluating the microbiology of the enhanced biological phosphorus removal process. Curr. Opin. Biotechnol. 57, 111–118. doi:10.1016/j.copbio.2019.03.008

Nielsen, P.H., Mielczarek, A.T., Kragelund, C., Nielsen, J.L., Saunders, A.M., Kong, Y., Hansen, A.A., Vollertsen, J., 2010. A conceptual ecosystem model of microbial communities in enhanced biological phosphorus removal plants. Water Res. 44, 5070–5088. doi:10.1016/j.watres.2010.07.036

Nittami, T., Mukai, M., Uematsu, K., Yoon, L.W., Schroeder, S., Chua, A.S.M., Fukuda, J.,

Fujita, M., Seviour, R.J., 2017. Effects of different carbon sources on enhanced biological phosphorus removal and "Candidatus Accumulibacter" community composition under continuous aerobic condition. Appl. Microbiol. Biotechnol. 101, 8607–8619. doi:10.1007/s00253-017-8571-3

Nittami, T., Oi, H., Matsumoto, K., Seviour, R.J., 2011. Influence of temperature, pH and dissolved oxygen concentration on enhanced biological phosphorus removal under strictly aerobic conditions. N. Biotechnol. 29, 2–8. doi:10.1016/j.nbt.2011.06.012

Oehmen, A., Keller-Lehmann, B., Zeng, R.J., Yuan, Z., Keller, J., 2005a. Optimisation of poly-beta-hydroxyalkanoate analysis using gas chromatography for enhanced biological phosphorus removal systems. J. Chromatogr. A 1070, 131–136. doi:10.1016/j.chroma.2005.02.020

Oehmen, A., Lemos, P.C., Carvalho, G., Yuan, Z., Keller, J., Blackall, L.L., Reis, M.A.M., 2007. Advances in enhanced biological phosphorus removal: From micro to macro scale. Water Res. 41, 2271–2300. doi:10.1016/j.watres.2007.02.030

Oehmen, A., Vives, M.T., Lu, H., Yuan, Z., 2005b. The effect of pH on the competition between polyphosphate- accumulating organisms and glycogen-accumulating organisms. Water Res. 39, 3727–3737. doi:10.1016/j.watres.2005.06.031

Oehmen, A., Yuan, Z., Blackall, L.L., Keller, J., 2005c. Comparison of acetate and propionate uptake by polyphosphate accumulating organisms and glycogen accumulating organisms. Biotechnol. Bioeng. 91, 162–168. doi:10.1002/bit.20500

Oehmen, A., Yuan, Z., Blackall, L.L., Keller, J., 2004. Short-term effects of carbon source on the competition of polyphosphate accumulating organsisms and glycogen accumulating organisms. Water Sci. Technol. 50, 139–144.

Oehmen, A., Zeng, R.J., Yuan, Z., Keller, J., 2005d. Anaerobic metabolism of propionate by polyphosphate-accumulating organisms in enhanced biological phosphorus removal systems. Biotechnol. Bioeng. 91, 43–53. doi:10.1002/bit.20480

Patel, J., Nakhla, G., 2006. Interaction of denitrification and P removal in anoxic P removal systems. Desalination 201, 82–99. doi:10.1016/j.desal.2006.03.522

Philips, S., Laanbroek, H.J., Verstraete, W., 2002. Origin, causes and effects of increased nitrite concentrations in aquatic environments. Rev. Environ. Sci. Biotechnol. 1, 115–141. doi:10.1023/A:1020892826575

Pijuan, M., Baeza, J.A., Casas, C., Lafuente, J., 2004a. Response of an EBPR population developed in an SBR with propionate to different carbon sources. Water Sci. Technol. 50, 131–138.

Pijuan, M., Casas, C., Baeza, J.A., 2009. Polyhydroxyalkanoate synthesis using different carbon sources by two enhanced biological phosphorus removal microbial communities. Process Biochem. 44, 97–105. doi:10.1016/j.procbio.2008.09.017

Pijuan, M., Guisasola, A., Baeza, J.A., Carrera, J., Casas, C., Lafuente, J., 2005. Aerobic phosphorus release linked to acetate uptake : Influence of PAO intracellular storage compounds. Biochem. Eng. J. 26, 184–190. doi:10.1016/j.bej.2005.04.014

Pijuan, M., Guisasola, A., Baeza, J.A., Casas, C., Lafuente, J., 2006. Net P-removal deterioration in enriched PAO sludge subjected to permanent aerobic conditions. J. Biotechnol. 123, 117–126. doi:10.1016/j.jbiotec.2005.10.018

Pijuan, M., Saunders, A.M., Guisasola, A., Baeza, J.A., Casas, C., Blackall, L.L., 2004b. Enhanced Biological Phosphorus Removal in a Sequencing Batch Reactor Using Propionate

as the Sole Carbon Source. Biotechnol. Bioeng. 85, 56–67. doi:10.1002/bit.10813

Puig, S., Coma, M., Monclús, H., van Loosdrecht, M.C.M., Colprim, J., Balaguer, M.D., 2008. Selection between alcohols and volatile fatty acids as external carbon sources for EBPR. Water Res. 42, 557–566. doi:10.1016/j.watres.2007.07.050

Qin, Y., Cao, Y., Ren, J., Wang, T., Han, B., 2017. Effect of glucose on nitrogen removal and microbial community in anammox-denitrifi cation system. Bioresour. Technol. 244, 33–39. doi:10.1016/j.biortech.2017.07.124

Qiu, G., Zuniga-Montanez, R., Law, Y., Thi, S.S., Nguyen, T.Q.N., Eganathan, K., Liu, X., Nielsen, P.H., Williams, R.B.H., Wuertz, S., 2019. Polyphosphate-accumulating organisms in full-scale tropical wastewater treatment plants use diverse carbon sources. Water Res. 149, 496–510. doi:10.1016/j.watres.2018.11.011

Rahman, A., De Clippeleir, H., Thomas, W., Jimenez, J.A., Wett, B., Al-Omari, A., Murthy, S., Riffat, R., Bott, C., 2019. A-stage and high-rate contact-stabilization performance comparison for carbon and nutrient redirection from high-strength municipal wastewater. Chem. Eng. J. 357, 737–749. doi:10.1016/j.cej.2018.09.206

Rahman, A., Meerburg, F.A., Ravadagundhi, S., Wett, B., Jimenez, J., Bott, C., Al-Omari, A., Riffat, R., Murthy, S., De Clippeleir, H., 2016. Bioflocculation management through high-rate contact-stabilization: A promising technology to recover organic carbon from low-strength wastewater. Water Res. 104, 485–496. doi:10.1016/j.watres.2016.08.047

Rahman, A., Wadhawan, T., Khan, E., Riffat, R., Takács, I., Clippeleir, H. De, Wett, B., Jimenez, J.A., Al-Omari, A., Murthy, S., 2014. Characterizing and quantifying flocculated and adsorbed chemical oxygen demand fractions in high-rate processes. Glob. challenges Sustain. Wastewater Treat. Resour. Recover. IWA Spec. Conf. doi:10.1103/PhysRevB.91.155112

Ramsay, I.R., Pullammanappallil, P.C., 2001. Protein degradation during anaerobic wastewater treatment: Derivation of stoichiometry. Biodegradation 12, 247–257. doi:10.1023/A:1013116728817

Reino, C., Suárez-Ojeda, M.E., Pérez, J., Carrera, J., 2018. Stable long-term operation of an upflow anammox sludge bed reactor at mainstream conditions. Water Res. 128, 331–340. doi:10.1016/j.watres.2017.10.058

Reino, C., Suárez-Ojeda, M.E., Pérez, J., Carrera, J., 2016. Kinetic and microbiological characterization of aerobic granules performing partial nitritation of a low-strength wastewater at 10 °C. Water Res. 101, 147–156. doi:10.1016/j.watres.2016.05.059

Rongsayamanont, C., Limpiyakorn, T., Khan, E., 2014. Effects of inoculum type and bulk dissolved oxygen concentration on achieving partial nitrification by entrapped-cell-based reactors. Bioresour. Technol. 164, 254–263. doi:10.1016/j.biortech.2014.04.094

Rosenberg, E., Delong, E.F., Lory, S., Stackebrandt, E., Thompson, F., 2014. The Prokaryotes. Springer Heidelberg New York Dordrecht London. doi:10.1007/978-3-642-38954-2

Rössle, W., Pretorius, W., 2001. A review of characterisation requirements for in-line prefermenters: Paper 1: Wastewater characterisation. Water SA 27, 405–412. doi:10.4314/wsa.v27i3.4985

Rubio-Rincón, F.J., Lopez-Vazquez, C.M., Welles, L., van Loosdrecht, M.C.M., Brdjanovic, D., 2017a. Cooperation between Candidatus Competibacter and Candidatus Accumulibacter clade I, in denitrification and phosphate removal processes. Water Res. 120, 156–164. doi:10.1016/j.watres.2017.05.001

Rubio-Rincón, F.J., Welles, L., Lopez-Vazquez, C.M., Abbas, B., Van Loosdrecht, M.C.M., Brdjanovic, D., 2019. Effect of lactate on the microbial community and process performance of an EBPR system. Front. Microbiol. 10, 1–11. doi:10.3389/fmicb.2019.00125

Rubio-Rincón, F.J., Welles, L., Lopez-Vazquez, C.M., Nierychlo, M., Abbas, B., Geleijnse, M., Nielsen, P.H., van Loosdrecht, M.C.M., Brdjanovic, D., 2017b. Long-term effects of sulphide on the enhanced biological removal of phosphorus: The symbiotic role of Thiothrix caldifontis. Water Res. 116, 53–64. doi:10.1016/j.watres.2017.03.017

Rud, I., Kolarevic, J., Buran, A., Berget, I., Calabrese, S., 2017. Deep-sequencing of the bacterial microbiota in commercial-scale recirculating and semi-closed aquaculture systems for Atlantic salmon post-smolt production. Aquac. Eng. 78, 50–62. doi:10.1016/j.aquaeng.2016.10.003

Saad, S.A., Welles, L., Abbas, B., Lopez-vazquez, C.M., Loosdrecht, M.C.M. Van, Brdjanovic, D., 2016. Denitrification of nitrate and nitrite by '*Candidatus* Accumulibacter phosphatis' clade IC. Water Res. 105, 97–109. doi:10.1016/j.watres.2016.08.061

Saito, T., Brdjanovic, D., Loosdrecht, M.C.M. Van, 2004. Effect of nitrite on phosphate uptake by phosphate accumulating organisms. Water Res. 38, 3760–3768. doi:10.1016/j.watres.2004.05.023

Sancho, I., Lopez-Palau, S., Arespacochaga, N., Cortina, J.L., 2019. New concepts on carbon redirection in wastewater treatment plants: A review. Sci. Total Environ. 647, 1373–1384. doi:10.1016/j.scitotenv.2018.08.070

Satoh, H., Mino, T., Matsuo, T., 1998. Anaerobic uptake of glutamate and aspartate by enhanced biological phosphorus removal activated sludge. Water Sci. Technol. 37, 579–582. doi:10.1016/S0273-1223(98)00163-2

Schomburg, D., 2015. Brenda. The comprehensive enzyme information system. URL http//www.brenda-enzymes.org/enzyme.php.

Sekine, M., Akizuki, S., Kishi, M., Toda, T., 2018. Stable nitrification under sulfide supply in a sequencing batch reactor with a long fill period. J. Water Process Eng. 25, 190–194. doi:10.1016/j.jwpe.2018.05.012

Shen, N., Zhou, Y., 2016. Enhanced biological phosphorus removal with different carbon sources. Appl. Microbiol. Biotechnol. 100, 4735–4745. doi:10.1007/s00253-016-7518-4

Shon, H.K., Vigneswaran, S., Kandasamy, J., Cho, J., 2007. Characteristics of Effluent Organic Matter in Wastewater. UNESCO - Encycl. life Support Syst. Water wastewater Treat. Technol. 1–17.

Sliekers, A.O., Derwort, N., Campos Gomez, J.L., Strous, M., Kuenen, J.G., Jetten, M.S.M., 2002. Completely autotrophic nitrogen removal over nitrite in one single reactor. Water Res. 36, 2475–2482. doi:10.1016/S0043-1354(01)00476-6

Smitshuijzen, J., Pérez, J., Duin, O., Loosdrecht, M.C.M. van, 2016. A simple model to describe the performance of highly-loaded aerobic COD removal reactors. Biochem. Eng. J. 112, 94–102. doi:10.1016/j.bej.2016.04.004

Smolders, G.J.F., van der Meij, J., Van Loosdrecht, M.C.M., 1994a. Stoichiometric model of the aerobic metabolism of the biological phosphorus removal process. Biotechnol. Bioeng. 44, 837–848.

Smolders, G.J.F., van der Meij, J., van Loosdrecht, M.C.M., Heijnen, J.J., 1995. A structured metabolic model for the anaerobic and aerobic stoichiometry of the biological phosphorus removal process. Biotechnology and Bioengineering. Biotechnol. Bioeng. 47, 277–287. doi:10.1002/bit.260470302

Smolders, G.J.F., van der Meij, J., van Loosdrecht, M.C.M., Heijnen, J.J., 1994b. Model of the anaerobic metabolism of the biological phosphorus removal process: Stoichiometry and pH influence. Biotechnol. Bioeng. 43, 461–470. doi:10.1002/bit.260430605

Stokholm-Bjerregaard, M., McIlroy, S.J., Nierychlo, M., Karst, S.M., Albertsen, M., Nielsen, P.H., 2017. A critical assessment of the microorganisms proposed to be important to enhanced biological phosphorus removal in full-scale wastewater treatment systems. Front. Microbiol. doi:10.3389/fmicb.2017.00718

Strous, M., Heijnen, J., Kuenen, J., Jetten, M., 1998. The sequencing batch reactor as a powerful tool for the study.pdf. Appl. Microbiol. Biotechnol. 50, 589–596. doi:10.1007/s002530051340

Tayà, C., Garlapati, V.K., Guisasola, A., Baeza, J.A., 2013a. The selective role of nitrite in the PAO/GAO competition. Chemosphere 93, 612–618. doi:10.1016/j.chemosphere.2013.06.006

Tayà, C., Guerrero, J., Vanneste, G., Guisasola, A., Baeza, J.A., 2013b. Methanol-driven enhanced biological phosphorus removal with a syntrophic consortium. Biotechnol. Bioeng. 110, 391–400. doi:10.1002/bit.24625

Tchobanoglous, George, Burton, F.L., Stensel, H.D., 2003. Wastewater Engineering: Treatment, Disposal and Reuse. McGraw-Hill , New York, USA.

Tchobanoglous, G, Burton, F.L., Stensel, H.D., 2003. Wastewater Engineering: Treatment and Reuse, Metcalf & Eddy, Inc., Fourth. ed. McGraw-Hill, New York.

Tomei, M.C., Soria Pascual, J., Mosca Angelucci, D., 2016. Analysing performance of real textile wastewater bio-decolourization under different reaction environments. J. Clean. Prod. 129, 468–477. doi:10.1016/j.jclepro.2016.04.028

Turk, O., Mavinic, D.S., 1989. Maintaining nitrite build-up in a system acclimated to free ammonia. Water Res. 23, 1383–1388. doi:10.1016/0043-1354(89)90077-8

UNEP, 2015. Good practices for Regulating Wastewater Treatment: Legislation, Policies and Standards.

UNESCO, 2014. Water and Energy.The United Nations World Water Development Report. Paris, France.

Vaiopoulou, E., Melidis, P., Aivasidis, a., 2007. Growth of filamentous bacteria in an enhanced biological phosphorus removal system. Desalination 213, 288–296. doi:10.1016/j.desal.2006.02.101

Valverde-Pérez, B., Wágner, D.S., Lórant, B., Gülay, A., Smets, B.F., Plósz, B.G., 2016. Short-sludge age EBPR process - microbial and biochemical process characterisation during reactor start-up and operation. Water Res. 104, 320–329. doi:10.1016/j.watres.2016.08.026

Van Loosdrecht, M.C.M., Brdjanovic, D., 2014. Anticipating the next century of wastewater treatment. Science (80-.). 344, 1452–1453. doi:10.1126/science.1255183

Vargas, M., Casas, C., Baeza, J.A., 2009. Maintenance of phosphorus removal in an EBPR system under permanent aerobic conditions using propionate. Biochem. Eng. J. 43, 288–296. doi:10.1016/j.bej.2008.10.013

Vargas, M.D.M., Casas, C., Baeza, J.A., 2009. Maintenance of phosphorus removal in an EBPR system under permanent aerobic conditions using propionate. Biochem. Eng. J. 43, 288–296. doi:10.1016/j.bej.2008.10.013

Vazquez, J.R.P., 2009. Autotrophic nitrogen removal in granular sequencing batch reactors 20–25.

Versprille, A.I., Zuurveen, B., Stein, T., 1985. The A-B process : A novel two stages wastewater treatment system. Water Sci. Technol. 17, 235–246.

Verstraete, W., Vlaeminck, S.E., 2011. ZeroWasteWater: Short-cycling of wastewater resources for sustainable cities of the future. Int. J. Sustain. Dev. World Ecol. 18, 253–264. doi:10.1080/13504509.2011.570804

Vieira, A., Galinha, C.F., Oehmen, A., Carvalho, G., 2019. The link between nitrous oxide emissions, microbial community profile and function from three full-scale WWTPs. Sci. Total Environ. 651, 2460–2472. doi:10.1016/j.scitotenv.2018.10.132

Wan, J., Gu, J., Zhao, Q., Liu, Y., 2016. COD capture: A feasible option towards energy self-sufficient domestic wastewater treatment. Sci. Rep. 6, 1–9. doi:10.1038/srep25054

Wang, X., Hu, M., Xia, Y., Wen, X., Ding, K., 2012. Pyrosequencing analysis of bacterial diversity in 14 wastewater treatment systems in china. Appl. Environ. Microbiol. 78, 7042–7047. doi:10.1128/AEM.01617-12

Wanner, J., Kucman, K., Ottov, V., Grau, P., Ottová, V., Grau, P., 1987. Effect of anaerobic conditions on activated sludge filamentous bulking in laboratory systems. Water Res. 21, 1541–1546. doi:10.1016/0043-1354(87)90139-4

Welles, L., Tian, W.D., Saad, S., Abbas, B., Lopez-Vazquez, C.M., Hooijmans, C.M., van Loosdrecht, M.C.M., Brdjanovic, D., 2015. Accumulibacter clades Type I and II performing kinetically different glycogen-accumulating organisms metabolisms for anaerobic substrate uptake. Water Res. 83, 354–366. doi:10.1016/j.watres.2015.06.045

Wentzel, M., Ekama, G., Loewenthal, R.E., Dold, P., Marais, G., 1989. Enhanced polyphosphate organism cultures in activated sludge systems: Part II: Experimental behaviour. Water SA 15, 89.

Wenyi, D., Hong, D., Li-an, Z., Jia, M., Baozhen, W., 2006. Operational Retrofits of AB Process for Biological Removal of Nitrogen and Phosphorus. Water Pract. Technol. 1. doi:10.2166/wpt.2006.078

Wett, B., Omari, A., Podmirseg, S.M., Han, M., Akintayo, O., Gómez Brandón, M., Murthy, S., Bott, C., Hell, M., Takács, I., Nyhuis, G., O'Shaughnessy, M., 2013. Going for mainstream deammonification from bench to full scale for maximized resource efficiency. Water Sci. Technol. 68, 283–289. doi:10.2166/wst.2013.150

Willems, A., 2014. The Family Comamonadaceae, in: The Prokaryotes: Alphaproteobacteria and Betaproteobacteria. pp. 777–851. doi:10.1007/978-3-642-30197-1

Winkler, M.K., Straka, L., 2019. New directions in biological nitrogen removal and recovery from wastewater. Curr. Opin. Biotechnol. 57, 50–55. doi:10.1016/j.copbio.2018.12.007

Wong, M.T., Tan, F.M., Ng, W.J., Liu, W.T., 2004. Identification and occurrence of tetrad-forming Alphaproteobacteria in anaerobic-aerobic activated sludge processes. Microbiology 150, 3741–3748. doi:10.1099/mic.0.27291-0

Xu, G., Wang, H., Gu, J., Shen, N., Qiu, Z., Zhou, Y., Liu, Y., 2017. A novel A-B process for enhanced biological nutrient removal in municipal wastewater reclamation. Chemosphere 189, 39–45. doi:10.1016/j.chemosphere.2017.09.049

Yadav, D., Pruthi, V., Kumar, P., 2016. Journal of Water Process Engineering Enhanced biological phosphorus removal in aerated stirred tank reactor using aerobic bacterial

consortium. J. Water Process Eng. 13, 61–69. doi:10.1016/j.jwpe.2016.08.005

Yuan, Q., Oleszkiewicz, J., 2010. Interaction between Denitrification and Phosphorus Removal in a Sequencing Batch Reactor Phosphorus Removal System. Water Environ. Res. 82, 536–540. doi:10.2175/106143009x12529484815476

Zafiriadis, I., Kapagiannidis, A.G., Ntougias, S., Aivasidis, A., 2017. Inhibition of the respiratory chain reactions in denitrifying EBPR biomass under simultaneous presence of acetate and electron acceptor. N. Biotechnol. 36, 42–50. doi:10.1016/j.nbt.2017.01.003

Zeng, R.J., Saunders, A.M., Yuan, Z., Blackall, L.L., Keller, J., 2003. Identification and comparison of aerobic and denitrifying polyphosphate-accumulating organisms. Biotechnol. Bioeng. 83, 140–148. doi:10.1002/bit.10652

Zeng, T., Wang, D., Li, X., Ding, Y., Liao, D., 2013. Comparison between acetate and propionate as carbon sources for phosphorus removal in the aerobic / extended-idle regime. Biochem. Eng. J. 70, 151–157. doi:10.1016/j.bej.2012.10.014

Zeng, W., Zhang, L., Fan, P., Guo, J., Peng, Y., 2018. Community structures and population dynamics of “Candidatus Accumulibacter” in activated sludges of wastewater treatment plants using ppk1 as phylogenetic marker. J. Environ. Sci. (China) 67, 237–248. doi:10.1016/j.jes.2017.09.001

Zengin, G.E., Artan, N., Orhon, D., Satoh, H., Mino, T., 2011. Effect of aspartate and glutamate on the fate of enhanced biological phosphorus removal process and microbial community structure. Bioresour. Technol. 102, 894–903. doi:10.1016/j.biortech.2010.09.023

Zessner, M., Lampert, C., Kroiss, H., Lindtner, S., 2010. Cost comparison of wastewater treatment in Danubian countries. Water Sci. Technol. 62, 223–230. doi:10.2166/wst.2010.271

Zhang, B., Xu, X., Zhu, L., 2017. Structure and function of the microbial consortia of activated sludge in typical municipal wastewater treatment plants in winter. Sci. Rep. 1–11. doi:10.1038/s41598-017-17743-x

Zhao, J., Feng, L., Yang, G., Dai, J., Mu, J., 2017. Development of simultaneous nitrification-denitrification (SND) in biofilm reactors with partially coupled a novel biodegradable carrier for nitrogen-rich water purification. Bioresour. Technol. 243, 800–809. doi:10.1016/j.biortech.2017.06.127

Zheng, D., Sun, Y., Li, H., Lu, S., Shan, M., Xu, S., 2016. Multistage A-O Activated Sludge Process for Paraformaldehyde Wastewater Treatment and Microbial Community Structure Analysis. J. Chem. 2016. doi:http://dx.doi.org/10.1155/2016/2746715

Zhou, S., Zhang, X., Feng, L., 2010. Effect of different types of electron acceptors on the anoxic phosphorus uptake activity of denitrifying phosphorus removing bacteria. Bioresour. Technol. 101, 1603–1610. doi:10.1016/j.biortech.2009.09.032

Zhou, Y., Ganda, L., Lim, M., Yuan, Z., Jern, W., 2012. Response of poly-phosphate accumulating organisms to free nitrous acid inhibition under anoxic and aerobic conditions. Bioresour. Technol. 116, 340–347. doi:10.1016/j.biortech.2012.03.111

Zhou, Y., Ganda, L., Lim, M., Yuan, Z., Kjelleberg, S., Ng, W.J., 2010. Free nitrous acid (FNA) inhibition on denitrifying poly-phosphate accumulating organisms (DPAOs). Appl. Microbiol. Biotechnol. 88, 359–369. doi:10.1007/s00253-010-2780-3

Zhou, Y., Oehmen, A., Lim, M., Vadivelu, V., Ng, W.J., 2011. The role of nitrite and free nitrous acid (FNA) in wastewater treatment plants. Water Res. 45, 4672–4682. doi:10.1016/j.watres.2011.06.025

Zhou, Y., Pijuan, M., Yuan, Z., 2007. Free nitrous acid inhibition on anoxic phosphorus uptake and denitrification by poly-phosphate accumulating organisms. Biotechnol. Bioeng. 98, 903–912. doi:10.1002/bit

Zhou, Y., Pijuan, M., Zeng, R.J., Yuan, Z., 2009. Involvement of the TCA cycle in the anaerobic metabolism of polyphosphate accumulating organisms (PAOs). Water Res. 43, 1330–1340. doi:10.1016/j.watres.2008.12.008

Zhou, Z., Qiao, W., Xing, C., An, Y., Shen, X., Ren, W., Jiang, L., Wang, L., 2015. Microbial community structure of anoxic – oxic-settling-anaerobic sludge reduction process revealed by 454-pyrosequencing. Chem. Eng. J. 266, 249–257. doi:10.1016/j.cej.2014.12.095

ANNEX I

Annex I.1. Carbon storage

The fraction of the carbon stored consumed only by *Accumulibacter* was estimated based on the average value of COD load and solids production during the period II for the A/O SBR and period V for the A^2/O pilot plant.

FISH quantification was used to estimate the biovolume of *Accumulibacter* in both systems ($f_{PAO,FISH}$ = 36% for the SBR and $f_{PAO,FISH}$ = 49% for the A^2/O pilot plant, corresponding these values to the same periods aforementioned).

The amount of solids removed from the reactor (WAS, $g \cdot d^{-1}$) was calculated with Equation 1. Q_P is the purge flowrate ($L \cdot d^{-1}$), VSS_P is the concentration of volatile suspended solids purged ($gVSS \cdot L^{-1}$), Q_{in} is the feed flow ($L \cdot d^{-1}$) and $VSS_{effluent}$ is the solids concentration in the effluent ($g\ VSS \cdot L^{-1}$).

$$WAS = Q_P \cdot VSS_P + (Q_{in} - Q_p) \cdot VSS_{effluent} \quad (1)$$

The observed yield for PAO Y_{obs} ($gCOD_X \cdot g^{-1}COD$) was calculated with equation 2 (G Tchobanoglous et al., 2003) using the parameters reported by (Chan et al., 2017), where Y is the biomass growth yield coefficient (0.39 $gCOD_X \cdot g^{-1}COD$), k_d is the endogenous decay coefficient (0.06 d^{-1}), SRT is the average sludge retention time in the periods aforementioned (d) and f_d is the fraction of biomass that remains as cell debris (0.1).

$$Y_{obs} = \frac{Y}{1+k_d \cdot SRT}(1 + f_d \cdot k_d \cdot SRT) \quad (2)$$

Equation 3 was used to calculate $Y_{SX,PAO}$, which is the observed yield coefficient expressed in $gVSS \cdot g^{-1}COD$, by using the typical stoichiometric factor (1.416 $gCOD_X \cdot g^{-1}VSS$).

$$Y_{SX,PAO} = \frac{Y_{obs}}{1.416} \quad (3)$$

Equation 4 was used to estimate the fraction of the COD in the influent that was consumed by *Accumulibacter* ($\%COD_{PAO}$), where $f_{PAO,FISH}$ is the fraction of *Accumulibacter* detected by FISH (%), and COD_{in} is the concentration of soluble COD in the influent ($gCOD \cdot L^{-1}$).

$$\%COD_{PAO} = \frac{(WAS \cdot f_{PAO,FISH})/Y_{SX,PAO}}{Q_{in} \cdot COD_{in}} \cdot 100 \quad (4)$$

Considering these equations and the values measured during the period II for the A/O SBR and period V for the A^2/O pilot plant (Table A.1.1), it was estimated that

Accumulibacter could be responsible of around 77.5% and 45% of the available COD respectively.

Table A.I.1. Average values for the estimation of the fraction of the carbon stored consumed only by *Accumulibacter*.

System	SBR	A^2/O
Average SRT (d)	15	10
Q_P ($L \cdot d^{-1}$)	0.4 ± 0.1	5.0 ± 0.1
VSS ($g \cdot L^{-1}$)	0.71 ± 0.05	1.54 ± 0.36
Q_{in} ($L \cdot d^{-1}$)	19.7 ± 0.1	239 ± 17
$VSS_{effluent}$($g \cdot L^{-1}$)	0.012 ± 0.001	0.024 ± 0.008
WAS ($g \cdot d^{-1}$)	0.48 ± 0.08	13.4 ± 3.0
$f_{PAO,\ FISH}$ (-)	0.36	0.49
Y_{obs} ($gCOD_X \cdot g^{-1}COD$)	0.22	0.26
$Y_{SX,PAO}$ ($gVSS \cdot g^{-1}COD$)	0.16	0.18
COD_{in} ($gCOD \cdot L^{-1}$)	0.072 ± 0.008	0.32 ± 0.06
COD_{PAO} (%)	77 ± 21	45 ± 9

Annex I.2. Glutamate fermentation pathways

Glutamate is converted via 3-methylaspartate to ammonia, acetate and butyrate through the classical pathway (Buckel and Barker, 1974) (equation 5), although another variant of this pathway is also reported (equation 6) (Buckel, 2001):

$$5\ \underbrace{C_5H_8NO_4^-}_{glutamate} + 6\ H_2O + 2\ H^+ \longrightarrow 5\ NH_4^+ + 5\ CO_2 + 6\ \underbrace{C_2H_3O_2^-}_{acetate} + 2\ \underbrace{C_4H_7O_2^-}_{butyrate} + H_2 \quad (5)$$

$$3\ \underbrace{C_5H_8NO_4^-}_{glutamate} + 4\ H_2O \longrightarrow 3\ NH_4^+ + 2\ CO_2 + 5\ \underbrace{C_2H_3O_2^-}_{acetate} + \underbrace{C_3H_5O_2^-}_{propionate} \quad (6)$$

The ratios of mole of acetate, propionate and butyrate per mole of glutamate were calculated for these two reactions:

$$\text{Reaction 3: } 0.48\ \frac{\text{mol C}_{\text{acetate}}}{\text{mol C}_{\text{glutamate}}} \text{ and } 0.32\ \frac{\text{mol C}_{\text{butyrate}}}{\text{mol C}_{\text{glutamate}}}$$

$$\text{Reaction 4: } 0.67\ \frac{\text{mol C}_{\text{acetate}}}{\text{mol C}_{\text{glutamate}}} \text{ and } 0.20\ \frac{\text{mol C}_{\text{propionate}}}{\text{mol C}_{\text{glutamate}}}$$

Assuming an equal contribution for each of the reactions, the average ratios obtained are:

$$0.57\ \frac{\text{mol C}_{\text{acetate}}}{\text{mol C}_{\text{glutamate}}}$$

$$0.16\ \frac{\text{mol C}_{\text{butyrate}}}{\text{mol C}_{\text{glutamate}}}$$

$$0.10\ \frac{\text{mol C}_{\text{propionate}}}{\text{mol C}_{\text{glutamate}}}$$

Annex I.3. Anaerobic balance and stoichiometry of *Accumulibater* and non-*Accumulibacter* PAO

The bibliographic anaerobic yields when the carbon sources are acetic, propionic and butyric are shown in Table A.1.2.

Table A.1.2. Anaerobic yields obtained from the literature.

Study/Anaerobic yields	P_{rel}/C_{upt}	PHB/C_{upt}	PHV/C_{upt}	Gly/C_{upt}	Carbon source
Welles et al. (2015)	0.64	1.27	0.09	0.29	Acetic acid
Oehmen et al. (2005d)	0.42	0.04	0.55	0.32	Propionic acid
Pijuan et al. (2004)	0.22	0.36	0.08	0.49	Butyric acid

Note: All data expressed in mol $C \cdot mol^{-1}C$, apart from P_{rel}/C_{upt}, which is expressed in mol $P \cdot mol^{-1}C$.

The COD distribution was assumed as described in the section I.1 of this Annex (carbon storage), while the theoretical anaerobic yields (Table A.1.2) were corrected with the average ratios obtained in the section I.2 of this Annex (Glutamate fermentation pathways) in order to express them per mole of glutamate (Table A.1.3).

Table A.1.3. Anaerobic yields expressed on glutamate basis

Anaerobic yields	P_{rel}/C_{upt}	PHB/C_{upt}	PHV/C_{upt}	Gly/C_{upt}	Carbon source
Welles et al. (2015)	0.37	0.73	0.05	0.17	Acetic acid
Oehmen et al. (2005d)	0.04	0.06	0.01	0.08	Propionic acid
Pijuan et al. (2004)	0.03	0.004	0.06	0.03	Butyric acid
Calculated total contribution	**0.44**	**0.79**	**0.12**	**0.28**	**Glutamate**

Note: All data expressed in mol $C \cdot mol^{-1}C$, apart from P_{rel}/C_{upt}, which is expressed in mol $P \cdot mol^{-1}C$.

The total contribution ratios are compared with the measured ratios in order to study the contribution of the *Accumulibacter* and non-*Accumulibacter* to the EBPR process (Tables 4.9 and 4.10).

Annex I.4

Table A.I.4. Enzymes of special interest reported for the main genus under study. Data for *Accumulibacter* was obtained from Kristiansen et al. (2013) and the rest of data from the BRENDA database (Schomburg, 2015).

	EC number	*Accumulibacter*	*Thiothrix*	*Comamonadaceae*
Glycolysis				
fructose-bisphosphate aldolase	4.1.2.13		Yes	Yes
phosphoglycerate mutase	5.4.2.1	Yes	Yes	Yes
glucokinase	2.7.1.2			Yes
phosphoglycerate kinase	2.7.2.3	Yes		Yes
phosphopyruvate hydratase	4.2.1.11	Yes		Yes
pyruvate kinase	2.7.1.40	Yes		Yes
phosphogluconate dehydratase	4.2.1.12			Yes
2-dehydro-3-deoxy-phosphogluconate aldolase	4.1.2.14			Yes
Gluconeogenesis				
fructose-bisphosphatase	3.1.3.11	Yes	Yes	
Glycogen synthesis				
glucose-1-phosphate adenylyltransferase	2.7.7.27	Yes		Yes
glycogen phosphorylase	2.4.1.1	Yes		Yes
Pyruvate metabolism				
Pyruvate synthetase	1.2.7.1	Yes	Yes	
phosphoenolpyruvate carboxylase	4.1.1.31	Yes		Yes
Polyphosphate metabolism				
polyphosphate kinase	2.7.4.1	Yes	Yes	
TCA cycle				
Citrate synthase	2.3.3.1	Yes	Yes	Yes
Aconitate hydratase	4.2.1.3	Yes	Yes	Yes
Oxoglutarate dehydrogenase	1.2.4.2	Yes	Yes	
Isocitrate dehydrogenase	1.1.1.41	Yes	Yes	
Succinate dehydrogenase	1.3.5.1	Yes	Yes	Yes
Malate dehydrogenase	1.1.1.37	Yes	Yes	Yes
PHA synthesis				
poly(3-hydroxybutyrate) depolymerase	3.1.1.75	Yes		Yes
Amino acid metabolism				
Glutamate dehydrogenase	1.4.1.2		Yes	Yes
aspartate kinase	2.7.2.4		Yes	
aspartate transaminase	2.6.1.1		Yes	
aspartate-semialdehyde dehydrogenase	1.2.1.11		Yes	

aspartate ammonia-lyase	4.3.1.1	Yes